

**Imperial College
London**

Stretch-Activated Channels in Heart Valve Cells

A thesis submitted to Imperial College London for the
degree of Doctor of Philosophy

Hessah F. Alshammari
January 2019

National Heart and Lung Institute
Faculty of Medicine
Imperial College London

Abstract

The aortic valve is a sophisticated structure that performs complex functions to preserve the unidirectional flow of blood and maintenance of myocardial function. Valve endothelial cells (VECs) cover the two surfaces of aortic valve cusps in a continuous layer consisting of the endocardium and the sinus wall endothelium. Valve interstitial cells (VICs) are a heterogeneous and dynamic population of cells that form the body of valve cusps and are located within the extracellular matrix. VECs experience continuous and different mechanical forces in both side and VICs are experience continuous and varying mechanical forces, including stretch. These mechanical forces are translated to the cells via electrochemical or biochemical signals through mechanotransduction pathways, which may include stretch-activated ion channels (SACs) which are membrane proteins capable of responding to mechanical force and activate intracellular signalling pathways that mediate the functional response of the cells. The overall aim of this study was to investigate SACs presence and their functional roles in VECs and VICs. The presence of stretch-activated ion channels was studied electrophysiologically and biochemically in VECs from each side of the valve and different phenotypes of VICs. The role of SAC on alignment of and proliferation VECs, migration and collagen production in VICs were assessed. Stretch-activated ion channels receptors including (KCNK2, KCNJ8, TRPM4, TRPV4 and TRPC6) were present in VECs and VICs. SACs have the same channel activity in VECs from aortic and ventricular sides, but the expression level of some SACs

are significantly more in VECs isolated from the ventricular side. Additionally, functional roles of SACs in VECs was demonstrated where blocking of SACs significantly reduced VECs alignment under shear stress. SACs activity and expression varied in VICs of a fibroblast, myofibroblast and osteoblast phenotype, which correlated with changes in fibroblast and osteoblast markers. SACs blockers significantly reduced migration and collagen production of VICs in response to mechanical stretch. Also, SACs activators regulated VICs proliferation in static condition. In conclusion, SACs are present in VECs and VICs and have regulatory roles in some mechanically-mediated cells responses or function. This study shows a role for SACs in the mechanobiology of valve cells, and information provides a new insight towards understanding valve cell function in health and disease.

Declaration

I, Hessah Alshammari, hereby declare that I wrote this thesis; the work and experiments presented in this thesis were performed by me unless properly referenced. Data, information and work done of patch clamp technique are included in this thesis and performed in collaboration with Remi Peyronnet.

Copyright Declaration

‘The copyright of this thesis rests with the author. Unless otherwise indicated, its contents are licensed under a Creative Commons Attribution-Non Commercial 4.0 International Licence (CC BY-NC).

Under this licence, you may copy and redistribute the material in any medium or format. You may also create and distribute modified versions of the work. This is on the condition that: you credit the author and do not use it, or any derivative works, for a commercial purpose.

When reusing or sharing this work, ensure you make the licence terms clear to others by naming the licence and linking to the licence text. Where a work has been adapted, you should indicate that the work has been changed and describe those changes.

Please seek permission from the copyright holder for uses of this work that are not included in this licence or permitted under UK Copyright Law.’

Acknowledgements

First and foremost, all praise immeasurable gratitude is due to Almighty Allah for all His blessing, mercy and guidance as this work has been accomplished by His grace. Then, I would like to dedicate this thesis to my parents, this study would not have been possible without their support. I would like to express profound gratitude to my husband Dr Saud for his love, help and support throughout my life. Deepest gratitude is also due to my brothers and sisters for their support. I wish to express my love and gratitude to my beloved small family; for their understanding & endless love, through the duration of my studies.

I would like to thank my supervisor Dr Adrian Chester for the continuous support of my PhD study, for his patience, motivation, and immense knowledge. His guidance, participation and input helped me in all the time. I am also highly thankful to my second supervisor Dr Najma Latif. I would like to express profound gratitude to Padmini Sarathchandra, Ann McCormack, and Gary in tissue engineering group for their invaluable support, encouragement, supervision and useful suggestions throughout this research work. I would like to thank Remi Peyronnet for all his works and guidance in patch clamp experiments.

This research was supported by King Fahad cardiac centre at King Saud University. I would like to express my gratitude to King Fahad cardiac centre who provided insight and financial support that greatly assisted the research. I would also like to acknowledge imperial college London for giving me this opportunity to study PhD.

Abstracts

Hessah Alshammari, Adrian Chester, Najma Latif, & Peter Kohl. Stretch Activated Channels in Valve Endothelial Cells. The 8th Biennial Heart Valve Biology & Tissue Engineering Meeting Royal Society of Medicine. London, UK. September 2018.

Hessah Alshammari, Adrian Chester, Najma Latif, & Remi Peyronnet, Padmini Sarathchandra, Ann McCormack, Peter Kohl, Magdi Yacoub. Stretch Activated Channels in Valve Interstitial Cells. The 8th Biennial Heart Valve Biology & Tissue Engineering Meeting Royal Society of Medicine. London, UK. September 2018.

Abbreviations

APD	Action potential duration
α -V β 3	Alpha- vitronectin beta 3
ALP	Alkaline phosphatase
AV	Aortic valve
ANP	Atrial natriuretic peptide
BMP	Bone morphogenetic protein
BSA	Bovine Serum Albumin
Ca ²⁺	Calcium ions
CaM	Calmodulin
TRPC	Canonical transient receptor potential
coll	Collagen
Cx43	Connexin43
Cx45	Connexin45
COX	cyclooxygenase
eNOS	Endothelial nitric oxide synthase
ET-1	Endothelin 1
EMT	Endothelial-to-mesenchymal transformation
ECM	Extracellular matrix
EDA-fn	Extra Domain A- fibronectin
CD90	Fibroblast surface antigen
FN	Fibronectin
FACS	Fluorescence-activated cell sorting analysis
Gd ³⁺	Gadolinium
GAPDH	Glyceraldehyde 3-phosphate dehydrogenase
GAGs	Glycosaminoglycans
GsMTx4	Grammostola spatulata mechanotoxin 4
COX	cyclooxygenase
ICAM-1	Intercellular Adhesion Molecule 1
IL-6	Interleukin 6
MMP	Matrix metalloproteinase

TRPM	Melastatin transient receptor potential
MSCs	Mesenchymal stem cells
MV	Mitral valve
MRTFA	Myocardin-related transcription factor A
NO	Nitric oxide
PBS	Phosphate-buffered saline
PECAM	Platelet endothelial cell adhesion molecule
PMA	Phorbol 12-myristate 13-acetate
PUFAs	polyunsaturated fatty acids
SACK	Potassium-selective channels
SMmyhc	Smooth muscles heavy chain
SACs	Stretch-activated channels
SACNS	Stretch-activated channels cation nonselective
RUNX2	Runt-related transcription factor 2
TIMP2	Tissue inhibitor of metalloproteinases 2
TGF- β	Transforming growth factor beta
TRP	Transient receptor potential channels
K2p	Two-pore-domain channels
TNF- α	Tumor necrosis factor
VECs	Valve endothelial cells
VICs	Valve interstitial cells
TRPV	Vanilloid transient receptor potential
VCAM-1	Vascular cell adhesion molecule 1
VE-cadherin	Vascular endothelial cadherin
VWF	Von Willebrand factor
WB	Western Blot
α SMA	α -smooth muscle actin
4 α PDD	4 α -phorbol 12,13-didecanoate

Table of Contents

Abstract	I
Declaration	II
Copyright Declaration	III
Acknowledgements	IV
Abstracts	V
Abbreviations	VI
Table of Contents	VIII
List of Figures	XII
List of Tables	XV
Chapter 1: Introduction	1
1.1 Heart Valves	2
1.2 Mechanical Environment of Aortic Valve	4
1.2.1 Shear Stress	5
1.2.2 Pressure	5
1.2.2.1 Stretch	6
1.3 Effect of Mechanical Forces on Cell Function	7
1.3.1 Shear Stress	7
1.3.2 Pressure	8
1.3.2.1 Stretch	8
1.4 Mechanotransduction in Heart Valve Cells	9
1.4.1 Mechanotransduction Elements	10
1.4.1.1 ECM & Cytoskeleton Elements	10
1.4.1.2 Mechanosensitive Channels	13
1.5 Stretch-Activated Channels	14
1.5.1 Stretch-Activated Channels Classification	15
1.5.1.1 Cation Non-Selective Channels	16
1.5.1.1.1 TRP Channels	16
1.5.1.1.2 Piezo Channels	22
1.5.1.2 Potassium-Selective Channels	23
1.5.1.2.1 Inwardly Rectifying (Kir)	24
1.5.1.2.2 Two-pore-domain (K2p)	25
1.7.1 Stretch-Activated Channels in the Heart Valve Cells	27
1.6 Hypothesis & Aims	29
Chapter 2: General Materials and Methods	30
2.1 Cell Culture	31
2.1.1 Endothelial cells Isolation and Culture	31
2.1.2 Interstitial Cells	32
2.2 Cells Sorting	32
2.3 FACS	33
2.4 Immunohistochemical Staining	33
2.5 Immunohistochemistry	34
2.6 Western Blot	35
2.7 RT-PCR	36
2.7.1 RNA extraction	36
2.7.2 cDNA synthesis	37

2.7.3	Real-time PCR	37
2.8	Statistical Analysis	38
Chapter 3: Isolation and Phenotype of Valve Cells		39
3.1	Rational	40
3.2	The Specific Aims	44
3.3	Methods	45
3.3.1	Isolation of Side-Specific VECs	45
3.3.2	Maintenance of VICs Fibroblast Phenotype of VICs	46
3.3.3	Differentiation of VICs to Myofibroblast	46
3.3.4	Differentiation of VICs to Osteoblast	47
3.4	Results	48
3.4.1	Valve endothelial cells	48
3.4.2	Side-specific Valve Endothelial cells	50
3.4.3	Valve Interstitial Cells	52
3.4.4	Differentiated Valve Interstitial Cells	56
3.4.4.1	Myfibroblast cells	57
3.4.4.2	Osteoblast cells	62
3.5	Discussion	65
3.6	Limitations and Future Studies	69
3.7	Conclusion	70
Chapter 4: Expression of Stretch-Activated Channels in Valve Cells		71
4.1	Rational	72
4.2	The specific Aims	73
4.3	Methods	74
4.3.1	Patch xClamp	74
4.4	Results	76
4.4.1	SAC expression in Valve Endothelial Cells	76
4.4.2	SACs activity in Valve Endothelial Cells	79
4.4.3	SACs expression in side-specific Valve Endothelial Cells	79
4.4.4	SACs activity in side-specific Valve Endothelial Cells	81
4.4.5	SACs expression in Valve Interstitial Cells	84
4.4.6	SACs activity in Valve Interstitial Cells	86
4.4.7	SACs expression in the differentiation of Valve Interstitial Cells	86
4.4.8	SACs activity in the differentiation of Valve Interstitial Cells	89
4.4.1	SAC expression in Valve Tissues Samples	93
4.5	Discussion	95
4.6	Limitations and Future Studies	98
4.7	Conclusion	99
Chapter 5: Stretch-Activated Channels in Calcified Aortic Valve		100
5.1	Rational	101
5.2	The Specific Aims	103
5.3	Methods	104
5.4	Result	105
5.4.1	Stretch-Activated Channels in VICs Isolated from Non-Calcified & Calcified Valves	105
5.4.2	Stretch-Activated Channels in Tissues from Non-Calcified & Calcified Valves.	107
5.5	Discussion	112

5.6	Limitation and future work	114
5.7	Conclusion	114
Chapter 6: Functional Effects Modulated by Stretch-Activated in VECs		115
6.1	Rationale	116
6.2	Aims	117
6.3	Methods	118
6.3.1	Shear stress	118
6.3.2	Inhibition of SACs	119
6.4	Result	120
6.4.1	The Role of SACs in the Alignment of VECs from Aortic and Ventricular Side	120
6.4.2	The Effect of Different Channels Inhibitors in the Alignment of VECs from Aortic and Ventricular Side	124
6.3.1	The Effect of Different Concentration of TRPC6/3 Channels Inhibitor in the Alignment of VECs from Ventricular Side	127
6.5	Discussion	129
6.6	Limitations and Future Work	131
6.7	Conclusion	132
Chapter 7: Functional Effects Modulated by Stretch-Activated Channels in VICs		133
7.1	Rationale	134
7.2	Aims	136
7.3	Methods	137
7.3.1	Activation of SACs	137
7.3.1.1	Activation of SACs by application of stretch	137
7.3.1.2	Activation of SACs by pharmacological activators	138
7.3.2	Inhibition of SACs	138
7.3.3	Migration assay	139
7.3.4	Proliferation Assay (MTS)	140
7.3.5	Live/dead cells assay	140
7.4	Results	142
7.4.1	Role of SACs in Collagen production by VICs	142
7.4.2	Role of SACs on migration of VICs	146
7.4.3	Role of SACs on the proliferation of VICs	151
7.5	Discussion	156
7.6	Limitations and Future Work	160
7.7	Conclusions	162
Chapter 8: Discussion and limitations and Future Work		163
8.1	Discussion	164
8.2	Limitations	170
8.3	Future Work	171
Reference		172

List of Figures

Figure 1.1	Photograph of an open aortic root.	3
Figure 1.2	Diagram of different mechanical stimuli experienced by the Aortic valve.	4
Figure 1.3	Gating Mechanism of SACs.	15
Figure 1.4	Overview of cation non-selective (SACNS) and potassium-selective (SACK) channel.	28
Figure 3.1	Isolation descriptions of side-specific endothelial cells.	46
Figure 3.2	Light microscope images of aortic VECs.	48
Figure 3.3	Confocal microscopy of ECs from aortic VEC stained for ECs markers.	49
Figure 3.4	FACS analysis of VECs isolated from aortic valve.	50
Figure 3.5	The morphology of side-specific endothelial cells.	51
Figure 3.6	Result of FACS analysis of site-specific endothelial cells.	52
Figure 3.7	Light microscope images of isolated aortic VICs	53
Figure 3.8	Confocal laser scanning microscopy of double-stain of interstitial markers of ICs	55
Figure 3.9	FACS analysis of VICs isolated from aortic valve	56
Figure 3.10	Confocal laser scanning microscopy of VICs stained with fibroblast and myofibroblast markers	58
Figure 3.11	A) Western blots bands of fibroblast& myofibroblast markers in differentiated VICs	60
Figure 3.12	Confocal laser scanning microscopy of differentiated VICs stained with osteoblastic markers	63
Figure 3.13	Western blots bands of Osteoblast markers in differentiated VICs	64
Figure 4-1	Illustration of the single-channel cell-attached patch-clamp mode	75
Figure 4.2	Protein expression of the SACs in VECs isolated from aortic and mitral valves.	77
Figure 4.3	Confocal microscopy of the immune-fluorescence stain of SACs in VECs.	78
Figure 4.4	Patch-clamp recordings of cultured VECs from aortic valve	79
Figure 4.5	Proteins expression of the SACs in side-specific VECs	80

Figure 4.6	Immuno-fluorescence stain of SACs in side-specific VECs.	81
Figure 4.7	SACs currents recording in side-specific VECs	82
Figure 4.8	The relation between relative current and pressure of side specific VEC.	83
Figure 4.9	Relative protein expression of the SACs in VICs isolated from aortic and mitral valves.	85
Figure 4.10	Patch-clamp experiments performed on VIC using cell-attached mode at -80 Mv.	86
Figure 4.11	Protein expression of SACs in three VICs phenotypes	88
Figure 4.12	Immune-fluorescence stain of SACs in VICs in three phenotypes.	89
Figure 4.13	Recordings of cation non-selective channels in Fibro, DMEM and osteogenic media.	91
Figure 4.14	Representative recordings obtained from VIC in fibroblastic and osteogenic media.	92
Figure 4.15	A representative trace of a potassium-selective stretch-activated channel before and after excision.	92
Figure 4.16	Representative single-channel events from VICs cultured in the fibroblastic vs osteogenic media.	93
Figure 4.17	Images in transmitted light of aortic valve paraffin sections stained for SACs.	94
Figure 5.1	Protein expression of SACs in VICs isolated from non-calcified and calcified valve specimens.	106
Figure 5.2	Paraffin section stain of calcified and non-calcified valve tissues	108
Figure 5.3	Protein expression of SACs in calcified and non-calcified valve tissues.	110
Figure 5.4	Relative gene expression of SACs in calcified and non-calcified valve tissues.	111
Figure 6.1	Computational fluid dynamic analysis showing radial shear stress (dyne/cm ²) in the edge and low oscillatory in the centre	118
Figure 6.2	Diagram of Feret angle calculation	119
Figure 6.3	The effects of different concentrations of streptomycin on the alignment of VECs from the aortic side.	122
Figure 6.4	The effects of different concentrations of streptomycin on the alignment of VECs from the ventricular side.	123
Figure 6.5	The effects of different SAC inhibitors on the alignment of VECs from the aortic side.	125
Figure 6.6	The effects of different SAC inhibitors on the alignment of VECs from the ventricular side.	126
Figure 6.7	The effects of different concentrations of TRPC6/3 channel inhibitors on alignment of VECs from the ventricular side.	128
Figure 7-1	Scratch Assay	139

Figure 7.2	The effects of stretch on the gene expression of collagen I, collagen III, elastin, and HSP47 in VICs.	142
Figure 7.3	The effects of specific channels blockers on collagen I and collagen III gene expression under stretch conditions.	145
Figure 7.4	Migration percentages of VICs under active and blocked SAC conditions.	146
Figure 7.5	The migration percentage of VICs under the stimulation and inhibition of TRPV4 and TRPC3/6.	147
Figure 7.6	The effects of TRPC6/3 channel activation on VIC migration.	148
Figure 7.7	The effect of TRPC6/3 channel inhibition on VICs migration.	149
Figure 7.8	The effects of TRPV4 channel activation on VIC migration.	150
Figure 7.9	The effect of TRPV4 channel inhibition on VICs migration.	151
Figure 7.10	The effects of different channel activator in VIC proliferation in 2% FCS medium.	153
Figure 7.11	The effects of different channel activator in VIC proliferation in 10% FCS medium.	155

List of Tables

Table 1.1	Summary of some effects of shear stress on valve cells function and phenotype	7
Table 1.2	Summary of some effects of pressure on valve cells function and phenotype	8
Table 1.3	Summary of some effects of shear stretch on valve cells function and phenotype	9
Table 2.1	List of antibodies	36
Table 2.2	list of RT-PCR primers	38
Table 3.1	Phenotypic and functional classification of aortic valve interstitial cells	42
Table 6.1	Different SACs channel inhibitors	120
Table 7.1	Different SACs channel activators	138
Table 7.2	Different SACs channel inhibitors	139

Chapter 1

General introduction

1.1 Heart Valves

Heart valves maintain the unidirectional flow of blood through the heart throughout the cardiac cycle and maintain coronary blood flow. Four valves are present in a normal human heart, which are: two atrioventricular valves and two semilunar valves:

1. Atrioventricular valves separate the atria from the ventricles and have large asymmetric leaflets that are hinged to a ring-shaped structure and tethered to the papillary muscles of the ventricles by chordae tendineae. The atrioventricular valves are the mitral valve and tricuspid valve. The mitral valve regulates flow from the left atrium to the left ventricle and prevents flow back of blood into the atrium when the left ventricle contracts. The tricuspid valve performs a similar function on the right side of the heart, controlling the flow of blood from the right atrium into the right ventricle. Accordingly, the tricuspid valve prevents blood from coming flowing back into the right atrium when the right ventricle contracts.
2. The semilunar valves separate the ventricles from the great arteries. The pulmonary valve controls the flow of oxygen-depleted blood from the right ventricle, through the pulmonary artery to the lungs. Aortic valve (AV) controls the flow of oxygen-rich blood from the left ventricle through aorta and onwards to the rest of the body (Weinhaus and Roberts, 2005). Semilunar valves are composed of three symmetric, semilunar-shaped cusps attached to a crown-shaped annular ring. The cusps of the AV are termed the left coronary, right coronary, and non-coronary cusps, according to the location of the coronary arteries, which originate from two of the three sinus bulges above the annulus and behind each cusp. The end-to-end cusps are adjoined (the commissures) at the highest point of the attachment. The boundary between the valve and the ascending aorta is identified as a small ridge called the sinotubular junction. The annulus bulges at the basal point of the cusps attachment, forming three “pockets”

called the sinuses of Valsalva. The left coronary and right coronary cusps have ostia that give rise to the left and right coronary arteries. The area of the fibrosa sheet that extends from fibrous arches supporting the cusps to the wall of the right atrium is called the subaortic curtain, and it blends with the fibrous core of the anterior mitral leaflet. The left and right fibrous trigones are an extensive thickening of the most inferior part of the fibrous skeleton underlying the left coronary and right coronary AV cusps, respectively. The left and right fibrous trigones connect the part of the fibrous skeleton to the mitral valve. A membranous septum separates the subaortic curtain from the lower part of the right atrium and upper part of the right ventricle. The muscular septum is thick and muscular, separating the left ventricle from the right ventricle (**Figure 1.1**) (Weinhaus and Roberts, 2005).

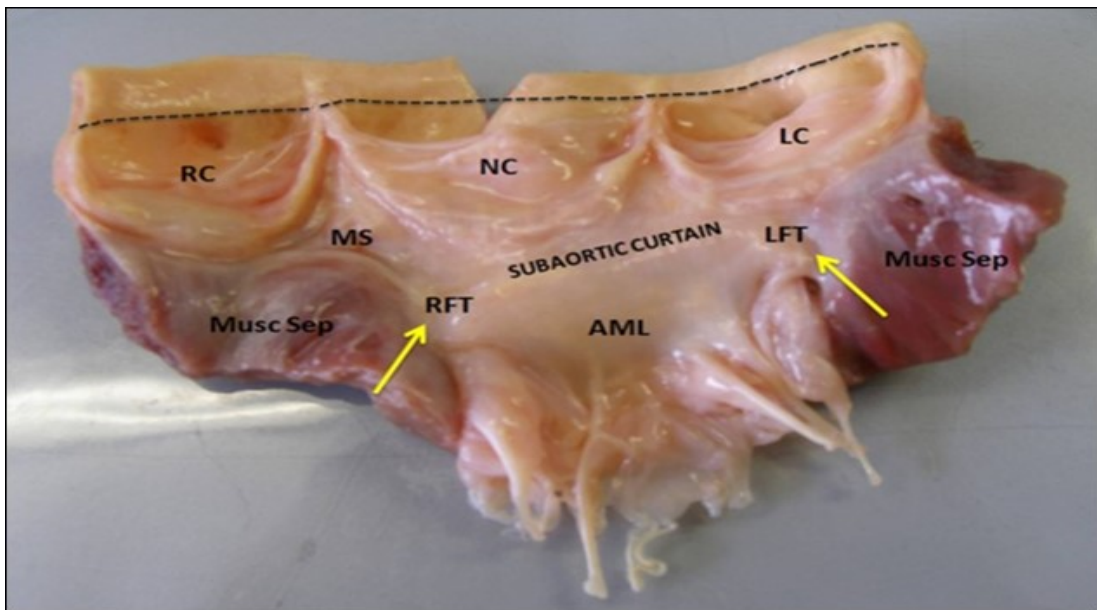


Figure 1.1: Photograph of an open aortic root showing its structural components (annulus, cusps, sinuses of Valsalva, and sinotubular junction [dashed line]) as well as their relationship with the left ventricular outflow tract and mitral valve. AML, anterior mitral leaflet; LC, left coronary cusp; LFT, left fibrous trigone; MS, membranous septum; Musc Sep, muscular septum; NC, non-coronary cusp; RC, right coronary cusp; RFT, right fibrous trigone (adapted from (Chester et al., 2014)).

The focus of this thesis is the study of the AV, further description of valve structure, mechanobiology and function will therefore focus on AV.

1.2 Mechanical Environment of Aortic Valve

AV is a sophisticated structure that performs complex functions to preserve the unidirectional flow of blood out of the left ventricle and controls coronary blood flow, which leads to the maintenance of myocardial function. AV opens and closes due to the changes in transvalvular pressure and myocardial contraction/relaxation. AV geometry is precise and provides a suitable distribution of the stress, leading to efficient valve function without complications over a human lifetime (Rajamannan, 2011). AV cusps are exposed to a unique profile of haemodynamic forces, including shear stress from the flow of the blood and the cyclical pressure of the blood. Notably, the different sides of the cusps are exposed to a different pattern of shear stress, as the ventricular side is exposed to high velocity and high shear stress, whereas the aortic side is exposed to interrupted low-velocity flow and low shear stress. The effects of the diastolic pressure on the valve as it closes cause the cells to be stretched in both the radial and circumferential directions. These mechanical forces act as a stimulus to initiate functional responses from valve cells (Balachandran et al., 2010)(Figure 1.2).

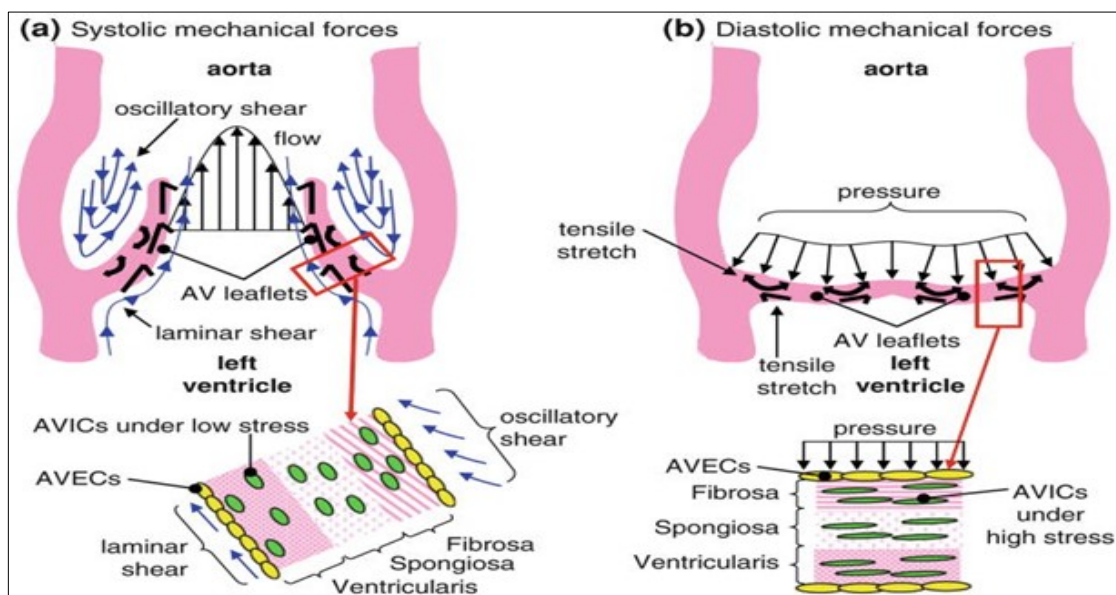


Figure 1.2: Diagram of different mechanical stimuli experienced by the Aortic valve during a cardiac cycle: (a) mechanical forces during systole and (b) mechanical forces during diastole (adapted from (Balachandran et al., 2010)).

1.2.1 Shear Stress

Physiologically, shear stress is generated by friction between the AV leaflet surface and blood flow; however, this depends on blood flow conditions and the cyclical dynamic motion of the valve leaflets. The VECs are directly affected by shear stress and subsequently, transmit signals to the VICs and the underlying matrix by integrins. The VECs respond differently to shear stress depending on shear stress patterns and changes to shear stress during valve development and pathological conditions. Therefore, a precise estimation of how shear stress affects the AV under physiological and pathological conditions is essential for valve mechanobiology and pathology studies (Arjunon et al., 2013). Several techniques have been used to estimate and magnitude of shear stress on the AV; for example using laser Doppler velocimetry and computational modelling (Jermihov et al., 2011). As a result, shear stress on the aortic surface of AV is estimated by two-component laser Doppler velocimetry to be approximately 20 dynes/cm² during diastole with a disrupted pattern of flow (Yap et al., 2012a), while the ventricular side is more laminar type of flow with a magnitude of approximately 80 dynes/cm² during systole (Yap et al., 2012e).

1.2.2 Pressure

In a single cardiac cycle, the pressure on the AV cusps changes continually in a cyclic manner. During systole, when the valve is open only a few mmHg of pressure is applied on the AV as a result of the negligible resistance to blood flow (Butcher et al., 2004). During diastole, the AV closes under the diastolic blood pressure of approximately 80mmHg of distending pressure that acts on the aortic side of the AV and is transmitted to the ECM, and sensed by the VIC (Arjunon et al., 2013).

1.2.2.1. Strain

The mechanical environment of the AV is a highly non-linear, stress-strain complex relation. The pressures applied during each cardiac cycle to the valve results in tissue strain. This applied strain changes the internal structure of the AV cusps due to elongation and bending of the matrix and the cells contained within. The AV leaflet is formed with integrated curvature to make it adaptable to stretching so that it can maintain long-term functionality and viability of the valve cusp (Arjunon et al., 2013). Different studies have extensively characterized the flexural mechanical properties of AV leaflets and estimated the maximum extension (~3 mm), stiffness (~6 N/mm), and load (~13 N) (Ragaert et al., 2012).

The stretch in AV cusps is anisotropic due to the circumferential alignment of collagen, which increases tensile strength. The AV cusps lose their ability to stretch and extend as they age because, over time, collagen fibrillogenesis increases the diameter of the constituent fibrils, requiring more force to extend the collagen fibrils (Arjunon et al., 2013). The amount of stretch experienced by AV leaflet has been reported *in vivo* as being approximately 10% in a circumferential direction and 40% in the radial direction (Arjunon et al., 2013, Brewer et al., 1977, Missirlis and Chong, 1978). These studies were performed on different species such as porcine and dog, yet the results were similar. Studies have also measured stretch under different hypertensive pressure conditions in an *ex vivo* flow loop system by using stereophotogrammetry to track markers on the leaflet surface. The diastolic strain of the leaflets followed the transvalvular pressure gradient and the systolic strain followed the flow curve (Arjunon et al., 2013).

1.3 Effect of Mechanical Forces on Cell Function

A number of studies have shown the role of different mechanical forces on cell function, including effects on gene expression, cell morphology and phenotype, ECM secretion and ultimately valve function (Arjunon et al., 2013). This is discussed in more detail within this section, in addition to the effect of all mechanical forces on valve function.

1.3.1 Shear Stress

It is presently well known that different shear stress patterns engender different responses from VECs; For example, disturbed flow affects cell proliferation, morphology, and gene expression, whereas laminar flow does not affect cell proliferation, morphology, and gene expression, (Chandra et al., 2012, Chiu and Chien, 2011). The VECs also respond to shear stress in a site-specific manner with reports of different responses in ECM production and cytokine release from VECs cultured from either side of the valve (Arjunon et al., 2013). Several studies have characterized the effect of shear stress on VECs using Cone and Plate bioreactors to expose VECs to shear stress patterns that mimic the *in vivo* environment (Sucosky et al., 2008). The main focus of these studies was to define the regulatory roles of shear stress on alignment, ECM composition, remodelling, proliferation, and phenotypic changes. Table (1.1) summarizes the critical effects of shear stress on endothelial cells.

Table 1.1: Summary of some effects of shear stress on valve cells function and phenotype.

Markers	Effects of Shear Stress	References
ECM	Collagen ↑, sGAG ↓, MMP-2, 9 ↑, TIMP-2 ↑, cathepsin-L ↓ on ventricularis	(Platt et al., 2006, Xing, 2005)
Inflammation	ICAM-1 and VCAM-1 ↑ on fibrosa	(Hoehn et al., 2010, Sucosky et al., 2009, Sun et al., 2012)
Osteogenesis	BMP-2, 4 ↑, TGF-β ↑ on fibrosa, higher in Bicups aortic valves	(Hoehn et al., 2010, Sucosky et al., 2009, Sun et al., 2012)

1.3.2 Pressure

The role of pressure in valve function has been studied *in vivo* and *in vitro*. Many studies have focused on the regulation of gene expression in response to pressure, showing down-regulation of α -SMA and osteopontin and up-regulation of VCAM-1 (Arjunon et al., 2013). A summary of the effects observed are summarized in table (1.2) (Weston and Yoganathan, 2001). Approximately 50% of the genes in VICs are affected by hypertensive conditions for example, α -SMA, Calponin and Caldesmon. VCAM-1, which are involved in inflammation are all up-regulated in response to hypertensive pressures, suggesting that pressure plays a contributory role in inflammatory and remodelling responses in VICs. Although all studies have separately investigated the effect of pressure in isolated porcine AV endothelial cells cultured on BioFlexTM culture plates, it is important to note that pressure generates greater stretch on the leaflets through tensile and bending forces. Therefore, future studies should consider a combination of pressure and stretch (Arjunon et al., 2012, Thayer et al., 2011).

Table 1-2: Summary of some effects of pressure on valve cells function and phenotype.

Markers	Effects of pressure	References
ECM	Collagen \uparrow , sGAG \uparrow , MMP-2, 9 \downarrow , MMP-1, 3 \uparrow , osteopontin	(Warnock et al., 2006, Warnock et al., 2011, Xing et al., 2004c)
Inflammation	VCAM-1 \uparrow , pentraxin-3 \uparrow , TNF- α \uparrow , IL-6 \uparrow	(Warnock et al., 2006, Warnock et al., 2011)
Phenotype	SMA \downarrow	(Xing et al., 2004a)

1.3.2.1. Stretch

Application of stretch on AV leaflets in *ex vivo* and *in vitro* studies has been performed on both intact valve leaflets and isolated cells grown on deformable membranes or in scaffold or gels. These studies have investigated remodelling, inflammatory and calcification processes. Importantly, AV leaflets respond to different magnitudes of stretch in a biphasic

manner in terms of the amount stretch and its direction. Expression of BMP-2 and BMP-4 in porcine AV leaflets was significantly greater in response to 15% stretch than 10% (Frishman et al., 1995). The remodelling potential, quantified by metalloproteinase (MMP) activity and tissue inhibitor of metalloproteinase (TIMP) ratio, it was greater after 15% stretch than after 10% stretch or in fresh un-stretched tissue. Also, the collagen content of AV leaflet was greater after stretch at a pathological level compared to static leaflets, whereas GAGs content was less in the stretch tissue than the static leaflets (Balachandran et al., 2009). These findings suggest that AV leaflets respond to stretch by alteration in synthesis or degradation of ECM proteins. Finally, a summary of some studies of the effect of different mechanical forces on valve cells and their finding is in Table (1.3).

Table 1.3: Summary of some effects of shear stretch on valve cells function and phenotype.

Markers	Effects of stretch	References
ECM	Preserved elastin, MMP-1, 2, 9 ↑, TIMP-1 ↓, sGAG ↓, collagen ↑, cathepsin-L ↓, cathepsin	(Balachandran et al., 2006, Balachandran et al., 2010)
Inflammation	ICAM-1 and VCAM-1 ↑	(Smith et al., 2010)
Phenotype	α-SMA ↑	(Balachandran et al., 2009, Balachandran et al., 2010)
Osteogenesis	BMP-2, 4 ↑, TGF-β ↑	(Balachandran et al., 2010, Clark-Greuel et al., 2007, Metzler et al., 2008)

1.4 Mechanotransduction in Heart Valve Cells

Mechanotransduction, can be defined as converting mechanical forces into intracellular signals and molecular changes that affect cell behaviour. Mechanotransduction regulates different cellular functions, such as cell morphology, alignment, secretory responses, and gene or protein expression.

Consequently, when mechanotransduction pathways are altered, this can contribute to diseases processes. For example, disturbance in fluid shear stress contributes to atherosclerosis and dysfunctional vascular remodelling (Jaalouk and Lammerding, 2009). Studies continue to attempt to identify and better describe the nature of mechanotransduction elements which include studying the molecular identity of mechanosensors, signalling molecules, and the resultant biochemical cascade that cause observable changes in cell behaviour (Tan and Coroneo, 2009). The following section summarizes the mechanotransduction elements and their relationship to heart valve cells.

1.4.1 Mechanotransduction Elements

Mechanotransduction consists of three phases force recognition, force transduction and a corresponding response. Force transduction is performed by different elements including, but not limited to, membrane-associated proteins. Mechanotransduction elements can be divided into two main categories described in greater detail below (Muhammed et al., 2017).

1.4.1.1. ECM & Cytoskeleton Elements

The ECM's involvement in mechanotransduction has been determined in several studies, providing considerable insight into its role in this process. Mechanical forces are sensed by cells via linkages between the cells and the ECM. These linkages are formed by integrins. Integrins are transmembrane proteins in the plasma membrane and connect the cytoskeletal components (such as actin) to the ECM (Ingber et al., 2014). These forces are transmitted across the matrix-integrin interactions which initiate intracellular signalling by unfolding protein domains and modulating protein binding affinities. Applying forces locally onto cell surface integrins (but not other transmembrane receptors) leads to modification of the nuclear and nucleolar shape inside the cell (Ingber et al., 2014). The integrin-ligand bond displays "catch bond" action, altering to a long-lived state in response

to applied mechanical force (Humphrey et al., 2014). The integrins act as part of a highly complex mechanism with contributions from other downstream signalling such as protein tyrosine phosphatase alpha (RPTP α) (Humphrey et al., 2014). Studies have found that inhibiting some integrins inhibits mechanotransduction (Tan and Coroneo, 2009). For example, the integrin binding peptide GRGDTP blocked the mitogenic response to strain in neonatal rat vascular smooth muscle cells (Wilson et al., 1995). In addition, cellular adhesion molecules (integrin $\alpha 5\beta 1$) may contribute to responding to mechanical forces by strengthening the connections with new cytoskeletal proteins to resist the applied force (Schwartz, 2010). Cytoskeletal molecules, such as actin, and cadherins and selectins, are proposed molecular mediators of mechanotransduction, which are highly sensitive to the mechanical environment (Tan and Coroneo, 2009). ECM-integrin interactions transduce mechanical forces via an integrated mechanism involving focal adhesions kinases (Li et al., 2016). Cellular adhesion molecules (such as vascular endothelial cadherin (VE-cadherin) and platelet endothelial cell adhesion molecule (PECAM)) also modulate different functions in response to mechanical forces. For example, PECAM-1 and VE-cadherin convert shear forces that result from laminar blood flow into endothelial cell alignment with the direction of the flow (Tzima et al., 2005) .

The ECM responds to mechanical forces by remodelling, which activates the expression of collagen, fibronectin, and metalloproteinase genes. Collagen, and fibronectin fibrils are assembled and aligned according to the direction of applied force. Many studies have found that cells arrange their ECM in a force-dependent manner. Two possible explanations exist for this. First, exposing cells to mechanical forces regulates gene expression for both ECM proteins and ECM-remodelling enzymes. Second, mechanical forces directly affect the ECM polymerization or organization; the forces extend through the ECM to organize the cells' positions within the ECM and maintain cellular functions.

In addition, transforming growth factor beta (TGF- β), a cytokine that promotes fibroblasts to secrete ECM proteins, is upregulated by a mechanical strain. Although the mechanism for this is unclear, mechanical strain modulates ECM production under both physiological and pathological conditions in the tissues (Ingber et al., 2014).

Matrix remodelling can lead to changes in matrix stiffness. The compliance of the matrix regulates different functions including cell differentiation. For example, mesenchymal stem cells tend to differentiate towards osteogenic lineages on stiffer matrices and to neurogenic lineages on a softer matrix (Schwartz, 2010).

- **Molecular Regulators of Mechanotransduction**

It is apparent that multiple mechanotransducers coexist in the same cell and are connected through shared components and interact with each other and the environment. Any changes to the mechanical stimulus can lead to activation of different signalling pathways and pathological responses of the cells (Pagnozzi and Butcher, 2017). Several molecules have been identified as mechanotransducers in AV cells. A study conducted by Holliday *et al.* found that some shear-dependent mRNAs and side-specific miRNAs act as potential master mechano-regulators in human AVECs. These include genes and transcription factors such as Ctsk, Hdac1, Id1, Dhh, Thbs1, NFkB, Atf3, Egr1, and FosB. All of these are related to proliferation, apoptosis, migration, and disease-related changes in AV cells (Holliday et al., 2011). Moreover, Klf2 and eNOS proteins have been identified as mechanosensitive genes in ECs (Holliday et al., 2011). Additionally, several integrins, including α 2 and β 1 subunits and α 5 β 1, have been recognized as mechanotransducers that are strongly expressed in VICs (Latif et al., 2005). These integrins are important to the binding that occurs between VICs and collagen I, as well as to mediate the VIC contraction, migration, ECM synthesis, and myofibroblastic and osteogenic differentiation (Pagnozzi and Butcher, 2017). Blocking the 67kDa laminin receptor, which is highly

affinitive to laminin and elastin, causes the formation of calcific nodules (Gu and Masters, 2010), which suggests an anticalcific effect of integrin binding. Another study has shown that disruption VIC binding, via the $\alpha 5\beta 1$ integrin, dramatically stimulates calcification in AVICs (Latif et al., 2005). The RhoA protein (family of GTPases) is a mechanotransducer that regulates cell migration, differentiation, proliferation, and mediates endothelial-mesenchymal transition during valvulogenesis (Pagnozzi and Butcher, 2017).

In summary, mechanical forces are initially sensed by different cytoskeletal molecules and the ECM and subsequently propagate throughout the cell to modulate different functions. Cytoskeletal molecules respond to mechanical forces in a complex set of interactions, and their roles in mechanotransduction have often been widely studied. The following section discusses elements that are more closely related to this study.

1.4.1.2. Mechanosensitive Channels

Mechanosensitive channels (MSCs) are cell receptors that open in response to a mechanical stimulus and allow for the movement of ions across the membrane. They are considered to be universal sensors in the transduction of mechanical forces in living cells. Mechanosensitive channels are present in many cell membranes, as they have involved in the physiology of many different types of cells mechanotransduction. Mechanotransduction through MSCs control touch, hearing, osmotic gradients, cell swelling, and several other functions. Abnormalities in MSCs can cause diseases, such as muscular degeneration, cardiac arrhythmias and hypertension (Martinac, 2004). In the heart, a passive stretch of the atrial chamber is controlled by inward cationic channels; abnormalities can result in mechanical dysfunction and atrial fibrillation. Notably, blocking of the stretch-activated cation non-selective channels (SA-CAT) can inhibit or reduce this action (Hu and Sachs, 1997).

Recent work has categorized MSCs into different groups depending on their stimuli. These are: volume-activated ion channels, voltage-activated ion channels, and stretch-activated ion channels (SAC). Volume-activated ion channels are activated in response to increases in cell diameter without effects on length, due to cell swelling. Volume-activated ion channels are unlikely to participate in the functioning of the heart, because the contraction and relaxation cycle is not related to changes in cell volume (Reed et al., 2014). Stretch-activated ion channels (SAC) are activated in response to stretch, shear stress and pressure. They are expressed in a range of tissues, with the greatest abundance in the brain and heart. The next section focuses in more detail on stretch-activated ion channels (SAC) and the possible roles of SACs in the heart (Wang, 2017).

SACs have the potential to participate in the mechanotransduction processes of heart valve cells due to the dynamic environment in which valve cells reside. Despite the fact that many studies have analysed the importance of SAC in the myocardium (Reed et al., 2014), little is known regarding their presence and role in valve cell function.

1.5 Stretch-Activated Channels

It has been strongly suggested that stretch-activated ion channels (SACs) are involved in these responses to stretch and modulate membrane currents, and the major stretch-induced changes are mediated by activation of SACs (Youm et al., 2005). SACs are defined as cell receptors in the plasma membrane and respond to membrane stress by changing their open probability to ion transients and converting a mechanical signal into an electrochemical flux, leading to different inter -and intra-cellular functions being regulated (**Figure 1.3**) (Hu and Sachs, 1997, Sackin, 1995). The first study to describe the SACs was in chick skeletal muscles (Guharay and Sachs, 1984). More recently, SACs have been detected in many cells types in different organisms, including , bacteria, fungi, plants, different animal species and humans (Hu and Sachs, 1997).

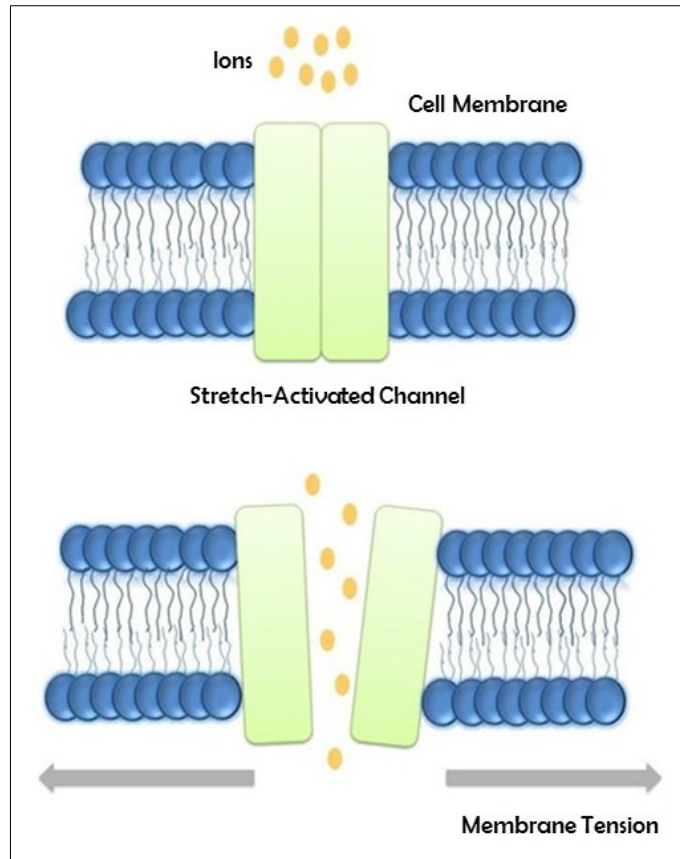


Figure 1.3: Gating Mechanism of SACs. Membrane tension triggers conformational changes which open the channel and allow for ion transients. Figure adapted from (Lumpkin and Caterina, 2007).

Although profound differences appear among SACs in their kinetics and mechanisms, there are some common properties in all SACs classes. First, all SACs respond to mechanical force and increase open probability without changes in single-channel conductance or ion selectivity.

1.5.1 Stretch-Activated Channels Classification

Stretch-activated channels can be either cation nonselective (SACNS) or potassium-selective (SACK), and they have ionic selectivity, voltage dependence, and stretch-dependence properties that mediate electrical activity changes. In addition, the channels are classified into the following groups and subgroups (Prevarskaya et al., 2010).

1.5.1.1. Cation Non-Selective Channels

Cation-non selective stretch-activated channels (SACNS) comprised the original family SACs and were discovered in chick skeletal muscle (Guharay and Sachs, 1984) and embryonic *Xenopus* muscle (Brehm et al., 1984). These channels are selectively permeable to cations over anions and are selective for Ca and Na with a preference for Ca over Na. There have been several investigations into the importance of SACNS channels in cellular function, and a great permeability of Ca may allow for Ca to act as a second messenger. For example, in the choroid plexus, SACNS channels open in response to hypotonic shock and significantly increase cytosolic Ca, activating Ca-dependent channels (Christensen, 1987). SACNS channels also regulate chloride currents which are necessary for hypotonic volume regulation (Odell et al., 1981). There are two main groups of SACNS channels: TRP channels and the recently discovered Piezo channels (Prevarskaya et al., 2010). The structures, functions, classification of these two main groups are discussed in more detail in the following section.

1.5.1.1.1. TRP channels

Transient receptor potential (TRP) channels are non-selective ion channels that serve as mechanotransducer for a wide range of mechanical forces (Benemei et al., 2015). TRP channels were discovered in a mutant strain of *Drosophila* where the lack of the TRP gene caused impairment in the fly's visual system (Zheng, 2013). TRP channels comprise four pore-forming TRP protein subunits that are gathered as homo-tetramers and hetero-tetramers. TRP channels are regulated and formed by intracellular C-terminus and N-terminus, and TRP channels subfamilies are differentiated by either ankyrin repeats, different domains, or coiled-coil regions. TRP channels are broadly expressed in many tissues, and some of these channels are universally expressed, while others are related to specific conditions. At a cellular level, TRP channels are found in plasma and intracellular

membranes. Nonetheless, knowing the distribution and expression patterns of TRP channels helps to explain their functions and their molecular mechanisms.

TRP channels activation alters the membrane potential and transports the ions across the cell membrane, activating intercellular and intracellular signalling. Also, TRP channels show exquisite sensitivity to different types of stimuli (Zheng, 2013). For example, TRP channels can be activated by strain, shear stress, pressure, voltage, oxidative stress, chemical activation, intracellular Ca^{2+} -store depletion in some channels, lipids, and inflammation products (Smani et al., 2015). The regulation of Ca^{2+} channels in cells is one of the most vital mechanisms for governing short-term cell functions such as contraction and governing long-term functions such as proliferation (Balachandran et al., 2006). Although the physiological role of TRPs remains unclear, active research in the TRP channel field has generated significant information about the activation of molecular pathways, functional roles, and inhibitors of the TRP channels (Zheng, 2013). Understanding the activation mechanisms of TRP channels will help to realise the complex roles that TRP channels have in physiological and pathophysiological conditions

TRP channels have been classified into six subfamilies according to their sequence homology: TRPC (canonical, seven members), TRPV (vanilloid, six members), TRPM (melastatin, eight members), TRPA (ankyrin, one member), TRPP (polycystin, three members) and TRPML (mucolipin, three members). Every subfamily shares some common features and differences in their expression patterns, functions, and molecular mechanisms (Benemei et al., 2015). TRPM4, TRPV4, and TRPC6 are present in some cardiac cells and interact to regulate the cardiac pacemaker, the conduction system, cardiac fibrosis, cardiomyopathies, cardiac remodelling, and ventricular contractility in during cardiogenesis (Nishida et al., 2015). However, it is unknown if these channels are present in heart valves, or if they are involved in mechanotransduction mechanisms.

The following section presents three TRP channels that are activated by stretching and are related to this research, and the section shows their roles and importance in the cardiovascular system and its diseases.

- **TRPC6**

Among the TRP channels, TRPC channels are one of the most extensively characterised channels. TRPC channels are divided according to their amino acid sequences into four subgroups (TRPC1; TRPC4 and TRPC5; TRPC3, TRPC6, and TRPC7; and TRPC2). TRPCs channels are broadly distributed in human tissue, and their roles in regulating several functions have been demonstrated. A growing body of evidence has suggested that TRPCs channels are involved in cardiac pathology and inhibiting these channels improves cardiac remodelling in vivo and in vitro (Nishida et al., 2015). TRPC6 is a non-selective cation channel and is directly activated by stretch, intracellular lipid mediators such as Diacylglycerol and other activators. Similar to all TRPC channels, TRPC6 has six transmembrane helices formed tetrameric transmembrane pore (Zheng, 2013). TRPC6 channel is widely distributed in human tissue and has important roles in several physiological or pathological processes such as kidney function and wound healing. Interestingly, TRPC6 represents an important element in therapeutic targets for drug development in cardiovascular diseases (Nishida et al., 2015).

- **TRPV4**

Transient receptor potential vanilloid channels (TRPV) are a sub-family of the TRP channel that is relatively more permeable to Ca²⁺ ions. TRPV channels are divided into six channels, TRPV1-TRPV6, that are similar in architecture structure to some interesting variations in their structure in their domain arrangements and these differences highlight structural diversity between relatively correlated tetrameric cation channels and

potentially different gating mechanisms (Deng et al., 2018). TRPV channels respond to a variable range of stimuli, for example, chemical activators, mechanical stimuli, low pH, temperature and hypotonicity. TRPV channels are widely distributed in the human body such as the colon, lungs, urinary bladder, vascular smooth muscle, vascular endothelial cells, aorta, and coronary blood vessels (Balachandran et al., 2006). Within the TRPV subfamily, TRPV4 has been one of the most intensively investigated because of essential physiological and pathological roles of TRPV4.

TRPV4 is characterised as an outwardly rectifying current-voltage, and is 5–10 times more permeable for Ca^{2+} than for Na^{+} . TRPV4 is a single-channel conductance of about 60 pS at negative potentials and 90–100 pS at positive potentials (Nilius et al., 2004b). Different studies have shown the involvement of TRPV4 channel in a range of cells function in different cell types, for example, in the regulation of vascular tone and brain signalling, and the control centre of thermogenesis in the preoptic and anterior hypothalamus (Nilius et al., 2004b). The TRPV4 role in vasodilatation has been documented by different studies, and the presence of aberrant TRPV4 function has been detected in all diseases associated with endothelial dysfunction (Darby et al., 2018, Hartmannsgruber et al., 2007, Mendoza et al., 2009). TRPV4 responds to different stimuli involved in the endothelium such as hypo-osmolarity, shear stress, and pressure. TRPV4 is a mechanosensitive channel for Ca^{2+} entry in vascular endothelial cells and is involved in the shear stress-induced Ca^{2+} entry (Balachandran et al., 2006). In 2018, Darby et al. described the role of TRPV4 channel in the vasodilatation mediated by endothelial cells. TRPV4-dependent vasodilatation is also related to endothelium-dependent hyperpolarisation and causes the opening of calcium-dependent potassium channels that hyperpolarise the cell membrane and leads to relaxation, independently from the release of nitric oxide or cyclooxygenase products. (Darby et al., 2018). This role has also has been documented in human coronary

arterioles (Bubolz et al., 2012), mouse mesenteric arteries (Mendoza et al., 2009) and carotid arteries (Hartmannsgruber et al., 2007). In addition, the activation of TRPV4 targeted an endothelium-dependent contractile response in the mesenteric arteries (Mendoza et al., 2009) and endothelium-independent relaxation in pulmonary vessels (Sukumaran et al., 2013). In conclusion, TRPV4 channel is highly expressed in endothelial cells influences several critical functions, including regulation alignment with blood flow, vasomotor activity, production of nitric oxide, vasoconstriction and vasodilatation of peripheral blood vessels (Nilius et al., 2004b). In this respect, TRPV4 might be a new target for studying valve function and diseases.

- **TRPM4**

The melastatin-related transient receptor potential (TRPM) channels were named based on the first discovered member, melastatin, which is a gene that was identified in the comparison between benign and malignant melanocytes. Similar to TRP channels, TRPMs channels have N- and C-terminals in the cytoplasm and six putative transmembranes (TM) domains with the pore-forming region between them, while N-terminal is longer (by 300–400 amino acids) than the same regions in other TRP channels. TRPM channels are the most novel, broadly expressed, and are functionally diverse TRP channels. The TRPM channels share some features and cellular functions such as the combination of pore-forming structures with enzymatic domains that are permeable to some cations and are activated by voltage, stretch, temperature and other activators. However, many studies have suggested the vital roles of TRPMs channels in tumourigenesis, vascular angiogenesis, cell proliferation, and cell death and cell differentiation. Regarding the ion selectivity, TRPM channels were classified into impermeable to Ca^{2+} (TRPM4/5) and semi-permeable to Ca^{2+} (TRPM1/2/3/6/7/8) channels. The next section focuses on TRPM4, which displays mechanosensitive properties expressed in the heart and its role in

myogenic constriction has been documented in several studies (Brayden et al., 2008, Earley et al., 2007, Earley et al., 2004).

TRPM4 is a monovalent cation-selective ion channel that mediates plasma membrane depolarisation. The TRPM4 channel makes calcium-activated sodium channels impermeable for calcium (Harteneck, 2005) and is composed of putative binding sites that are in the N terminus and bind to calmodulin (CaM) and ATP and protein kinase C (PKC) phosphorylation sites. In the intracellular side, C-terminal sites bind to either CaM or PKC phosphorylation links to the second and third transmembrane domain, and this link regulates the Ca²⁺-sensitivity of the TRPM4 channel. The TRPM4 channel is expressed ubiquitously, and its expression in human kidney, heart pancreatic beta-cells, and many other tissues have been detected (Abriel et al., 2012). The evidence is being accumulated for the important physiological and pathological roles for TRPM4 channels in many tissues, such as the regulation of the resting membrane potential in vascular smooth muscle cells and myocyte contraction (Abriel et al., 2012). TRPM4 physiologically modulates the pacemaker cells automaticity and has been recorded in pacemaker cells of the sino-atrial node in mice. In 2006, Guinamard et al. suggested a modulatory role of TRPM4 in current and arrhythmogenic remodelling after a significant upregulation in TRPM4 at the mRNA level in hypertrophied ventricular cardiomyocytes from spontaneously hypertensive rats (SHR) compared to normotensive WKY rats (Guinamard et al., 2006). Furthermore, TRPM4 channel exists in atrial cells and Purkinje fibres but not in the Bundle of His and ventricular cardiomyocytes. This suggests the regulatory role of TRPM4 in the cardiac conduction velocity system via a mechanism of the supernormal conduction where supernormal conduction depends on extracellular K⁺ concentration.

TRPM4 is activated by stretch, but the way the channel is activated is still not fully understood, although it has been related to the release of Ca²⁺. Also, the TRPM4 channel

is activated by intracellular calcium or by pharmacological activators (Harteneck, 2005). The sensitivity to stretch of the TRPM4 channel make it a potential candidate for mediation of mechanotransduction mechanisms in the heart valve cells (Nilius et al., 2004a).

1.5.1.1.2. Piezo Channels

Piezo channels were recently discovered in human and plants but not in bacteria and are one of the last major SACs to be identified. Two families of Piezo channels have recently been characterised in many mechanosensitive tissues: Piezo1 (over 2,500 amino acids in size) and Piezo2 (2,800 amino acids).

Piezo1, also known as Fam38a, assembles as a 900 kDa homotrimeric complex to form SAC with a central pore and a propeller-like structure around it. It is a membrane channel that detects any changes in membrane tension without the presence of cellular components. Activation of Piezo1 channels produces cationic non-selective currents, membrane depolarisation, and Ca²⁺ entry into the cell to intracellular Ca²⁺ signalling pathways. The channels are also permeable of monovalent cations, (Na⁺ and K⁺), and to divalent cations, (Ca²⁺ and Mg²⁺) (Parpaite and Coste, 2017). The Piezo1 channels are detected by quantitative RT-PCR in many tissues such as the kidney, blood vessel, bladder, and lung. The primary biological function of Piezo1 is likely to be as sensors and transducers of mechanical force. Since the discovery of Piezo1, it rapidly showed physiological relevance to Piezo1. Recent studies have shown that Piezo1 channels regulate different functions in endothelial cells for vascular remodelling and developing blood vessels. Also, a Piezo1 knockout in vivo causes embryo lethality at mid-gestation due to vascular defects, while in vitro Piezo1 knockout of piezo1 channel results in the distribution of cellular alignment in response to laminar shear stress (Li et al., 2014). It remains unknown whether Piezo1 channels are involved in only vasculature development or if they are also involved in adult physiology. Regarding diseases, Piezo1 mutations have been linked to genetic diseases,

but none of them has been electrophysiologically characterised (Parpaite and Coste, 2017). Also, the Piezo1 channels are activated by many mechanical stimuli such as stretch and shear stress. However, there is a lack of pharmacological regulation of Piezo1 channels; only a synthetic small molecule called Yoda1 can activate Piezo1 channels (Parpaite and Coste, 2017, Volkers et al., 2015). The inhibition of Piezo1 channels could be achieved by some non-specific blockers such as ruthenium red, gadolinium, and streptomycin. Recently, the peptide GsMTx4 (*Grammostola spatulata* mechanotoxin 4) was discovered as a widely used inhibitor of Piezo1 channels (Smith et al., 2010).

The knowledge of Piezo1 channels is growing rapidly, but major answers remain unanswered. How is the channel response to stretch? How is channel gating occurring? What are other important roles? Follow-up studies are required to offer a better understanding regarding the mechanism of Piezo1 channel and the physiological role of piezo1 channels in more tissue (Smith et al., 2010).

1.5.1.2. Potassium-Selective Channels

Potassium-selective (SACK) channels comprise a smaller family than the SA-cat family of SACs and have less distribution in species. SACK channels show a predominant selectivity for potassium ions. SACK can be activated by Ca, pH, and ATP levels. The volume regulation of cells occurs via a barium-sensitive K efflux and chloride flux where K and Cl ions depart from the cell via different channels, independent of calcium. illustrating (Welling and O'Neil, 1990). However, many SACK channels are directly activated by stretch. SACK channels are classified into two families: inward rectifier channels (Kirs), which have a higher K⁺ ions conductance for entering into the cell than outwards and two-pore-domain (K2p), which contain two copies of the selectivity filter (Sansom et al., 2002). Ca-sensitive SAKS is activated by voltage and Ca concentration as well as stretch, and named big potassium (BK) or Maxi-K channels due to large amounts

of potassium ions passed via the cell membrane. An example Ca-sensitive SAKS is by the identification of Maxi-K channels in rat and rabbit cortical collecting tubule (CCT), where these channels are independently activated by voltage, Ca concentration, and membrane stretch (Pacha et al., 1991).

1.5.1.2.1. Inwardly rectifying (Kir)

Inwardly rectifying potassium (Kir) channels were first discovered in skeletal muscle. Kir channels display greater flow current into the cells rather than out of the cells, and their actions depend on the electrochemical K gradient. The primary structure of Kir channels comprises two putative membrane-spanning domains (TM1 and TM2) connected by an extracellular pore-forming region (H5) which is considered as the “ion-selectivity filter” and cytoplasmic amino (NH₂)- and carboxy (COOH)- terminal domains. Also, there are four such subunits in a tetrameric complex transferring this structure into a functional structure. Kir channels are insensitive to membrane voltage because of the absent of the S4 voltage sensor region. To date, 15 Kir channels have been identified and divided into seven subfamilies (Kir1.x to Kir7.x). Every subfamily is categorised into four groups based on their function: 1. classical Kir channels (Kir2.x), 2. G protein-gated Kir channels (Kir3.x), 3. ATP-sensitive K channels (Kir6.x), and 4. K-transport channels (Kir1.x, Kir4.x, Kir5.x, and Kir7.x) where x is multiple member. These channels can form a homomeric or heteromeric combination of two channels to produce functional Kir channels. Also, the majority of Kir channels effectively can be blocked by Barium cation (Ba²⁺) and Cesium cation (Cs⁺) and they are commonly used to study the physiological roles of Kir channels in cells and tissues (Isomoto et al., 1997).

The Kir6.1 (KCNJ8) channel is expressed in cardiac myocytes, pancreatic-cells, skeletal muscle, vascular smooth muscle, and neurons. Also, the KCNJ8 has been physiologically and pharmacologically characterised in different tissues, which the KCNJ8 channel single-

channel conductance is 30 pS. KCNJ8 channel can be inhibited by sulfonylureas agents, such as chlorpropamide, tolbutamide, and glibenclamide. It can also be stimulated by different agents such as pinacidil, nicorandil, and diazoxide.

An experimental demonstration of the effect of KCNJ8 on blood pressure was performed by Aziz et al. Their major findings were that the KCNJ8 channel controlled vascular reactivity and blood pressure, KCNJ8 (-/-) mice showed no obvious arrhythmic phenotype and vascular smooth muscle cells failed to respond to vasodilators in a normal manner (Aziz et al., 2014). Interestingly, KCNJ8 channel regulates vascular tone and vascular reactivity including vasodilators, vasoconstrictors (such as angiotensin II and histamine), and the vasorelaxant tone that occurs under physiological conditions (Kakkar et al., 2005). Furthermore, the KCNJ8 channel has essential roles in other cell phenotypes; for example, endothelial cells, peripheral nerve endings, and central nervous system. The KCNJ8 channel is functionally expressed in endothelial cells, and different studies show that the KCNJ8 channel significantly increases the endothelin-1 release and coronary perfusion pressure (Malester et al., 2007). The presence and functional roles of the KCNJ8 channel in heart valve have not been investigated.

1.5.1.2.2. Two-pore-domain (K2p)

Potassium (K⁺) current is essential in generating a negative membrane potential in excitable tissues. An entire channel family has been characterised by generating the negative membrane potential in relative time- and voltage-independence manners, as well as regarding potassium selectivity. These channels are called “two-P domain” or “two-pore-domain” because of the presence of two pore-forming loops (P domains) instead of one in their subunit structure (Talley et al., 2003). Physicochemical parameters such as oxygen tension, pH, and mechanical forces, including membrane stretch can modulate K2p channels (Talley et al., 2003). K2p channels have been involved in different physiological

processes such as HCO₃⁻ transport in the kidney, modulation of heart rate, regulation of breathing, maintenance of body temperature T cells volume regulation, and aldosterone secretion (Szüts et al., 2012).

K2p channels are classified into different members based on the analysis of the nematode genome. To date, 14 members of K2p channels have been identified in the human genome. Currently, there are two terminology systems of K2p channels: 1- prefix KCNK was assigned to K2p channels by the Human Genome Organization and is followed by the number for every gene. These numbers represent the order in which gene was discovered and did not mean any classification of sequence or function. 2- It based on abbreviations derived from the main physical features of the cloned channels. The functional expression of K2p channels in different tissues paves the way for more definitive work to investigate their roles in physiological and pathological scenarios. To date, there are no blockers or activators of K2p channels which limit definitive identification of the role of K2p channels in different tissues. However, genetically modified animals or knockdown of these genes help explain the functions of K2p channels (Talley et al., 2003).

KCNK2 or TREK-1 channel is a K⁺-selective channel from the K2p family. KCNK2 can be stimulated directly by stretching through the lipid bilayer, and it is membrane tension-gated channels. Also, KCNK2 can be activated by voltage, acidic cytosolic pH, lipids and lysolipids, phosphorylation and chemical stimuli such as arachidonic acid, and other polyunsaturated fatty acids (PUFAs). Some of KCNK2 channel inhibitors such as norfluoxetine and paroxetine are clinically utilised drugs such as volatile anaesthetics, antidepressants, neuroleptics, and sedatives (Enyedi and Czirják, 2010, Honoré, 2007).

KCNK2 channels have shown a functional expression in smooth muscle cells (SmMC) and cardiomyocytes. KCNK2 regulates different cellular process such as the migration of immune cells in the blood-brain barrier, muscle cell differentiation and regeneration, and

interaction between muscle cell and immune cell (Afzali et al., 2016). KCNK2 inhibits membrane stretch-induced contraction in the hollow organs such as bladder and colon. Also, KCNK2 performs a protective role against mechanically induced apoptosis in epithelial cells in the kidney (Peyronnet et al., 2012). Additionally, the dysregulation of KCNK2 channel is related to pathophysiologies such as cancer (Brohawn, 2015).

Less known about KCNK2 in comparison to other SACs, but among K2ps, the KCNK2 channel has most widely investigated, and many essential roles of KCNK2 have been reported. The presence and function of KCNK2 in some tissues such as heart valves remain to be seen, and future efforts to clarify the functional expression and role of KCNK2 in different tissues are essential to understanding physiological and pathological conditions in heart valves and developing novel therapeutic strategies for valve diseases.

1.5.2 Stretch-Activated Channels in the Heart Valve Cells

SACs are primary mechanical transducers in cardiomyocytes, and the major pathway for heart mechanotransduction is in the cardiomyocytes. The electrical activity in cardiomyocytes is regulated by SACs via modulating ion transients during activation. Opening SACNS channels allow sodium and possibly calcium to enter the cells, causing plasma membrane depolarisation during diastole, repolarisation during early systole, and depolarisation during systole. The opening of SACK allows potassium ions to exit from cell cytoplasm, causing hyperpolarisation of the plasma membrane during diastole and repolarisation of the plasma membrane during systole (Reed et al., 2014) (**Figure 1.4**). Stacy et al. have highlighted the role SACs in the cardiac function where they found that increasing the diastolic stretch increases the diastolic depolarisation up to the threshold, and this targets the action potential and generates the stretch-induced depolarisation or arrhythmia (Stacy Jr et al., 1992).

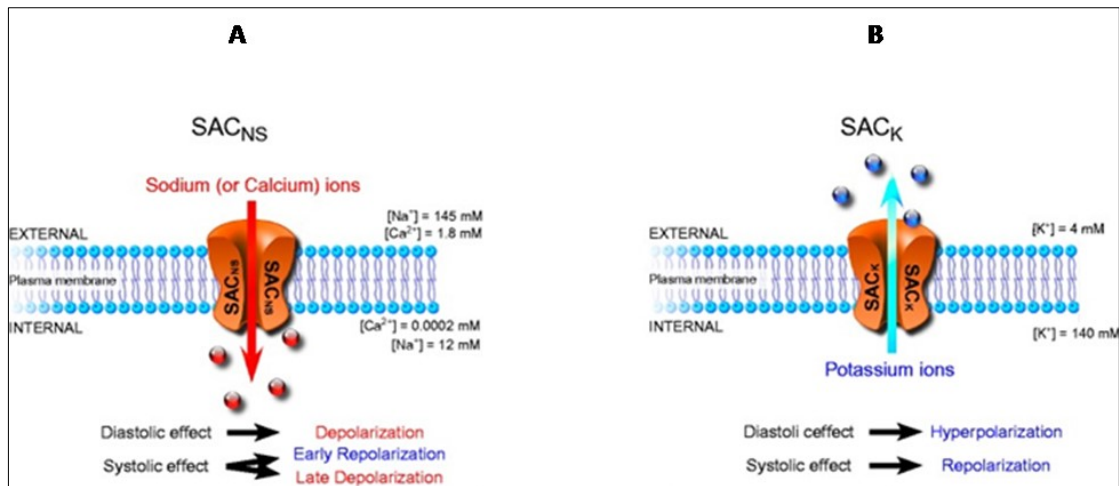


Figure 1.4: Overview of cation non-selective (SACNS) and potassium-selective (SACK) channel function, effects, and pharmacological modulators. A. SACNS opening leads to sodium and possibly calcium entry (in addition to also present potassium fluxes); this opening depolarises the plasma membrane during diastole, repolarises it during early systole, and may cause after-depolarisation-like behaviour in later stages of action potential repolarisation, depending on the current's reversal potential (usually in the mid-region between systolic and diastolic peak potentials). B. SACK opening leads to potassium ions exiting from the cytoplasm; this opening act to hyperpolarise the plasma membrane during diastole and to repolarise it during systole (Reed et al., 2014).

Despite many SACs having been identified and their roles in regulating cardiomyocytes function having been proven, SACs in valve cells have not yet been investigated. AV cusps are exposed to a unique profile of haemodynamic forces, including shear stress and stretch. These forces are well-known to have a number of biological effects on valve cells, however, there is a lack of mechanistic data that establishes how the cell sense mechanical force and transmitted it into intracellular responses. Therefore, identification of SACs and their roles in the mechanotransduction process in heart valves will provide important information towards understanding valve function in health and disease and will be useful in the design and construction of future tissue engineered heart valves.

1.6 Hypothesis & Specific Aims

This study hypothesized that SACs are present in valve endothelial and interstitial cells, and play a vital role in helping transduce and modulate the responses of endothelial and intestinal valve cells to mechanical forces.

A comprehensive exploration of this hypothesis would require a great deal of time and effort. Therefore, my thesis targets only six SACs and investigates the following aims.

This framework will achieve an initial understanding of my general hypothesis.

Specific Aims

- **Expression of SACs:**

- I. Detect the expression of SACs in VECs and VICs.
- II. Characterise the presence SACs in VECs from the aortic and ventricular side of AV cusps.
- III. Describe the changes in the expression of SACs in different phenotypes of VICs.
- IV. Characterize the expression changes of SACs in non-calcified and calcified AV.

- **The functional role of SACs in VECs and VICs:**

- I. Investigate the role of SACs on VEC alignment in response to shear.
- II. Examine the effect of SACs on collagen production by VICs in response to stretch.
- III. Study the role of SACs in the migration of VICs.
- IV. Investigate the role of SACs in the proliferation of VICs.

Chapter 2

General Materials and Methods

The methods common to all the results chapters are described in this chapter. Those methods specific of certain chapters are described in the respective chapters.

2.1 Cells Isolation and Cells Culture

The healthy heart valve samples that were collected from the heart valve bank were unsuitable for clinical usage due to different reasons including damage in valve tissue , early signs of calcification and potential risk of infection. The donors' ages (of both genders) were between 23–81 years.

2.1.1 Endothelial Cells Isolation and Culture

Upon arrival at the laboratory, the valve was placed in 90mm diameter Petri dish in a sterile hood. Immediately, the valve leaflets were removed and thoroughly washed with sterile Phosphate-Buffered Saline (PBS). For VECs isolation, leaflets were placed in a conical tube filled with PBS, shaken several times to remove all debris, and refilled with 0.3% collagenase in PBS. They were then incubated for 5–10 mins on the shaker in a water bath at 37°C. Then, the valve leaflets were removed into 90mm diameter Petri dish for VICs isolation and DMEM (Sigma) containing serum was added to neutralise collagenase. The mixture was then centrifuged at 300-500g for 5 min. Finally, cell pellets were re-suspended in Endothelial Cell Growth Medium 2 (PromoCell) supplemented with Supplement Mix Endothelial Cell Growth Medium (PromoCell), 2 mM glutamine (Sigma), 20% fetal bovine serum (FCS) (Sigma), 100 U/mL penicillin (Sigma), and 100 µg/mL streptomycin (Sigma) in 1% gelatin-coated tissue culture T25 flasks (gelatin solution from bovine skin from Sigma). The ethical approval number is 11-L01055.

2.1.2 Interstitial Cells Isolation and Culture

After VECs isolation, removed leaflets were rinsed with PBS and finely minced and dissociated with a blade in 90mm diameter Petri dish. Then, leaflets pieces were suspended in 0.3% collagenase solution in PBS at 37°C in a shaking water bath for 3-4 hours. After, released cells were separated from undigested tissue by passing the incubation material through 40mm cell strainer. Then, DMEM with calf serum was added to rinse strainer and inhibit collagenase. Finally, cells were pelleted after centrifugation at 300-500g for 6 mins and the cells were then re-suspended in Dulbecco's Modified Eagle's medium (Sigma) supplemented with 10% Fetal bovine serum (Sigma) 2 mM glutamine (Sigma), 100 I.U./mL penicillin and 100 (µg/mL) streptomycin (Sigma).

All cells were grown at 37°C in 5% CO₂ and their specific medium was changed every 3 days. Additionally, cells were passaged using Trypsin (Sigma) at optimal confluency (70-80%) where too low confluency inhibits proliferation and too high confluency leads to cell transformation. After phenotyping by FACS or stain, all cells have been frozen in DMEM, 40% FBS and 10% Dimethyl sulfoxide (Aldrich) for experiment usage.

2.2 Cells Sorting

Magnetic cell sorting of labelled VEC was performed using CD31 MicroBead kit (Miltenyi Biotec, Lot: 5100315069). Initially, cells were labelled with CD31-Biotin and magnetically labelled Anti-Biotin MicroBeads. Afterwards, the cell suspension was loaded into a MACS Column which is placed in the magnetic field of a MACS Separator. Due to the magnetic field, CD31 labelled cells were attached to the magnet and unlabelled cells run through it. The column was washed for three times to remove all unlabelled cells. After removal of the magnet from the column and addition of the medium, the selected magnetically labelled cells were eluted and plated in 1% gelatin-coated tissue culture T25 flasks.

2.3 FACS Analysis

To confirm valve ECs and ICs phenotype, cells were trypsinized and re-suspended in wash buffer (2% FCS in PBS). For each sample, 10×10^4 cells were stained by incubation with CD31 (1/100,BD, Lot:550369), CD90 (1/100,RUO, Lot:110616/03), CD14 (clone,26IC), CD34 (1/5,Becton, Lot:348050), CD45 (1/5,Becton, Lot:347460), CD105 (1/100,BD, Lot:555690), CD106 (clone,1.4C3), ICAM (clone,6.5B5), CD133 (1/10,MACS, Lot:5100312013), α -SMA (1/200,Dako, Lot:20019176), and vimentin (1/100, Dako, Lot:0038354), CD29 (1/50,BD,556048), α -V β 3 (1/100,Santa cruz, lot:23C01), CD44 (1/5,Becton, Lot:347940), VE-cadherin, CD49A (1/50,BD,559594), CD49B (1/50,BD, 555668), CD49E (1/50,Harlan,p9713658), CD49D (1/50,BD,555502) conjugated antibodies for 30 min. A negative control sample was included and incubated with fluorescein isothiocyanate (FITC) conjugated IgG or IgG2a isotype. Samples were washed twice using the wash buffer and re-suspended secondary antibody. Finally, samples were washed twice and re-suspended in 400 μ L of PBS. The percentage of positive cells was determined using BD FACS flow cytometer.

2.4 Immunocytochemical Staining

Cells were cultured on size 22 mm \times 22 mm coverslips (20,000 cells /coverslip) for 2 days. The cells were then fixed with 4% Paraformaldehyde for 10 min at room temperature (RT), washed three times with PBS and stored at 4 $^{\circ}$ C until use. For staining, cells were exposed to Triton X-100 for 3 minutes at RT to improve antibody penetration. The slides were blocked with 3% Bovine Serum Albumin (BSA) in PBS containing 0.1% Tween-20 (PBS-T). Then, the slides were incubated with the required unconjugated primary antibody (see **table 2.1** for a list of antibodies used) for 1 hour at RT. After cells were washed three times and incubated again for 1 hour at RT with the appropriate fluorochrome-conjugated secondary antibody diluted 1/1000 in PBS-T. For the negative control, an identical

procedure was carried out, but with the omission of the primary antibody in each case. After being washed, the slides were incubated with DAPI for 10 mins and mounted using Mountant, Permaflour (Thermo Scientific, Lot: 150202).

Images were acquired using Confocal Laser Scanning Microscopy LSM 510 META, ZWISS and LSM5 software. For quantitative analysis of eNOS, CD31, vWF, vimentin, α -SMA, and CD90 expression, ten microscopic fields were imaged and the number of positive cells was counted in each field.

2.5 Immunohistochemistry

Valve tissue was fixed in a 10% formal saline solution for 24 h, proceeding in the paraffin block using tissue processor (TP1020). Sections were cut into 5 μ m thin pieces using a microtome and were placed on glass slides. Prior to immunoperoxidase staining, 5 μ m thick paraffin wax sections were dewaxed and rehydrated in water and then washed in PBS for 5 minutes. Then the slides were immersed in 0.1M citrate buffer (pH 6) and microwaved for 10 minutes before blocking for endogenous peroxidases using 0.3% hydrogen peroxide in PBS for 10 minutes. The sections were washed twice in PBS and blocked using 3% (w/v) BSA in 0.5% Tween in PBS (PBS-T) for 30 minutes. Sections were incubated separately for 1 hour with a respective antibody and negative control consisting of 3% BSA in PBS (see **Table 2.1**). Primary antibodies were then removed by washing the sections 3 times in PBS followed by a second layer of biotinylated goat anti-mouse immunoglobulins (GAM IgG-Vector Laboratories) diluted 1/250 in PBS for 1 hour. Sections were then washed 3 times in PBS before 1 hour incubation with Avidin-Biotin Complex (ABC-Vector Laboratories). Reactivity was detected using diaminobenzidine tetrahydrochloride (DAB tablets, - Sigma) (25mg/ml) and hydrogen peroxide (0.01% W/V). Sections were then counter-stained with haematoxylin and viewed on a Ziess LSM 510 confocal microscope.

2.6 Western Blotting

Cell pellets from T25 flask were washed two times in PBS, solubilised and homogenised in Radioimmunoprecipitation assay (RIPA) buffer supplemented with protease inhibitor cocktail 1X. The cell lysate was vortexed and kept for 20 min on ice before freezing. Proteins were quantified with a Pierce bicinchoninic acid (BCA) protein assay after a 10,000g centrifugation for 10 minutes at 4°C. Total protein homogenates (25-50 µg) were denatured and separated on 10% Bis-Tris gels. Electrophoretic bands were resolved at 200V for 60 min; resolved bands were transferred on nitrocellulose membranes (Hybond C, Amersham). Membranes were blocked in PBS-T and 5% (w/v) non-fat powdered milk for 1 hour. Membranes were then incubated overnight with the respective primary antibody (see **table 2.1**) in PBS-T containing 5% (w/v) non-fat powdered milk. Membranes were then washed three times in PBS-T and incubated with corresponding horseradish peroxidase conjugated secondary antibody for 1 h at room temperature. Membranes were washed with PBS-T four times for 15 min on shaker prior to visualization of the protein bands using an enhanced chemiluminescence (ECL) substrate. The membrane was scanned, and bands were quantified using the ChemiDoc Touch Imaging System from Biorad. Levels of expression were normalised to one of the house-keeping proteins including GAPDH, Vimentin or T-tubulin.

Table 2.1: list of antibodies.

Antibody	Lot number	company	Concentration in		
			Fluorescence	paraffin section	WB
CD31	20023423	Dako	1/40		
vWF	00060129	Dako	1/400		
eNOS	610296	BD Biosciences	1/200		
CD90	110616/03	RUO	1/100		
α SMA	20019176	Dako	1/200		1/5000
vimentin	307021	PROGEN	1/100		1/50k
SmmyHC	10053253	Doka			1/100
SM22	ab14106	Abcam	1/10000		1/100
Calpain	10107080	Doka	1/50		1/500
myHC	10053253	Doka	1/200		1/100
MRTF	SG21558	Santa Cruz	1/100		1/250
EDA-fib	ab6328	Abcam	1/10000		
Mycardian	Pab0604	covalab	1/2000		1/200
KCNK2	ab90855	Abcam	1/50	1/100	1/100
TRPM4	ab123936	Abcam	1/50	1/50	1/100
TRPV4	ab191580	Abcam	1/200	1/50	1/500
KCNJ8	Bs-6468R	BIOSS	1/50	1/50	1/250
TRPC6	ab62461	Abcam	1/50	1/50	1/500
osteopontin	Ab91655	Abcam	1/100	1/50	1/1000
ALP	Ab133602	Abcam	1/100	1/25	1/1000
RUNX2	Ab23981	Abcam	1/100	1/200	1/500
Phalloidin	49409	Invitrogen	1/100		

2.7 RT-PCR

RT-PCR experiments were performed in three steps: RNA extraction, cDNA synthesis, and RT-PCR.

2.7.1 RNA Extraction

RNA samples were extracted from cells in one well of 6-well plate using a RNeasy kit (QiaGen) following the manufacturers' instructions. Briefly, cell pellets were disrupted and homogenised by adding 350 μ l of RLT buffer and vortex. Next, 350 μ l of 70% ethanol was added to the lysate and mixed well by pipetting. The sample, including any precipitate, was transferred to an RNeasy Mini spin column placed in a 2ml collection tube, the lid was closed, and the sample was centrifuged for 15 seconds at 8000g, discarded the flow-

through. Then 700µl of RW1 buffer was added to the RNeasy Mini spin column, the lid was closed, and the sample was centrifuged for 15 seconds at 8000g, discarded the flow-through. Next, 500µl of RPE buffer was added to the RNeasy Mini spin column, the lid was closed, and the sample was centrifuged for 15 seconds at 8000g, discarded the flow-through. The RNeasy Mini spin column was placed in a new collection tube and centrifuged at full speed for 1 minute to dry the membrane. Finally, 30µl of RNase-free water was added to the RNeasy Mini spin column, and it was placed in a new 1.5ml collection tube, the lid was closed, and the sample was centrifuged for 1 minute at 8000g to elute the RNA.

2.7.2 cDNA Synthesis

The cDNA synthesis was the TaqMan Reverse Transcriptase Reagent (Applied Biosystems, lot: 175634), for which every reaction was loaded with 100ng of total RNA, 1X of 10X RT buffer, 5.5 mM of MgCl₂, 500 µM of dNTPs, 2.5 µM of random hexamer, 0.4U/µl of RNase inhibitor, 1.25U/µl of MultiScribe reverse transcriptase, 1 µl of primer in 10µl cDNA synthesis volume. All steps were performed on ice and, in the end, the tubes were vortexed to mix and spin briefly at 4°C to collect the reaction. They were subsequently left on the bench for 2 minutes in order to reach room temperature. The reaction tubes were then loaded into a thermocycler (T3thermocyclers, Biometra) for 10 minutes at 25°C to allow for primer binding, followed by 30 minutes at 48°C for an extension, and 5 minutes at 95°C for enzyme denaturation.

2.7.3 Real-Time PCR

All reagents of the TaqMan Fast Universal PCR Master Mix 2X (Applied Biosystem, Lot: 1802503) and cDNA samples were thawed at RT, and the primers (listed in **table 2.2**) were protected from the light. Master Mix of the 2X universal master mix, primer and RNA-

free water were aliquoted into 96-well reaction plates, and cDNA was aliquoted into its own reaction plate as per the 96-well plate plan. The plate was tightly sealed and start a real-time run using Light Cycler 480 (Roche). The data were analysed using the comparative Ct method.

Table 2-2: list of RT-PCR primers

Primers	Cat no	Dye	Company
18S	HS99999901-sl	FAM- MGB	Applied Biosystems
Actin β	Hs0100665-gl	VIC-MGB	Applied Biosystems
COLL1A1	HS01097664-ml	FAM-MGB	Applied Biosystems
COLL3A1	SS03375691-gl	FAM-MGB	Applied Biosystems
ELASTIN	Hs00355783 ml	FAM-MGB	Applied Biosystems
HSP47	Hs01060397 gl	FAM-MGB	Applied Biosystems
RUNX2	HS00231692-ml	FAM-MGB	Applied Biosystems
KCNK2	HS01005159- ml	FAM-MGB	Applied Biosystems
KCNJ8	HS00958961-ml	FAM-MGB	Applied Biosystems
TRPM4	HS00214167-ml	VIC-MGB	Applied Biosystems
TRPC6	HS00989190- ml	FAM-MGB	Applied Biosystems
TRPV4	HS01099348- ml	FAM-MGB	Applied Biosystems
Piezo1	Hs00207230 ml	FAM-MGB	Applied Biosystems

2.8 Statistical Analysis

Data were expressed as the box and whisker plot where the n number was ≥ 4 and a bar chart where the n=3 . Statistical analysis was performed by conducting a T-test (nonparametric) (Mann Whitney test) to compare two groups. A one-way ANOVA (nonparametric) (Friedman) to compare more than two groups, Dunn's post-test was used to compare between groups. Non-parametric tests were used because of small n numbers. All n number for all experiments are given in figure legends. A P value <0.05 was considered statistically significant. Graph-pad (prism) software (version 8.0.0) was used to perform all statistical analysis.

Chapter 3

Isolation and Phenotype of Valve Cells

3.1 Rationale

Although the AV cusp is a thin structure, it is extremely strong due to the organisation of the extracellular matrix. In addition to the extracellular matrix there are a population of cells that help maintain the extracellular matrix and thereby the durability of the valve. The valve cells include VEC that cover the surface of the cusps and VIC which populate the body of the valve cusp (Chester et al., 2014).

VECs cover the two surfaces of valve cusps in a continuous layer with the endocardium and the sinus endothelium. However, VECs were once thought to be a minor candidate in valve function when the valve was believed to be a passive structure that just opened and closed in response to transvalvular pressure change. Nonetheless, recent studies suggest the VECs possess unique properties that allow them to regulate valve homeostasis under varying haemodynamic conditions. Alternations in VEC function are believed to be associated with pathological conditions (Poggianti et al., 2003). VECs are considered vital in transducing mechanical stress imposed by haemodynamic forces to VICs (Butcher and Nerem, 2007).

AV is located in a unique mechanical environment within the circulation wherein the opposing sides of the valve experience different hemodynamic forces including pressure and shear stress. Valve endothelial from the ventricular side are exposed to unidirectional shear stress, while the aortic side is experienced oscillatory shear. This has led to the suggestion that the VEC on each side of the valve responds to shear stress in different ways. Recently, it has been shown that side-specific endothelial cells possess different mechanical properties (Miragoli et al., 2014), which suggests the cells on each side of the valve have differential properties that allow them to respond appropriately to the respective pattern of flow that they are exposed to. Therefore, it is relevant to consider

endothelial cells from the aortic and ventricular surfaces of the valve as two separate cell phenotypes.

Valve interstitial cells are heterogeneous and dynamic populations of cells derived from embryonic mesenchymal outgrowths (the cardiac cushions) (Eisenberg and Markwald, 1995). They populate the body of valve cusps and are located within the ECM. VIC turnover in the valve leaflet remains unknown, but has been documented that VIC numbers decrease in with age, which is accompanied by collagen degeneration (Sell and Scully, 1965). VICs maintain valve structure by the release of growth factors and synthesising matrix components such as collagen, elastin, proteoglycans, and chemokines, as well as the matrix remodelling enzymes, matrix metalloproteinases (MMPs), and their tissue inhibitors (TIMPs). Furthermore, VICs have the capacity to release a range of pro- and anti-inflammatory cytokines including IL-12, IL-10, and TNF- α , although the role of VICs in inflammatory response has yet to be addressed (Segura et al., 1998). Furthermore, it has been shown that several valve pathologies are associated with an increase in expression or activity of matrix remodelling enzymes and cytokine secretion (Sell and Scully, 1965) and the expression of markers of either myofibroblasts or osteoblast-like cells (Osman et al., 2006). In the healthy valve, the VIC cells are predominately a fibroblast-like cell, but as a range of phenotypes also exist according to their microenvironment, mechanical environment, and the effects of soluble factors (Taylor et al., 2000) (**Summarized in Table 3-1**). It has been well established that valve interstitial cells can express five identifiable phenotypes, which include embryonic progenitor endothelial/mesenchymal cells, fibroblast VICs (fVICs), activated VICs (aVICs), progenitor VICs (pVICs), and osteoblastic VICs (obVICs).

Table 3-1. Phenotypic and functional classification of AV interstitial cells [adapted from (Chester et al., 2014)].

Cell type	Location	Function
Embryonic progenitor endothelial/ mesenchymal cells	Embryonic cardiac cushions	Give rise to fVICs through an activated stage or EMT.
fVICs	Valve leaflet	Maintain valve structure and function by secreting ECM. Prevent angiogenesis.
pVICs	Bone marrow, blood, the valve leaflet	Provide aVICs for valve repair.
aVICs	Valve leaflet	SMA-containing VICs with activated cellular repair processes (proliferation, migration, and remodelling). Respond to valve injury and abnormal hemodynamic or mechanical forces.
obVICs	Valve leaflet	Calcification, chondrogenesis, and osteogenesis in the leaflet. Secrete ALP, osteocalcin, osteopontin, and bone sialoprotein.

The sections below describe the phenotype, presence, and functions of three former interstitial cells.

- **Fibroblast cells**

Fibroblast cells are a population of cells that consists of spindle-shaped elongated cells with around the elliptic nucleus, rough endoplasmic reticulum, large Golgi apparatus, and an absence of the basement membrane. Fibroblast VICs are non-activated cells that are actively involved in ECM production and express prolyl 4-hydroxylase, the essential enzyme for stabilisation of the collagen triple helix (Janin et al., 1990, Konttinen et al., 1989). Valve fibroblasts are linked to each other and to the ECM via gap junctions, primarily Connexin43 (Cx43) and Connexin45 (Cx45) (Baum and Duffy, 2011, Latif et al., 2005). A considerable amount of studies have documented the role of valve fibroblast cells in valve function by modulation of ECM. Valve fibroblast cells govern a balance

between the synthesis and degradation of ECM by harmonic production of ECM, cytokines, growth factors, and matrix metalloproteinases (MMPs). Finally, valve fibroblast cells have a low turnover rate under normal physiological conditions (Baum and Duffy, 2011).

- **Myofibroblast cells**

Valve leaflets arise from endocardial cushions during valve development. Endocardial cells differentiate into valve cells through the endothelial-to-mesenchymal transformation process. These foetal valve cells exist as myofibroblasts, expressing α -smooth muscle actin (α -SMA). After birth the cells gradually lose α -SMA expression. In normal valves, myofibroblasts are normally present in AV leaflets, though at an extremely low population (Latif et al., 2015) and characterised by prominent stress fibres and express smooth muscle α -actin (Taylor et al., 2000). Myofibroblasts are large cells, have ruffled membranes, and a very active endoplasmic reticulum (Baum and Duffy, 2011). A layer of these cells exists in the ventricular side of the AV of both humans and porcine (Taylor et al., 2003). These contractile cells are believed to proliferate and migrate more than the fibroblast population (Arora and McCulloch, 1994). In pathological conditions, VICs are re-activated and differentiated into myofibroblasts after mechanical and chemical stimulation by haemodynamic changes and/or inflammatory mediators. These cells form an activated population of VICs. Finally, in vitro culture of VIC isolated from healthy valve adopt a myofibroblast phenotype, therefore, most studies using cultured human valve represent the response of myofibroblasts.

- **Osteoblast cells**

Previous studies with VICs have highlighted the role of VICs in valve calcification by differentiation of VICs into osteoblast-like cells in response to different factors such as

specific pro-inflammatory cytokines (Osman et al., 2006). The differentiation of VICs into osteoblast-like cells, occurs via transition initially into myofibroblasts, and then into a calcifying cell phenotype that expresses phenotypic markers that are usually associated with osteoblasts (Wyss et al., 2012). Several studies have revealed that osteoblasts and osteoclasts are present in calcified AV (Mohler, 2004). Osteoblastic differentiation of VICs is akin to physiological osteogenesis, and it is mediated by Runx-related transcription factor 2 (RUNX2) and bone morphogenetic proteins (BMPs) (Miller et al., 2011). VICs differentiated into osteoblast express proteins that are also secreted by bone tissue, including osteocalcin, alkaline phosphatase (ALP), and osteopontin. In vitro osteoblastic differentiation of VICs provides a useful model to investigate AV calcification. A considerable number of studies have published prominent findings regarding AV calcification based on this approach (Liu et al., 2007).

This chapter sets out to validate the cells used in this study, and provide a confirmation that methods used to isolate and culture the cells in the subsequent experimental chapters can be categorised according to the currently accepted classification of valve cells phenotypes.

3.2 The Specific Aims of This Chapter were to:

- Isolation and phenotype of valve endothelial cells and side-specific valve endothelial cells.
- Isolation and phenotype of valve interstitial cells and to differentiate valve interstitial cells into three distinct phenotypes.

3.3 Methods

The general methods employed in this chapter include: cells isolation, cells culture, immunocytochemical staining, and western blot are listed previously in Chapter 2 in detail. The methods specific for this chapter are described here.

3.3.1 Isolation of Side-Specific VECs

A new technique was developed to isolate valve side-specific endothelial cells (Figure 3-1). The human AV was opened in a Petri dish and the leaflets were removed. Valve leaflets were thoroughly washed with sterile PBS, and then placed and spread on the top of a filter that was inserted into a 35cm² dish filled with 3ml of 3% collagenase in PBS. Finally, the top surface of the leaflets was covered with a glass slip; the entire set was placed in a larger dish, and then onto an orbital shaker at 37°C for 5-10 minutes. Then, the collagenase mixture was collected and centrifuged at 300-500g for 5 min. Finally, cell pellets were re-suspended in Endothelial Cell Growth Medium 2 (PromoCell) supplemented with Supplement Mix Endothelial Cell Growth Medium (PromoCell), 2 mM glutamine (Sigma), 20% fetal bovine serum (FCS) (Sigma), 100 U/mL penicillin(Sigma), and 100 µg/mL streptomycin (Sigma) in 1% gelatin-coated T25-tissue culture flasks (gelatin solution from bovine skin from Sigma).

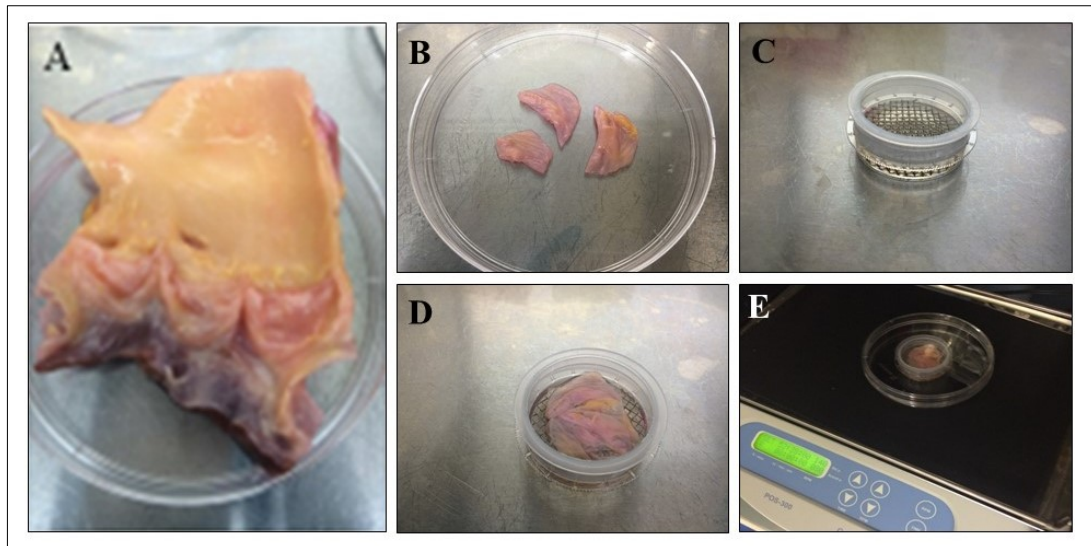


Figure 3-1: Isolation descriptions of side-specific endothelial cells: A) human valve opened. B) Valve leaflets were removed and thoroughly washed with sterile PBS. C) A 35cm² dish was filled with 3ml of 3% collagenase and a filter was placed on the top. D) Three valve leaflets were speared on the filter and covered with a glass slip. E) The dish was placed in a larger dish, then onto an orbital shaker at 37°C for 5-10 min.

3.3.2 Maintenance of Fibroblast Phenotype of VICs

A fibroblast culture medium, containing DMEM , and supplemented with 2% FBS, 2 mM glutamine (Sigma), 100 U/ml penicillin (Sigma), 100 µg/ml streptomycin (Sigma) , 5µg/ml insulin (Sigma) , and 10ng/ml FGF-2 (PERRO Tech) was used to maintain the VICS in a fibroblast-like phenotype as previously described (Latif et al., 2015) was used and fibroblast phenotype was checked by FACS.

3.3.3 Differentiation of VICs to Myofibroblast

The standard culture media DMEM (Sigma) supplemented with 10% FCS (Sigma), 2 mM glutamine (Sigma), 100 I.U/mL penicillin (Sigma) and 100 (µg/mL) streptomycin (Sigma) was used to maintain VICs in a myofibroblast phenotype and myofibroblast phenotype were checked by FACS.

3.3.4 Differentiation of VICs to Osteoblast

VICs were differentiated to osteoblast-like cells using osteogenic medium, containing DMEM supplemented with 1M of β -glycerophosphate (Sigma), 10^{-6} M of dexamethasone (Sigma), and 5mg/ml of ascorbic acid (Sigma) for 21 days and osteoblast phenotype were checked by western blot of calcification markers such as osteopontin, RUNX2 and ALP. β -Glycerophosphate is an organic donor of phosphate groups and forms crystals of calcium phosphate. Dexamethasone plays a well-known role in mineralised nodule formation. Ascorbic acid is a cofactor for enzymes that forms collagen chains via hydroxylate proline and lysine in pro-collagen. Therefore, ascorbic acid facilitates osteogenic differentiation by increasing Coll production.

3.4 Results

3.4.1 Valve Endothelial Cells

In this study, isolation of VECs produced a usable number of pure VECs that allows for further investigation on VECs biology. Valve endothelial cells formed colonies after isolation and began to show a typical endothelial morphology in culture, which is generally a cobblestone morphology (**Figure 3-2**).

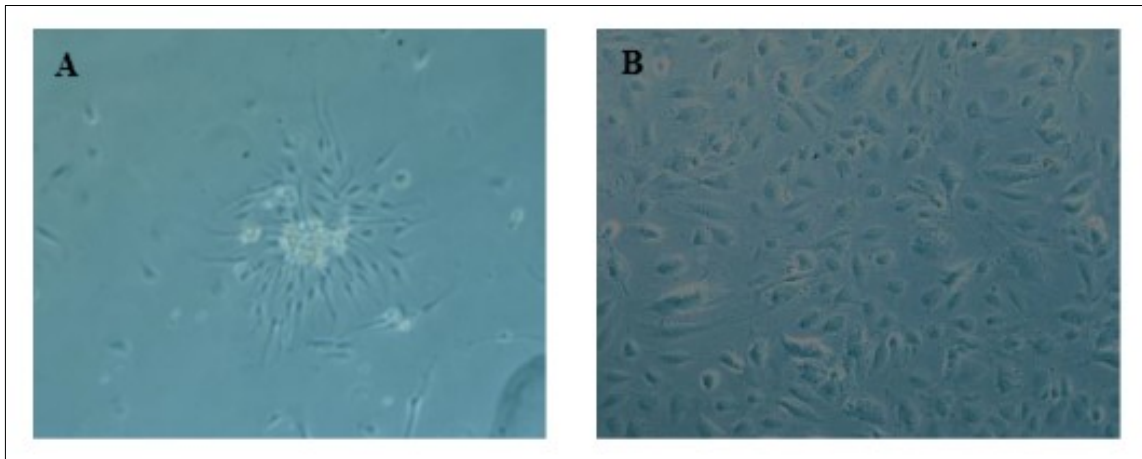


Figure 3-2: Light microscope images of A) aortic VECs at day 1 post-isolation, showing typical endothelial morphology and forming clusters to promote growth, and B) aortic VECs at day 4 post-isolation showing a typical endothelial morphology, which is generally cobblestone morphology. 20X

Following isolation, VECs were additionally purified using magnetic selection methods based on the selection of only endothelial cells (described in Chapter 2 in detail in the Methods section). To confirm the identity of isolated cells, an immunocytochemical stain for EC markers was performed. Approximately 95% of VECs were positive for PECAM-1 (platelet endothelial cell adhesion molecule) (CD31), which was expressed in the cell membrane. Also, 80% of the EC population tested positive for Endothelial Nitric Oxide Synthase (eNOS) and it was expressed in nuclei and cytoplasm. Additionally, 50% of VECs was positive for Von Willebrand factor (vWF), where it expressed in the cytoplasm around the nucleus (**Figure 3-3**).

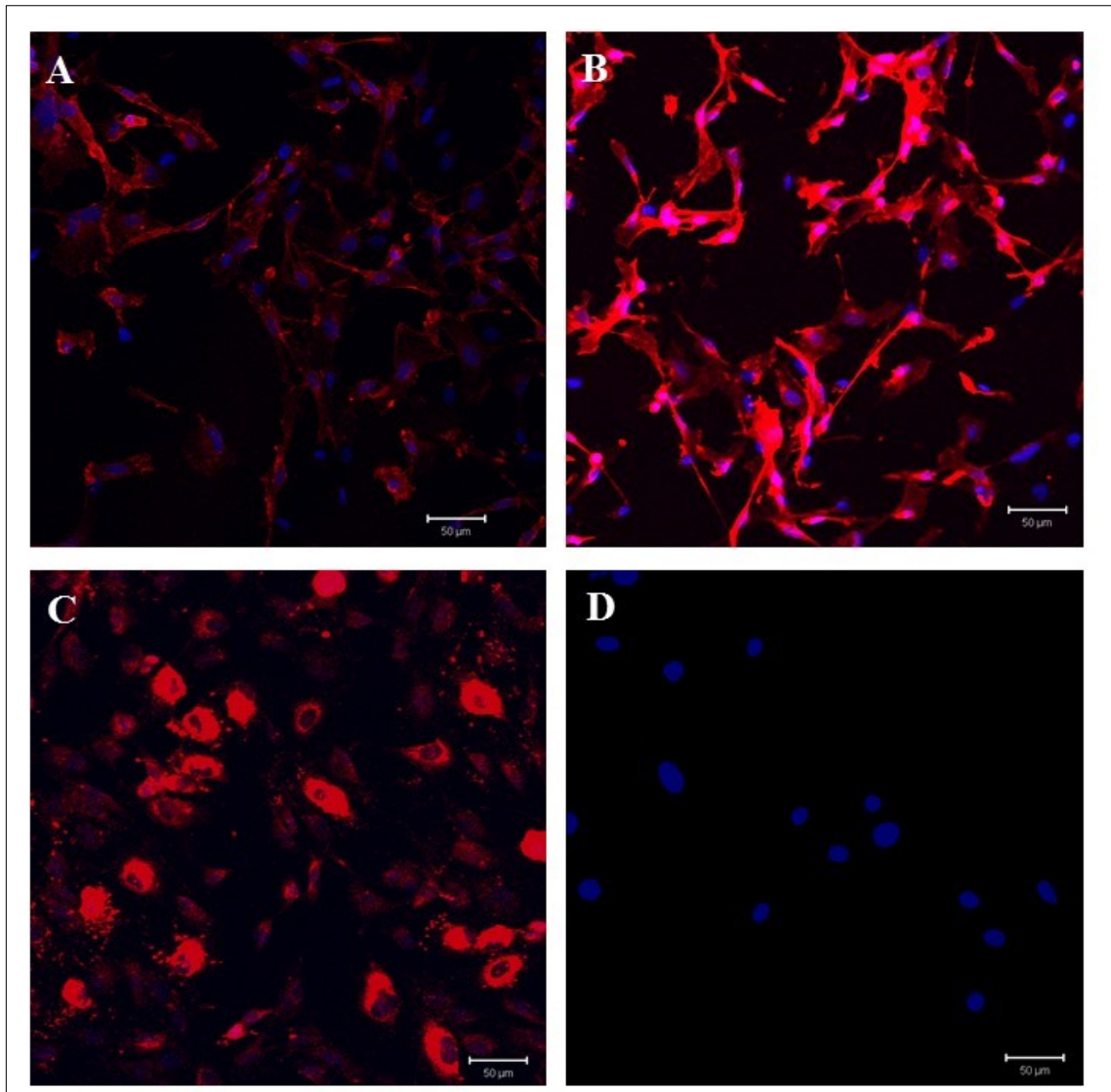


Figure 3-3: Confocal microscopy of ECs from aortic P2 stained for EC markers A) CD31, B) eNOS, C) vWF (red), and DAPI (blue) for nuclear counterstaining. Panel D) shows the negative control. X20; scale bars present 50 μ m.

For further identification, a FACS analysis of the aortic ECs was performed for VEC markers. To increase the validity of the phenotyping, FACS analysis included markers for mesenchymal stem cells (CD45), monocytes, macrophages (CD14), endothelial progenitor cells (CD34), and hematopoietic stem cells (CD133) as exclusion markers. Therefore, CD14, α -V β 3, CD105, CD133, CD45, and CD34 were included in the FACS analysis. The results obtained are comparable with the immunocytochemistry staining results and show >90% of VECs populations expressed CD31. In terms of exclusion markers, the isolated cells were negative for markers of endothelial progenitors cells (CD34),

monocyte/macrophage (CD14), mesenchymal stem cells (CD45), and hematopoietic stem cells (CD133). All isolated VECs that were analysed by FACS, and expressed > 95% of CD31 were considered a sufficiently pure population to use for experiments (**Figure 3-4**).

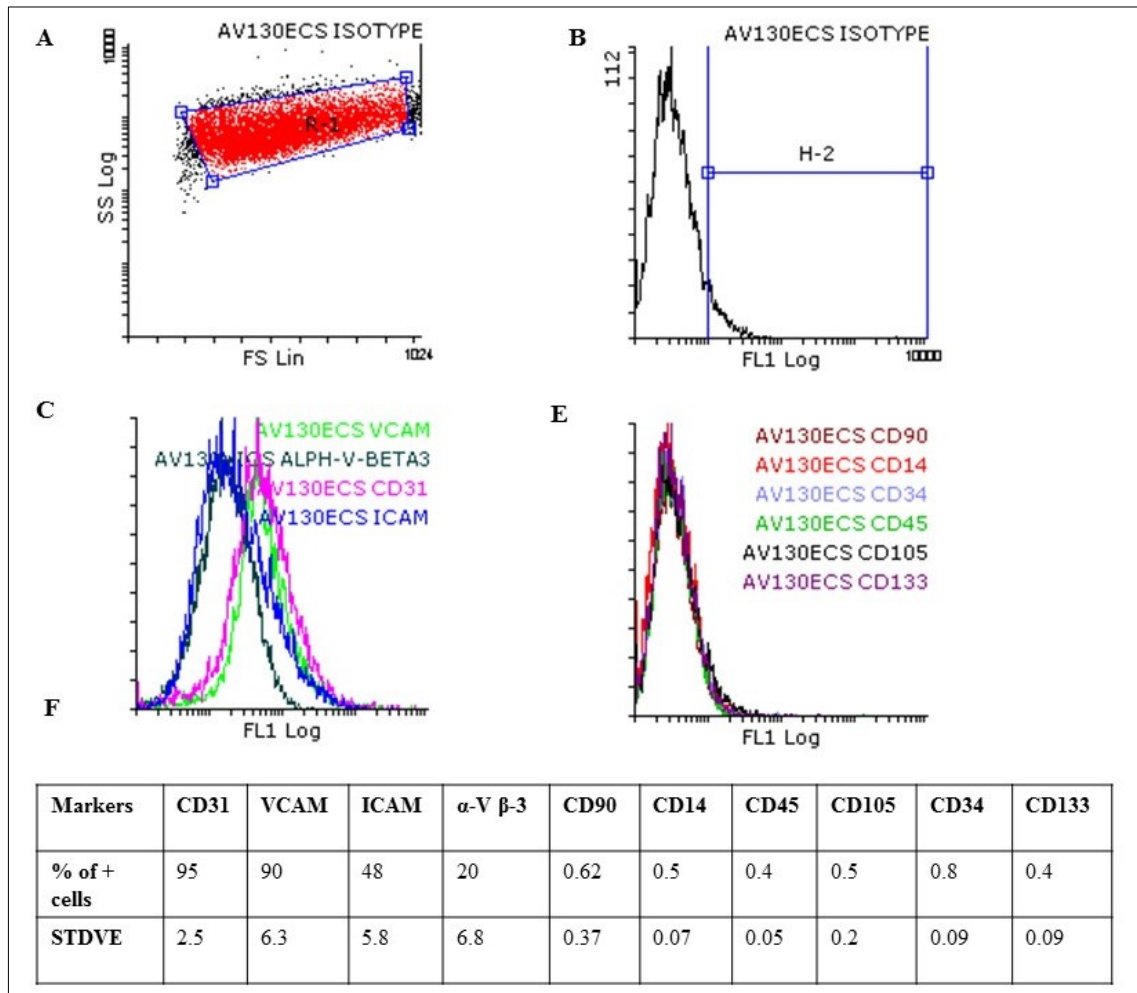


Figure 3-4: FACS analysis of VECs isolated from AV: A) a dot plot histogram of analysed cells. B) Histogram analysis of isotype as a negative control. C) Overlay showing the cell population expresses VCAM, α -V β -3 CD31, and ICAM. D) Cell population is negative for CD90, CD14, CD34, CD45, CD105 and CD133. E) A summary of FACS analysis representing the means + SD of data obtained in three different isolates of VECs. Data is Means \pm SEM, n =3.

3.4.2 Side-Specific Valve Endothelial Cells

As stated above, it is of value to study site-specific endothelial cells as two separate cell phenotypes. To begin, I used a custom-made device previously developed by members of our group (Drs Najma Latif and Ivan Carubelli). A Perspex plate with a number of holes

1 cm in diameter was then placed over the one side of the valve tissue and firmly tightened, creating a tight seal, so one side of valve tissue was exposed to enzymatic digestion (Miragoli et al., 2014). However, using this method the cell yield was too low and was not enough to process the cells isolation to further experiments because it utilizes a small area of the valve leaflet. To try and improve on this method, a new technique was developed as described above and it exposed the all leaflet surface to collagenase enzyme. This method has produced a sufficient number of VECs. Valve endothelial cells from aortic and ventricular side displayed similar morphology in culture, both were exhibiting a typical endothelial morphology, which is generally cobblestone morphology. (**Figure 3-5**).

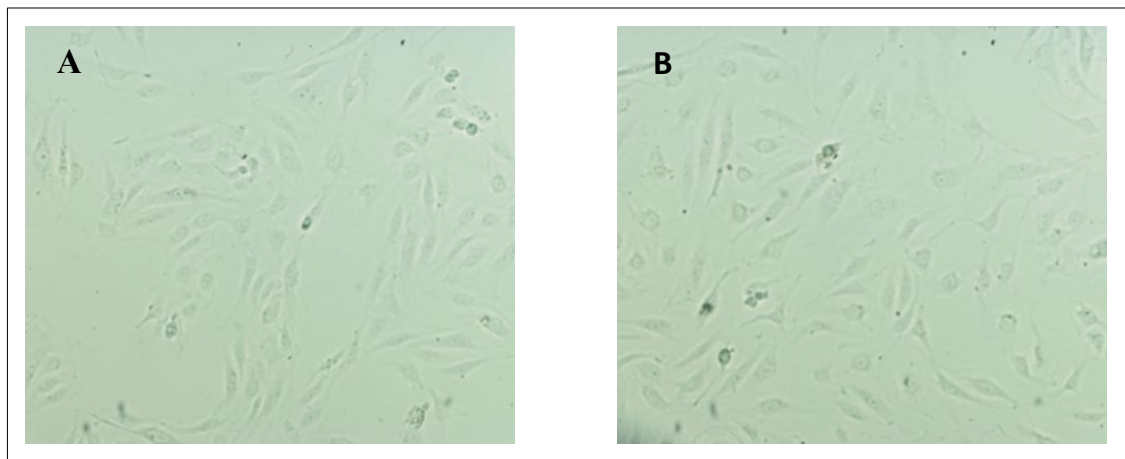


Figure 3-5: The morphology of side-specific endothelial cells at 3 days' post isolation. A) VEC from the aortic side, and B) VEC from the ventricular side. 20X.

After successful isolation of side-specific endothelial cells, FACS analysis was used to characterize side-specific endothelial cells. The panel included the following markers: positive markers of ECs (CD31, vWF), exclusion markers of valve interstitial cells (CD90), smooth muscle cells (α -SMA), human mesenchymal cells (CD45 and CD29), monocytes/ macrophages (CD14), endothelial progenitor cells (CD34), and hematopoietic stem cells (CD133). Side-specific endothelial cells were negative to all the exclusion markers and positive for ECs markers. (**Figure 3-6**).

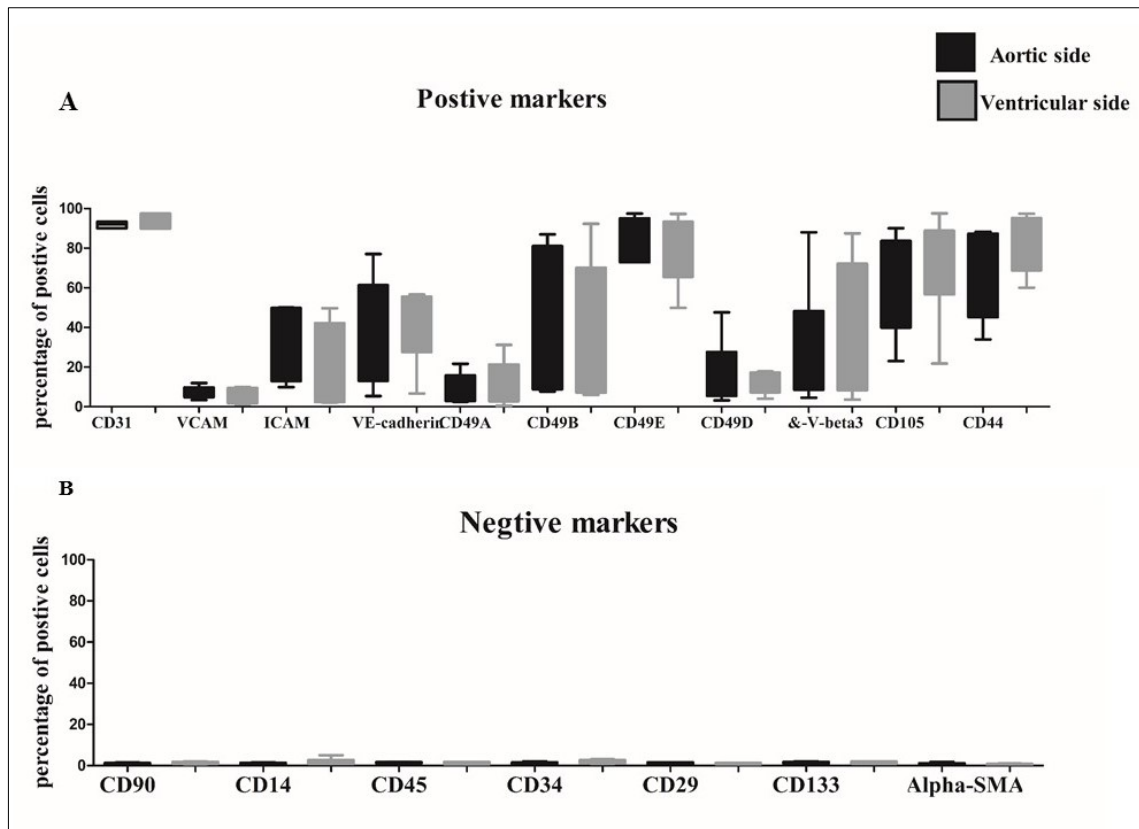


Figure 3-6: Result of FACS analysis: A) expression levels of endothelial cells markers in valve endothelial cells from aortic and ventricular sides. B) Endothelial cell exclusion markers in valve endothelial cells from aortic and ventricular sides. The data were statistically analysed by t-test and presented in the whisker plot format, n = 6. *P < 0.05.

3.4.3 Valve Interstitial Cells

In this study, the isolation of VICs was performed using enzymatic digestion of the underlying basal matrix via utilisation of collagenase (Manduteanu et al., 1988). VICs generally show a typical VICs, spindle-shaped morphology. However, two cell morphologies are observed in VICs culture after isolation: small islands of cuboidal cells and elongated cells that are spindle-shaped. When ICs are confluent, they become more fibroblastic in morphology and show a swirling pattern (**Figure 3-7**).

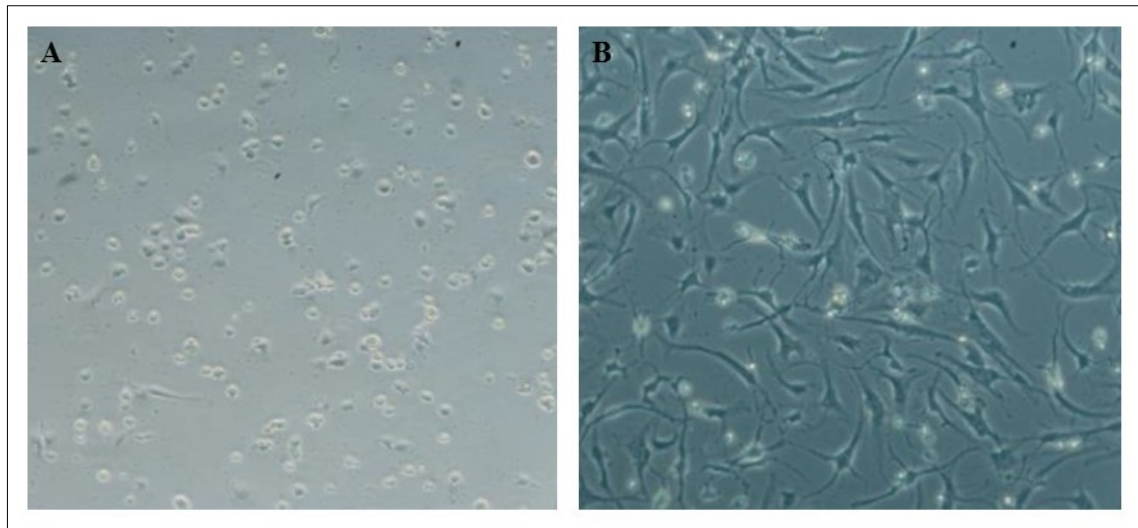


Figure 3-7: Light microscope images of isolated aortic VICs: A) At day 1 post-isolation, the images are blurred due to the incomplete attachment of aortic VICs and the presence of debris after isolation. Aortic VICs are showing a round shape and no typical interstitial cell morphology. B) At day 1 post-isolation, aortic VICs showing spindle-shaped morphology and spreading evenly throughout the flask. Phase contrast; X10.

Following isolation, VICs were cultured in standard DMEM with 10% FCS for 4–10 days. It has been shown that VICs differentiate into myofibroblasts and express α -SMA after isolation in the presence of 10% FCS (Taylor et al., 2000). It was reported that a fibroblast medium containing 10ng/ml of FGF2/low serum/insulin was used to determine that the fibroblast phenotype is associated with healthy valves (Latif et al., 2015). It is believed that reducing serum concentration leads to suppression of myofibroblast differentiation due to the high concentration of active growth factors such as TGF β in serum. To avoid the negative impact of low serum concentration, insulin as a mitogenic factor and FGF2 as a growth factor were added to promote proliferation. FGF2 is one of 23 members of the fibroblast growth factor family (FGF), and it is present in nearly all human tissues (Latif et al., 2015). Therefore, VICs that were cultured from non-calcified human AV were maintained in fibroblast media for up to 10 days prior to phenotyping to maintain the fibroblast phenotype. To confirm the identity of isolated cells, VICs were stained by immunocytochemistry for a range of markers that well-known to be expressed in fibroblast cells. However, approximately 97% of VICs tested positive for Fibroblast Surface Antigen

(CD90), and VICs were highly positive for other fibroblast markers including α -SMA and vimentin (**Figure 3-8**). For further identification, a FACS analysis of the VICs was performed for VIC markers. Similarly to VECs phenotype, exclusion markers were included, which included markers of VECs, human mesenchymal cells, monocytes, macrophages, endothelial progenitor cells, and hematopoietic stem cells. Therefore, CD31, CD14, α -V β 3, CD105, CD133, CD45, and CD34 were included in the FACS analysis. The obtained results are compatible with the immunocytochemistry staining results and show that >90% of VICs expressed CD90, confirming their phenotype. Cells were negative for markers of endothelial cells (CD31), endothelial progenitor cells (CD34), monocyte/macrophage (CD14), Mesenchymal stem cell (CD45), and hematopoietic stem cells (CD133). Additionally, vimentin expression was between 60 and 80%, while α -SMA was very low due to the culture of VICs in fibroblast medium. All isolated cells were analysed by FACS, and samples expressing > 95% of CD90 were considered a sufficiently pure population to be utilised in experiments (**Figure 3-9**).

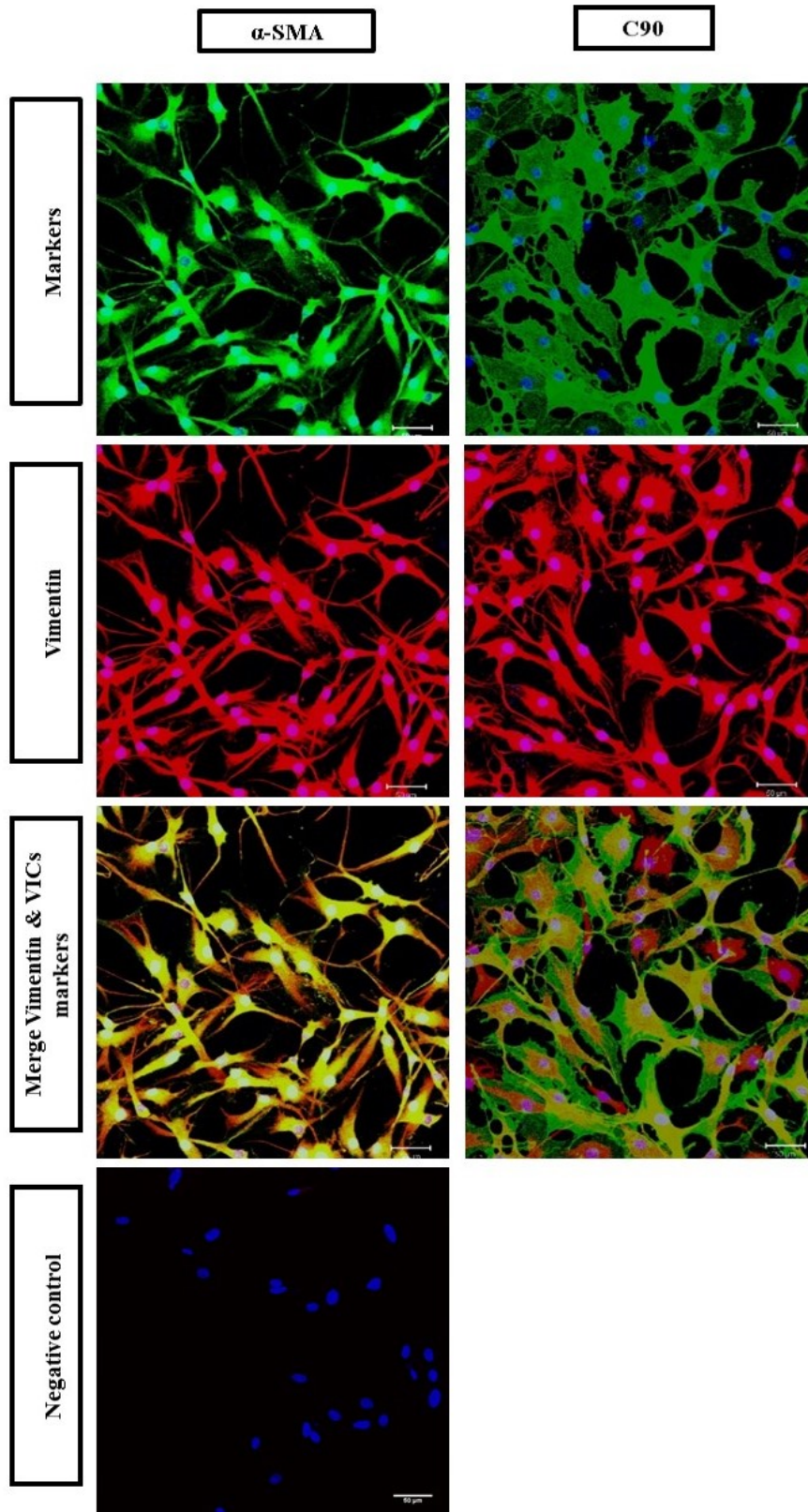


Figure 3-8: Confocal laser scanning microscopy of double-stain ICs isolated from aortic in P2: the first row represents CD90 and α -SMA (green), the second row represents Vimentin stain (red), the third row is merged images for both stains, and the last row is the negative control. The nucleus was counterstained with DAPI. X20, Scale bars present 50 μ m.

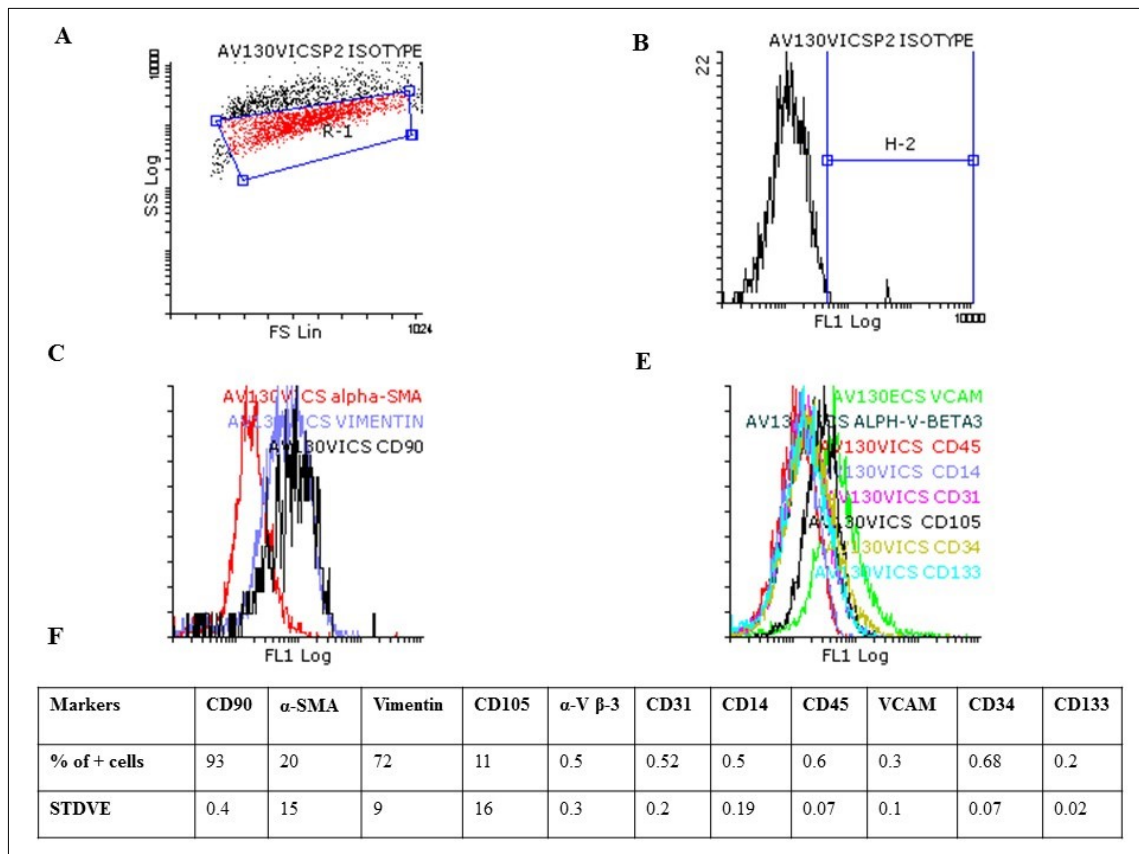


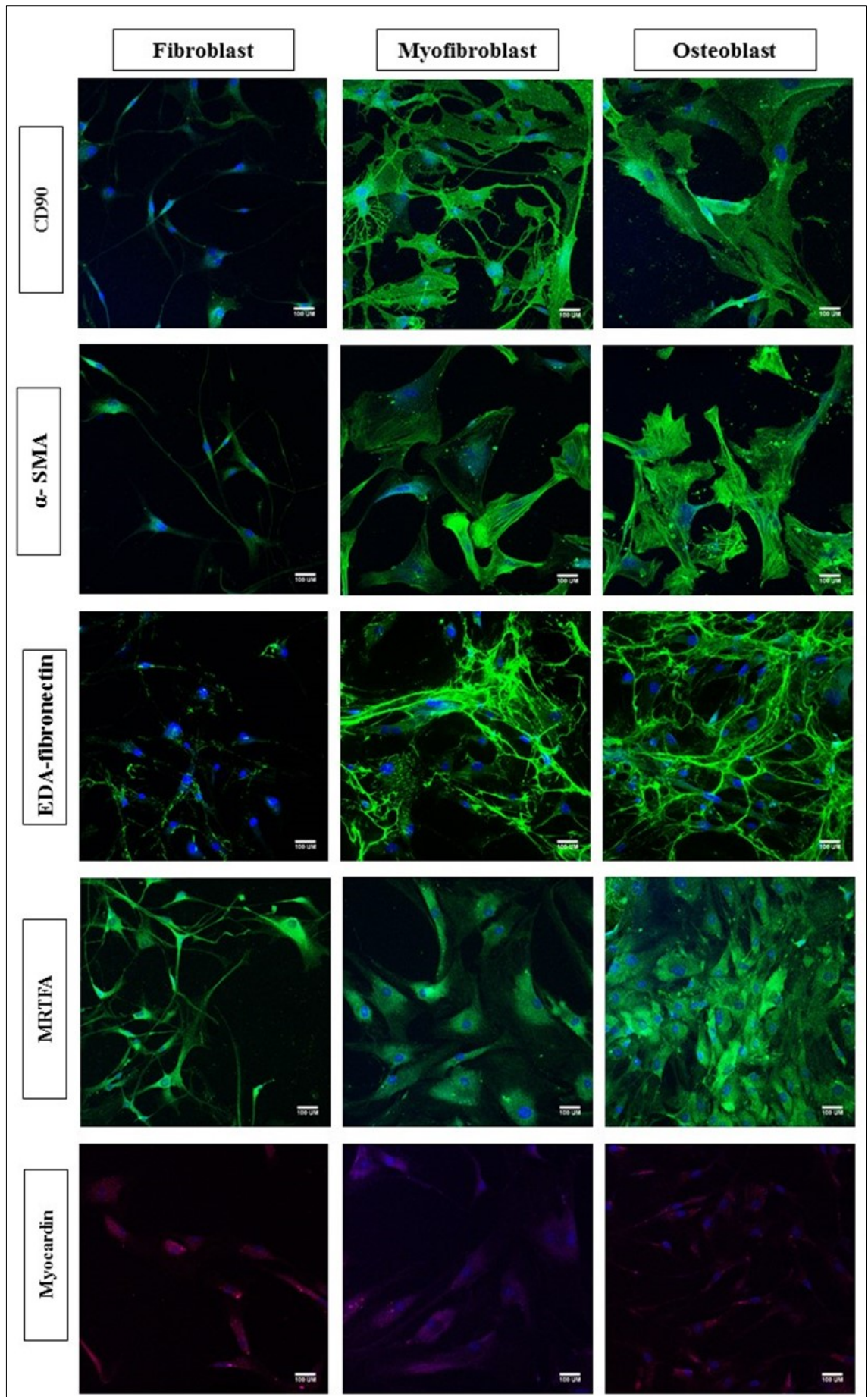
Figure 3-9: FACS analysis of VICs isolated from AV: A) a dot plot histogram of analysed cells. B) Histogram analysis of isotype as a negative control. C) Overlay showing the cell population expresses α -SMA, Vimentin and CD90. D) Overlay showing the cell population negative for VCAM, α -V β 3, CD45, CD14, CD31, CD105, CD34, and CD133. E) A summary of FACS analysis representing means + SD of data obtained from three different VICs.

3.4.4 Differentiation of Valve Interstitial Cells

It has been well established that valve interstitial cells can differentiate into myofibroblast and osteoblast (Chester and Taylor, 2007). The fibroblast media formulation (fibroblast media) provides a cells good model to investigate biological and pathological conditions of AV by preventing myofibroblastic differentiation and maintaining a fibroblastic phenotype of VICs (Latif et al., 2015). Therefore, VICs maintained in fibroblast media was used to compared to myofibroblast cells and osteoblast cells.

3.4.4.1 Myfibroblast Cells

Generally, fibroblasts isolated from different organs are differentiated into myofibroblasts in the culture of standard medium with 10% FCS and exhibited large cells with spread morphology. Therefore, isolated VICs from human and porcine valves become myofibroblasts and positive for α -SMA within one week of culture in standard culture medium with 10% FCS (Baum and Duffy, 2011). All myofibroblast markers including α -SMA, EDA-fibronectin, SM22, MRTFA, Myocardin, Calponin, and smooth muscle heavy chain (SMmyhc) were clearly reduced in VICs in fibroblast conditions compared to myofibroblastic and osteoblastic conditions. To begin, a stain of α -SMA, as a marker of myofibroblast, was reduced in VICs under the fibroblastic condition and strong staining in stress fibres under myofibroblastic and osteoblastic conditions. A focal adhesion protein EDA-fibronectin is a sign of myofibroblast differentiation (Latif et al., 2015), is markedly low in fibroblastic condition compared to myofibroblastic and osteoblastic conditions. In fibroblast condition, SM22, and Calponin were barely detectable and increased in myofibroblastic and osteoblastic conditions. VICs demonstrated lower staining of MRTFA, myocardia and SMmyhc in fibroblastic condition compared to myofibroblastic and osteoblastic conditions. However, no difference in the effect of fibroblast condition was observed on fibroblast surface antigen (FSA, CD90), and the stain was similar among the three groups. In terms of vimentin staining, long filaments were separated in the large body of VICs in myofibroblast media while in fibroblast media, and cells extensions are very thin and compressed; therefore, the staining was stronger (**Figure 3-10**).



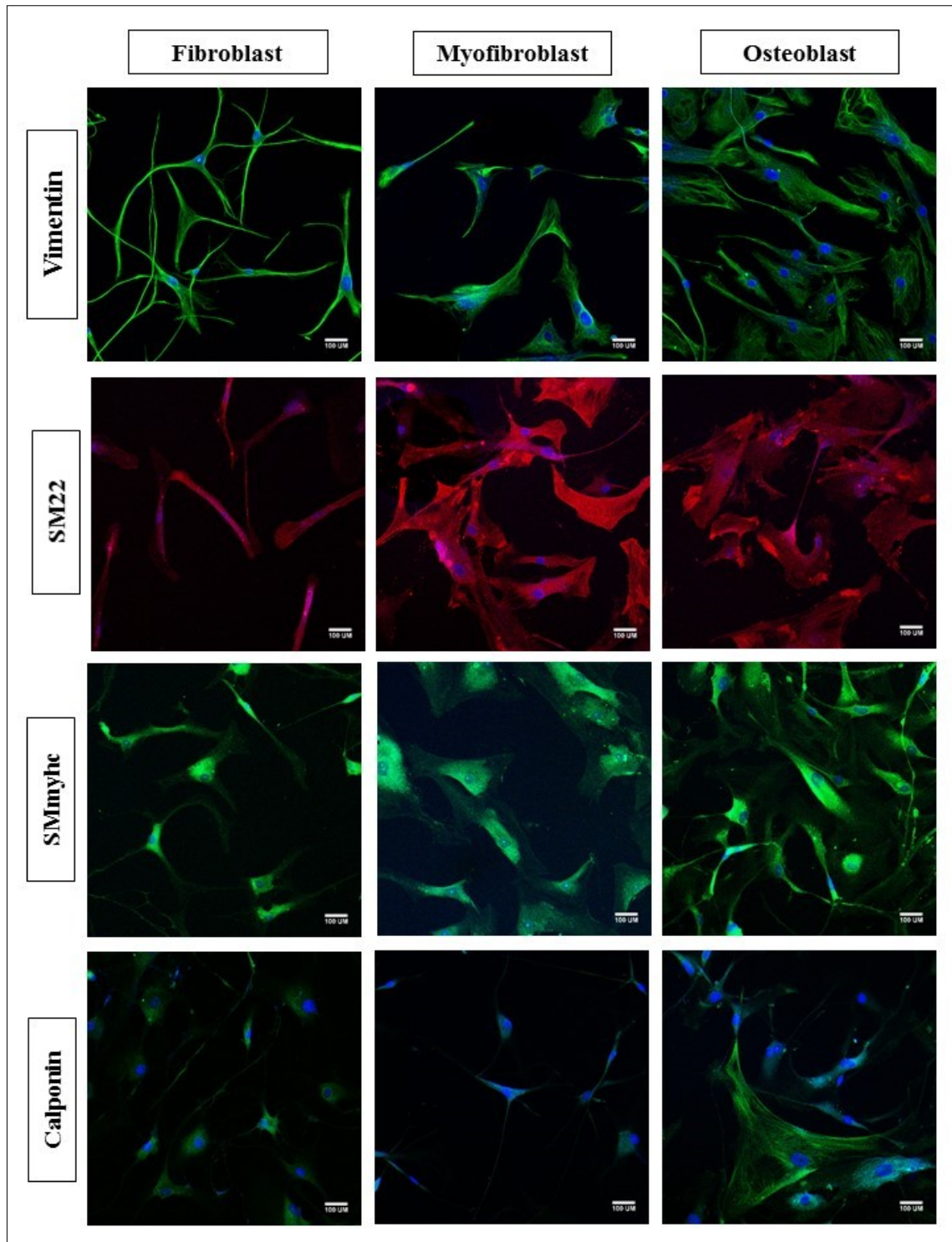
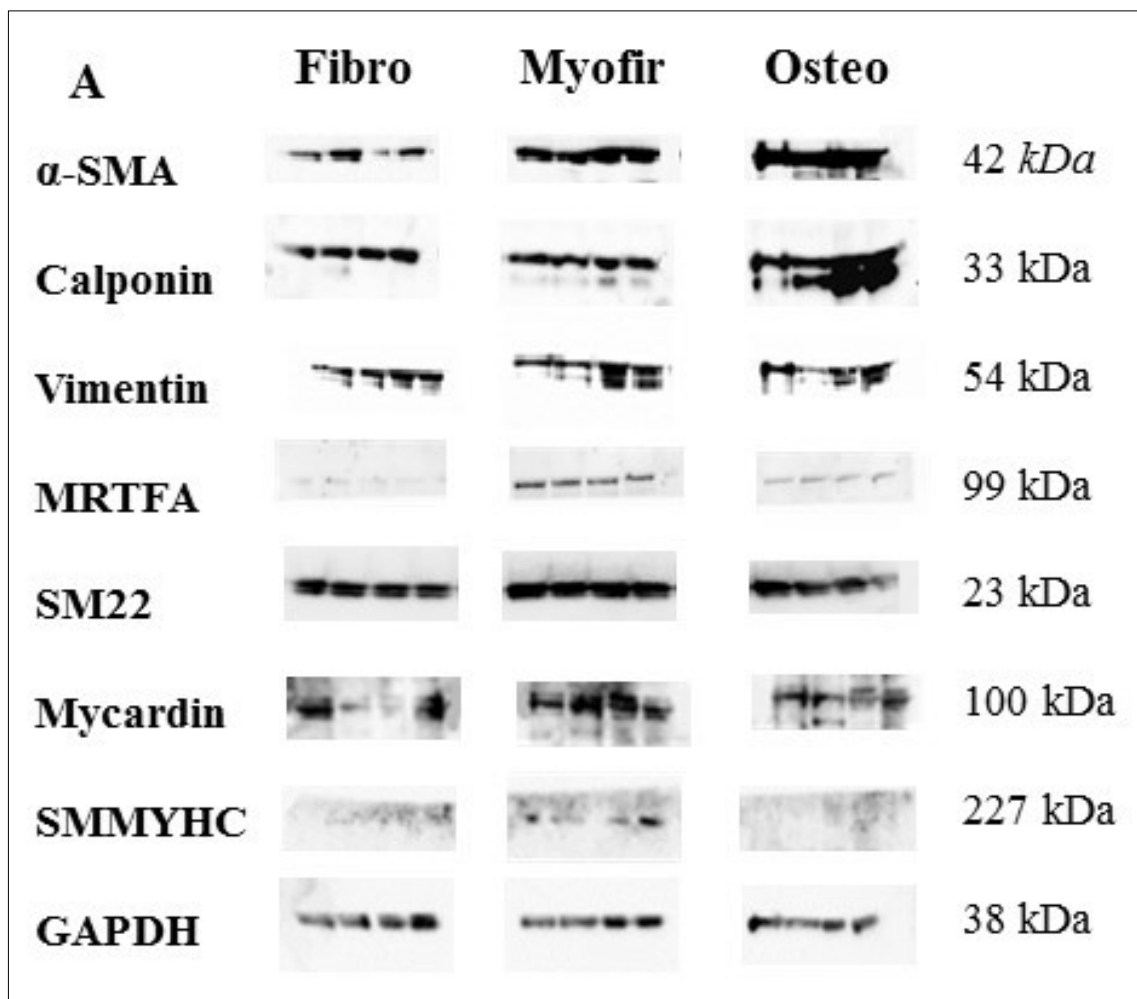


Figure 3-10. Confocal laser scanning microscopy of VICs stained with α -SMA (green), EDA-fibronectin (green), SM22 (red), Calponin (green), MRTFA (green), Myocardin (red), and SMMyhc (green), (FSA, CD90) (green), and vimentin (green) in fibroblast media (first column), myofibroblast media (second column), and osteoblast media (third column). The nucleus was counterstained with DAPI. X20; scale bars present 100 μ m.

Additionally, Western blotting was included to quantify the myofibroblast markers at the protein level. An equal amount of protein was loaded and expression was normalised to Glyceraldehyde 3-phosphate dehydrogenase (GAPDH). All Myofibroblast markers exhibited significantly reduced fibroblast compared to Myofibroblast and osteoblasts (Figure 3-11).



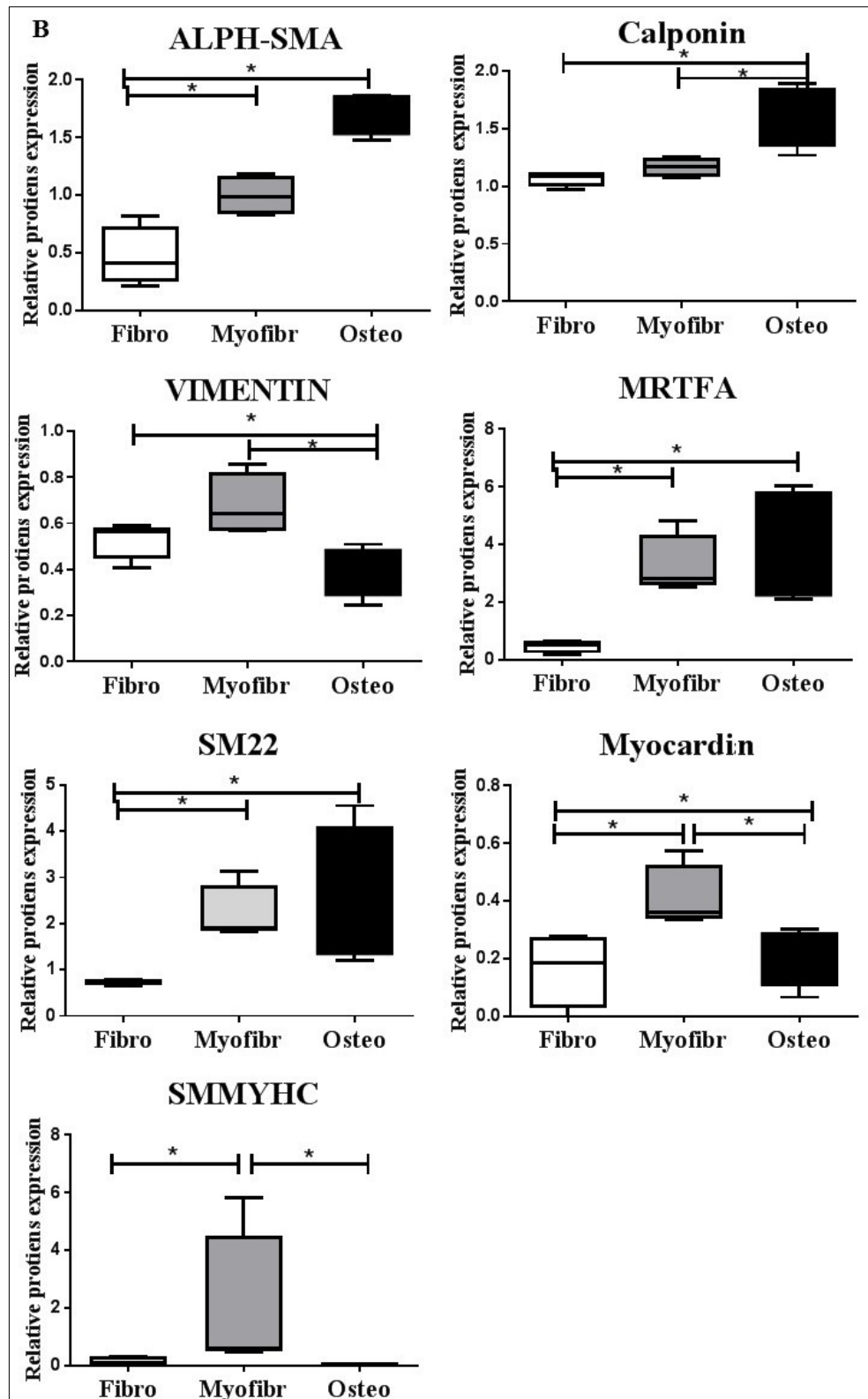


Figure 3-11: A) Western blots bands of fibroblast & myofibroblast markers in VICs in fibroblast media, myofibroblast media, and osteoblast media. B) Graphs are showing median levels of protein expression of fibroblast & myofibroblast markers in VICs in fibroblast media, myofibroblast media, and osteoblast media as assessed by Western blotting. The data-labelled fibre was cultured in fibroblast media, myofibroblast was cultured in standard media, and osteoblast was cultured in osteoblast media. One-way ANOVA followed by the Friedman test was used. Data are presented in the format of the box-and-whisker plot, n = 4. *P < 0.05.

3.4.4.2 Osteoblast Cells

The *in vitro* osteoblastic differentiation of VICs provides a useful model to investigate AV calcification. A considerable number of studies have published prominent findings regarding AV calcification based on this approach. As such, *in vitro* osteoblastic differentiation of VICs could be achieved by using appropriate stimuli. The most common and efficient stimulation is standard osteogenic medium, which is DMEM-supplemented with 1M of β -glycerophosphate, 10^{-6} M of dexamethasone, and 5mg/ml of ascorbic acid for 21 days. Calcification signs are typically flagged by expression of osteoblast markers such as RUNX2 and an increase in ALP activity. In this experiment, osteoblastic differentiation was induced and assessed in comparison to fibroblast and myofibroblast cells from the same samples. VICs differentiated into osteoblast showed clear signs of osteoblast cells compared to the other groups. Expression of osteoblast cells markers was assessed using immunostaining and Western blot. Immunostaining has shown high expression of osteopontin and RUNX2, osteocalcin, and ALP in osteoblast differentiation compared to fibroblast and myofibroblast cells, osteoblast markers were reduced in fibroblast and myofibroblast media but not quantified (**Figure 3-12**). At the protein level, osteopontin and RUNX2 were significantly upregulated in osteoblast differentiation compared to fibroblast and myofibroblast cells (**Figure 3-13**).

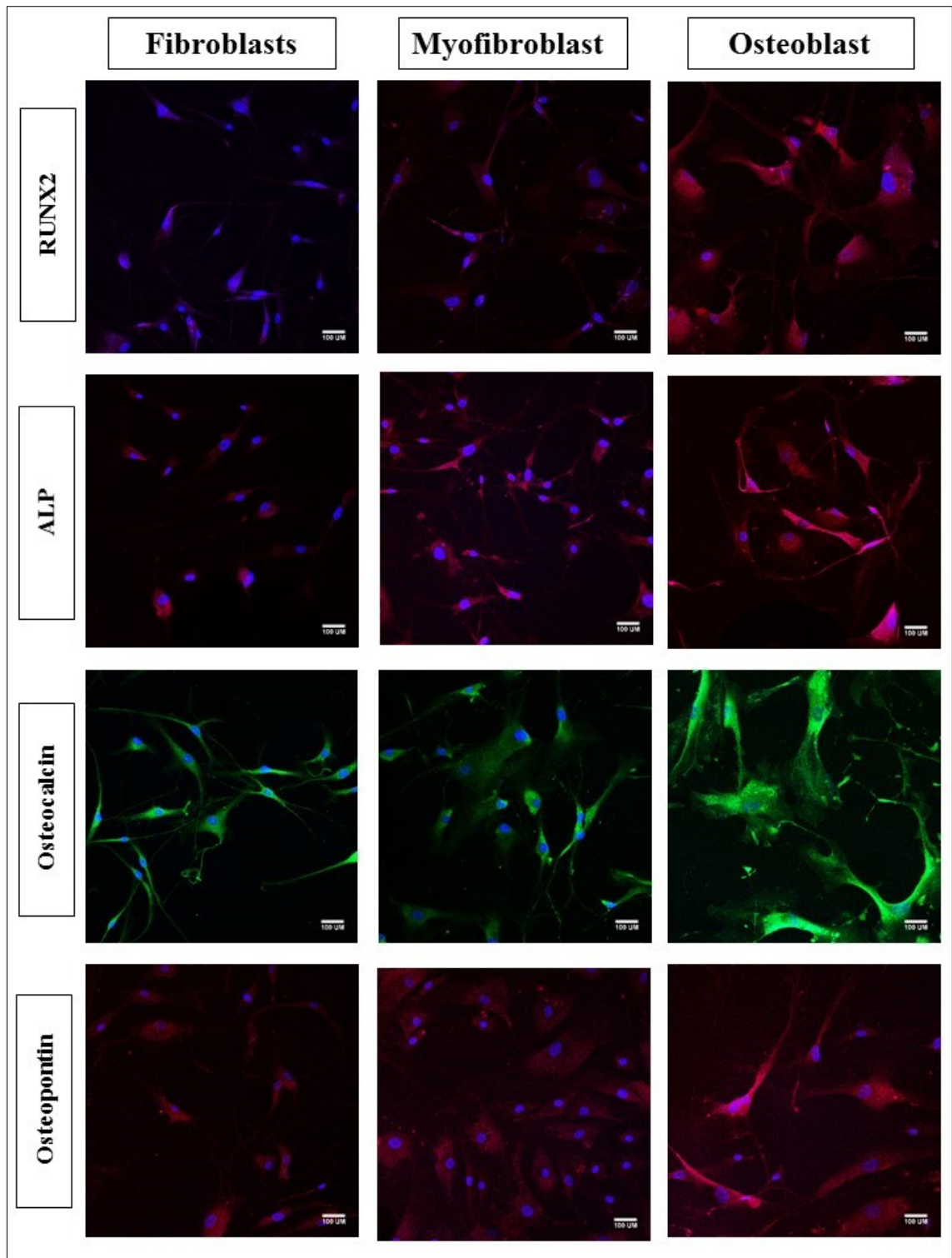


Figure 3-12. Confocal laser scanning microscopy (LSM 510 META) of VICs stained with RUNX2 (red), ALP (red), osteocalcin (green) and osteopontin (red), and in fibroblast media (first column), myofibroblast media (second column), and osteoblast media (third column). The nucleus was counterstained with DAPI. X20; scale bars present 100 μ m.

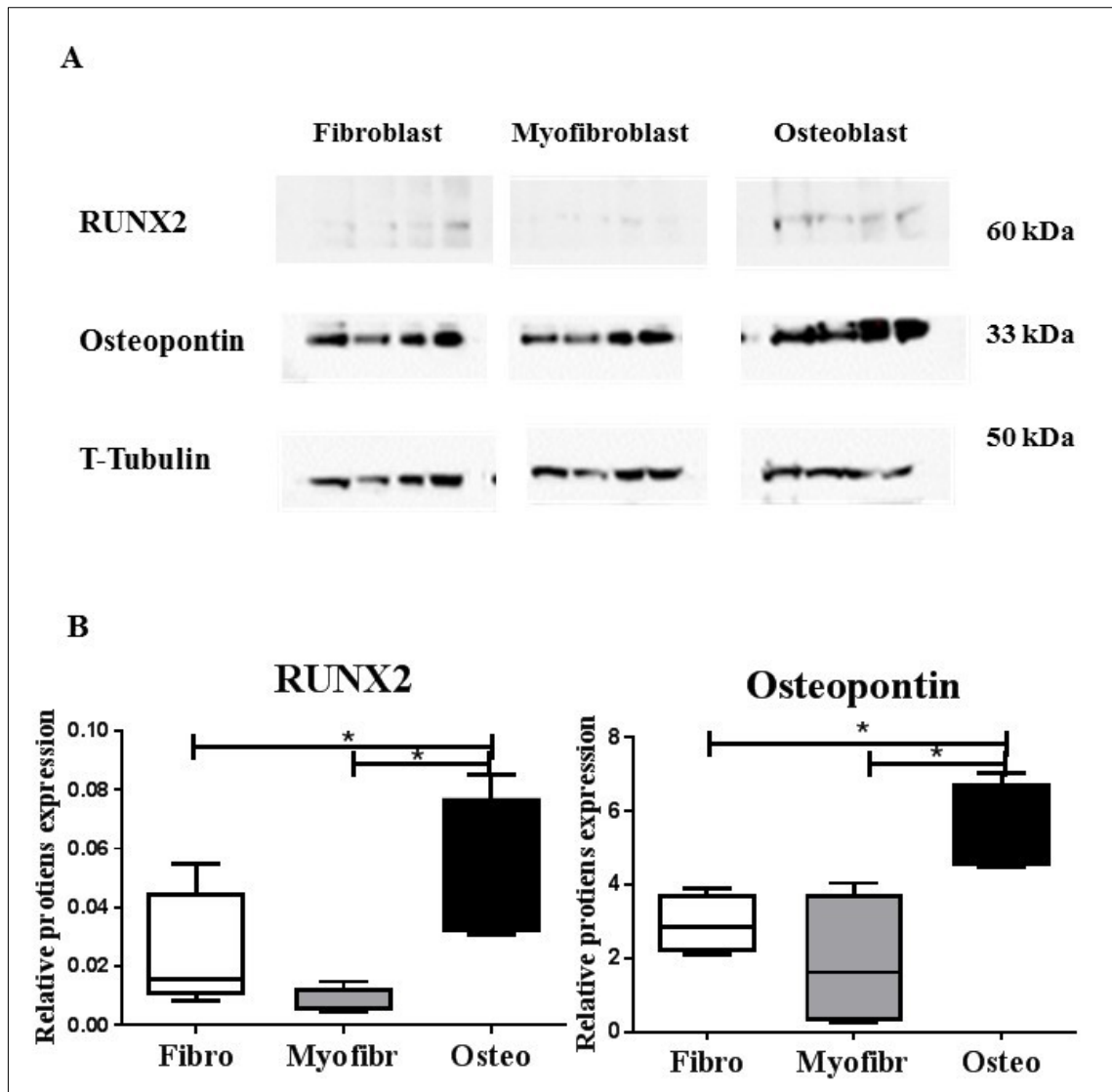


Figure 3-13. A) Western blots bands of Osteoblast markers in VICs in fibroblast media, myofibroblast media, and osteoblast media. B) Graphs are showing levels of protein expression of Osteoblast markers in VICs in fibroblast media, myofibroblast media, and osteoblast media as assessed by Western blotting. The data-labelled fibre was cultured in fibroblast media, myofibroblast was cultured in standard media, and osteoblast was cultured in osteoblast media. One-way ANOVA followed by the Friedman test was used. Data are presented in the box-and-whisker plot format, $n = 4$. * $P < 0.05$.

3.5 Discussion

The isolation of valve cells provides a useful tool for understanding diseases mechanisms and therapeutic strategies. In this study, VECs and VICs were successfully isolated from human AV according to a protocol that utilising the collagenase digestion (Taylor et al., 2000). The major practical concern of valve cell isolation is cross-contamination between VECs and VICs. Despite the many precautions of different methods, cross-contamination still represents up to 10% in VIC and VECs after isolation (Wang et al., 2013). Therefore, it was essential to separate VIC from VEC cultures via magnetic cell sorting based on CD31-positive selective cells.

Expression of a ‘pro-calcific’ genes is observed exclusively more in the VEC from the aortic side compared to the ventricular side, suggesting differences in the biological features of each side (Simmons et al., 2005). Thus, it is essential to study and phenotype side-specific endothelial cells separately. In the present study, isolation of side-specific endothelial cells was a fundamental step, which was practically successful. The device has been optimised to minimize cross-contamination between aortic and ventricular side. The collagenase volume was enough for only one side, and the other side was covered with glass slip. It is hoped that this method will help in further research regarding the differences of side-specific endothelial cells in their phenotypes and mechanical properties. These results must therefore be interpreted through a phenotypic study of site-specific endothelial cells in terms of endothelial markers and exclusion markers. Here, valve endothelial cells from both the aortic and ventricular side have similar expression patterns in terms of positive and negative markers. The side-specific endothelial cells are likewise expressed with intercellular adhesion molecules, integrin, and antigen. Additionally, exclusion markers were included in the FACS analysis to obtain greater accuracy and reliable analysis. One disadvantage of the FACS analysis is that it cannot distinguish between

VECs from each side of AV, due to the absence or presence of a specific marker. Despite the lack of a specific marker, different studies have demonstrated differences in site-specific endothelial cells in the AV. One study has shown that side-specific endothelial cells differ in their mechanical properties and that endothelial cells from the ventricular side were stiffer (less compliance) than endothelial cells from the aortic side (Miragoli et al., 2014). Another study noted a difference in their response to shear stress, oscillatory and laminar flow modulated production of collagen, and GAGs in a site-independent manner (Mongkoldhumrongkul et al., 2016). Interestingly, there was a significant difference in the proliferation rate between endothelial cells from the aortic and ventricular sides.

VICs are considered as experimental models to study disease condition due to their ability to differentiate into myofibroblasts and osteoblasts; this process imitates the pathological process in the body (Latif et al., 2015). Although the term “valve fibroblasts” is widely used, VICs should be used as the proper term due to their specific embryonic origin via endothelial-to-mesenchymal transformation (EMT) of valve progenitor cells in the endocardial cushions and their functional characteristic in the mechanical environment in which they function (Liu et al., 2007). In this study, the identity of isolated VICs was confirmed by a range of fibroblast markers that well-known expressed in VIC. However, mesenchymal stem cells and fibroblasts exhibit similar features including spindle-like morphology, adhesion to plastic, and similar expression patterns in several surface markers, Therefore, it is essential to include MSC-specific surface markers (Kundrotas, 2012). Furthermore, inflammatory cells such as macrophages are present in diseased heart valves; therefore, these cells types must be included in analysed cells and their presence must be assessed (Liu et al., 2007).

As previous studies have mentioned, VICs display the ability to differentiate into myofibroblasts and osteoblasts. Under certain culture conditions (DMEM+10% foetal calf serum) VIC spontaneously adopt a myofibroblast phenotype in culture. Myofibroblast differentiation, which may occur due to mediators such as transforming growth factors (TGFs) and bone morphogenetic proteins (BMPs) present in the serum, begins with the formation of stress fibres that are bundles of organized α -SMA (Latif et al., 2015). Previous studies of VICs have demonstrated the ability of VICs to differentiate from myofibroblasts into osteoblast-like, a process that occurs as part of the calcification process. Also, one study has indicated the presence of bone markers such as osteopontin and osteocalcin in VICs (Rajamannan et al., 2003). The exact molecular mechanisms of osteoblast differentiation are not fully understood, though bone morphogenetic protein (BMP)-2 and BMP-4 and transforming growth factor- (TGF-) 1 have been identified as mediators of osteoblast differentiation (Osman et al., 2006). In vitro treatment with osteogenic medium promotes the formation of calcifying colonies and nodules in VICs. The earliest signs of calcification include increased ALP activity and expression of the master transcriptional factor of the osteoblastic differentiation osteoblast-specific transcription factor Cbfa1 (RUNX2). Recently, a new approach was used to maintain the fibroblastic phenotype of VICs in culture and retain a low α SMA level over a prolonged period by using a specific fibroblast medium formulation (Latif et al., 2015). Previous experience in the Harefield Lab has shown that human VICs have a low proliferation rate (Chester and Taylor, 2007).

In this study, the fibroblast medium successfully maintains the fibroblastic phenotype of VICs and prevents their differentiation into myofibroblasts and reduction of myofibroblast markers were systematically observed after 7 to 10 days. This result is consistent with a study that confirmed a reduction in myofibroblast markers following treatment with

fibroblast medium formation (Latif et al., 2015). Myofibroblastic differentiation occurs in the standard culture medium, and the hallmark of myofibroblasts is α -SMA. Also, VICs were able to differentiate into osteoblasts with upregulation of osteoblastic markers such as RUNX2 and ALP. Osteoblast differentiation efficiency decreases with passage number; therefore, early cells passages were used in all experiments (Osman et al., 2006).

In conclusion, Fibroblast medium represents the optimal condition for studying VIC biology, which also implies that all studies of VICs in standard culture medium most likely studied myofibroblasts (Latif et al., 2015). Controlling phenotype of VICs is important to modulate the response of VICs in healthy or diseased valves. Therefore, all the experiments in this study were performed in VICs in fibroblast medium.

3.6 Limitations and Future Studies

The valve samples were obtained from the heart valve bank, all valves are considered unsuitable for clinical use due to contamination potential -; this source of valve samples is limited by the number and the quality of the valves sample. All valve samples were maximally utilized where some tissues were fixed and VECs and VICs were isolated and expanded in cell culture for further experiments. In spite of this, there were shortages of cells for experiments because all experiments were performed at low passage ($P < 5$). The isolation protocols of VECs and VICs were well-optimized and successful. In contrast, isolation of side-specific valve endothelial cells was not well-established. In the beginning, a custom made device was used. It was technically difficult to use, and the yield was too low. Therefore, a new filter was used, and the cell yield was good but there is a potential of mixing cell populations from both valve sides. In cell culture, VECs preferentially grow in their specific endothelial cell growth media and VICs grow in fibroblast medium and maintain their phenotype but their growth rate was often slow. This is often a problem of working with human cells from older people. The best prospect to improve this is to find a fibroblast medium that can increase the growth rate of VICs without affecting the phenotype of VICs.

In future, a new design of the device should be developed to isolate side-specific valve endothelial cells without the potential for contamination between cell populations from both valve sides. However, another limitation is the absence of site-specific markers for VEC. This problem would ultimately be resolved by the identification of a phenotypic marker that would differentiate VEC from each side of the valve. Currently, no such marker has been identified. Additionally, the fibroblast medium has to be improved to increase the growth rate of VICs without effects on or changes in fibroblast phenotype of VICs.

3.7 Conclusion

- The isolation of valve cells was successful and showed the ideal phenotype of VECs and VICs.
- VECs from aortic and ventricular side showed a similar phenotype.
- VICs exhibit plasticity that allows them to differentiate into myofibroblast and osteoblast.

Chapter 4

Expression of Stretch-Activated Channels in Valve Cells

4.1 Rationale

Heart valve interstitial and endothelial cells sense mechanical forces and translate them into inter-cellular signalling to regulate a range of different cell functions which contribute to the regulation of valve durability and function in both physiological and pathological conditions. While many functional responses have been reported, there is little information about how the cells sense changes in mechanical forces and translate them into a biological response (Arjunon et al., 2013). One of the potential ways this may occur is via the activation of ion channels that are sensitive to mechanical force, so-called stretch-activated channels (SACs) (Youm et al., 2005).

SACs form pores in the plasma membrane and opens in response to mechanical stimuli resulting in membrane stretch and/or membrane curvature. SACs generate currents across membranes by passively diffusing ions. SACs display ion selectivity based on the nature of the ions capable of passing through the selectivity filter. There are many published studies describing the presence of SACs and their roles in physiologic and pathologic states such as in cardiomyocytes SACs regulate polarisation and depolarise resting tissue functions (Reed et al., 2014). In recent years, growing evidence has been accumulated regarding the fundamental roles of potassium channels in SMCs and cardiomyocytes (Afzali et al., 2016). Different studies have shown a fundamental role of TRP channels in cardiovascular cell function. For example, down-regulation of TRPC6 or TRPM4 significantly reduces pressure-induced depolarisation in arterial smooth muscle and decreases the myogenic vasoconstriction in an intact cerebral artery (Afzali et al., 2016, Smani et al., 2015). Additionally, TRP channels have essential roles in VSMC growth and vascular remodelling, cardiac myocytes contraction, angiogenesis, and various vascular disorders (Smani et al., 2015).

However, their presence or function had not been examined in heart valves. Thus, the focus of this chapter is to define the expression of SAC on valve endothelial and interstitial cells, with regard to expression in valve interstitial cell phenotypes associated with healthy and diseased valves and the endothelial cells present on either side of the AV.

Based on their possible contributions to valve cell function and the availability of suitable antibodies and pharmacological probes, the following six SACs were selected to be investigated: four cation-non-selective channels (three members of the TRP family (TRPM4, TRPV4, and TRPC6) and piezo1) and two potassium channels (inwardly rectifying (KCNJ8) and two-pore-domain (KCNK2)). SACs were studied with respect to gene and protein expression, localisation and their electrochemical activity, using RT-PCR, western blotting and immunostaining and patch clamping.

4.2 The Specific Aims of This Chapter were to:

- Determine the expression and activity of SACs in side-specific valve endothelial cells.
- Determine the presence of SACs in valve interstitial cells.
- Study the effect of valve interstitial cell phenotype on the expression of SACs.

4.3 Methods

The general methods used in this chapter including western blot, immunocytochemical staining, and cell culture are listed previously described in Chapter 2. The methods specific for this chapter are described here.

4.3.1 Patch-Clamp

The patch-clamp technique was used to detect SACs activity in VECs and VICs from AV. Initially, the presence of SACs was studied in VICs and mixed isolation of VECs from both valve side. Then, the presence of SACs was investigated in side-specific VECs and differentiated VICs that maintained in specific media (described in Chapter 3). The recording was performed at room temperature with a patch-clamp amplifier (200B, Axon Instruments, FosterCity, CA, USA) and a Digidata 1440A interface (Axon Instruments). Currents recording was digitized at 3 kHz, low-pass filtered at 1 kHz and analysed with pCLAMP10.3 and ORIGIN9.1 software (Axon Instruments). The recordings were made in the cell-attached and inside-out patch-clamp mode (**Figure 4-1.**), and bath and pipette solutions previously described in (Peyronnet et al., 2013). Pipette medium contained: 150mM NaCl, 5mM KCl, 1mM CaCl₂, and 10mM HEPES (pH 7.4 with NaOH), 10 mM TEA (tetraethylammonium), and 5 mM 4-aminopyridine as a blocker of voltage-gated K⁺ (K_v) channel. 10 mM glibenclamide was added to inhibit putative contaminating potassium channels when potassium channels only recorded. The bath medium contained: 155mM KCl, 5mM EGTA, 3mM MgCl₂, and 10mM HEPES (pH 7.2 with KOH). Initially, the culture medium was removed and exchanged for the bath solution. Brief (500 ms) negative pressure pulses of 10 mm Hg increments were applied on membrane patches by the recording electrode and using a pressure-clamp device (ALA High-Speed Pressure Clamp-1 system; ALA Scientific, Farmingdale, USA). The holding voltage was -80 mV in all experiments. Pressure effect curves were fixed with a standard Boltzmann function

$(I = (I_{max} - I_{min}) / (1 + e^{(P - P_{0.5}) / k}) + I_{min})$, where I_{max} is the highest value of current, I_{min} is the lowest one and $P_{0.5}$ is the required pressure to get the half-maximal current activation. The kinetics of the current were set up at a standard exponential function at a pressure of -80 mm Hg.

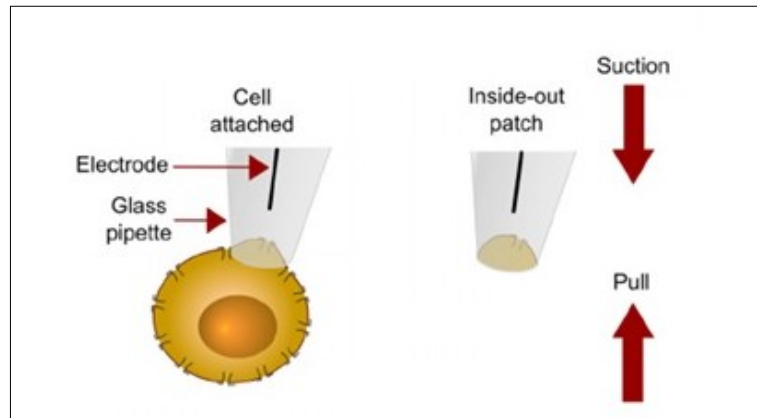


Figure 4-1. Illustration of the single-channel cell-attached and inside-out patch-clamp mode. The patch electrode remains sealed to the cell membrane, allowing the single-ion channels recording through the patch of membrane surrounded by the tip of the electrode. In inside-out patch, after the gigaseal is formed, the micropipette is quickly withdrawn from the cell, pulling off a patch of membrane from the cell, to rupture the cell membrane, hence allowing access to the intracellular space and cellular soluble contents will slowly be replaced by contents of the electrode.

4.4 Result

4.4.1 Expression of SAC in Valve Endothelial Cells

Presence of six SACs in mixed isolation of VEC from both valve side, including TRPM4, TRPV4, TRPC6, piezo1, KCNJ8, and KCNK2, were detected by western blot in VECs and the expression was consequently seen in all 6 isolates of VECs isolated from the aortic and mitral valve. Interestingly, quantitative analysis by western blot showed that the protein expression of SACs in VECs from AV was not similar to the same in the mitral valve where KCNK2 expression was significantly higher in VECs from the mitral valve than in VECs from the AV ($P < 0.05$). In contrast, KCNJ8 and Piezo 1 protein expression were more in VECs from AV than in VECs from the mitral valve but did not reach the significant level ($P=0.09$). The protein expressions of TRP channels including TRPM4, TRPV4, and TRPC6 were similar in VECs from aortic and ventricular valves (**Figure 4-2**).

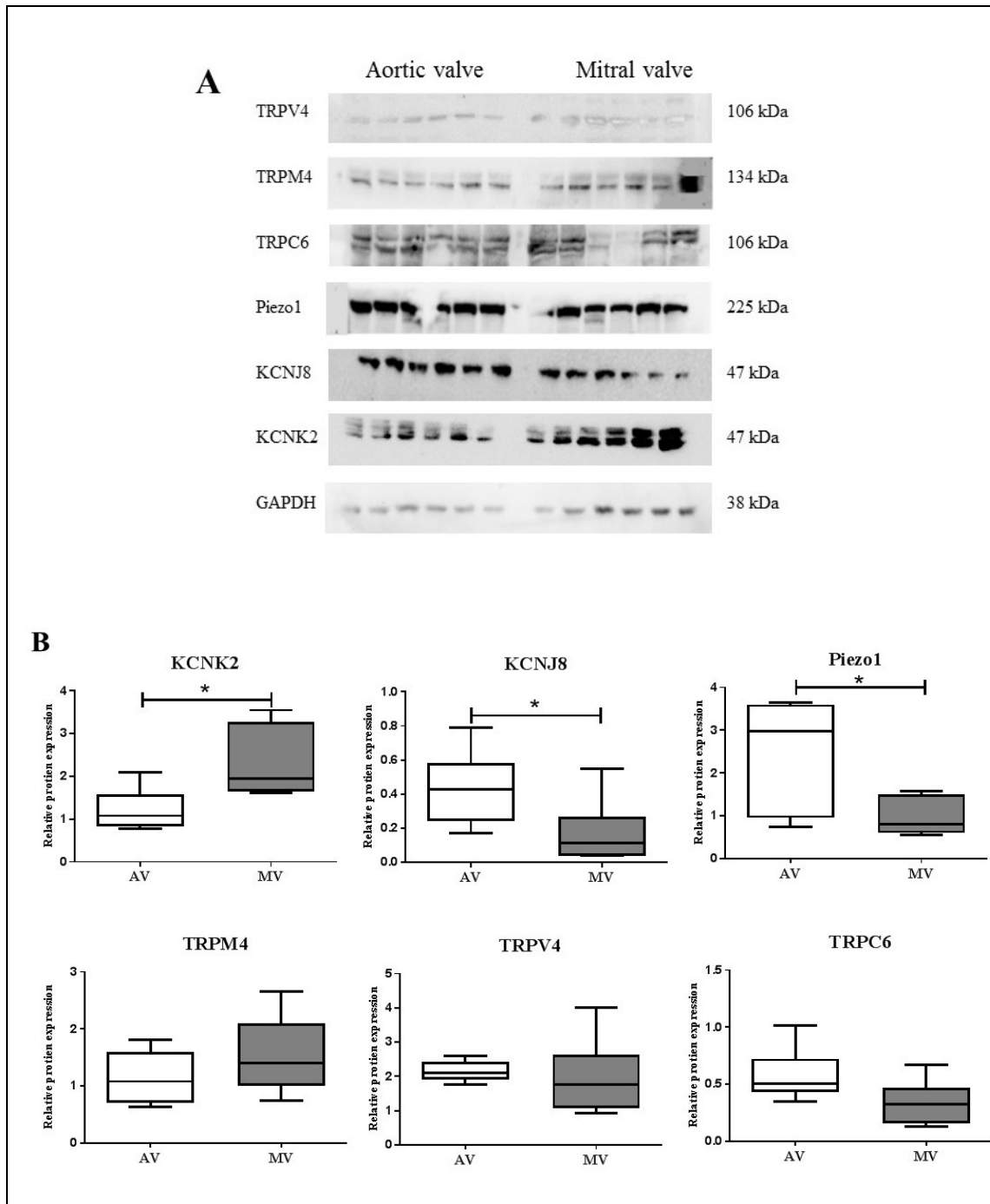


Figure 4-2. Protein expression of the SACs in VECs isolated from aortic and mitral valves. A) Western blot band of protein expression of TRPV4, TRPM4, TRPC6, Piezo1, KCNJ8, and KCNK2, in VECs isolated from aortic (AV) and mitral valves (MV). B) The corresponding charts SACs, KCNK2 was significantly less in the AV than in the MV and $p < 0.05$. KCNJ8 and Piezo1 expressions were more in the AV than in the mitral valve, and the p values are 0.0649 and 0.0649, respectively. In contrast, there were no significant differences in TRPM4, TRPV4 and TRPC6 expression between VECs isolated from AV and MV. The values were statistically analysed by t-test and Friedman test and presented in the box-and-whisker plot format, $n = 6$. * $P < 0.05$.

The antibodies of KCNK2, KCNJ8, TRPM4, and Piezo1 gave only one band at the specific molecular weight, whereas TRPC6 and TRPV4 gave multiple bands and were not used in immunostaining due to the non-specificity binding. Immune-fluorescence stain of Piezo 1, TRPM4, KCNK2, and KCNJ8 stretch-activated channels in VECs from AV shown strong expression of these channels in the cytoplasm and nucleus of all the cells (**Figure 4-3**).

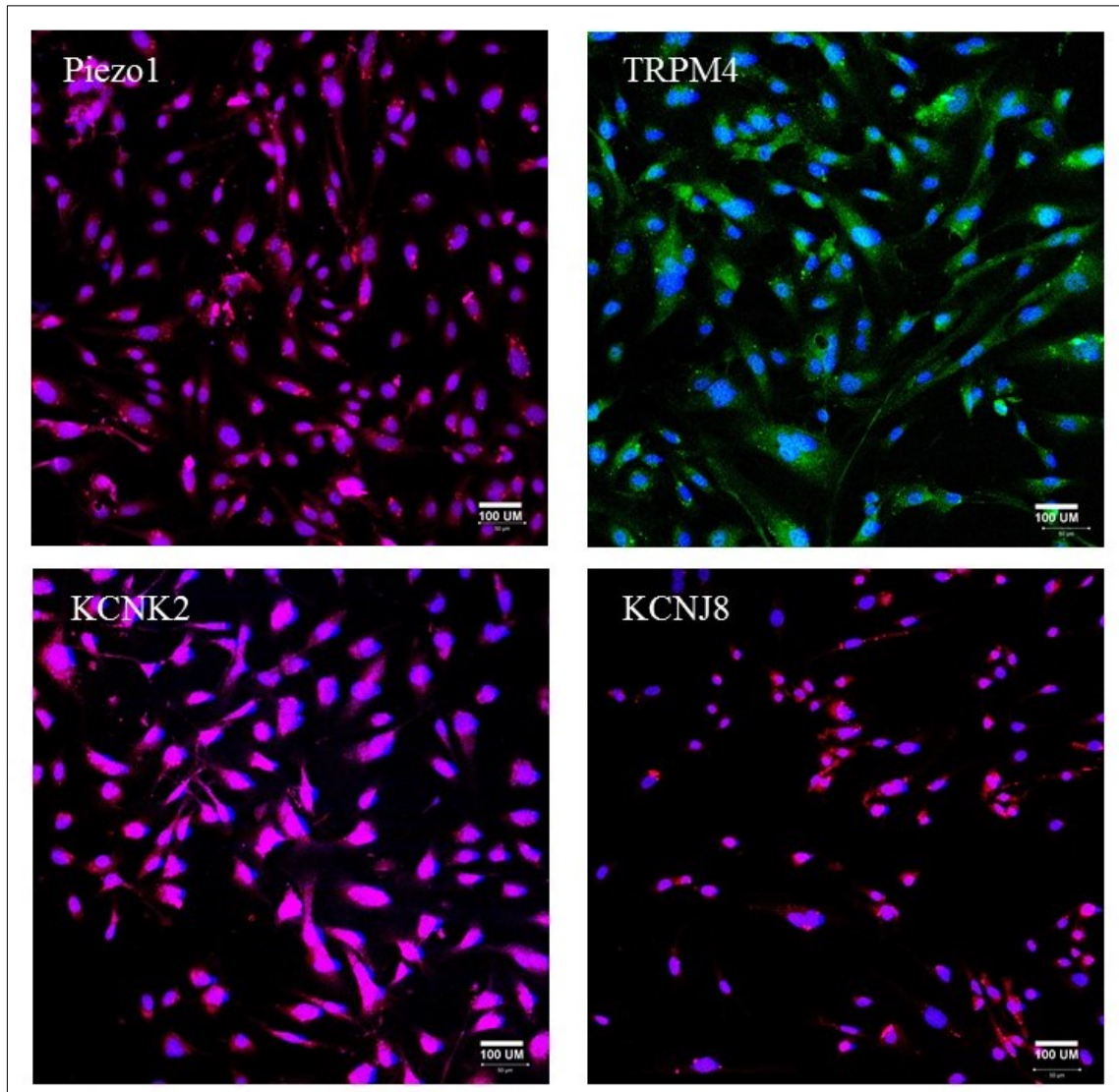


Figure 4-3. Confocal microscopy of the immune-fluorescence stain of SACs in VECs from AV and P2 stained with Piezo 1 (red), TRPM4 (green), KCNK2 (red), and KCNJ8 (red). Nucleus counterstained with DAPI. Scale bar represents 100 μ m.

4.4.2 Channel Activity in Valve Endothelial Cells

Electrophysiologically, SACs activity was recorded by patch clamping VEC isolated from AV. The membrane potential was held at -80 mV and 200 ms negative pressure pulses were applied via the recording electrode to activate SAC. There was an activity of cationic non-selective channels in VEC from AV which increased in response to increases in negative pressure pulses applied to the membrane (**Figure 4-4**).

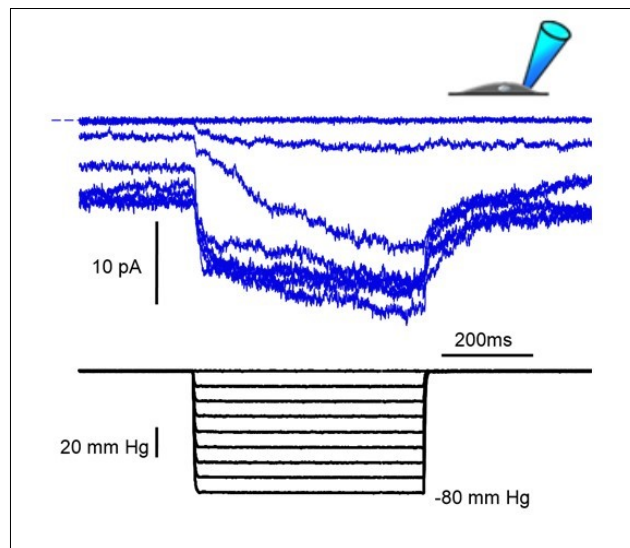


Figure 4-4. Patch-clamp recordings of cultured VECs from AV. Cationic non-selective stretch-activated channels are active on EC from AV. The upper tracings show the cell-attached mode (see insets) recorded currents activated in response to 200-ms long negative pressure pulses from 0 to -80 mm Hg in increments of -10 mm Hg (lower tracings), Membrane potential was clamped at -80 mV. (Experiment is performed with Dr Remi Peyronnet assistance).

4.4.3 SACs Expression in Side-Specific Valve Endothelial Cells

Shear stress on the ventricular side of the valve is laminar and estimated to be approximately 80 dynes/cm² during systole, whereas on the aortic side and is a disturbed pattern of flow with a maximum value estimated to be 20 dynes/cm during diastole (Yap et al., 2012a, Yap et al., 2012e). The different environment in which VECs on each side function could affect the expression and activity of SAC. Therefore the expression of SACs in VECs from the aortic and ventricular side was compared. SAC expression was semi-quantified with western blots, which showed that the relative expression levels of

KCNK2, KCNJ8 and Piezo1 were significantly higher in VEC from the ventricular side compared to the aortic side, whereas the expression of TRPM4, TRPC6 and TRPV4 were similar in VECs from both sides of the valve (**Figure 4-5**).

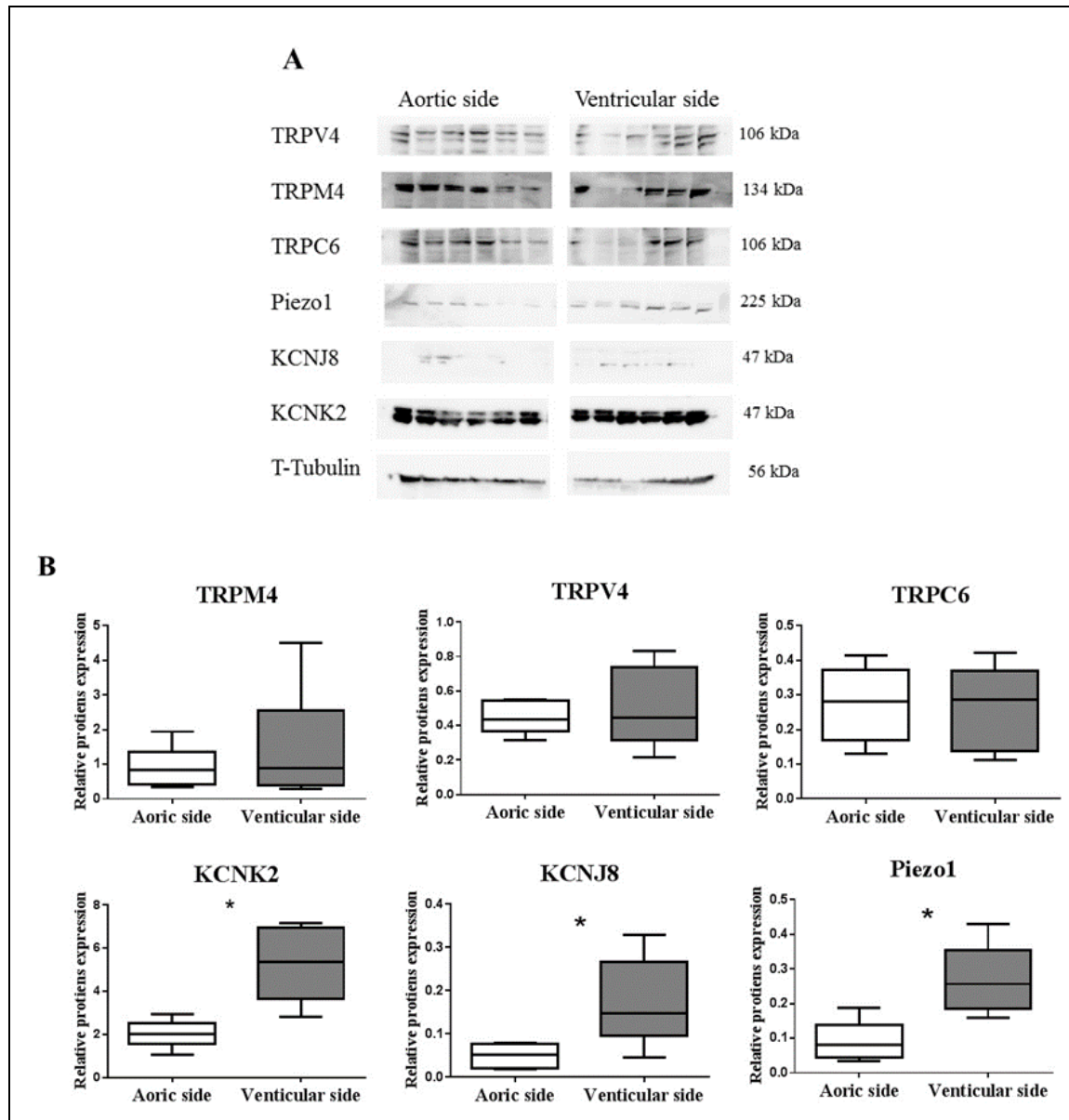


Figure 4-5. SACs expression in VECs isolated from aortic and ventricular sides. A) Western blots bands of TRPM4, TRPV4, TRPC6, KCNK2, KCNJ8 and Piezo1 channels at predictable molecular weights. B) The corresponding charts showed that there were no differences in TRPM4, TRPV4 and TRPC6 expression between VECs from aortic and ventricular sides. In contrast, the expression of KCNK2, KCNJ8 and Piezo1 expression was significantly greater in VECs from the ventricular side than the aortic side of the AV, $p < 0.05$. The values were statistically analysed by t-test and Friedman test. Data are presented in the box-and-whisker plot format, $n = 6$. * $P < 0.05$.

Immuno-fluorescence staining showed that the expression of KCNK2, and Piezo1 channels were stronger in VECs isolated from the ventricular side than VECs isolated from the aortic side, whereas KCNJ8 was similar on VECs from both sides (**Figure 4-6**).

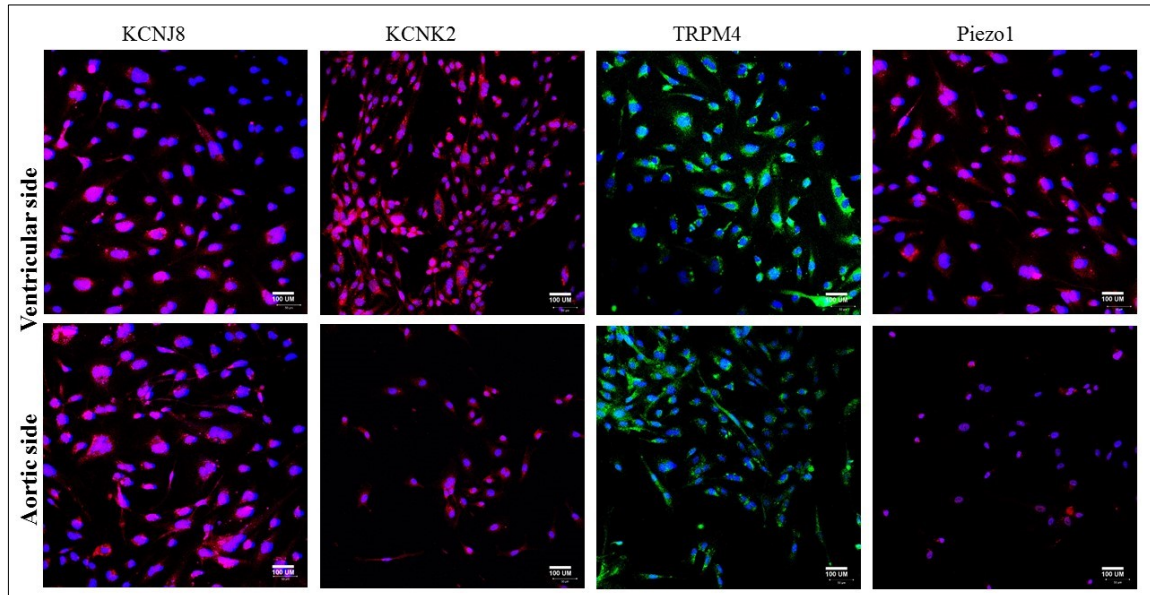


Figure 4-6. Confocal images of the immuno-fluorescence stain of SACs including KCNK2, KCNJ8, TRPM4 and Piezo1 in valve endothelial cells from the aortic side (first row) and ventricular side (second row). Scale bar represents 100 μ m.

4.4.4 SACs activity in Side-Specific Valve Endothelial Cells

SAC activity is similar in valve endothelial cells isolated from aortic and ventricular valve sides. The averaged recordings currents increased in response to increases in negative pressure pulses applied to the membrane. The averaged recordings of cationic non-selective stretch-activated channels were similar in patch current amplitudes between VECs isolated from the ventricular side and the aortic side (**Figure 4-7**). Also, the peak currents recorded during the stimulation was similar in VEC isolated from aortic and ventricular side (**Figure 4-8**).

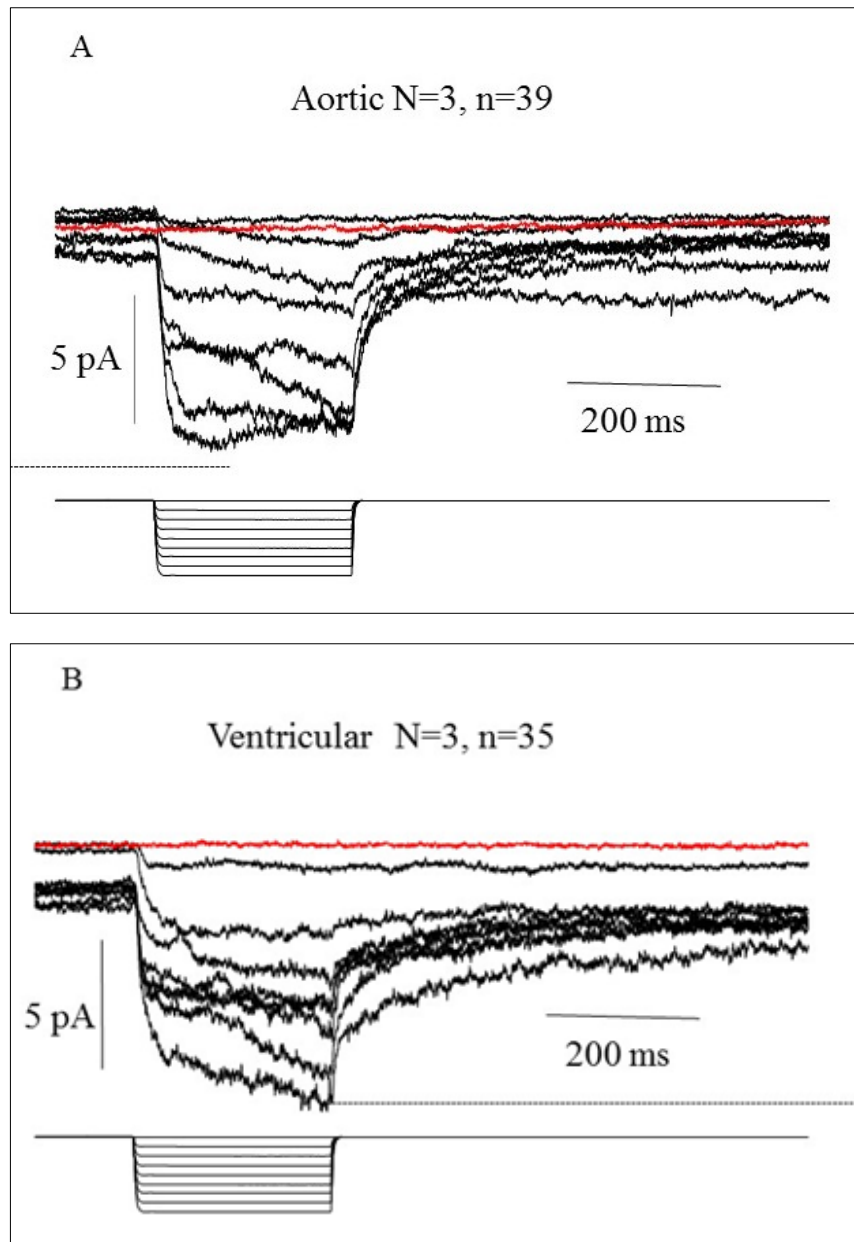


Figure 4-7. SACs currents are recording in side-specific VECs isolated from the aortic and ventricular side. A) Averaged recordings currents of SACs in three isolates of VECs isolated from the aortic side, n=39 (where n is recording number in every isolate). B) Averaged recordings currents of SACs in three isolates of VEC isolated from the ventricular side, n=35 (where n is recording number in every isolate). The upper tracings showed the cell-attached mode recorded (insets) and activated in response to 200-ms long negative pressure pulses from 0 to -80 mm Hg in increments of -10 mm Hg, and lower tracings are a holding potential of -80 mV. (Experiment is performed with Dr Remi Peyronnet assistance).

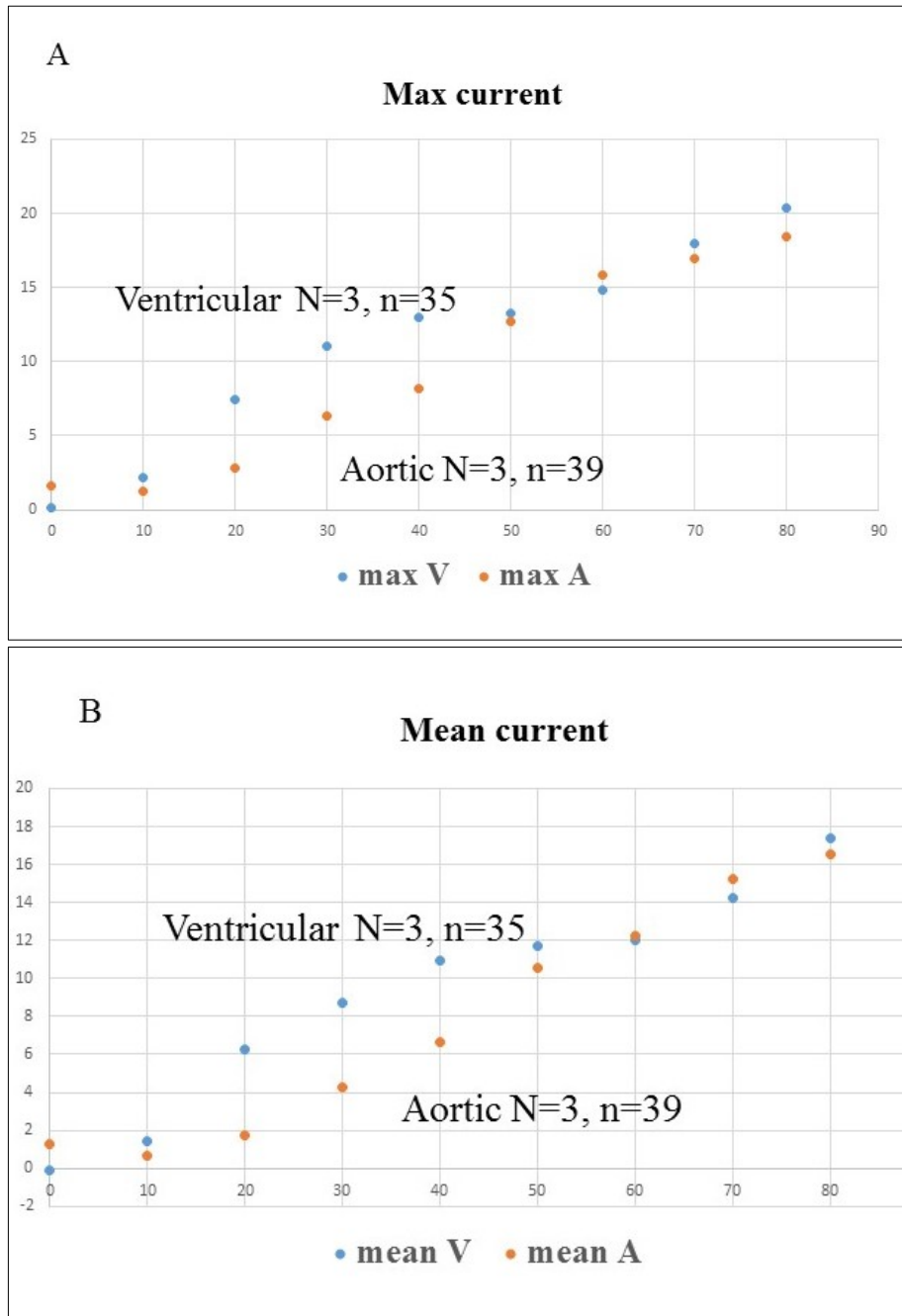


Figure 4-8. The relation between relative current and pressure of side specific VEC isolated from the human AV. A) Peak currents recorded during the stimulation of VEC isolated from aortic (max A in red) and ventricular side (max V in blue). B) A mean current recorded during the pulse of pressure in VEC isolated from aortic (mean A in red) and ventricular side (mean V in blue). Recordings were obtained from 3 isolates and in 39 recordings. Student t-test was used, data are presented in the format of mean \pm SEM, $P < 0.05$. (Experiment is performed with Dr Remi Peyronnet assistance).

4.4.5 SACs Expression in Valve Interstitial Cells

The SAC TRPM4, TRPV4, TRPC6, Piezo1, KCNJ8, and KCNK2 were all expressed in VICs from aortic and mitral valves. The results of western blot analysis are presented in **(Figure 4.9)**. All the channels were present in all isolates of VICs from aortic and mitral valves except KCNJ8 was absent in 3 isolates of both aortic and mitral valve VICs. Analysis of the relative levels of expression showed that there are no significant differences in expression of TRPM4, TRPV4, TRPC6, piezo1, KCNJ8, and KCNK2 channels between VICs from the aortic and mitral valves.

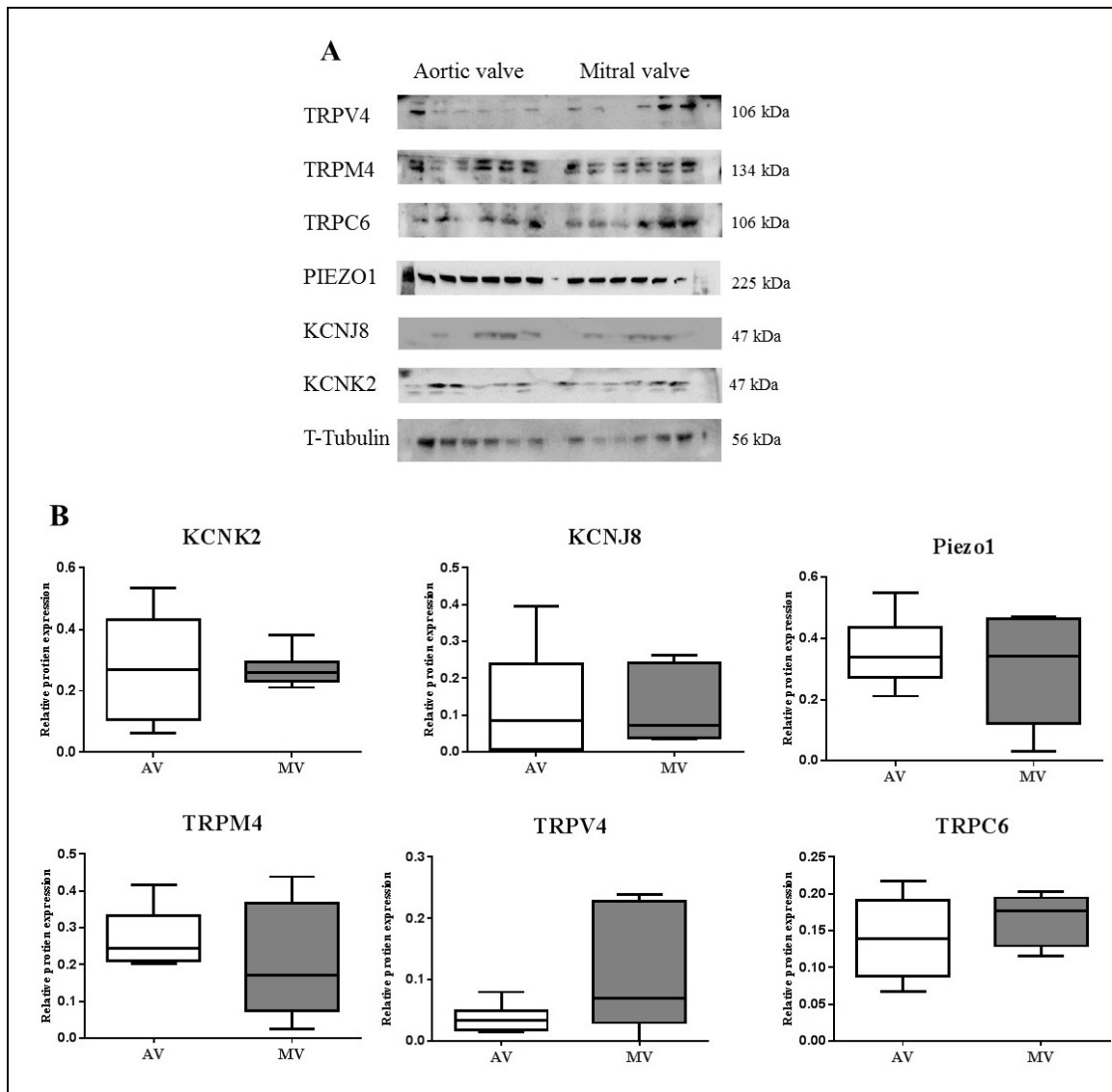


Figure 4-9: Protein expression of the SACs in VICs isolated from aortic (AV) and mitral valves (MV). A) Western blot bands of TRPV4, TRPM4, TRPC6, Piezo1, KCNJ8, and KCNK2 channels in VICs isolated from aortic and mitral valves. B) Charts of corresponding western blot band showing the relative protein expression of the SACs in VICs isolated from aortic and mitral valves. The expressions of KCNK2, KCNJ8, Piezo1, TRPM4, TRPV4, and TRPC6 in AV were similar to the mitral valve. The values were statistically analysed by t-test and Mann Whitney test. Data are presented in the box-and-whisker plot format, n = 6. *P < 0.05.

4.4.6 SACs Activity in Valve Interstitial Cells

Electrophysiologically, using patch-clamping I detected cationic non-selective stretch-activated channels activities of SACs at -80 mV mode in VICs isolated from AV. There was an activity of cationic non-selective channels in VIC from AV which increased in response to increases in negative pressure pulses applied to the membrane (**Figure 4.10**).

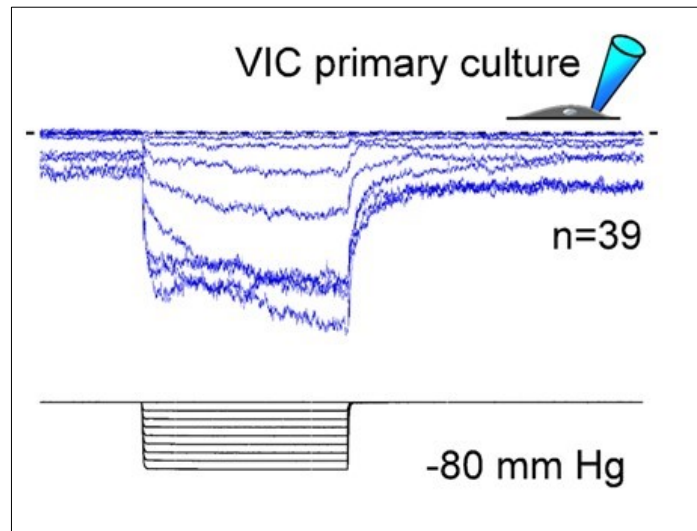


Figure 4-10: Patch-clamp experiments performed on VIC using cell-attached mode at -80 mV. The first trace reveals the presence of a stretch-activated channel cationic non-selective current. The second trace shows the applied pressure. Average recordings of 39 and 30 cells are presented. (Experiment is performed with Dr Remi Peyronnet assistance).

4.4.7 SACs Expression in The Differentiation of Valve Interstitial Cell

As shown in Chapter 3, VICs are present in different phenotypes and can differentiate / de-differentiate from one phenotype to another under varying conditions, including development, normal physiological conditions, repair and pathological conditions. VICs may be present in three phenotypes, including fibroblast VICs predominant in healthy valves, myofibroblast VICs that occur at the early stages of diseases in remodelling valves, or osteoblastic VICs which are present in calcifying valves. Changes in proteins expressions of SACs were compared among three phenotypes using western blot. Interestingly, there were significant differences in TRPC6, TRPV4, TRPM4, KCNK2, and KCNJ8 protein expression in different VICs phenotype. KCNK2 and KCNJ8 were

expressed in fibroblast cells and their expression significantly decreased upon differentiation into myofibroblast and osteoblast VICs. In contrast, the protein expressions of TRP channels including TRPM4, TRPV4, and TRPC6 were significantly upregulated upon differentiation into myofibroblast and osteoblast. The expression of Piezo 1 channels was not changed in the three VICs phenotypes (**Figure 4-11**). Also, the immunofluorescence stain images in (**Figure 4-12**) show expression patterns similar to western blot, where expression of KCNK2 and KCNJ8 were weak upon myofibroblast and osteoblast differentiation and TRPM4 was stronger in myofibroblast and osteoblast differentiation; no changes in Piezo1 expression appeared among the three phenotypes. In summary, expression and activity of SACs were increased in the differentiation of VICs to osteoblast cells, this could be important to understand the pathophysiological status of valve calcification in which abnormal SACs are involved.

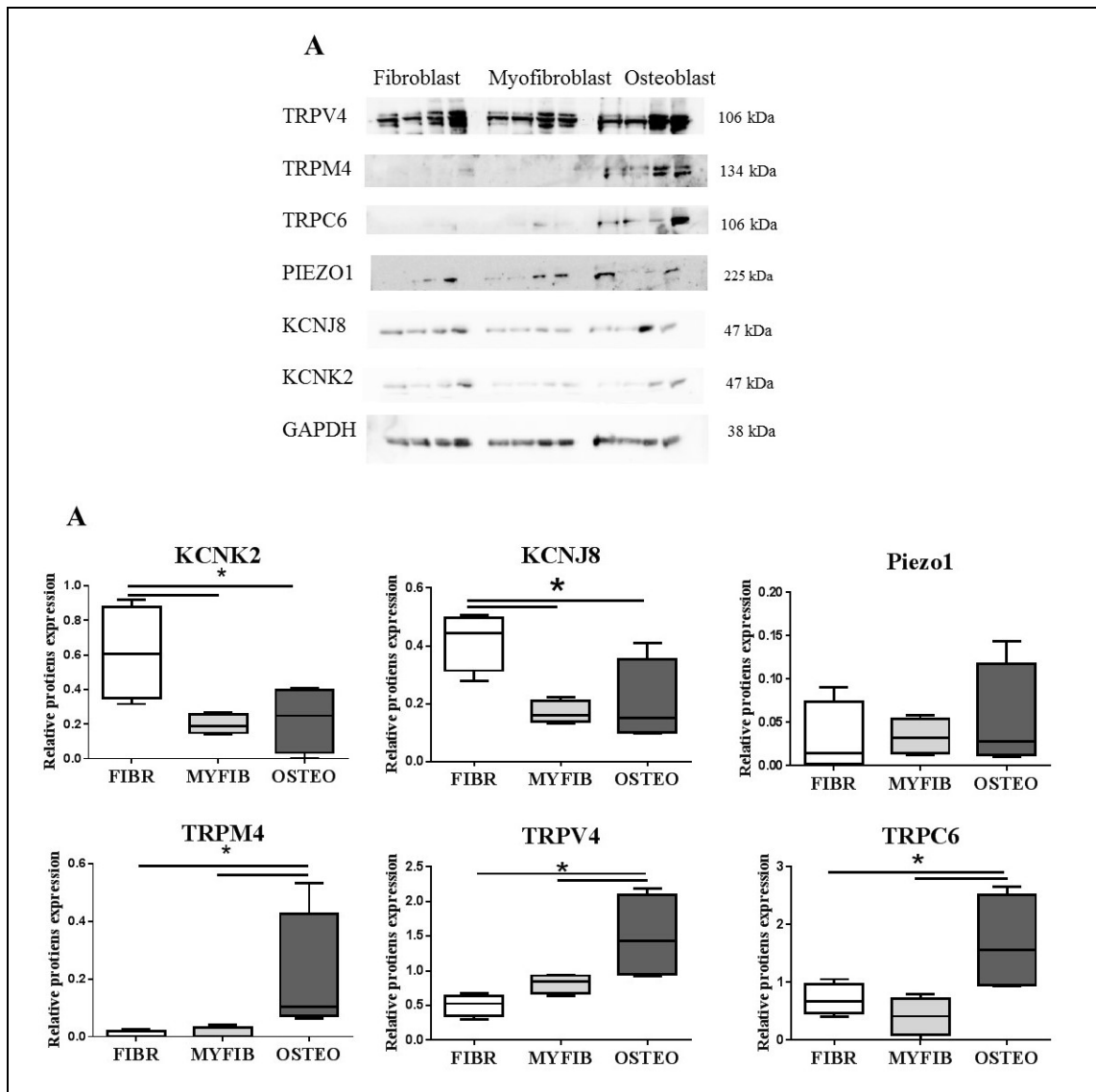


Figure 4-11: A) Western blot band at predicted molecular weights of protein expression of SACs in three VICs phenotypes. B) Bar charts show the relative protein expression of SACs in three VICs phenotypes of corresponding. One-way ANOVA followed by the Friedman test was used. Data are presented in the box-and-whisker plot format, $n = 4$. * $P < 0.05$.

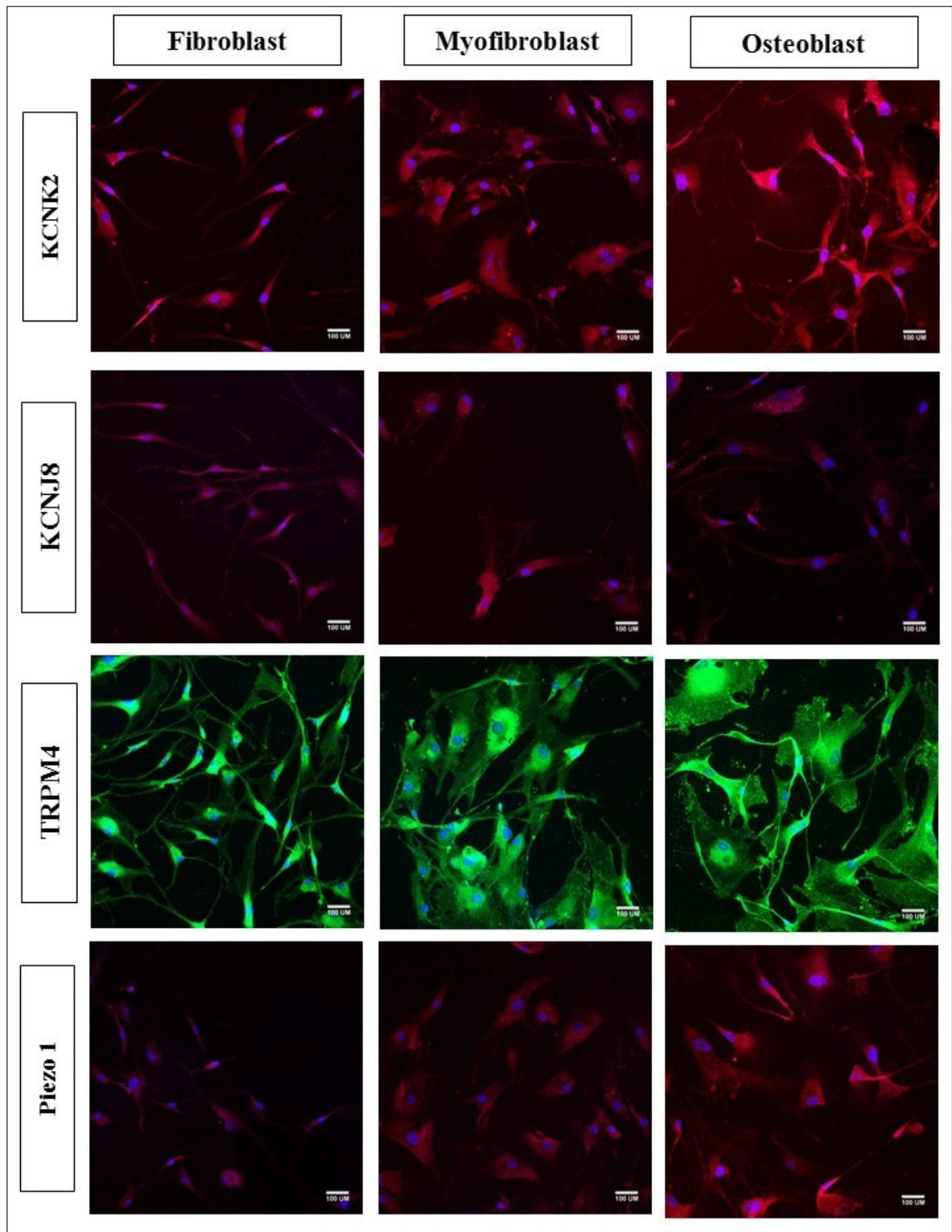


Figure 4-12: Confocal microscope images of the immuno-fluorescence stain of SACs in VICs in three phenotypes: fibroblast (left column), myofibroblast (middle column), and osteoblast (right column).

4.4.8 SACs Activity in The Differentiation of Valve Interstitial Cells

The activities of SACs channels current were assessed by a patch-clamp to compare the activity of SACs in fibroblast VICs, myofibroblast VICs, and osteoblastic VICs to test the potential effect of VICs differentiation on channel activity. Fibroblastic and myofibroblastic VICs displayed the same channel activity. Interestingly, the osteoblastic and fibroblast conditions showed similar current amplitudes, but ion channel kinetics were changed. Osteoblast VIC was more sensitive to stretch and was activated significantly faster compared to VICs cultured in the fibroblast media: $P_{0.5}$ (the pressure required to obtain half-maximal current activation) was -38.5 ± 1.0 mm Hg for fibroblast VIC, compared to -49.8 ± 1.1 mm Hg for osteoblast VIC. In addition, in osteoblastic conditions, recordings displayed an increase in SAC mediated current during the increase of constant pressure stimuli at all pressure levels, unlike cells in fibroblast condition where the activity of the channel did not increase after increase pressure stimuli (**Figure 4-13**).

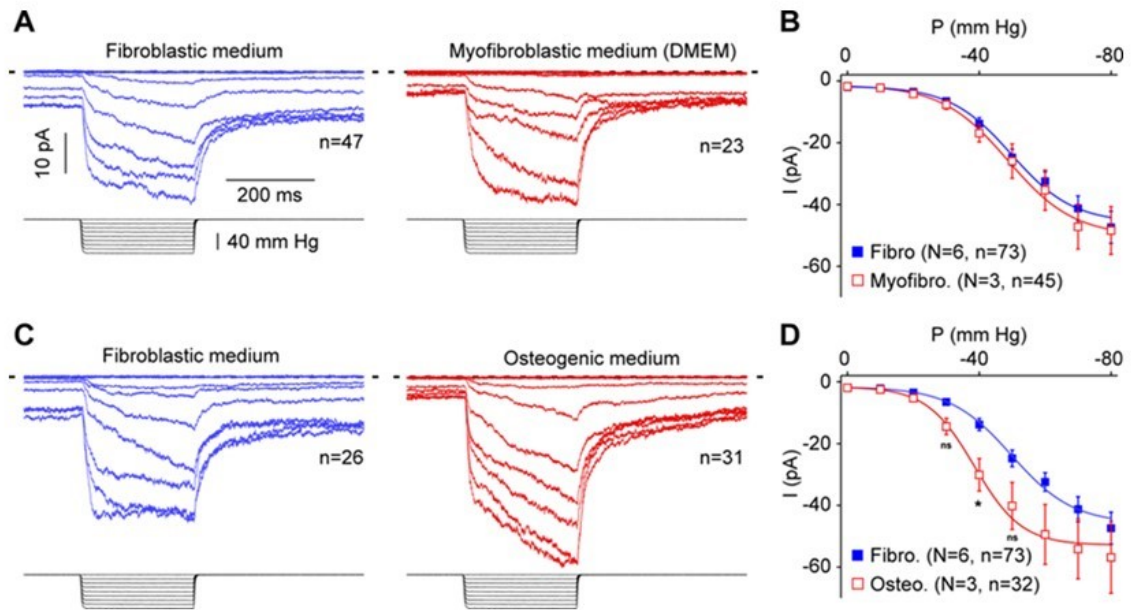


Figure 4-13: Recordings of cation non-selective channels of VICs in Fibro, DMEM and osteogenic media from passage 1 to 4-5. A) Averaged recordings from VIC fibroblastic (6 isolates, n=73) and in myofibroblastic medium cells (3 isolates, n=45). B) Average currents obtained during pulses of pressure from VIC cultured in the two media. The cell-attached patch configuration was used and channels were stimulated by 250-ms long negative pressure pulses from 0 to -80 mm Hg in increments of -10 mm Hg (lower tracings) at a holding potential of -80 mV. C) Recordings obtained upon similar stimulation in fibroblastic and osteogenic media. D) Corresponding averaged currents obtained upon pulses of pressure from VIC cultured in the two media. Student t-test was used, data are presented in the format of mean \pm SEM, $P < 0.05$. (Experiment is performed with Dr Remi Peyronnet assistance).

In parallel, activities of stretch-activated potassium-selective channels were recorded. In a single-channel cell-attached patch-clamp mode where it was possible to see some single channel openings in osteoblast VICs and fibroblast VICs as a control group (**Figure 4-14A**). Interestingly, the activity, from the same patch of membrane, was strongly enhanced when changing to the inside-out configuration (**Figure 4-14B**). These stretch-activated potassium-selective channels were induced after excision, as demonstrated in (**Figure 4-15**). The percentage of cells activated by negative pressure steps without inactivation and slow deactivation is significantly more in the osteoblast VIC than in the fibroblast VIC (**Figure 4-16**). In conclusion, differentiation of fibroblastic VICs to myofibroblast VICs

did not affect the activity of SACs, but their differentiation to osteoblasts affects channel kinetics and currents.

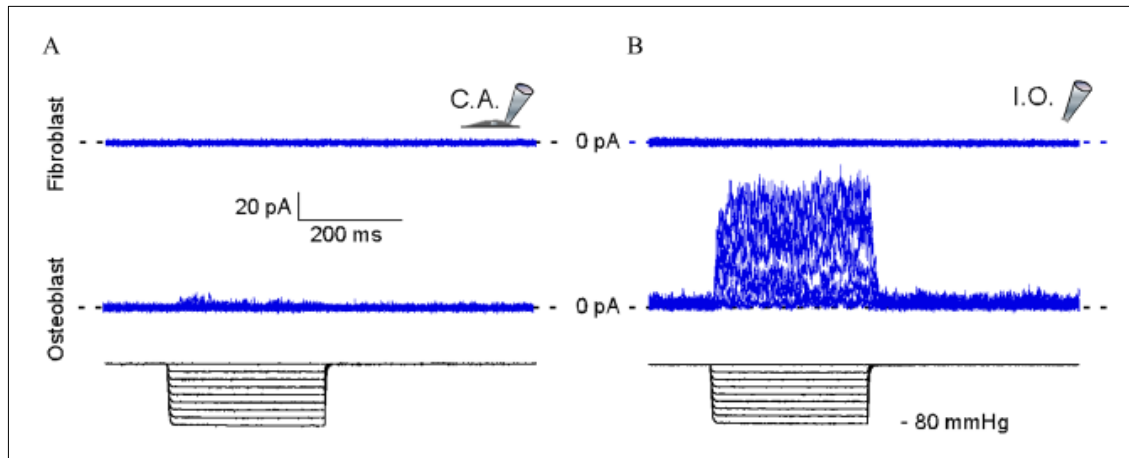


Figure 4-14: Representative recordings of potassium channels obtained from VIC in fibroblastic and osteogenic media. A) No channel opening was observed in cell-attached mode (C.A) in fibroblastic conditions (upper trace) while some single channels event were detected in the osteogenic medium (lower trace). B) Representative recordings obtained in the inside-out configuration from VICs in fibroblastic (upper trace) and osteogenic (lower trace) media. The membrane potential was held at 0 mV. The pressure protocol is similar to what was described previously. (Experiment is performed with Dr Remi Peyronnet assistance).

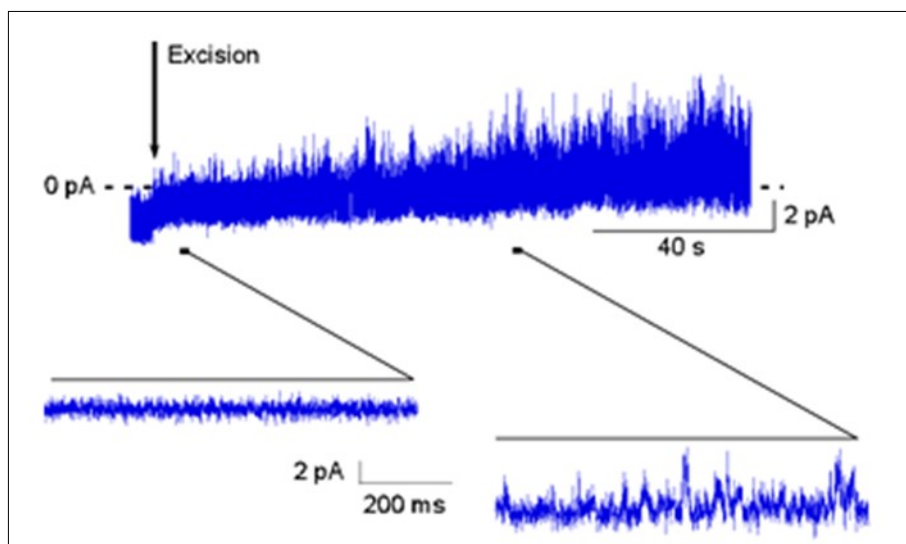


Figure 4-15: A representative trace of a potassium-selective stretch-activated channel before and after excision of a VIC in osteoblast condition. No activity is detected at the beginning of the recording (bottom left inset) and strong activation is observed upon excision. (Experiment is performed with Dr Remi Peyronnet assistance).

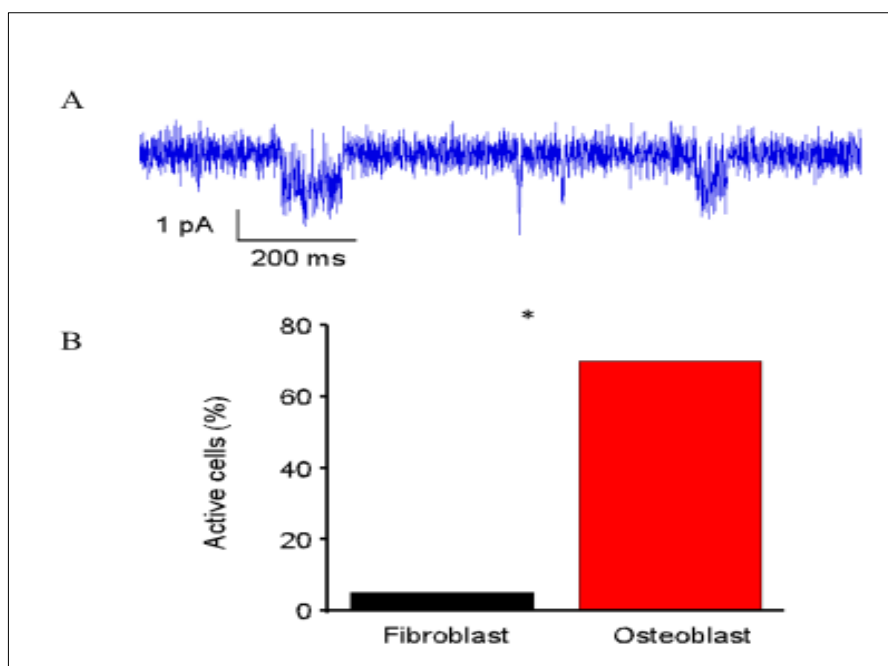


Figure 4-16: A) Representative single-channel events. B) Percentage of active cells from VICs cultured in the fibroblastic vs osteogenic media. Student t-test was used, data are presented in the format of mean \pm SEM, $P < 0.05$. (Experiment is performed with Dr Remi Peyronnet assistance).

4.4.9 Expression of SAC in Valve Tissues Samples

In order to assess if the expression of SAC obtained in cultured valve cells, was also the case of intact tissue samples, expression studies were conducted on samples of AV tissue from patients without AV calcification. Immunohistochemical staining paraffin sections of fixed AV tissues indicated that SACs are present in valve intestinal and endothelial cells. The expression patterns of the SACs were different in endothelial cells between the aortic and ventricular sides, where KCNK2, KCNJ8 and Piezo1 channels were expressed a greater extent on the ventricular side compared to the aortic side of the valve, but there is no difference in TRPM4, TRPV4, and TRPC6 channel expressions. Also, KCNK2, KCNJ8, Piezo1, TRPM4, TRPV4, and TRPC6 were all present in VICs, but not all VICs were expressed these channels. Together, these results provide important insights into the role of SACs in regulating the function of valve cells (**Figure 4-17**).

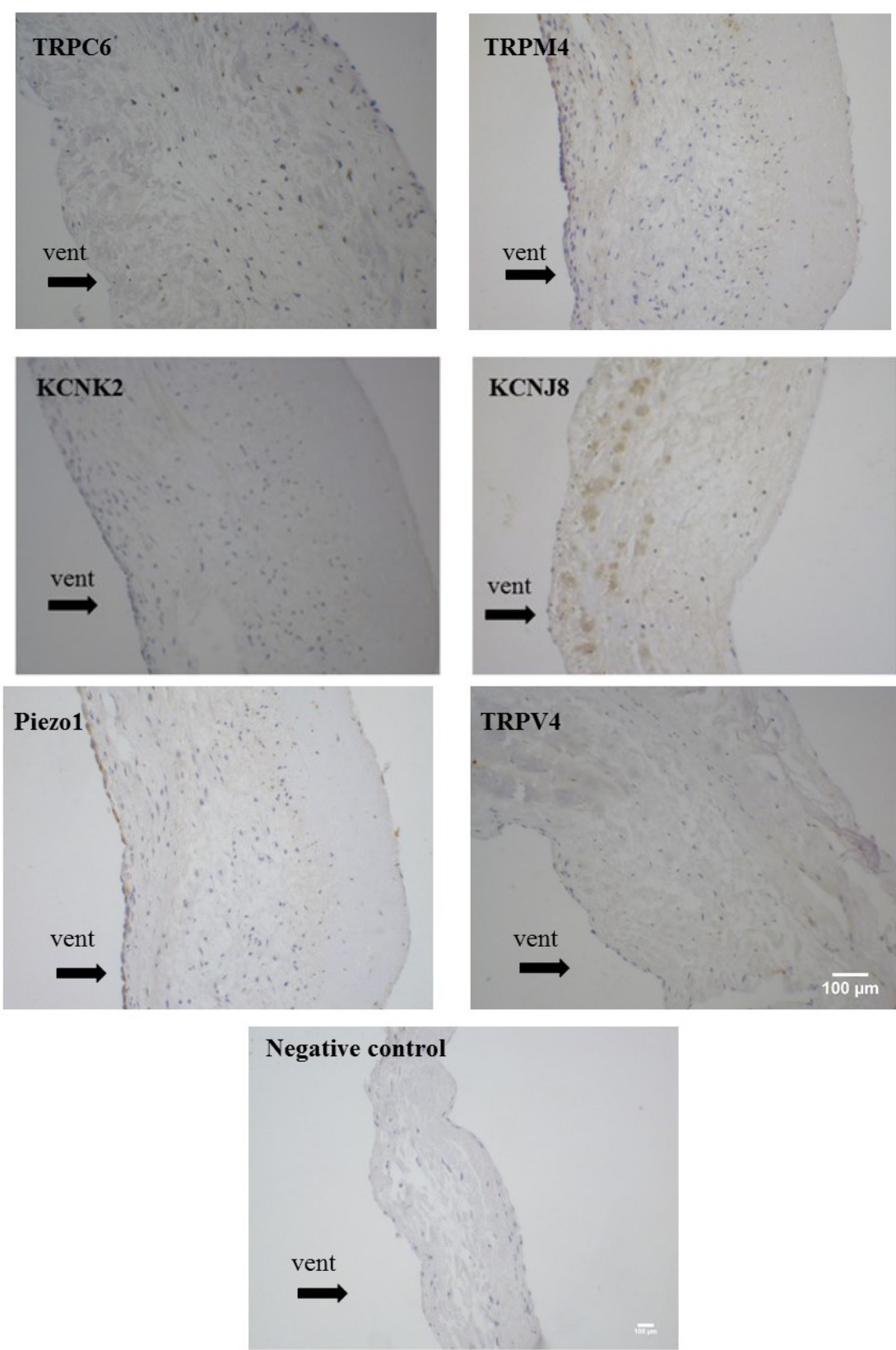


Figure 4-17. Images in transmitted light microscopy of AV paraffin sections stained for TRPV4, TRPM4, TRPC6, KCNK2, KCNJ8, and Piezo1. Scale bar represents 100 µm.

4.5 Discussion

This study characterised the expression of six SACs on AV cells and demonstrated that stretching of the membranes of these cells leading to activation of electrical current across the membrane. This was achieved by immunocytochemistry and western blotting to assess the expression of the channels and by patch clamping to record the channel's activities. Patch clamping in this study recorded the activities of the channels in three optimized condition to record cation non-selective, potassium, and piezo1 channels. While channel activity could be recorded, it was not possible to characterise the contribution of different channels to the current recorded, due to the long optimization process and the lack of specific pharmacological and molecular tools with which to inhibit or knock-down specific channels. Nonetheless, techniques such as western blotting and immunocytochemistry were able to demonstrate the presence a variety of SACs, which included TRPM4, TRPV4, TRPC6, KCNK2, KCNJ8, and Piezo1 channels in VEC and VIC.

The present study makes several findings with respect to the expression of SAC on VEC. Firstly, the expression pattern of some SACs differed between VECs isolated from the aortic and mitral valve. The finding could be due to the fact that different heart valves are exposed to different mechanical environments and that their mechanical environment regulates their expression of SAC, to optimise the responses of the cells to the mechanical stimuli. Secondly, the finding was that KCNK2, KCNJ8, and Piezo1 expression in the VEC on the aortic side of the valve is different from the VEC on the ventricular side that could be due to the fact that different valve sides are exposed to different mechanical environments (Yap et al., 2012a, Yap et al., 2012e). Recently, different studies suggested that VECs on either side of AV vary in the expression of pro-inflammatory and pro-calcifying genes, and that the mechanical properties of the VEC on each side of the valve

differ, with those on the aortic side being less stiff than those from the ventricular side (Arjunon et al., 2013, Chester and Butcher, 2013). Furthermore, site-specific VECs were in different ways responsive to the particular patterns of flow. Oscillatory flow increases the amount of collagen and GAGs on the only aortic surface and not on the ventricular side of the valve (Mongkoldhumrongkul et al., 2016).

TRPM4, TRPV4, TRPC6, KCNK2, KCNJ8, and Piezo1 channels were also detected in VICs, and the expression levels were the same between the aortic and mitral valves. Our results show that the expression levels of SAC in VICs differ according to the phenotype of the cells. Potassium channels (KCNK2 and KCNJ8) were expressed more in fibroblast phenotypes than myofibroblast and osteoblast phenotypes. In contrast, TRP channels (TRPM4, TRPV4, and TRPC6) were expressed more in osteoblast phenotype than fibroblast and myofibroblast phenotypes. Given their expression pattern in VIC phenotypes, suggest that their expression and function may therefore change in disease processes -since myofibroblast and osteoblast are associated with pathological changes. In channels activity, differentiation of fibroblastic VICs to myofibroblast VICs did not affect the activity of SACs, but their differentiation to osteoblasts affects channel kinetics and currents. A better understanding of how SACs regulate valve interstitial cell differentiation will provide us with more tools to control VIC differentiation, this to regulate better tissue remodelling occurring during most valve diseases. More research is required to investigate whether SACs mediate the differentiation or whether they are simply part of the changes that occur in VIC cells. One study has shown that calcium-activated potassium channels influence the differentiation of mesenchymal stem cells by regulating membrane potential and intracellular Ca^{2+} oscillations (Pchelintseva and Djamgoz, 2018). Moreover, several studies have indicated the essential role SACs play in the differentiation of prostate cancer cells (Mariot et al., 2002, Prevarskaya et al., 2007).

In conclusion, the study of SACs in AV is still in its infancy; it will be important to better characterise and identify further SACs and to determine the specific activity and stimulus for each channel. This chapter confirmed the presence of different SACs in valve endothelial and interstitial cells and identified differences in SACs between valve endothelial cells from either side of the valve. Also, this chapter highlighted the differences in expression of SACs between valve interstitial cells phenotypes and their potential to be involved in the pathological changes that occur during valve calcification.

4.6 Limitation & Future work

Prior studies have noted the importance of mechanical forces in regulating valve interstitial and endothelial cells function (Arjunon et al., 2013). Recently, many studies have focused on SACs and their role in cellular function, but no study has focused on SACs in heart valve cells. Therefore, the aim of this chapter was to detect the presence of SACs in valve cells. In the beginning, there was variability in well-known information about SACs; for example, TRPC6 has been intensively studied, while little is known about KCNK8. Nonetheless, investigating all a selection of SACs has found that SACs are expressed on valve cells and therefore have the capacity to mediate the response of these cells to mechanical stimulation. The ability to identify and localise the SAC was limited by the antibodies available. For example, the antibodies for TRPC6 and TRPV4 gave multiple bands and could not be used for immune-fluorescence stain due to non-specific binding. Also, in the electrophysiological studies the conditions have been optimized to record SACs activities for cation non-selective channels and potassium channels. Detecting specifically each channel of interest will need a long optimization process and the availability of selective inhibitors and molecular probes to identify the activities of individual channels. This was outside the scope of this study. Lastly, this study has focused mainly on AV. The semilunar valve function under different haemodynamic conditions, while the atrioventricular valve differs in their structure form the semilunar valves. A comprehensive study to map SAC in all four heart valves to see how valve structure and function affect the potential role for SAC in mechanotransduction of heart valves is required.

4.7 Conclusion

- TRPM4, TRPV4, TRPC6, KCNK2, KCNJ8, and Piezo1 channels were present aortic VECs.
- The expression patterns of KCNK2, KCNJ8, and Piezo1 channels were different between VECs from aortic and mitral valves whereas TRPM4, TRPV4, and TRPC6 were similarly expressed in VECs from aortic and mitral valves.
- KCNK2, KCNJ8, and Piezo1 channels were expressed more in VECs from the ventricular side than the aortic side of AV, TRPM4, TRPV4, and TRPC6 were similarly expressed in VECs from the ventricular side than the aortic side of AV.
- TRPM4, TRPV4, TRPC6, KCNK2, KCNJ8, and Piezo1 channels were present aortic VICs.
- The expression of KCNK2 and KCNJ8 were downregulated in VICs differentiated into osteoblast whereas TRPM4, TRPV4, and TRPC6 were upregulated in VICs differentiated into osteoblast.

Chapter 5

Stretch-Activated Channels in Calcified Aortic Valve

5.1 Rationale

Aortic stenosis is a significant health problem that affects 2-4% of people over 65 years. Replacement of the affected valve currently represents the only viable treatment. Every year, 6000 patients in the UK and 60 000 patients in the USA alone undertake valve replacement surgery. However, valve replacement is associated with some limitation including valve degradation and drug need (Bloomfield, 2002). Recently, Transcatheter aortic valve implantation (TAVI) procedure has been developed, it involves inserting a catheter into a blood vessel in the upper leg or chest and passing it towards the aortic valve and fix a replacement valve over the top of the old one. It is more suitable for people whom surgery would be difficult or risky where it doesn't need to stop the heart and incision in the chest. On the other hand, there is a high risk of having a stroke after the TAVI procedure (Yoon et al., 2018).

AV stenosis is defined as narrowing of AV opening; it is caused by the calcified lesion on the valve cusps that impair the opening of the valve. While these changes are associated with old age, in people with congenitally bicuspid aortic valves, calcification and progression to aortic stenosis can occur at a much younger age. AV calcification is an active cell-driven process related to the transformation of VICs too osteoblast like cells, endothelial dysfunction, and inflammation (Owens and Otto, 2009). Initially, AV calcification starts with progressive degeneration of the valve and loss of cell phenotype regulation. Valve cells including interstitial and endothelial cells play important roles in valve calcification. However, the precise mechanism of valve calcification process is still not fully understood and different aspects are investigated. Valve interstitial cells are the main orchestrator of valve calcification and direct the calcification process by trans-differentiation of AV interstitial cells into osteogenic-like cells lead to initiate valve calcification, increase valve stiffness and mechanical strain, and upregulation of

osteoblastic cell markers in response to mediators such as TGF β (Chawla et al., 1999, Osman et al., 2006). Some studies suggest that calcium accumulates in the matrix is resultant of apoptotic bodies after AV interstitial cells apoptosis. Also, valve endothelium modulates the valve stiffness through paracrine mediators that protect the valve against pro-calcifying factors. Endothelium damage leads to a loss of protection of the interstitial cells that suppress changes in VICs phenotype and function (Chester et al., 2014). Another aspect, nitric oxide (NO) is an important mediator of valve calcification and its role in AV calcification have been reported in different studies. eNOS protein expression was significantly lower in AV endothelial cells in valve diseases patients (Aicher et al., 2007). Richards study has reported the inhibitory role of NO in valve calcification where the diethylenetriamine NO adduct (DETA-NO) inhibited VIC osteogenic differentiation, whereas the NO blocker (N-nitro-l-arginine methyl ester) improved valve calcification (Richards et al., 2013). Also, calcifying nodules in *in vitro* culture of porcine aortic valve interstitial cell, formed in response to osteogenic factor, were inhibited by NO donors DETA-NO (Kennedy et al., 2009). The high cholesterol and smoking are considered as risk factors which increase oxidant stress on the endothelium and have been shown to have a significant role in valve calcification induction and calcific lesions on the surface of the valve occur preferentially at areas of high stress (Ngo et al., 2009).

Apart from biochemical factors, mechanical forces play an important role in the development of valve disease. Several studies have linked changes in these mechanical forces to initiate valve cells dysfunction and disease (Balachandran et al., 2009, Ku et al., 2006, Sucosky et al., 2008). For example, hypertension is a well-known risk factor for AV calcification, it causes raised stress and stretch in the AV cusp (Rabkin, 2005). In normal physiological conditions, AV is exposed to stretch due to pressure load approximately 10% stretch in the circumferential direction and 30% in the radial direction.

Any changes in stretch force initiate pathological responses such as increased release of matrix remodelling proteins and pro-inflammatory markers (Balachandran et al., 2009, Metzler et al., 2008). However, the intercellular signalling mechanisms by which stretch induces these changes are unclear. Previous discoveries have highlighted the importance of SACs in the function of the heart, and data presented in the previous chapter show that SACs are expressed in cultured heart valve cells and samples of healthy valve tissue. Defining SACs in valves affected will validate the observations made in cells that are differentiated into the pathogenic phenotypes of myofibroblast and osteogenic VICs. Therefore, this chapter aimed to define SACs and their expression in diseased valve. The real benefit of this is to reveal the potential roles of SACs in the disease process and consequently, identify pharmacological targets that may restore valve function by preventing the progression of AV disease.

5.2 The Specific Aims of This Chapter Were to:

- Compare the profile of SAC expression in non-calcified and calcified valve specimens.

5.3 Methods

The general methods employed in this chapter include: western blot, RT-PCR, immunocytochemical staining, and paraffin section stain are listed previously in Chapter 2 in detail. The diseased valve samples were collected from heart transplant recipients in Harefield hospital and valves that rejected from valve transplant. While the healthy valve samples that were collected from the heart valve bank were unsuitable for clinical usage because of damage in valve tissue and potential risk of infection. The causes of death were very general but they came with no medical history of heart valve diseases. The donors' ages (of both genders) were between 23–81 years.

5.4 Result

5.4.1 Stretch-activated channels in VICs isolated from non-calcified & calcified valves.

Initially expression of 6 SACs including TRPM4, TRPV4, TRPC6, KCNK2, Piezo1, and KCNJ8 was assessed in VICs in passages 3-4 isolated from the non-calcified and calcified valve by western blot. Comparison of protein expression of SACs and the osteoblast transcription factor (RUNX2) between valve interstitial cells isolated from non-calcified and calcified valves was performed by Western blot. The figure shows upregulation of TRPM4 and TRPV4 and down-regulation of KCNK2 and KCNJ8 in cells isolated from calcified valves compared to those from non-calcified samples. No changes were seen in the expression of TRPC6 and Piezo1 (**Figure 5-1**).

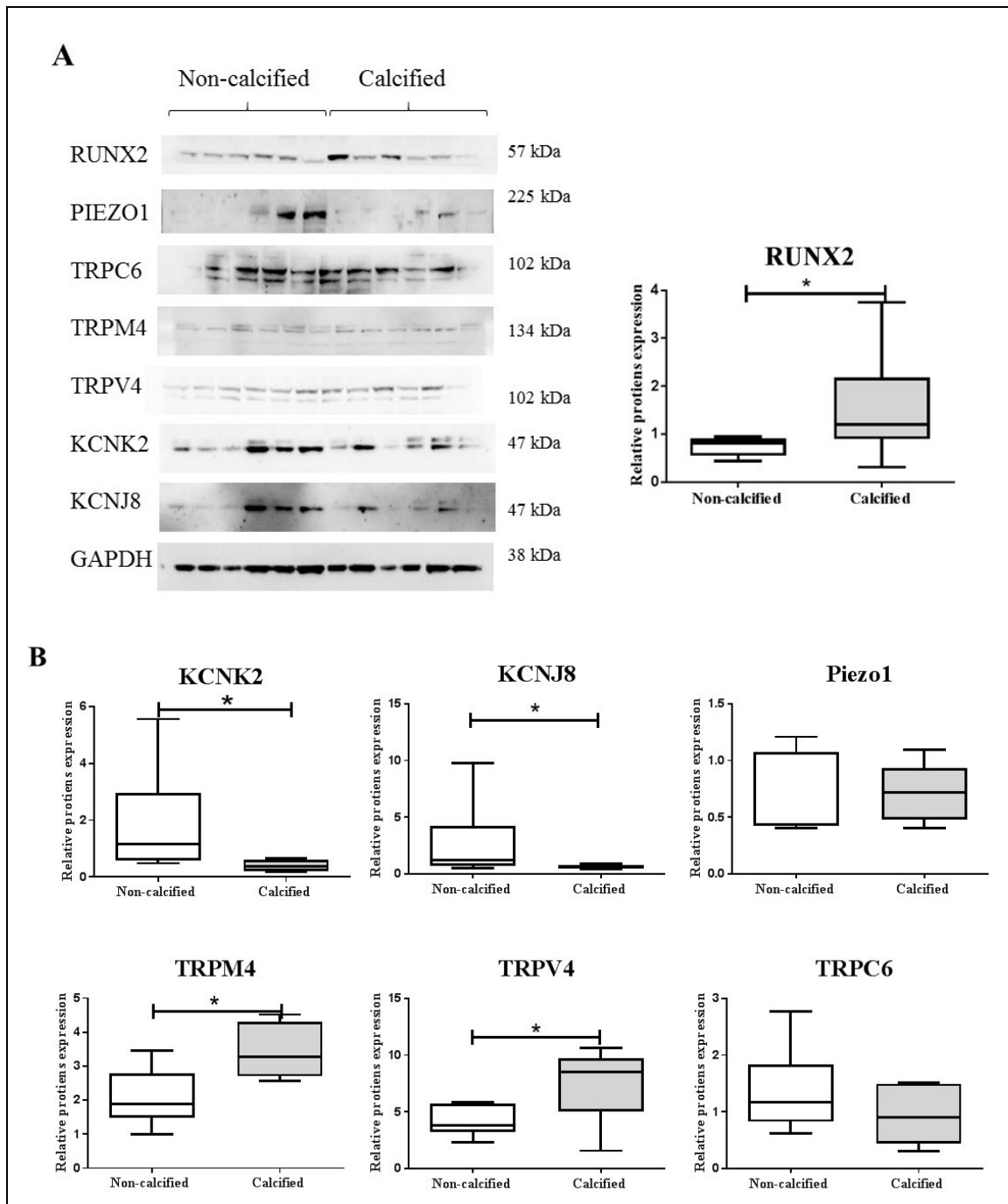


Figure 5-1: Protein expression of SACs in VICs in passages 3-4 isolated from non-calcified and calcified valve specimens. A) Western blots of at predicted molecular weight for each SACs and RUNX2 as a calcification marker. B) Charts show the relative protein expression of the SACs and RUNX2 in VICs isolated from the non-calcified and calcified valve. The values were statistically analysed by t-test and Mann Whitney test. Data are presented in the box-and-whisker plot format, n = 6. *P < 0.05

5.4.2 Stretch-activated channels in tissues from non-calcified & calcified valves.

Cultured cells may not be an accurate representation of how the cells are in the intact tissue, due to the artificial environment of in vitro conditions. Cultured cells may undergo phenotypic and functional changes during cell culture. Therefore, I also assessed SACs expression in intact valve tissue in addition to cultured cells. Paraffin sections of calcified and non-calcified valve tissue were stained with antibodies against TRPM4, TRPV4, TRPC6, KCNK2, KCNJ8, and Piezo1 channels in valve tissues. All of these channels were expressed in the valve endothelial cells and some of the interstitial cells in non-calcified valve tissues. In calcified valve tissues, these channels were strongly expressed on the endothelium and in most of VICs, expression was enhanced in around the calcification onsets in calcified valve tissues (**Figure 5-2**).

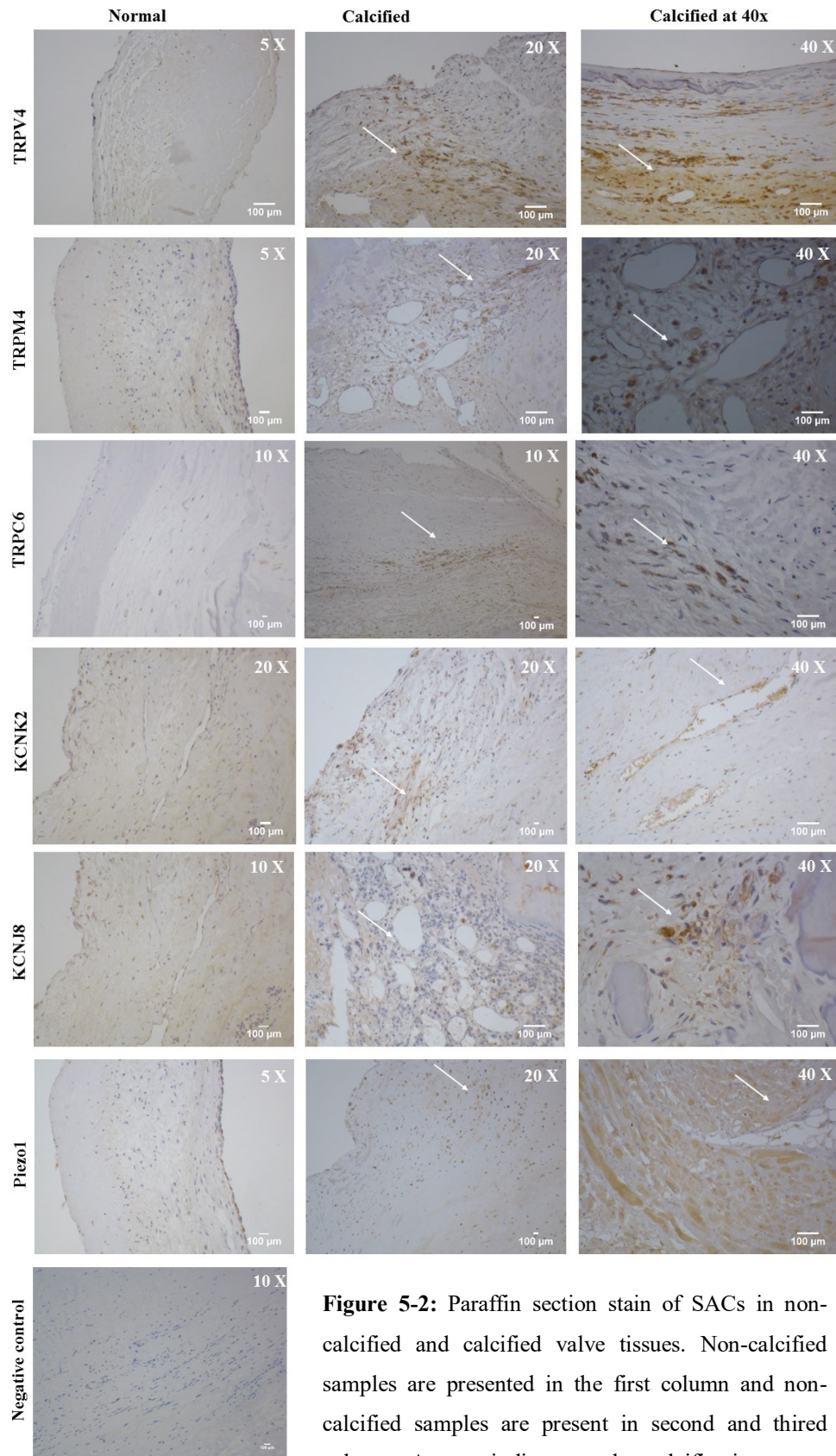


Figure 5-2: Paraffin section stain of SACs in non-calcified and calcified valve tissues. Non-calcified samples are presented in the first column and non-calcified samples are present in second and third column. Arrows indicate to the calcification areas.

Changes in SACs expression in non-calcified and calcified valve tissue were also compared using Western blot, and RT-PCR analysis. The results obtained from western blots show that the relative protein expression of TRPM4, TRPV4, KCNK2, and KCNJ8 channels was significantly greater in calcified than non-calcified valve tissues ($p < 0.05$) (**Figure 5-3**). Expression of the TRPC6 channel was also increased in calcified tissue but this difference did not reach significance ($p > 0.05$). The valve tissue was initially categorised according to the clinical diagnosis of the patients from whom the tissue was collected. This was confirmed experimentally by looking at the expression of calcification markers in these samples. Expression of RUNX2, ALP, and Osteopontin was assessed in non-calcified and calcified valve tissues.

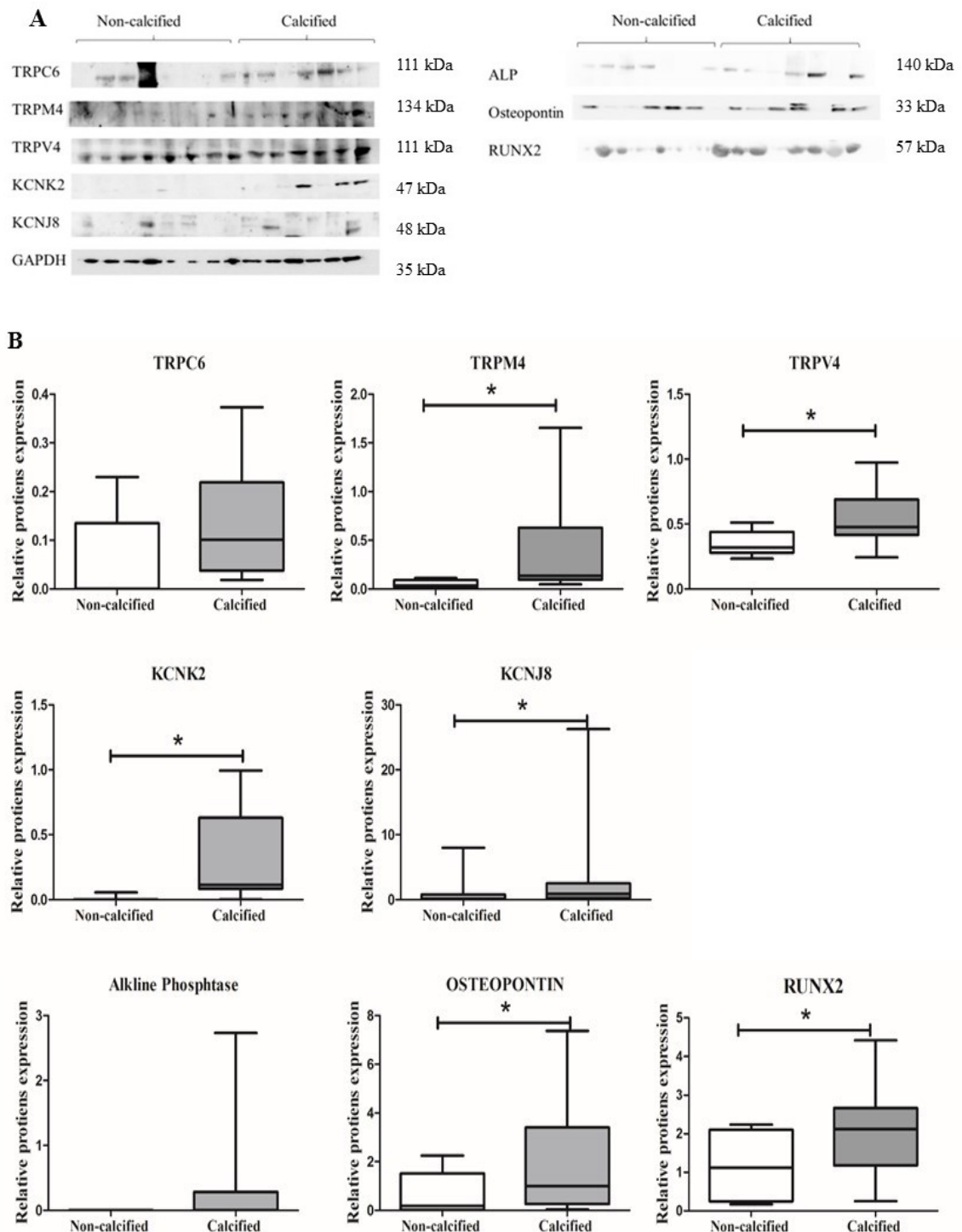


Figure 5-3: Protein expression of SACs in calcified and non-calcified valve tissues. A) Western blot band of SACs and calcification markers (Osteopontin, RUNX2 and Alkaline phosphatase) at the predicted molecular weight. Charts show the relative protein expression of the SACs and calcification markers in calcified and non-calcified valve tissues. The data were statistically analysed by t-test and Mann Whitney test. Data are presented in the box-and-whisker plot format, n = 6. *P < 0.05.

Additionally, gene expression was assessed by RT-PCR, which showed the genes for TRPM4, TRPC6, and TRPV4 channels were significantly up-regulated ($P < 0.05$) in calcified AV tissue in comparison to non-calcified tissue. Gene's expression of KCNJ8 and Piezo1 channels were expressed to a greater extent in calcified AV in comparison to non-calcified, but this difference was not significant ($P > 0.05$). KCNK2 was expressed more in non-calcified tissue, while Piezo1 expression was decreased in calcified samples, but this difference was not statistically significant (**Figure 5-4**).

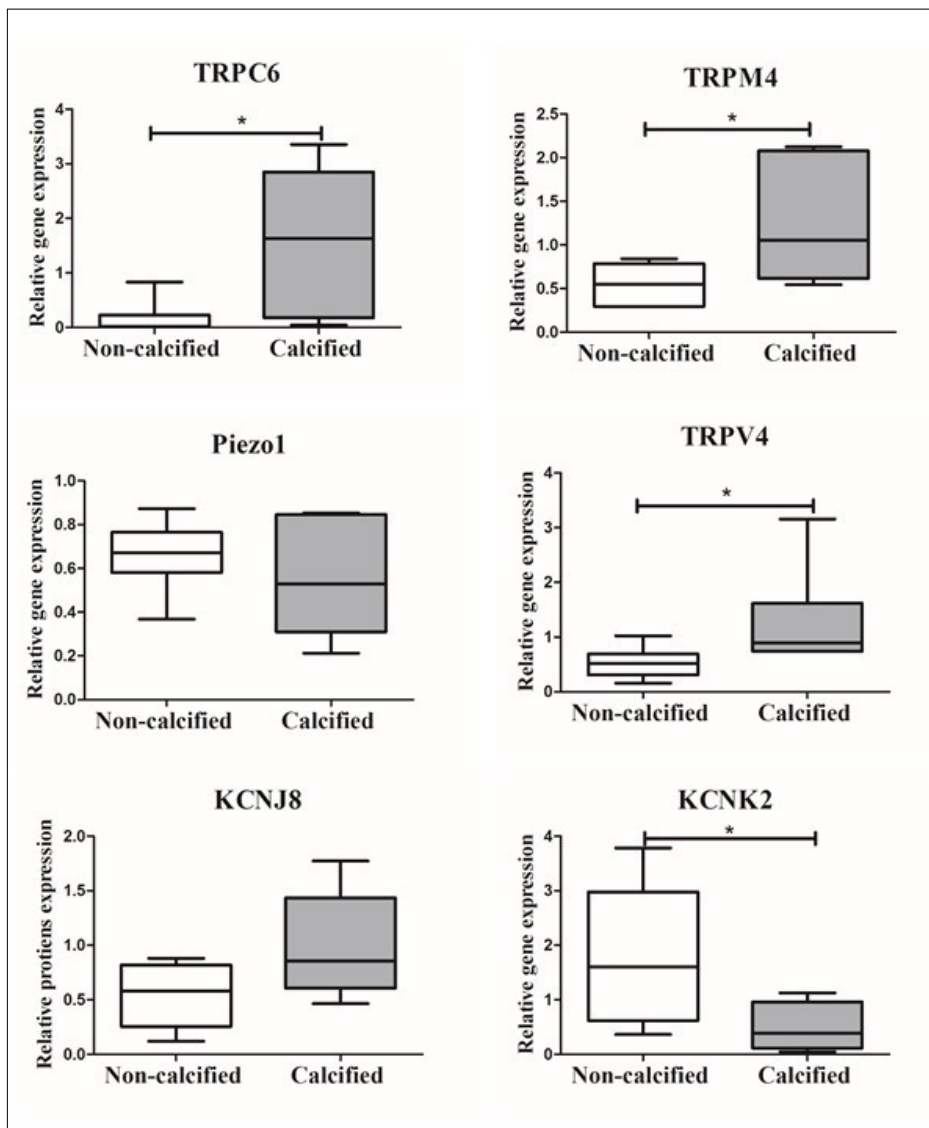


Figure 5-4: Relative gene expression of TRPM4, TRPV4, TRPC6, KCNK2, KCNJ8, and Piezo1 by RT-PCR in non-calcified and calcified valve tissues. The data were statistically analysed by t-test and Mann Whitney test. Data are presented in the box-and whisker plot format, $n = 6$. * $P < 0.05$.

5.5 Discussion

Different studies have suggested that AV calcification is induced by transdifferentiation of AV interstitial cells into osteogenic-like cells, and that this process may be exacerbated by valve stiffness and/or increased mechanical strain (Balachandran et al., 2010, Ferdous et al., 2013, Mohler, 2004, Osman et al., 2006, Chawla et al., 1999). These studies have highlighted the roles of mechanical forces in valve calcification. Several other studies have demonstrated the effects of mechanical forces on valve calcification (Chester and Taylor, 2007, Liu et al., 2007). It is well-known that mechanical forces are transmitted to cells by SACs that affect the phenotype and function of the cells in the heart valves.

In the previous chapter, six of SACs including: KCNK2 and KCNJ8, TRPC6, TRPV4, TRPM4, and Piezo channels have been identified in VECs and VICs. Recently, different studies suggested that side-specific VECs on either side vary in the expression of pro-inflammatory, pro-calcifying genes and mechanical properties (Arjunon et al., 2013, Chester and Butcher, 2013). The previous chapter has demonstrated different expression of SACs between VECs from the aortic and ventricular side. Importantly, differentiation of VICs to osteoblast a sign of valve calcification has been associated with up-regulated SACs expression. The expression of SACs on these cells suggest that SACs channels may play a role in valve calcification.

This chapter started to reveal the potential roles of SACs in the diseases process. Protein expression of SACs was up-regulated in VICs isolated from calcified valve tissue and potassium channels (KCNK2 and KCNJ8) were down-regulated in calcified cells, but this could be caused by the effect of cell culture time. Therefore, this chapter focused on expression patterns of SACs in non-calcified and calcified valves tissues. Overall, SACs were upregulated in calcified valve tissue comparing to non-calcified and these expressions were statistically significant. There was a discrepancy in KCNK2 expression:

It was upregulated in the calcified valve at the protein level and down-regulated in the calcified valve at the gene level. The staining of paraffin sections of intact valve tissue supported western blot result so, the decrease in KCNK2 gene expression in calcified valve in RT-PCR might be caused by primer troubles shoots. AV calcification is an actively regulated process associated with an osteoblast-like phenotype, and calcification markers are expressed in non-calcified AV and upregulated in calcified valves (Rajamannan, Subramaniam et al. 2003). While, calcification markers including RUNX2, ALP, and osteopontin were expressed in non-calcified valve these were found to be significantly upregulated in the calcified valve.

Valve calcification is accompanied by changing mechanical forces that disrupt the leaflet ECM, and consequently increase the stiffness of the leaflet. Additionally, VECs in the ventricular side is stiffer than VECs in the aortic side, whereas valve calcification occurs more in the ventricular side than in the aortic side of the AV (Rajamannan et al., 2011). However, the upregulation of SACs in calcified valves might be caused by more mechanotransduction. In conclusion, these findings further support the concept that changes in the expression of SAC may change the mechanotransduction processes that occur in calcified valves, thereby changing the response of the cells to mechanical stimuli. Further studies need to focus on the investigation of the functional effects mediated by SACs and determine if these are relevant to the calcification process.

5.6 Limitation and Future Work

The expression pattern of SACs has been measured and compared between non-calcified and calcified valves using different techniques. The valve tissues were well preserved, and there were no issues in processing these tissues for western blot, RT-PCR, and paraffin section stain, except for two minor issues. First, the calcified valve tissues originated from patients whose deaths were caused by different factors and who had received different treatments, which may affect SAC expression. Also, the non-calcified valve tissues were all post mortem samples; there may be a delay in obtaining the sample after death or there may be other factors related to donor conditions such as contamination.

Further studies are required to determine the role of SACs in valve calcification. It is important to determine the functional effects mediated by the SACs that are expressed in AV tissue in healthy and diseased valves. Additionally, investigation of specific SACs effect in valve calcification required, since this may identify targets for pharmacological or molecular interventions that could regress or prevent the development of valve calcification.

5.7 Conclusion

- This chapter demonstrates the effect of valve calcification on the expression of SACs in valve calcification.
- There seem to be some evidence to indicate that SACs were upregulated in calcified valve comparing to non-calcified valves.

Chapter 6

Functional Effects Modulated by Stretch-Activated

6.1 Rationale

Data from chapter 4 has shown that VEC from both AV side expressed a range of SAC including TRPM4, TRPV4, TRPC6, KCNK2, KCNJ8, and Piezo1 channels. The expression patterns of TRPM4, TRPV4, and TRPC6, channels were similar between VECs from the ventricular side than the aortic side of AV. In contrast, KCNK2, KCNJ8, and Piezo1 channels were expressed more in VECs from the ventricular side than the aortic side of AV. VECs are able to sense different mechanical forces and perform their function according to their response to mechanical stimulation. These include pressure, strain and shear stress. However, the two sides of the valve leaflet experience very different patterns of shear stress (Butcher and Nerem, 2007). Shear stress on the aortic surface of AV is low and of an oscillatory pattern, with a peak shear stress of approximately 20 dynes/cm² during diastole. In contrast, the ventricular side experiences high laminar shear, with a peak of approximately 80 dynes/cm² during systole (Weston et al., 1999). Interestingly, VECs respond in different ways to the different magnitudes and patterns of shear stress. For example, laminar shear stress downregulates some adhesion molecule proteins (vascular cell adhesion protein-1) and chemokines (interleukin 8), whereas oscillatory shear stress shows the opposite effect, upregulating adhesion proteins and chemokines (Butcher and Nerem, 2007). The occurrence of calcific lesions preferentially on the aortic side of the leaflet is believed to be contributed to by the different patterns of flow and function of the VEC on the aortic surface of the valve cusps (Gould et al., 2013). Also, it is well-known that VECs alignment is a definitive morphological response of the endothelial cell to shear stress where cell body of VECs elongate and align along the direction of flow (Steward Jr et al., 2015b). VEC alignment originally was reported by Deck et al after electron microscopic analysis of AV leaflet (Yap et al., 2012a, Yap et al., 2012e). It has also been shown that VEC, unlike vascular EC, aligns perpendicular to the

direction of flow, a process dependent of activation of specific signalling pathways including Rho-kinase and calpain pathway (Butcher et al., 2004). While it is known that VEC from each side of the valve responds differently, the mechanotransduction mechanisms in this cell are not fully understood. Nonetheless, the response of side-specific VECs to the shear stress via SACs and their effects on VEC alignment have not been investigated to date.

Thus this present chapter will investigate if SACs mediate the response of VEC to shear stress. This study will focus on the phenomena that VEC, in a similar manner of EC in the vascular system, align in response to flow. This study aims to determine whether SACs play a role in the response of side-specific-VEC-alignment-experienced flow shear stress by using pharmacological tools to inhibit or stimulate specific SAC to assess if they have a role in this functional response of VEC

6.2 Aims

This chapter sought to:

- Investigate whether SACs mediate the alignment of VECs in response to shear stress.
- Explore the effects of SACs in side-specific dependant functional effects.
- Determine which specific channels have effects on the alignment of side-specific VECs.

6.3 Methods

The general methods used in this chapter including immunocytochemical staining are listed previously in Chapter 2. The methods specific for this chapter are described here.

6.3.1 Shear stress

VECs were seeded in six-well plates at a density of 100,000 cells per plate and placed on an orbital shaker (POS-300, Grant-bio) rotating at 150 rpm. The culture medium swirled around in the wells and resulted in the cells being exposed to shear stress. Shear stress equal to 2 dyne/cm² using the protocol described in (Potter et al., 2011). The shear stress pattern applied to the endothelial cells by the orbital shaker was studied using the computational fluid dynamics solution. It revealed that the orbit wave of the shaker platform was circular with a radius of 5 mm and a rotation rate set to 150 rpm. This movement induced culture medium swirling motion over the cells, which generates shear stress around the edge and there is no, very low flow in the centre. The generated shear stress is relatively constant across the well edge (2 dynes/cm), although its direction is not similar. Resultant shear stress magnitudes are oscillatory in the centre of the well and radial near the periphery (**Figure 6.1**). Static controls were monolayers of VECs seeded in 6-well plate and placed in the incubator for 72 hours but not on the shaker platform, were included in each experiment.

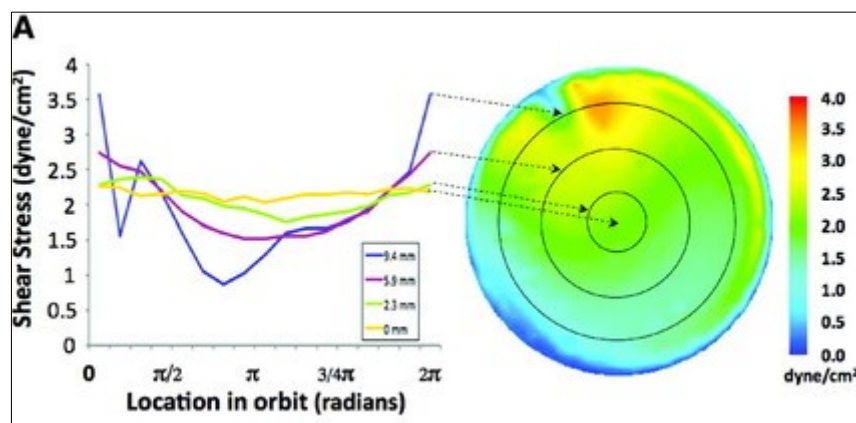


Figure 6.1. Computational fluid dynamic analysis showing radial shear stress (dyne/cm²) in the edge and low oscillatory in the centre.

After 72 hours, the cells were fixed and stained for cytoskeleton (phalloidin) and nucleus [4',6-diamidino-2-phenylindole (DAPI)] for alignment quantification purposes. The alignment was quantified based on the Feret angle; this method was developed by (Al-Yamani, 2016). It determines the feret angle for every cell, which is calculated at an angle of 90 degrees to that of the minimum Feret diameter. Then, the highest number of cells that falls within the same range of feret angle values are counted and presented as a percentage of the total number of cells in the field (**Figure 6.2**).

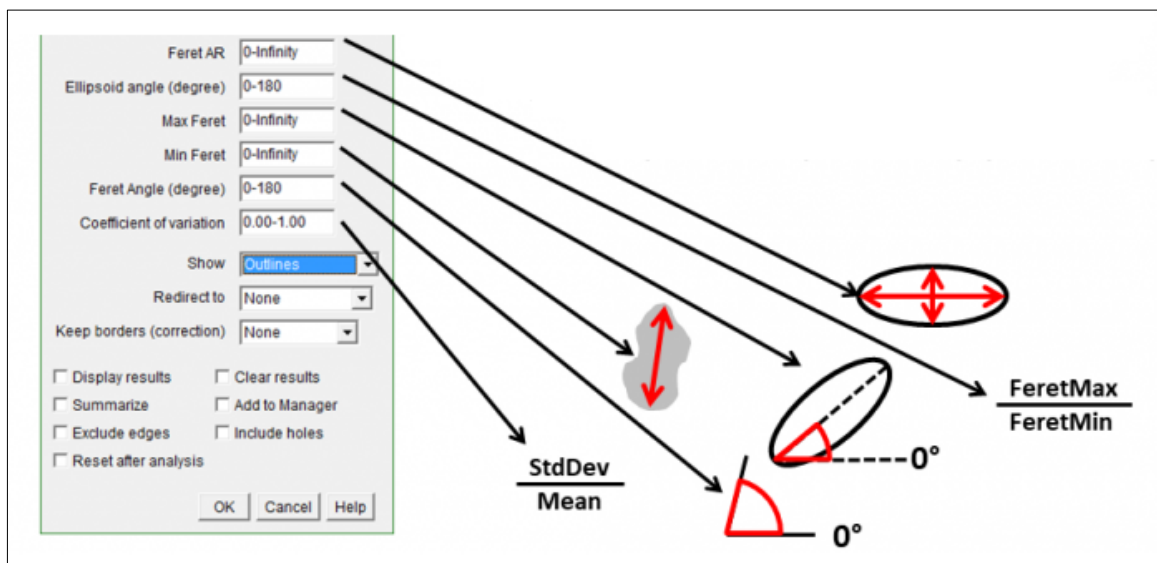


Figure 6-2. Diagram of Feret angle calculation. Feret angle (0–180 degrees) is the angle between the maximum Feret and a line parallel to the x-axis of the image. The maximum Feret is the longest distance between any two points along with an object.

6.3.2 Inhibition of SACs

Streptomycin is a nonspecific blocker of SACs, and was used in the experiments at a concentration of 100 μM (Gottlieb et al., 2004). Several specific blockers of SACs were also used to demonstrate the effects of specific channels in different mechanisms (Sackin, 1995). All of these blockers were tested at the specified concentrations (based on selective publications) and did not show any toxicity effects on the VICs. The summary of the blockers that were used and their features are presented in **Tables 6-1**.

Table 6-1: Different SACs channel blockers

Blocker	Selectivity	Dissolved in	Concentrations	Company
RN-9893	Specific blocker for TRPV4	DMSO	0.5 μ M	Sigma (cat:SML1547)
GSK4176 51A	Specific blocker for TRPC3/6 channels	DMSO	1 μ M	Focus biomolecules (cat:10-1434)
GsMTx4	Selective blocker of Piezo1	Water	0.5 μ M	Alomone labs (cat:STG-100)
Spadin	Selective blocker of K ⁺ channels	Water	1 μ M	Tocris (cat:5594)

6.4 Results

6.4.1 The Role of SACs in the Alignment of VECs from Aortic and Ventricular Side

A preliminary experiment was performed with a single concentration of non-specific blockers (100 μ M of streptomycin) (Stams et al., 2016) to investigate the potential role of SACs in VEC alignment. A confluent monolayer of VECs from the aortic and ventricular sides of AV grown in 6-well plates and were either maintained under static conditions or subjected to laminar shear stress applied by an orbital shaker. After 72 hours of exposure to shear stress, the VECs from the aortic and ventricular sides aligned parallel to one another; the percentage of alignment refers to the percentage of the cells that elongated and aligned to each other. In the absence of shear stress, VECs from both valve sides maintained a cobblestone morphology with less than 20% of cell alignment. After exposure to shear stress for 72 hours, VECs from both valve sides aligned to each other and their alignment was around 40% of cell alignment. In the presence of 100 μ M of streptomycin, percentage of alignment was significantly reduced to 30% in VECs from the aortic side and 20% in VECs from the ventricular side ($P < 0.05$). These findings were statistically analysed from six isolates of VECs from the aortic side and ventricular side of AV and showed that inhibition of SACs by streptomycin reduced the alignment of VECs from the aortic and ventricular side in response to shear stress.

The experiment was repeated with a range of streptomycin concentrations [e.g., 0 μM (control), 10 μM , 40 μM , 100 μM , and 500 μM]. With the onset of laminar shear stress, fluorescein stain showed that VECs from the aortic and ventricular side were aligned in all groups and, when percentages of alignment were calculated, such was decreased slightly from the lower concentration (10 μM) to the higher concentration (500 μM) of streptomycin. The decrease in alignment percentages became more significant in VECs from the aortic and ventricular side at 100 μM and 500 μM (**Figures 6-3 and 6-4**).

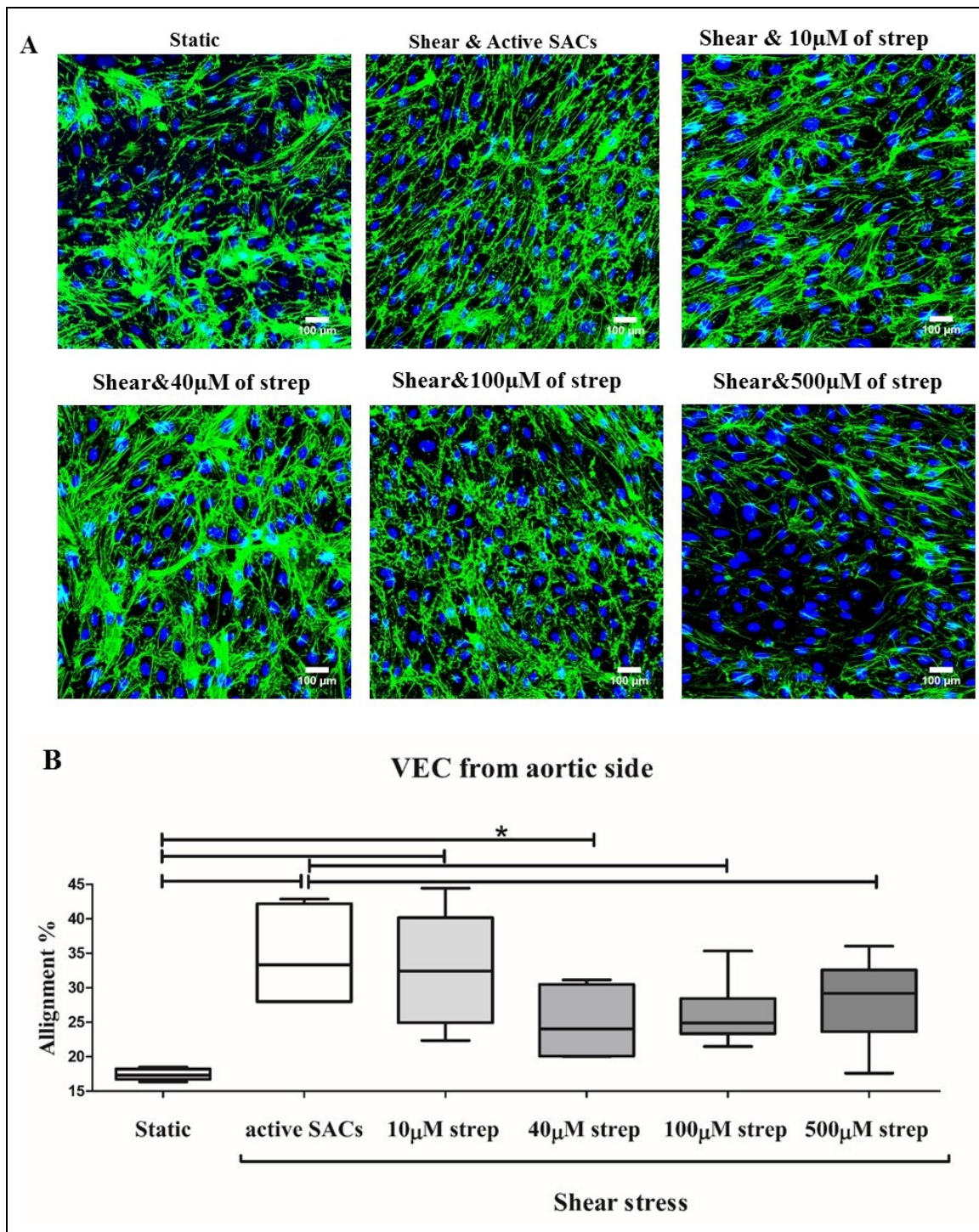


Figure 6-3. The effects of different concentrations of streptomycin on the alignment of VECs from the aortic side. A) Fluorescein stain with phalloidin (green) and DAPI (blue) of VECs from the aortic side exposed to shear stress for 72 hours, static, shear stress (active SACs), and shear stress with different concentrations of streptomycin. Scale bar present 100µm. B) The chart shows the alignment quantifications of all groups. The values were statistically analysed by analysis of variance (ANOVA) test and Friedman's test and compared by Dunn's test. Data are presented in the box-and-whisker plot format, n = 6 isolate of VECs. *P < 0.05.

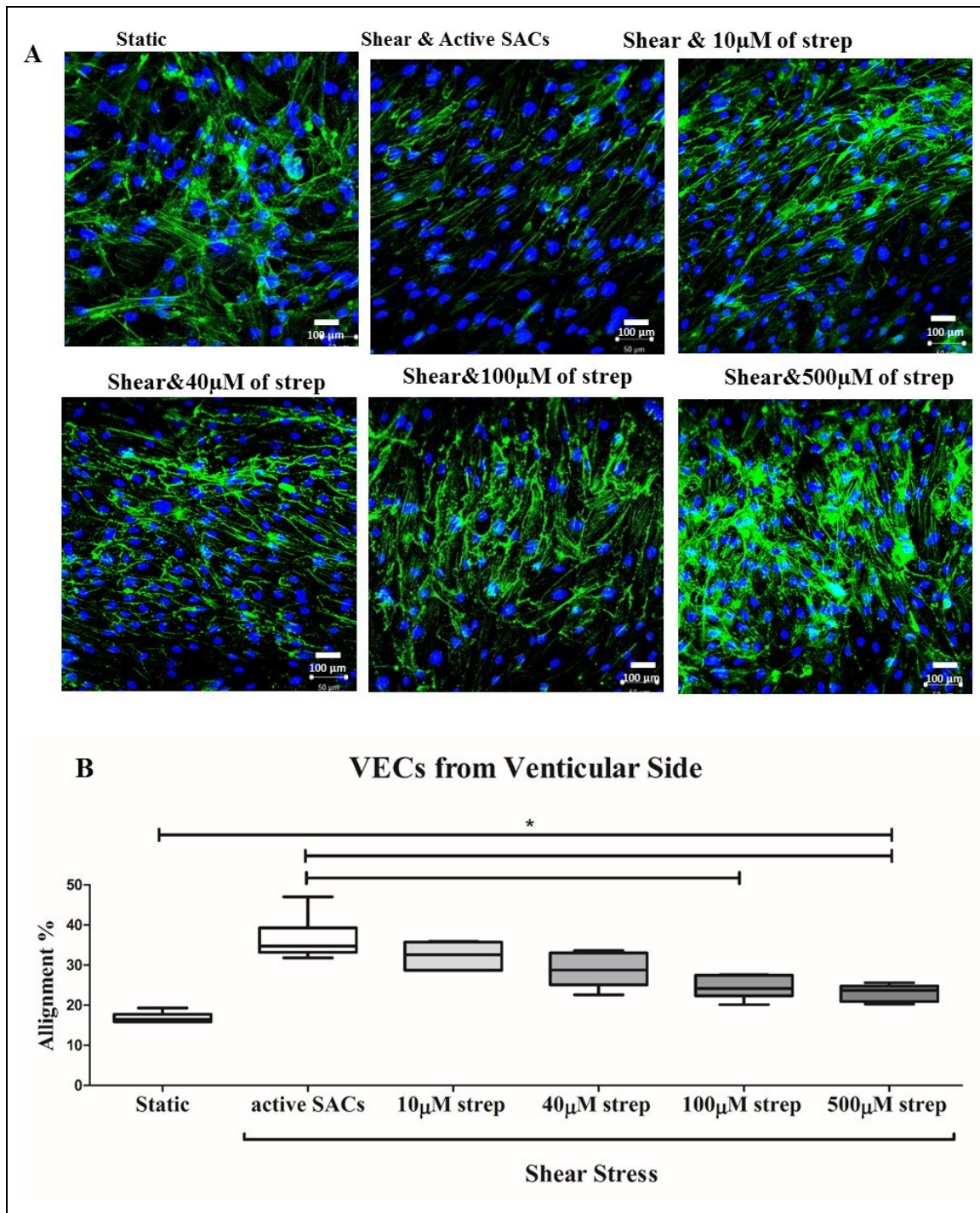


Figure 6-4. The effects of different concentrations of streptomycin on the alignment of VECs from the ventricular side. A) Fluorescein stain with phalloidin (green) and DAPI (blue) of VECs from the ventricular side exposed to shear stress for 72 hours, static, shear stress (active SACs), and shear stress with different concentrations of streptomycin. Scale bar present 100µm. B) The chart shows the alignment quantifications of all groups. The median values were statistically analysed by ANOVA test and Friedman's test and compared by Dunn's test. Data are presented in the box-and-whiskers plot format, n = 6 isolate of VECs. *P < 0.05.

6.4.2 The Effect of Different Channels Inhibitors in the Alignment of VECs from Aortic and Ventricular Side

To determine the effects of individual SACs on VEC alignment, specific channels inhibitors of TRPV4, TRPC3/6, Piezo1, and K⁺ channels were used on monolayers of VECs from the aortic and ventricular sides and under the same condition of shear stress as above. 0.5 μM of RN-9893 is a specific inhibitor of TRPV4 channel (Vincent and AJ Duncton, 2011), 1 μM of GSK417651A is a specific inhibitor of TRPC3/6 channels (Xu et al., 2013), 0.5 μM of GsMTx4 is a specific inhibitor of Piezo1 channel (Bae et al., 2011), and 1 μM of Spadin is a specific inhibitor of K⁺ channels (Mazella et al., 2010). Fluorescein stain of VECs from the aortic and ventricular sides show that a majority of the cells clearly aligned along both in the shear stress group versus in the static group. The alignment quantification demonstrated that inhibition of TRPV4, TRPC3/6, Piezo1, and K⁺ channels under shear stress did not have any effect on the alignment of VECs isolated from the aortic side (**Figure 6-5**). In contrast, the presence of TRPV4, TRPC3/6, and Piezo 1 channel inhibitors in VECs isolated from valve ventricular VECs in the shear stress condition were less aligned and disorganized as compared with in the case of the shear stress control group. The alignment of VECs from the ventricular side was quantified and the charts indicated that inhibition of TRPV4, TRPC6/3, Piezo1, and K⁺ channels reduced the alignment of VECs isolated from the ventricular side into 30%, 25%, 30%, and 35% respectively comparing to 40% in control group, but this was significant only in the inhibition of the TRPC6/3 channel ($P < 0.05$) (**Figure 6-6**).

VECs From Aortic Side

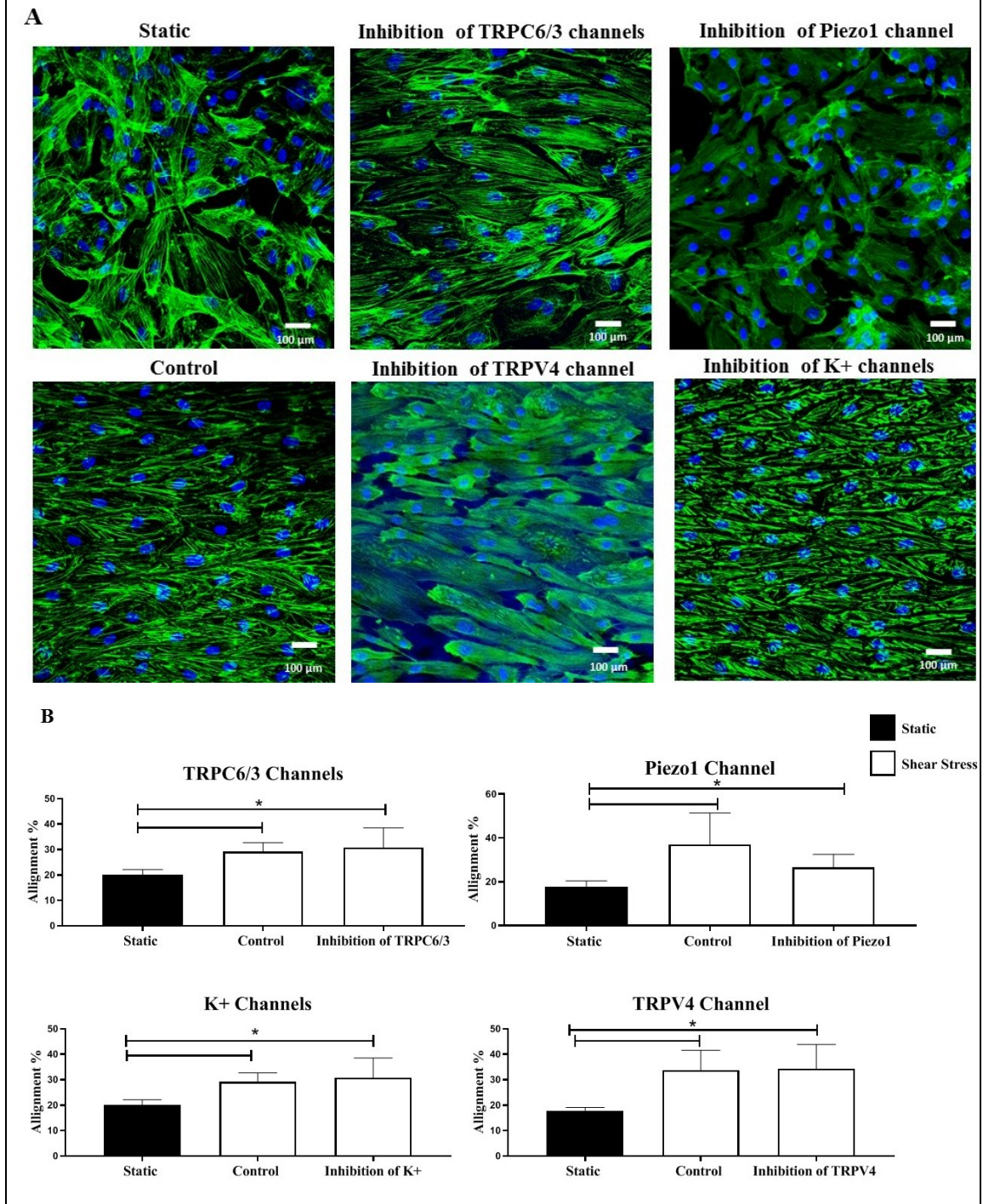


Figure 6-5. The effects of different SAC inhibitors on the alignment of VECs from the aortic side. A) Fluorescein stain with phalloidin (green) and DAPI (blue) of VECs from the aortic side exposed to shear stress for 72 hours; static; shear stress (control); and shear stress with 1 μ M of GSK417651A is a specific inhibitor of TRPC3/6 channels, 0.5 μ M of GsMTx4 is a specific inhibitor of Piezo1 channel, 1 μ M of Spadin is a specific inhibitor of K⁺ channels, and 0.5 μ M of RN-9893 is a specific inhibitor of TRPV4 channel. Scale bar present 100 μ m. B) The chart shows the alignment quantifications of all groups. The values were statistically analysed by ANOVA test and Mann Whitney test. Data are presented in the bar chart format, n = 3. *P < 0.05.

VECs From Ventricular Side

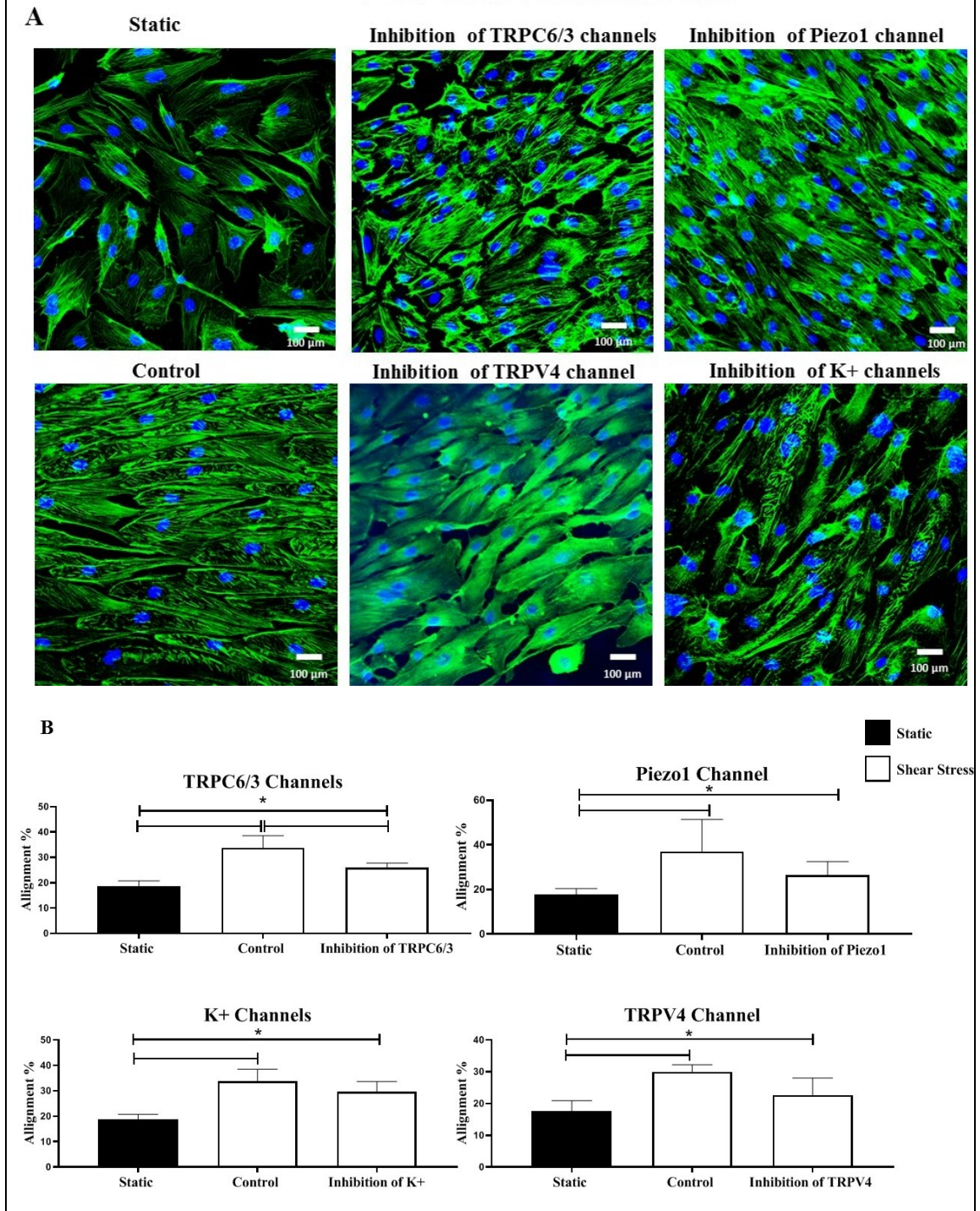


Figure 6-6. The effects of different SAC inhibitors on the alignment of VECs from the ventricular side. A) Fluorescein stain with phalloidin (green) and DAPI (blue) of VECs from the ventricular side exposed to shear stress for 72 hours; static; shear stress (control); and shear stress with 1 μ M of GSK417651A is a specific inhibitor of TRPC3/6 channels, 0.5 μ M of GsMTx4 is a specific inhibitor of Piezo1 channel, 1 μ M of Spadin is a specific inhibitor of K⁺ channels, and 0.5 μ M of RN-9893 is a specific inhibitor of TRPV4 channel. Scale bar present 100 μ m. B) The chart shows the alignment quantifications of all groups. The values were statistically analysed by ANOVA test and Mann Whitney test. Data are presented in the bar chart format, n = 3. *P < 0.05.

6.4.3 The Effect of Different Concentration of TRPC6/3 Channels Inhibitor in the Alignment of VECs from Ventricular Side

The difference in the alignment of VECs from the ventricular side in the presence of TRPC6/3 channel inhibitor was investigated further; consequently, different concentrations of TRPC6/3 channel inhibitor (e.g., 0.5 μM , 1 μM , and 2 μM) were used in the presence of shear stress. After exposure to shear stress for 72 hours, VECs from the ventricular side displayed elongation and alignment. This alignment was reduced in the presence of TRPC6/3 channel inhibitors and became even less prominent with an increasing concentration of TRPC6/3 channel inhibitor (**Figure 6-7**).

In conclusion, SACs influence the alignment of VECs from both sides of the valve in response to shear stress. TRPV4, TRPC3/6, Piezo1, and K^+ channels were investigated and only the TRPC3/6 channel showed an effect on VECs from the ventricular side. However, there was a trend toward the effect of Piezo channels on VECs from both valve sides, which did not prove to be significant. This may be due to the relatively low number of observations ($n = 3$) and additional experiments would be needed to establish a role of Piezo channels in the regulation of VEC alignment from both valve sides.

VECs From Ventricular Side

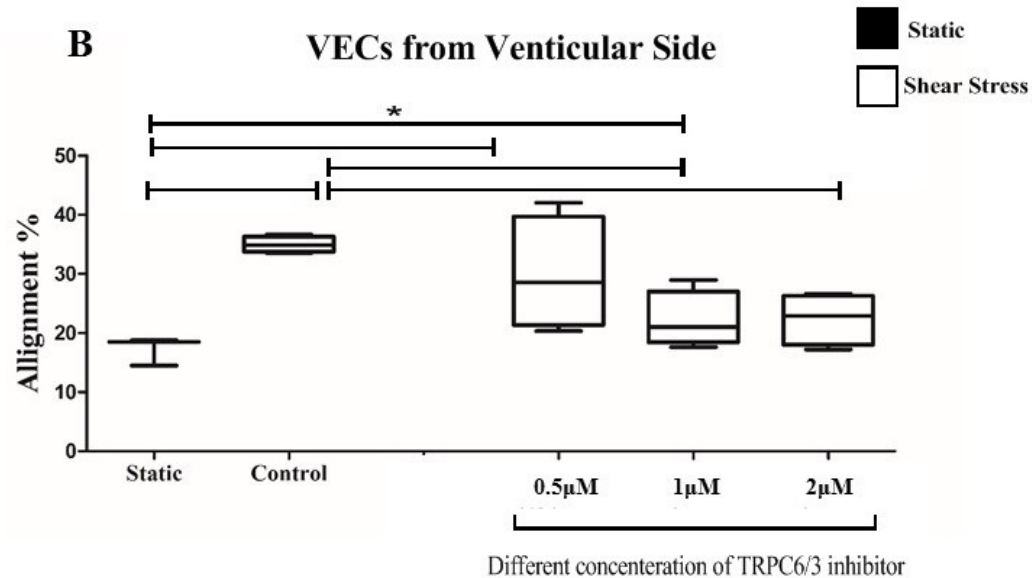
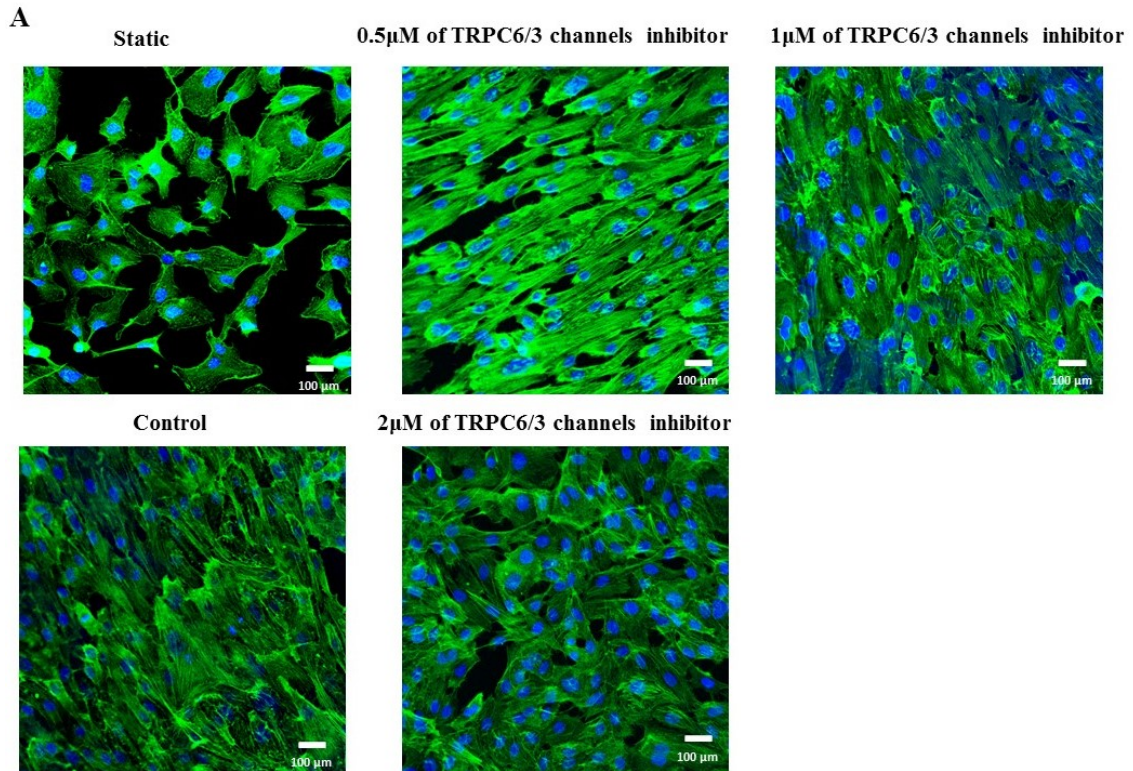


Figure 6-7. The effects of different concentrations of TRPC6/3 channel inhibitors on the alignment of VECs from the ventricular side. A) Fluorescein stain with phalloidin (green) and DAPI (blue) of VECs from the ventricular side exposed to shear stress for 72 hours; static; shear stress (active SACs); and shear stress with 0.5 μM, 1 μM, and 2 μM of TRPC3/6 channel inhibitors. Scale bar present 100μm. B) The chart shows the alignment quantifications of all groups. The values were statistically analysed by ANOVA test and Friedman’s test and compared by Dunn’s test. Data are presented in the box-and-whisker plot format, n = 4 isolate of VECs. *P < 0.05.

6.5 Discussion

Valve endothelial cells from the aortic and ventricular side were aligned with each other after 72 hours of exposure to shear stress to allow for completed VECs alignment. SACs have shown a regulatory role in the alignment of VECs from the aortic and ventricular side, since the percentage alignment was significantly reduced in the presence of SACs inhibitor (streptomycin). The alignment of VECs is a morphological indicator of their response to flow that starts by rapid alignment of the intercellular stresses fibres and forces along the direction of fluid flow within one hour, which is followed by changes in the cell bodies, and show more gradual and less precise alignment after 12 hours (Steward Jr et al., 2015a). Porcine aortic VECs are aligned perpendicular, rather than parallel, to the direction of flow even in the absence of an aligned substrate (Butcher et al., 2004). Recent observations of human aortic valve ECs have revealed this is not the case, suggesting that the VECs alignment is species dependent. Human aortic VECs appear to be aligned and elongated parallel to the direction of fluid flow. Holliday et al. identified that expression of microRNAs can account for some of the differential responses of VECs from each side of the valve (Holliday et al., 2011). The *in vivo* situation is much more complex than *in vitro*, with the presence of matrix and fluid shear stresses. In *vivo*, the two sides of the valve leaflet experience very different patterns of shear stress thus, VECs on the ventricular side showed more alignment than VECs in the aortic side due to high laminar shear stress in the ventricular side.

In Chapter 4, six SACs were defined in valve endothelial cells from both valve sides and, consequently, the protein expression levels of KCNK2, KCNJ8 and Piezo1 were significantly higher in VEC from the ventricular side compared to the aortic side, whereas the expression of TRPM4, TRPC6 and TRPV4 were similar in VECs from both side of

the valve. This current chapter aimed to determine whether SACs influence endothelial cell alignment under the condition of shear stress or not. Initially, this study was performed in site-specific VECs because of the heterogenous phenotypes of VECs on the aortic side and ventricular side of AV (Mongkoldhumrongkul et al., 2016). Different studies have suggested the existence of these heterogeneities in gene transcription profiles (Simmons et al., 2005), and, more importantly, they are different in terms of their response to flow in NOS III and Cx43 protein production in a flow-pattern independent manner (Holliday et al., 2011, Inai et al., 2000, Richards et al., 2013). In the confluent monolayer of endothelial cells from either side, steady laminar fluid shear stress was applied and caused alignment of endothelial cells to one another, VECs from both valve sides were aligned and the percentage of the cells that align to each other were calculated. The presence of nonspecific blockers (streptomycin) of all SACs showed an interesting observation revealing the effects of SACs on the flow response of VECs from the aortic and ventricular valve sides. Alignment of valve endothelial cells from either side was significantly reduced in the presence of streptomycin. In this experiment, the same patient isolates of the aortic and ventricular sides were used to reduce variations between cells from different individuals. Moreover, four specific blockers of TRPV4, TRPC6/3, Piezo1, and K⁺ channels were used to increase our knowledge about the roles of specific SACs in the alignment of VECs from both valve sides. The response of these inhibitors is different among VECs from the aortic and ventricular valve sides and only TRPC6/3 channel inhibitors were effective in VECs from the ventricular side. However, inhibition of Piezo1 channels displayed a trend in reduction of alignment of VECs from both sides, but this was not significant and could be due to low n number in the experiment. These findings could be due to the heterogeneity in the mechanical properties of VECs from both valve sides (Mongkoldhumrongkul et al., 2018). Also, it could be due to the difference in the level of channel expression between

the aortic and ventricular side, as shown in Chapter 4. In summary, SACs generally play a regulatory role in the alignment of VECs from both valve sides; however, TRPC6/3 channels were effective in VECs from the ventricular side but not the aortic side. Although TRPC6/3 channels have not been studied before in cells alignment, Piezo1 channel is well-known as a pivotal integrator in the alignment of vascular endothelial cells (Li et al., 2014).

6.6 Limitations and future work

This study has highlighted the role of SACs in the alignment of VECs for both valve sides. However, one pattern of shear was applied by orbital shaker in VECs from the aortic and ventricular sides of the valves. Compared with other existing methods of shear stress application, the orbital shaker is easy to use but has a major limitation. Specifically, it applies one pattern of shear stress while in vivo the VECs from the aortic and ventricular sides of the valve is exposed to different patterns of shear stress, the aortic surface of AV is low and of an oscillatory pattern, in contrast, the ventricular side experiences high laminar shear. To avoid this limitation, a Cone and Plate bioreactor could be used, which applies either aortic or ventricular shear flow patterns to isolated cells or tissue (Blackman et al., 2002) but could not be used in this study due to cells detachment after 24 hours of shear stress exposure. As such, our findings remain robust and should help to highlight the role of SACs in VEC function. On the other hand, more specific channel inhibitors should be included and, the number of cell isolates studied in some experiments could be increased. Finally, improving our understanding of the roles of SACs in the function of VECs can lead to promising advances in the development of endothelial cell-based therapies for valvular disease.

6.7 Conclusion

- SACs affect the alignment of VECs from the aortic and ventricular sides of AV in response to shear stress.
- The inhibition of these channels reduces the alignment of VECs from the aortic and ventricular sides of AV in response to shear stress.
- VECs from the aortic and ventricular sides respond differently to the inhibition of specific channels.
- The inhibition of the TRPC3/6 channels reduces the alignment of only VECs from the ventricular side of AV in response to shear stress.

Chapter 7

Functional Effects Modulated by Stretch-Activated Channels in Valve Interstitial Cells

7.1 Rationale

VICs work to actively maintain valve cusp integrity, structure and function (Gotlieb et al., 2002). ECM production is one of the main functions of VICs to maintain and AV cusp integrity and durability. VICs produce collagens, elastin, and glycoproteins (Chester et al., 2014). VIC also regulate the balance between the synthesis and degradation of ECM, via the expression of matrix metalloproteinases and their tissue inhibitors (Dreger et al., 2002). VIC and the ECM also plays a role in calcific AV disease with alterations in ECM composition including disorganisation of collagen bundles, fragmentation of elastin fibres, and high proteoglycan deposition occurring in calcified valves (Yip and Simmons, 2011). VICs synthesize ECM proteins and the enzyme that remodel the matrix in response to stimulation by mediators such as TGF- β and in response to the application of mechanical forces such as cyclic stretching and pressure (Balachandran et al., 2009, Merryman et al., 2007). Several studies have shown that stretch of VICs acts as a stimulus for collagen synthesis and the expression of matrix metalloproteinases and their tissue inhibitors (Dreger et al., 2002).

The migration of VICs is also a key process in valve repair and is regulated by different factors such as FGF-2 (Durbin and Gotlieb, 2002). Sheetz et al. proposed a model of fibroblast migration in which cells are able to move forward by attachment between integrins-ECM and the cytoskeletal protein actin (front lamellipodia) at the leading edge of the cells, which leads to a reduced integrin–extracellular matrix adhesion in the rear of the cell relative to the front lamellipodia (Sheetz et al., 1998). Migration processes activate downstream pathways that regulate different molecules such as integrin, cell surface receptors that mediate cell-cell and cell-extracellular matrix adhesion, and other membrane receptors that transduce external environment changes into intracellular signalling (Durbin and Gotlieb, 2002). The VIC population is maintained by an ongoing supply of new VIC

from the endothelium via a process of endothelial-to-mesenchymal transition, where endothelial cells differentiate into motile cells and migrate into the body of the valve to adopt a VIC phenotype (Paranya et al., 2001). This process has been shown to be enhanced during valve injury, for example during increased levels of strain (Baum and Duffy, 2011). VECs in mature semilunar valves demonstrated an ability to transdifferentiate in vitro to mesenchymal cells by induction of α -SMA, a well-known marker for this process. The differentiated cells co-expressed CD31, ECs marker, along with α -SMA and displayed obviously increased migration in response to platelet-derived growth factor-BB (PDGF-BB), consistent with a mesenchymal phenotype (Paranya et al., 2001). Also, mitral VECs display a propensity to multilineage mesenchymal differentiation potential, including osteogenic, adipogenic, and chondrogenic differentiation. The endothelium of mitral valves expressed osteocalcin (a marker of osteoblastic differentiation) in response to in vivo to mechanical stretch (Wylie-Sears et al., 2011). Different studies have explored the influences of different factors in VIC migration such as the activation of a protein complex at the focal adhesion site and ECM. Gotlieb et al. showed that VICs with myofibroblast morphology migrated less rapidly into the wound than did VICs with fibroblast morphology (Durbin and Gotlieb, 2002). Another study showed that VICs from the aortic and mitral valves have a similar migration ability (Sun et al., 2013).

Like ECM production and migration, the proliferation of VICs is an essential process in valve repair and remodelling. The proliferation of VICs is modulated by different factors such as mechanical forces and the overload of chronic and acute left ventricular pressure, which led to an increase in DNA synthesis in VICs in a rat model (Willems et al., 1994). The responses of mechanical force in VIC play an important role in regulating each of these properties of VICs. ECM secretion is known to be stimulated by increased strain on VIC, the migration of VICs generates tractional forces at the cell contacts and relaxes in

order to move forwards, cells also experience membrane forces as they divide and separate from each other during mitosis. In chapter 4, the presence of SACs including TRPM4, TRPV4, TRPC6, KCNK2, KCNJ8, and Piezo1 channels in VICs was detected. Given their expression pattern in VIC phenotypes, suggest that their expression may have a functional role in VICs differentiation. The purpose of this chapter was to investigate the potential regulatory role of SACs on these functions of VIC.

7.2 Aims

The specific aims of the research this chapter were to:

- Investigate the potential role of SACs on the main three functions of VICs in AV including: ECM production in aortic VICs, migration of aortic VICs, and proliferation of aortic VICs.

7.3 Methods

The general methods used in this chapter include: western blot, immunocytochemical staining, immunohistochemistry, RT-PCR, and cells culture are also listed in Chapter 2. The methods specific for this chapter are described here. It was reported in Chapter 4 that aortic VICs might differentiate in three phenotypes, with the fibroblast phenotype being associated with healthy valves. Therefore, in an attempt to model the physiological response of VICs, cells that were cultured from non-calcified human aortic valves were maintained in fibroblast media for up to 10 days prior to the experiments in order to maintain fibroblast phenotype.

7.3.1 Activation of SACs

The activation of SACs could be achieved using two different strategies, either by mechanical forces such as stretch or the use of specific channel activators. to limit the effect of biological action in a specific channel in a static condition.

7.3.1.1. Activation of SACs by Application of Stretch

Stretch force was applied by Flexercell FZ-4000T strain unit which has a vacuum pump to apply a negative pressure underneath of the culture plates and provides defined uniform stretch and can be monitored by a pressure transducer. VICs at passage (3-6) were seeded at 5×10^4 cells per well into BioFlex culture plates pre-coated with collagen type I (Bioflex 6-well plate, Dunn LabTech, Germany) and maintained in fibroblast medium with or without SAC blockers at 37°C in 5% CO₂ for 2 days to allow the cells to adhere to the membrane. After 2 days, cells were stretched gradually, starting at 3% for elongation for 5 minutes, then to 6% for 5 minutes, then 9% for 5 min, then 12% for 5 min and finally at 15% stretch, which was maintained for 24 hours. For the control group, VICs were culture

on BioFlex plates in the same way to that described above, was housed inside the incubator, but not stretched.

7.3.1.2. Activation of SACs by Pharmacological Activators

SACs can be activated by certain pharmacological agents. Binding of these activators is formed by the bending of lipids in the boundary layer surrounding the channel by hydrogen bonds between the channel and drug. SACs can segregate specific lipids around them based on the affinity between the channel and specific lipids, leading to activation processes that mimic normal physiological activations (Sachs, 2010). The activators were different in terms of their selectivity to the channels and efficacy in the ability to stimulate the receptor, all of these activators were tested at the specified concentrations (based on selective publications) and did not show any toxicity effects on the VICs. The summary of the activators that were used and their features are presented in **Tables 7-1**.

Table 7-1: Different SACs channel activators

Activator	Selectivity	Concentrations
Arachidonic acid	Selective activator for K ⁺ channels	5 μM
GSK1016790A	Selective activator for TRPV4	0.1 μM
GSK1702934A	Selective activator for TRPC3 and 6channels	1 μM
Yoda1	Selective activator for Piezo1	1 μM

7.3.2 Inhibition of SACs

To begin with, streptomycin as a nonspecific blocker of SACs was used in the experiments. Then, several specific blockers of SACs have been used to demonstrate the effects of specific channels in different mechanisms (Sackin, 1995). All of these blockers were tested at the specified concentrations (based on selective publications) and did not show any toxicity effects on the VICs. The summary of the blockers that were used and their features are presented in **Tables 7-2**.

Table 7-2: Different SACs channel blockers

Blocker	Selectivity	Concentrations
RN-9893	Selective blocker for TRPV4	0.5 μ M
GSK417651A	Selective blocker for TRPC3/6 channels	1 μ M
GsMTx4	Selective blocker of Piezo1	0.5 μ M
Spadin	Selective blocker of K ⁺ channels	1 μ M

7.3.3 Migration Assay

Migration assay was performed by making a scratch in the cells monolayer using a 200 μ l pipette tip (**Figure 7-1**).

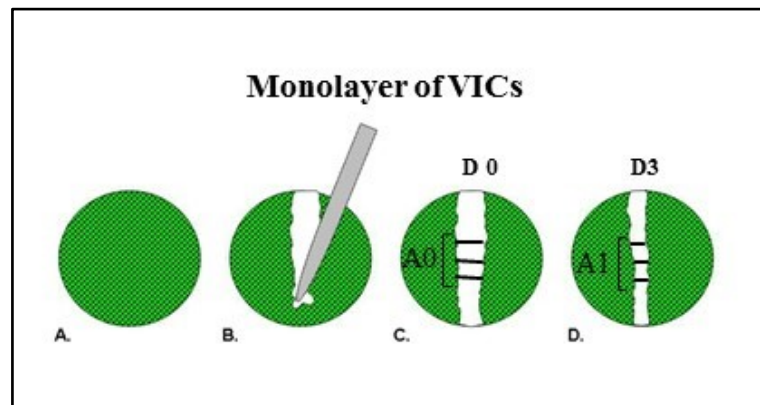


Figure 7-1: Scratch Assay: (A) a confluent monolayer of cells, (B) a wound is introduced into by drawing a tip across the cell layer, (C) the scratch area is imaged in day 0 to measure the boundary of the wound at 3 points, (D) the scratch area is imaged in day 3 to measure the boundary of the wound at 3 points.

The wound distance was measured at multiple points along the wound at time day 0 and at day 3 and the average value was used to calculate the scratch closure percentage (migration percentage) as follows:

$$\text{Scratch closure (\%)} = [(A_0 - A_t)/A_0] \times 100\%$$

Where A₀ is the area of scratch distances on Day 0 and A_t is the scratch distances on Day 5 after scratching.

The most important step during migration in the assay is to stop cell proliferation, since this closure of the wound close would then be based on cell proliferation rather than the

ability of cells to migrate. This was achieved by reducing the FCS concentration in culture media from 2% to 0.4% FCS to inhibit cell proliferation (Aguiar et al., 2016, Mun et al., 2014).

7.3.4 Proliferation Assay (MTS)

Cells were seeded into 96-well plates at a density of 2×10^3 per well and incubated in 0.4% FCS medium overnight. Then cells were exposed for 7 days to medium with and without treatment. At day 7, CellTiter 96 AQueous Non-Radioactive Cell Proliferation Assay kit (Promega G-5421) was used following the manufacturer's instruction. Briefly, 20 μ l of MTS/PMS solution and 100 μ l of medium were added into wells and incubated for one hour in 37°C and 5% CO₂ and absorbance of a coloured formazan product. The absorbance was determining the viable cells number and was detected at 490 nm with a Microplate Reader (a μ Quant universal microplate spectrophotometer made by Bio-Tek using KC junior software).

7.3.5 Live and dead cells assay

The LIVE/DEAD® Viability/Cytotoxicity Assay (Molecular Probes, cat: L3224) provides a two-colour fluorescence cell viability assay that is based on the simultaneous determination of live and dead cells using two probes. It measures two recognized parameters of cell viability: (1) intracellular esterase activity determined by the enzymatic conversion of the virtually nonfluorescent cell-permeant calcein AM to the intensely fluorescent calcein, which produces a uniform green fluorescence in live cells (495 nm/~515 nm), and (2) plasma membrane integrity determined by Ethidium homodimer-1, which enters cells with damaged membranes and binds to nucleic acids that produce a bright red fluorescence in dead cells (~495 nm/~635 nm). 20k of VICs at passage 2-4 were culture on size 22 mm \times 22 mm coverslips. The cells that adhered to the glass coverslips

were washed with PBS to remove all media and serum; 100–150 μL of the combined LIVE/DEAD® assay (2 μM calcein AM and 4 μM EthD-1 working solution in PBS) was then added directly to the cells. The cells were subsequently incubated in a covered dish for 30–45 minutes at room temperature. Following incubation, approximately 10 μL of PBS was added to the clean glass coverslips. Using fine-tipped forceps, the coverslips were carefully inverted and mounted on the microscope slide; The labelled cells were then viewed under the fluorescence microscope.

7.4 Results

7.4.1 Role of SACs in Collagen Production by VICs

VICs were cultured on collagen-coated Bioflex plates for 48 hours to allow for full attachment and then loaded into FlexCell for application of 15% stretch for 24 hours and treated with 100 μ M streptomycin to evaluate the role of SACs in collagen production by VICs. RNA samples were isolated from the cells at three-time points; 1 hour, 6 hours, and 24 hours. Expression of collagen I, collagen III, elastin, and heat shock protein 47 (HSP47) genes at the three-time points were measured and normalized to the housekeeping gene (β -actin).

At two time points (one hour and six hours), there was no significant changes in the gene expression of collagen I, collagen III, and elastin for three conditions: static, 15% stretch without blocking (active SACs), and 15% stretch with blocking of SACs. The results showed that expression of HSP47 (a procollagen-specific molecular chaperone that is also used as a marker of stretch response) (Widmer et al., 2012) was significantly upregulated in stretch groups versus static groups at two-time points (one hour and six hours). After 24 hours of stretch the relative levels of gene expression of collagen I and collagen III were upregulated under 15% stretch conditions versus under static conditions. In the presence of 100 μ M streptomycin the relative levels of gene expression of collagen I and collagen III were reduced. Also, HSP47 was increased in the active SACs group versus the blocked SACs group, though in a nonsignificant manner (**Figure 7-2**). The gene expression level of elastin was comparable among the two conditions between the presence of streptomycin and free of blocker, which was expected because elastin requires more time than just 24 hours to show an effect (data not shown). In conclusion, the blocking of SACs generally downregulates collagen I and collagen III production in VICs.

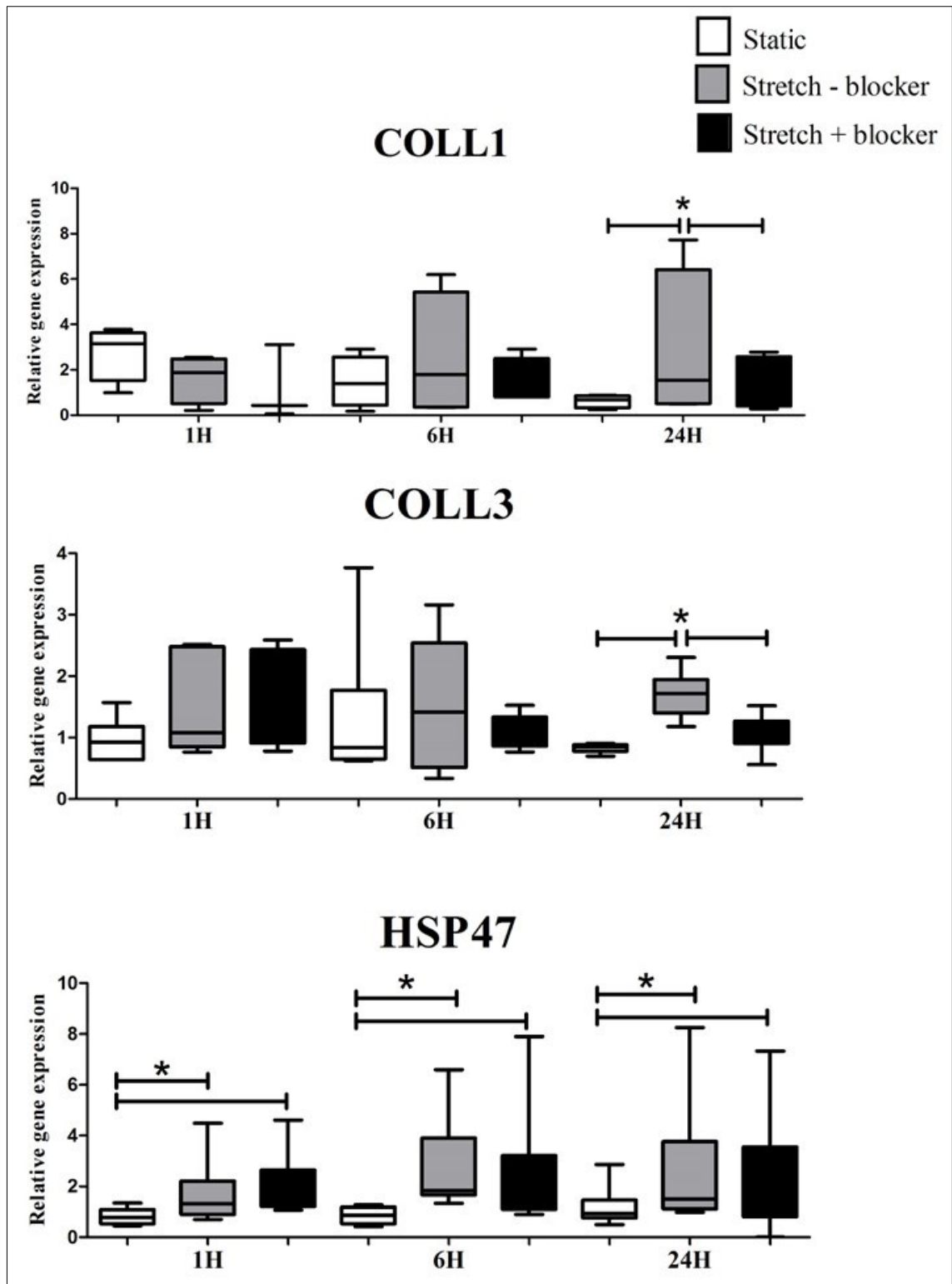


Figure 7-2: The effects of stretch on the gene expression of collagen I, collagen III, and HSP47 in VICs. The gene expression was measured at three-time points by RT-PCR and normalized to the housekeeping gene. Charts show the relative gene expression of collagen I, collagen III, and HSP47 under static and stretch conditions with and without nonspecific SAC blocking (100 μ M streptomycin). The values were statistically analysed by analysis of variance (ANOVA) test and the Friedman test and were compared by Dunn's test. Data are presented in the box-and-whisker plot format, n = 6. *P < 0.05.

Specific blockers of Piezo1, TRPV4, TRPC3/6, and +K channels were used to investigate and assess the role of these channels in collagen production in VICs. 0.5 μ M of RN-9893 is a specific inhibitor of TRPV4 channel, 1 μ M of GSK417651A is a specific inhibitor of TRPC3/6 channels, 0.5 μ M of GsMTx4 is a specific inhibitor of Piezo1 channel, and 1 μ M of Spadin is a specific inhibitor of K⁺ channels. As before, VICs were loaded on a FlexCell plate and exposed to 15% stretch for 24 hours, with RN-9893, GSK417651A, GsMTx4, and Spadin channels blockers added individually to plate wells. After 24 hours, the inhibition of the Piezo1 channel significantly decreased collagen I and collagen III gene expression under stretch conditions. Also, the inhibition of the TRPV4 and TRPC3/6 channels significantly lowered collagen I gene expression under stretch conditions comparing to stretch control, and this effect was not seen in collagen III gene expression under stretch conditions. In contrast, the inhibition of +K channels was not effective in both collagen I and collagen III gene expression under stretch conditions (**Figure 7-3**).

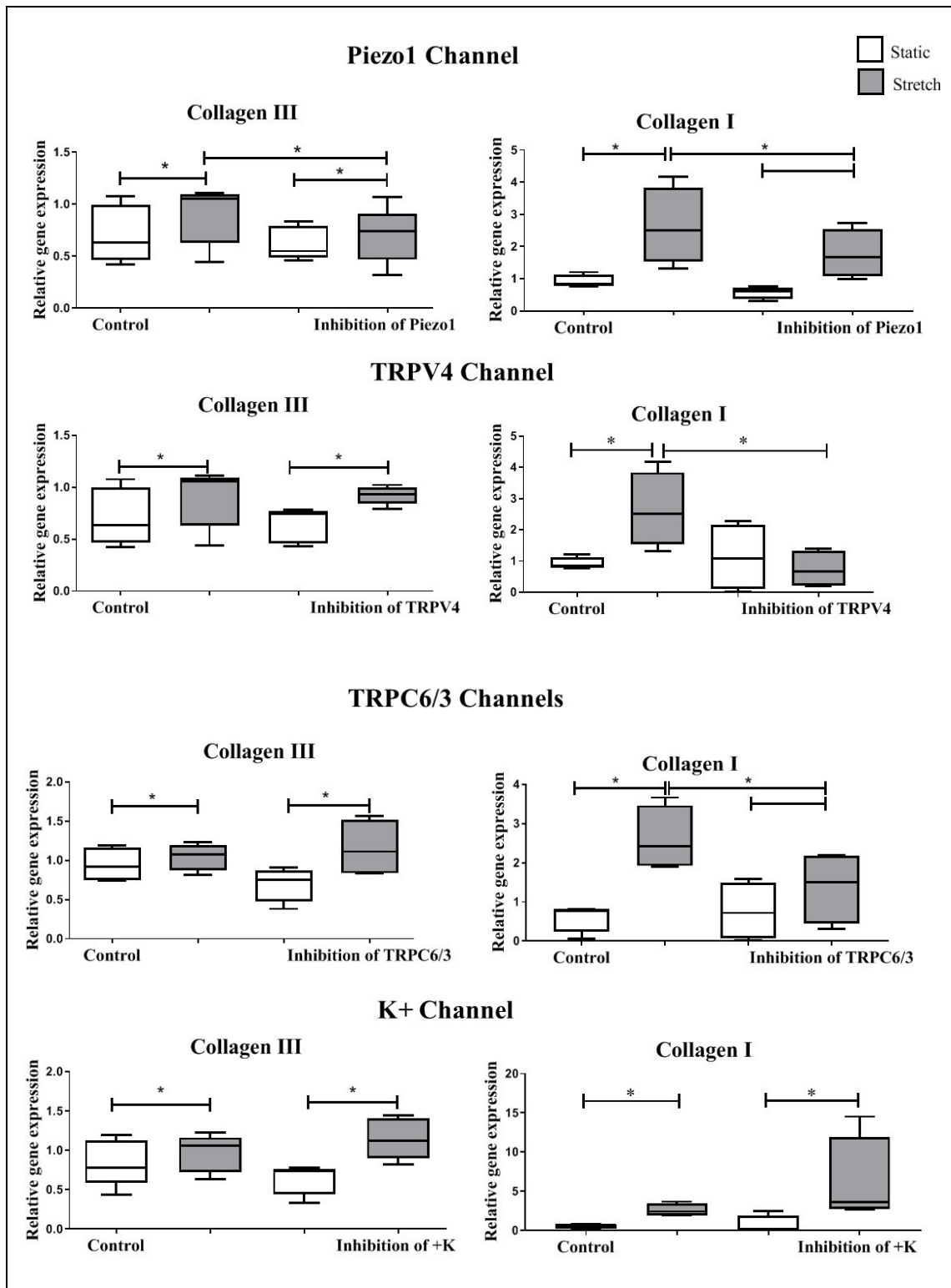


Figure 7-3: The effects of specific channels blockers (0.5 μ M of RN-9893 is a specific inhibitor of TRPV4 channel, 1 μ M of GSK417651A is a specific inhibitor of TRPC3/6 channels, 0.5 μ M of GsMTx4 is a specific inhibitor of Piezo1 channel, and 1 μ M of Spadin is a specific inhibitor of K⁺ channels) on collagen I and collagen III gene expression under stretch and static conditions. The gene expression of collagen I and collagen III was measured after 24 hours of stretch by RT-PCR and normalized to the housekeeping gene (18S). Charts show the effects of inhibition of Piezo1, TRPV4, TRPC3/6, and +K channels on collagen I and collagen III. The values were statistically analysed by ANOVA test and the Friedman test and compared by Dunn's test. Data are presented in the box and whisker plot format, n = 6. *P < 0.05.

7.4.2 Role of SACs on the migration of VICs

Results indicated VICs in the presence and absence of SAC inhibition with streptomycin migrated from the scratch edge into the scratch site. At Days 0 and 3, scratches distances were measured, and scratch closure percentages (indicated as migration percentages) were calculated for both groups. VICs in both groups were found to have migrated, but, interestingly, VICs in the blocked SACs group migrated less rapidly than did those in the control group (**Figure 7-4**). This result suggested a regulatory role of SACs on the migration ability of VICs in AV.

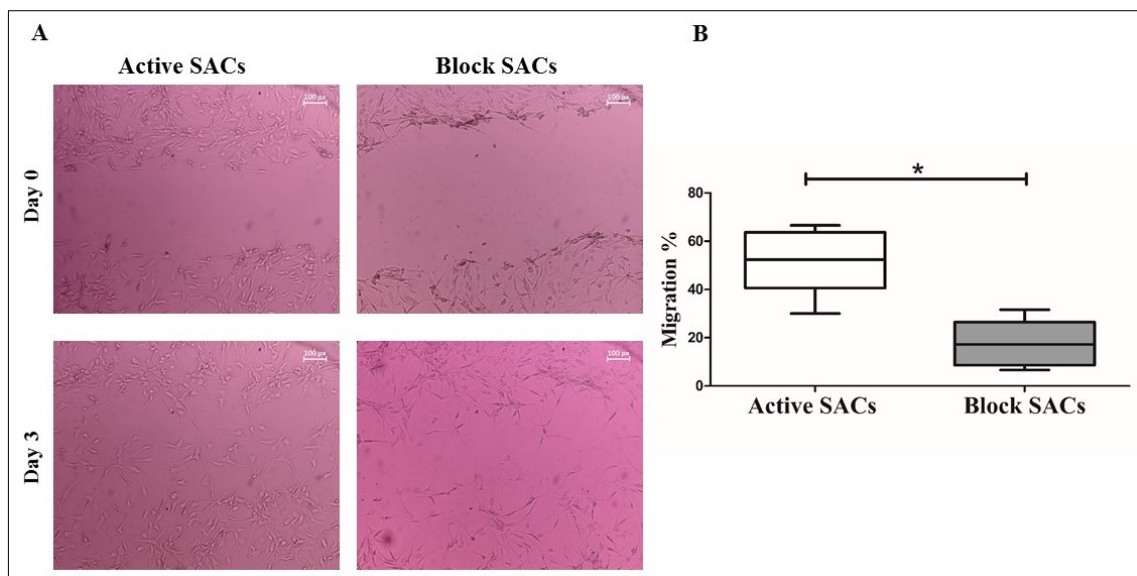


Figure 7-4. Migration percentages of VICs under active and blocked SAC conditions by 100μM streptomycin. A) Representative phase-contrast microscope image of a scratched monolayer of human aortic VICs at Days 1 and 3 in both the active SACs group (control) and the blocked SACs group (where streptomycin was added). The scale bar is 100 μm. B) The chart shows the migration percentage in the blocked SACs group and control group. The values were statistically analysed by t-test and Friedman test. Data are presented in the box and box and whisker plot format, n =6. *P < 0.05.

Preliminary experiments were performed with specific inhibitors and activators of TRPV4 and TRPC6/3 channels to stimulate or inhibit VIC migration. 0.1 μM of GSK1016790A was used to activate TRPV4 channels and 0.5 μM of RN-9893 to inhibit TRPV4 channels (Vincent and AJ Duncton, 2011). The inhibition of the TRPV4 channel significantly reduced the migration of VICs in comparison to the control group. There was not seen the effect when the cells were treated with 0.1 μM of GSK1016790A an activator of the

TRPV4 channels. Also, 1 μM of GSK1702934A was used to activate TRPC3/6 channels (Tiapko and Groschner, 2018) and 1 μM of GSK417651A to inhibit TRPC3/6 channels (Xu et al., 2013). Unlike TRPV4 channel, the activation of TRPC6/3 channel with 1 μM of GSK1702934A significantly increased the migration of VICs versus in the control group, and there was not seen effect under the inhibition effect of the TRPC6/3 channel by 1 μM of GSK417651A (**Figure 7-5**). This finding focused on the use of different concentration of specific inhibitors and activators of TRPV4 and TRPC6/3 channels as being an important regulator of VIC migration.

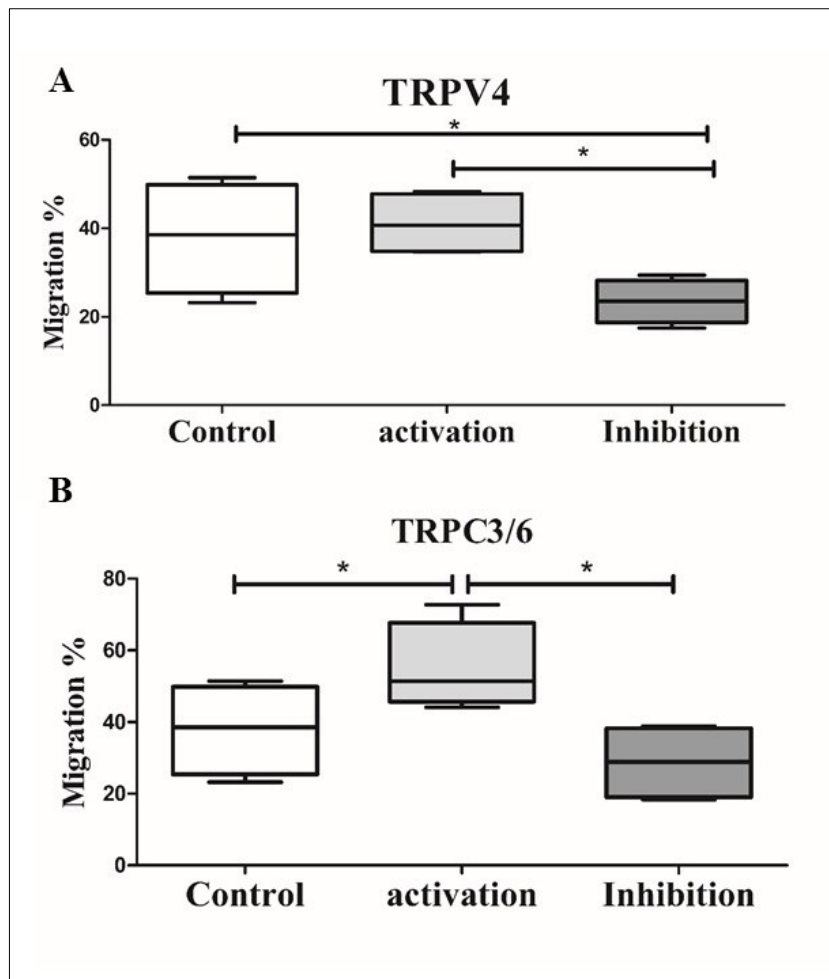


Figure 7-5: Charts show the migration percentage of VICs under the stimulation and inhibition of TRPV4 and TRPC3/6. A) The migration percentage of VICs in the control group and with activation and inhibition of the TRPV4 channel. B) The migration percentage of VICs in the control group and with activation and inhibition of the TRPC3/6 channel. One-way ANOVA followed by the Friedman test was used. Data are presented in the box and whisker plot format, n=4. *P < 0.05.

As TRPV4 and TRPC6/3 channels displayed an effect on the migration ability of VICs, different concentrations of TRPV4 and TRPC6/3 channel inhibitors and activators were tested. Concentrations of the TRPC3/6 channel activator (GSK1702934A) between 0.5 μ M and 2 μ M showed a concentration-dependent increase in the migration of VICs (**Figure 7-6**), while the same concentration range of (GSK417651A) the TRPC3/6 channel inhibitor gave a concentration-dependent decrease in the migration of VICs (**Figure 7-7**). The increases and decreases in migration were significant at the highest concentration used of 2 μ M of GSK1702934A channel activator and 2 μ M of GSK417651A channel inhibitor.

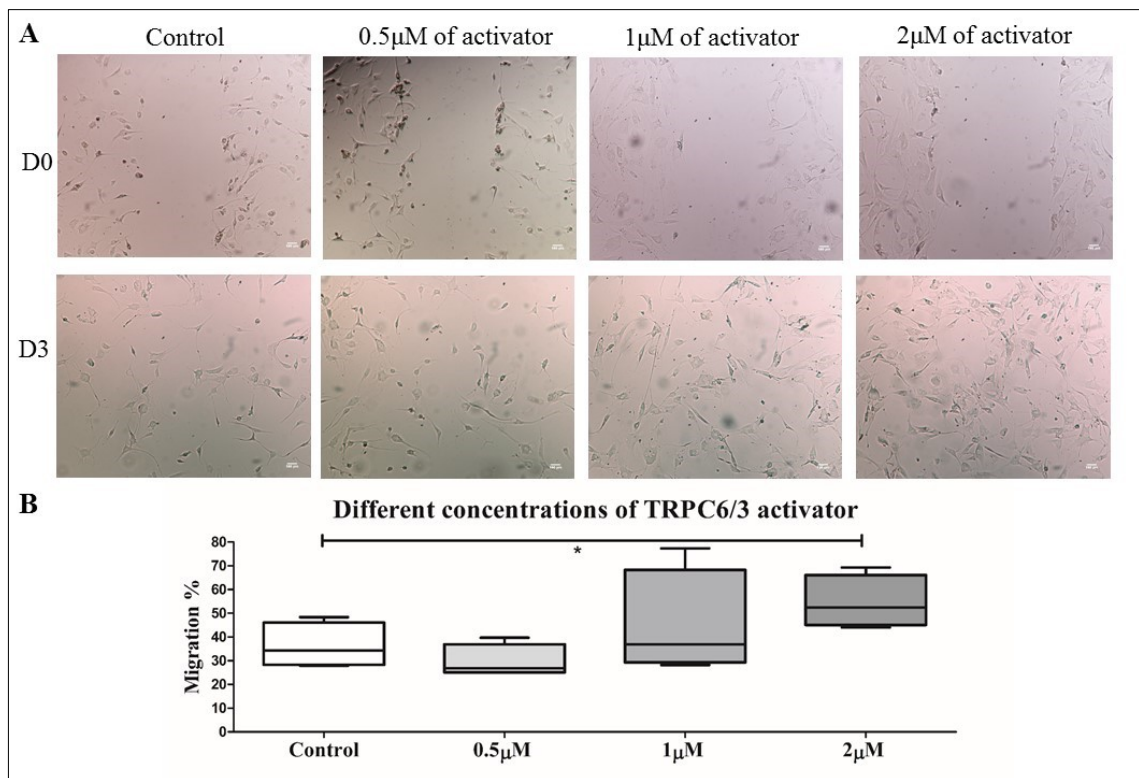


Figure 7-6: The effects of TRPC6/3 channel activation on VIC migration. A) Phase-contrast microscopy image of scratch assay shows patterns of migration of VICs along the wound edge at Day 0 (first row) and Day 3 (second row). VICs were grown in different concentrations (0.5 μ M, 1 μ M, and 2 μ M) of TRPC3/6 channel activator starting from Day 0 (control). Scale bar indicates 100 μ m. B) Charts show the migration percentage of VICs under different concentrations of the pharmacological activator of the TRPC3/6 channel. The median values were statistically analysed by one-way ANOVA followed by Friedman test. Data are presented in the box and whisker plot format, n =4. *P < 0.05.

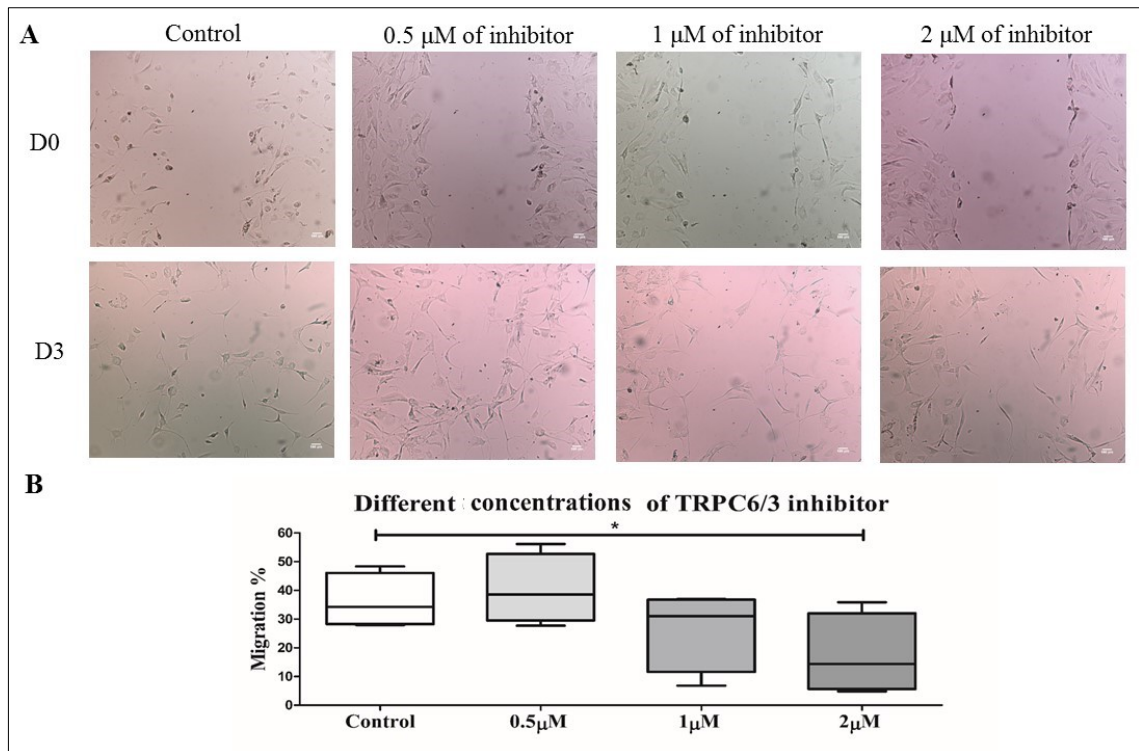


Figure 7-7: The effect of TRPC6/3 channel inhibition on VICs migration. A) Phase-contrast microscopy of scratch assay shows patterns of migration of VICs along wound edge at D0 (first row) and D3 (second row). VIC was growing in different concentration of TRPC3/6 channels inhibitor started from 0 (control), 0.5 μM , 1 μM , and 2 μM concentration. Scale bar indicates 100 μm . B) charts show migration percentage of VICs under different concentration of inhibitor of TRPC3/6 channels. The values were statistically analysed by one-way ANOVA followed by Friedman test. Data are presented in the box and whisker plot format, $n=4$. * $P < 0.05$.

In a similar manner, 0.1 μM - 1 μM of the TRPV4 channel activator (GSK1016790A) increased the migration of VIC (**Figure 7-8**), while a 0.5 μM - 2 μM of the TRPV4 channel inhibitor (RN-9893) decreased the migration of VIC (**Figure 7-9**). These increases and decreases, respectively, in migration percentage were significant at the highest used concentration of TRPV4 channel activator and inhibitor. Treatment with the activators and inhibitors of the TRPC3/6 and TRPV4 channels at the concentrations used in these experiments did not have any effects on cell morphology and viability which was examined before the experiment by proliferation assay (data not shown). Additionally, the VICs in all groups moved toward a scratch area as single cells; only their migration percentages were different.

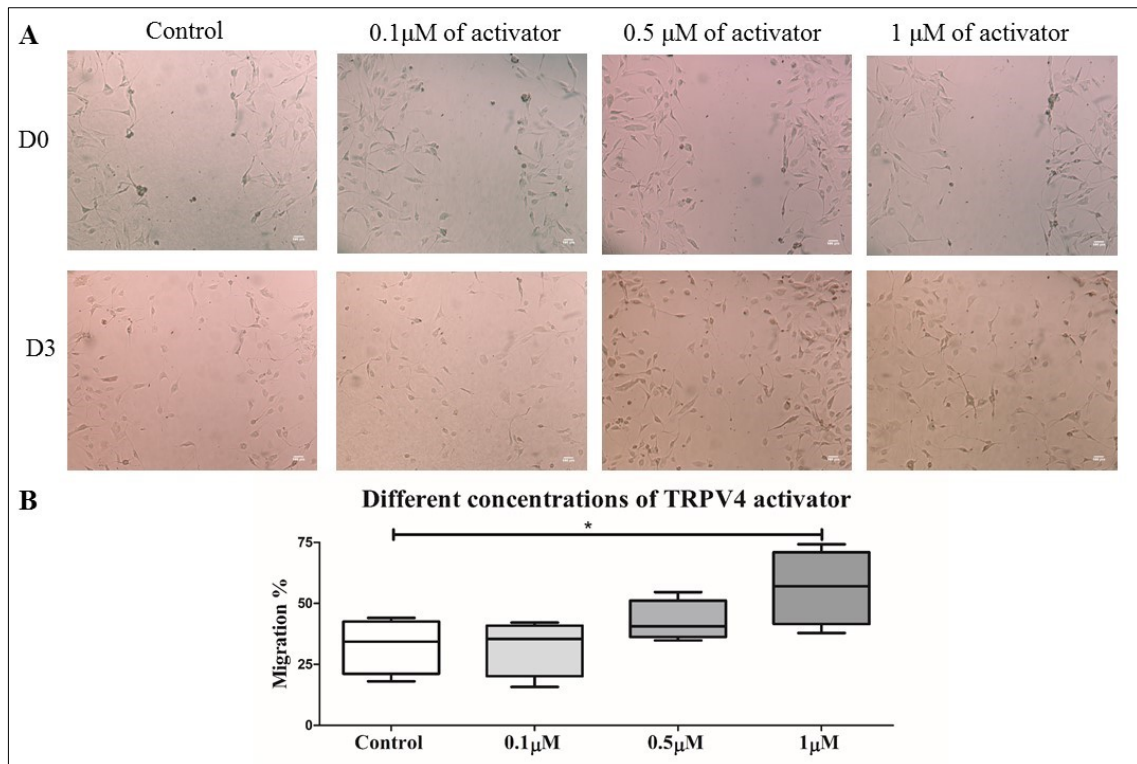


Figure 7-8: The effects of TRPV4 channel activation on VIC migration. A) Phase-contrast microscopy of scratch assay shows patterns of migration of VICs along the wound edge at Day 0 (first row) and Day 3 (second row). VICs were grown in different concentrations (0.1 μM, 0.5 μM, and 1 μM) of TRPV4 channel activator starting from Day 0 (control). Scale bar indicates 100 μm. B) Charts show migration percentage of VICs under different concentrations of the pharmacological activator of the TRPV4 channel. The median values were statistically analysed by one-way ANOVA followed by Friedman test. Data are presented in the box and whisker plot format, n = 4. *P < 0.05.

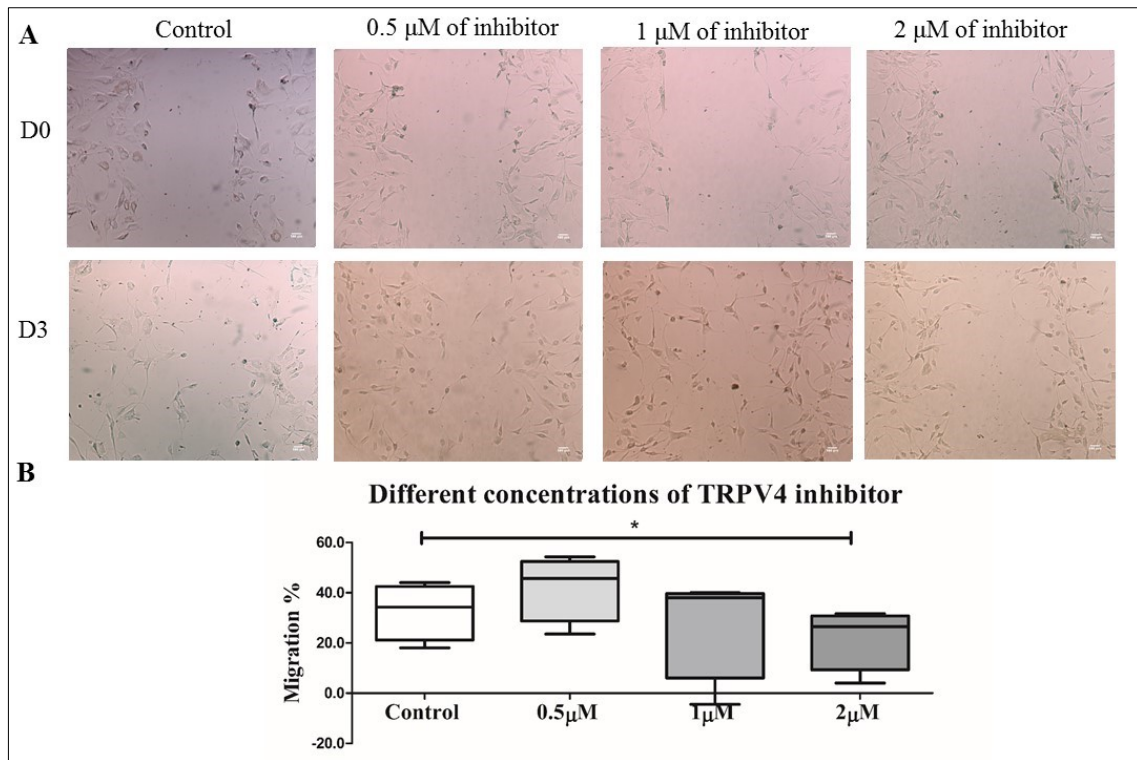


Figure 7-9: The effect of TRPV4 channel inhibition on VICs migration. A) Phase-contrast microscopy of scratch assay shows patterns of migration of VICs along wound edge at D0 (first row) and D3 (second row). VIC was growing in different concentration of TRPV4 channel activator started from 0 (control), 0.5 μM , 1 μM , and 2 μM concentration. Scale bar indicates 100 μm . B) charts show migration percentage of VICs under different concentration of pharmacological activator of TRPV4 channel. The median values were statistically analysed by one-way ANOVA followed by Friedman test. Data are presented in the box and whisker plot format, $n=4$. * $P < 0.05$.

7.4.3 Role of SACs on the proliferation of VICs

The proliferation of VICs is an essential process in valve repair and remodelling. The proliferation of VICs is modulated by different factors such as mechanical forces (Willems et al., 1994). This study assesses the contribution of SAC to the proliferation of VICs. This is tested in terms of stimulation and enhancement of VIC proliferation by activation of SACs as well as inhibition of proliferation by blocking of SACs' activity. The proliferation of VICs was studied and was found to be low in the case of a fibroblast phenotype which presents a normal condition of VICs, when low serum (2%) was used. The proliferation became higher after differentiation into the myofibroblast phenotype by using 10% FCS (Latif et al., 2015). Therefore, this investigation started with using some channel activators (TRPC3/6, TRPV4, and K^+ channels) in fibroblast medium (2% FCS), to examine the role

of SAC to stimulate proliferation. The proliferative capacity for VICs has changed for the groups with three specific channels activators as compared with the control group after 14 days [data are not shown because the changes were not significant due to a low n number (3)]. Therefore, the experiments were repeated with different doses of the activators and a high enough number of different VIC isolates. Experiments were performed in 2% FCS medium to minimize basal levels of proliferation, showed that after 14 days 2%FCS gave a small but non-significant increase in cell proliferation. Proliferative capacity for VICs was unchanged after 14 days of culture for different doses of GSK1016790A TRPV4 channel activator in 2% FCS versus the control group (**Figure 7-10, A**). The number of dead cells was measured by live and dead cells assay, dead cells rate was similar to the control group ($6.8\% \pm 7\%–11\%$) upon treatment with different doses of TRPV4 channel activator (1nM, 0.1 μM , 0.5 μM , and 1 μM). In contrast, it was noted that GSK1702934A the TRPC3/6 channel activator was effective in promoting VIC proliferation and, even though dead cells rate did not change with all doses ($6.8\% \pm 0\%–15\%$). In the presence of (0.25 μM) TRPC6/3 activator GSK1702934A, there was a small, but significant increase in cell proliferation at the lowest concentration used. At higher concentrations of GSK1702934A (0.5 μM , 1 μM , and 2 μM), there was a progressive reduction in cell number back to (0.25 μM) levels (**Figure 7-10, B**). Like the TRPV4 activator, (1 μM , 5 μM , 10 μM , and 20 μM) of Arachidonic acid the potassium channel activator also has no significant effect on the rate of proliferation of VIC after 14 days as compared to the control group (**Figure 7-10, C**). The VICs treated with lower doses of K^+ channel activator (1 μM and 5 μM) showed a similar percentage of dead cells to in the case of the control group ($6.8\% \pm 7\%–13\%$). The highest doses of K^+ channel activator (10 μM and 20 μM) were more toxic and a higher number of dead cells was observed in comparison to the control group ($6.8\% \pm 32\%–87\%$).

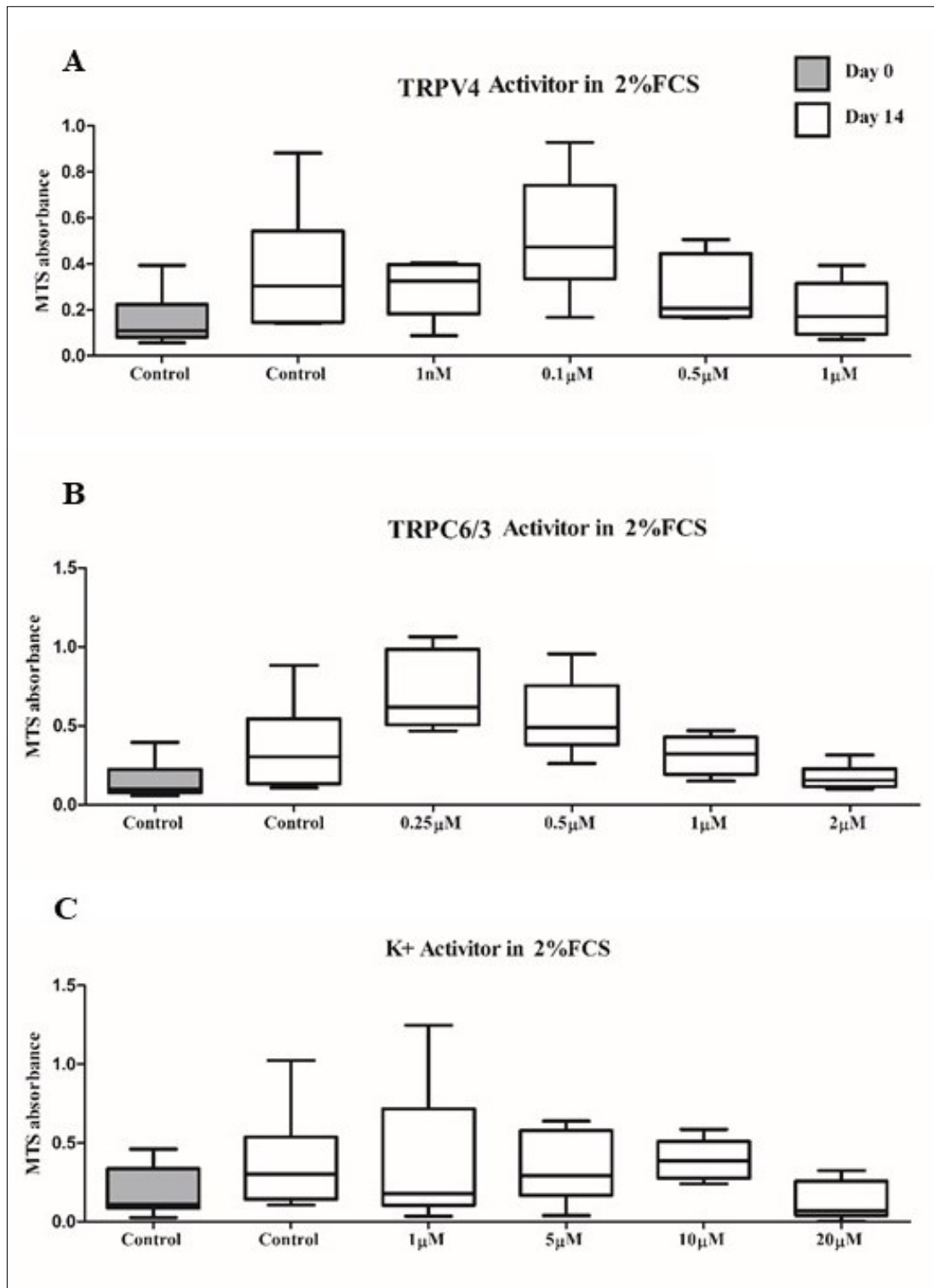


Figure 7-10: The effects of different channel activator in VIC proliferation in 2% FCS medium. Proliferation was measured by MTS absorbance. A) The chart shows the proliferation of VICs in the presence of TRPV4 channel activator on Day 0 and Day 14 for different groups (i.e., control, 1 nM, 0.1 μM, 0.5 μM, and 1 μM of the activator). B) The chart shows the proliferation of VICs in the presence of TRPC3/6 channels activator on Day 0 and Day 14 for different groups (i.e., control, 0.25 μM, 0.5 μM, 1 μM, and 2 μM of the activator). C) The chart shows the proliferation of VICs in the presence of K⁺ channels activator on Day 0 and Day 14 for different groups (i.e., control, 1 μM, 5 μM, 10 μM, and 20 μM of the activator). The median values were statistically analysed by ANOVA and the Friedman test and compared by Dunn's test. Data are presented in the box and whisker plot format, n=6. *P < 0.05.

In parallel, the same experiments were performed with three channels activators in 10% FCS medium to maximize the proliferation of VICs, to investigate whether SAC activation inhibited proliferating of VICs and ensure that high doses of the channel activators were not toxic to the VICs. VICs were proliferated in the presence of GSK1016790A TRPV4 channel activator in 10% FCS in the medium in all doses (1nM, 0.1 μ M, 0.5 μ M, and 1 μ M) (**Figure 7-11, A**). Also, GSK1702934A TRPC3/6 activator did not show a difference in VIC proliferation in the presence of 10% FCS in the medium in all doses (0.25 μ M, 0. 5 μ M, 1 μ M, and 2 μ M) (**Figure 7-11, B**). Also, the various doses (1 μ M, 5 μ M,10 μ M, and 20 μ M) of Arachidonic acid the potassium channel activator did not affect the proliferation in the presence of 10% FCS in the medium (**Figure 7-11, C**).

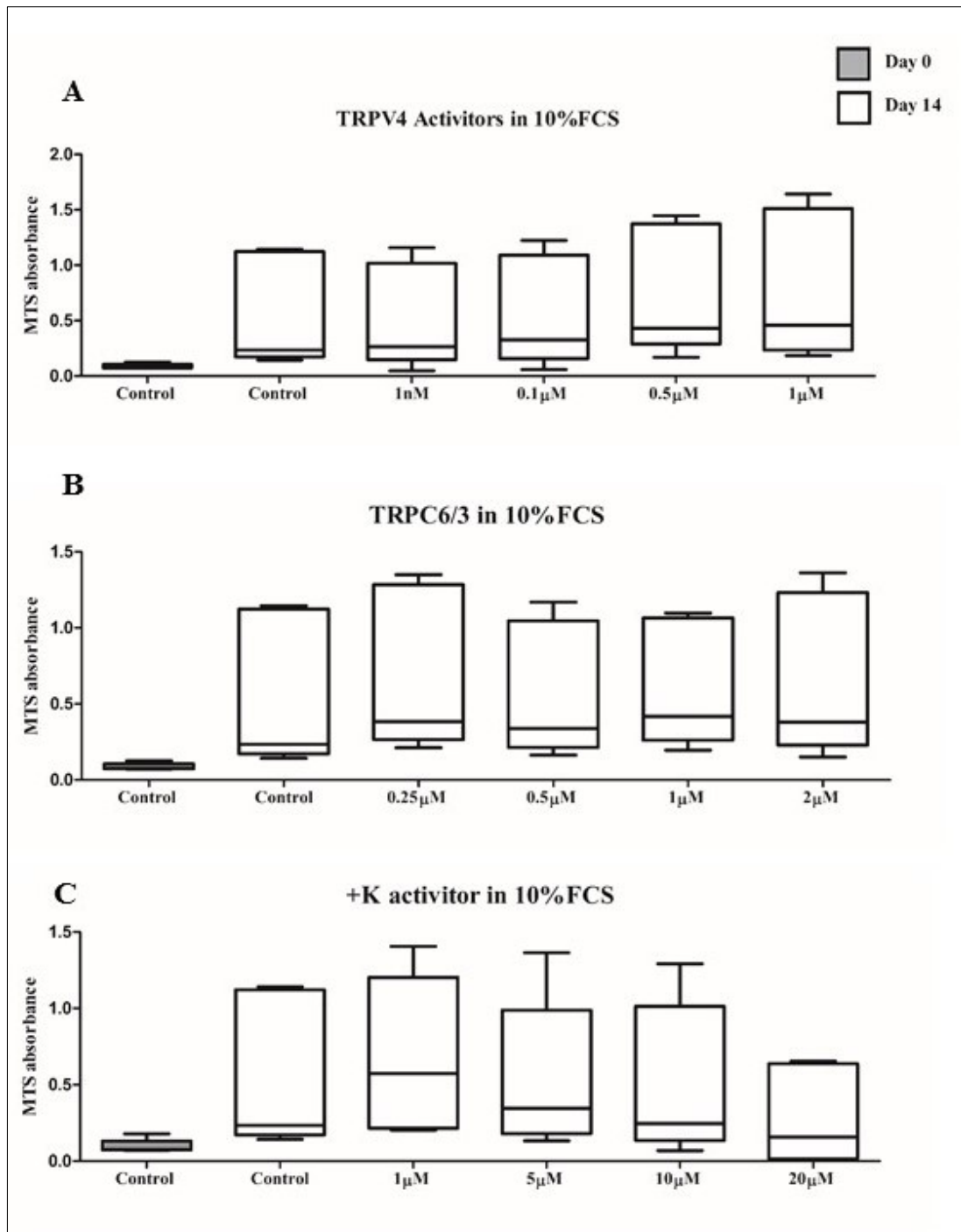


Figure 7-11: The effects of different channel activator in VIC proliferation in 10% FCS medium. Proliferation was measured by MTS absorbance. A) The chart shows the proliferation of VICs in the presence of TRPV4 channel activator on Day 0 and Day 14 for different groups (i.e., control, 1 nM, 0.1 μ M, 0.5 μ M, and 1 μ M of the activator). B) The chart shows the proliferation of VICs in the presence of TRPC3/6 channels activator on Day 0 and Day 14 for different groups (i.e., control, 0.25 μ M, 0.5 μ M, 1 μ M, and 2 μ M of the activator). C) The chart shows the proliferation of VICs in the presence of K⁺ channels activator on Day 0 and Day 14 for different groups (i.e., control, 1 μ M, 5 μ M, 10 μ M, and 20 μ M of the activator). The median values were statistically analysed by ANOVA and the Friedman test and compared by Dunn's test. Data are presented in the box and whisker plot format, n=4. *P < 0.05.

7.5 Discussion

Aortic VICs maintain valve function via ECM production, cell proliferation, and migration. Hemodynamic forces are applied to AV leaflets throughout the cardiac cycle, which are ultimately transduced to VICs within the valve cusps through different mechanotransduction pathways, which may include SACs. SACs are involved in cardiovascular biology and pathology such as arrhythmias (Hu and Sachs, 1997). However, the effects of SACs on VICs have not been previously studied or reported. Thus, in this chapter, the possible functional effects mediated by SACs in VICs were investigated using currently pharmacological activators and inhibitors of certain channels. In general, the data shown that SACs play a regulatory role in the collagen production, migration, and proliferation of VICs. The key goal of this work was to understand the contribution of individual SACs on the three functional responses that the data with streptomycin indicated SAC to be involved.

Collagen is the major component of ECM in AV, forming about 50% of the total ECM composition. There are three forms of collagen in AV, including collagen types I, III, and V. Collagen type I is the most abundant collagen type in AV and forms about 74% of the ECM, whereas type III (24%) and type V (2%) are less prevalent. The unique collagen fibre organization within AV provides mechanical strength to the valve by the existence of fibrils, allowing for leaflets to resist the load and expand during valve closure and ensure valve cell attachment and migration (Cheng et al., 2017). Therefore, collagen homeostasis maintenance is essential for proper valve function, and collagen disorganization is a common hallmark of valve calcification. It is known that VICs synthesize collagen in response to cyclic stretch *in vitro*, as the induction of collagen synthesis was measured by gene expression and secretion level of collagen (Ku et al., 2006, Xing et al., 2004a, Xing et al., 2004c). In many studies, it is believed that cells are stretched by 10% under

physiological conditions and 15% stretch under pathological conditions. Interestingly, one study determined that in dogs, leaflet length increased 31% from systole to diastole in the radial direction. This study also showed when the stretch of valve cusps was measured in vitro, it was more than twice that estimated in vivo, which appears to be due to the shielding effect of the ECM on VICs within the cusp (Thubrikar et al., 1986). The valve cells are shield by tissue stretch and the real degree of stretch that is experienced directly by the valve cells is about 15%, and this amount is comparable across different species (Lewinsohn et al., 2011). Therefore, the stretching protocol used in this study was 15% stretch. In conclusion, the role of stretch force in regulating collagen production in VICs is well-documented; however, the role of stretch-activated channels as a transducer of this stretch force has not been explored. SACs have been linked to collagen synthesis in other tissues such as chondrocytes. Synthesis of collagen was upregulated by stretch-induced matrix deformation. The calcium channel blocker (nifedipine) inhibited the stretch-induced increase of collagen (Wu and Chen, 2000). This study determined the effects of SACs in collagen synthesis in response to stretch. Non-specific blocker (streptomycin) decreased stretch-induced increase of collagen I and collagen III gene expression. On the other hand, elastin gene expression was not changed in the presence of streptomycin, which could be due to the short period of the experiment (24h). These results need to be confirmed by measuring protein expression of collagen I and collagen III gene expression. Also, this study investigated the role of TRPC6/3, TRPV4, +K, and Piezo channels in collagen production and showed that inhibition of TRPC6/3, TRPV4, and Piezo channels reduced the collagen production whereas inhibition of +K channels did not affect collagen production in VICs in response to stretch..

Also, it has presented and assessed new information, from in vitro studies, regarding the regulatory roles of SACs channels in VIC migration. The migration of VICs is a key

process in valve repair and maintenance (Durbin and Gotlieb, 2002). Tractional forces generated by the cells during cells migration that may act as the stimulus for the activation of SAC in the cells. SACs were also shown to have regulatory roles in the migration of different cells types. For example, the TRPM7 channel drives the migration and invasion of breast cancer cells via control EGF-induced signal transducer and activator of transcription 3 phosphorylation, while the TRPV2 channel controls the migration of PC3 prostate cancer cells by endogenous lysophospholipids. In this study, the regulatory role of SACs channels in the migration ability of VICs has been documented, where the inhibition of these channels by streptomycin reduced the migration percentage of VICs. Also, the migration ability of VICs was deemed controllable by specifically TRPC3/6 and TRPV4 channels, as channels' activation increased VIC migration and their inhibition reduced VIC migration in a dose-dependent manner. These findings are thus important from a therapeutic viewpoint because SACs appear to regulate valve repair and thus any valve therapies involving the modulation of SACs would affect valve repair.

Notably, SACs regulates Ca²⁺ entry, which plays an important role in cell proliferation. Some of these SACs have been shown to have regulatory roles in the proliferation of different cells types such as the TRPC6-modulated proliferation of several cancer cell types. Also, TRPM4 has a pro-proliferative effect in Wilms tumours and prostate cancer cells (Smani et al., 2015). In this study, it has have investigated the role of TRPC6/3, TRPV4, +K, and Piezo channels as a transducer of mechanical forces in cell proliferation. The role of SAC in VIC proliferation remains unclear, since the activation of TRPV4 and K⁺ channels did not increase VIC proliferation, even after minimizing proliferation by reducing the FCS concentration. However, the activation of the TRPC3/6 channel significantly increased VIC proliferation at low concentration of TRPC3/6 channel activator (0.25 μ M of GSK1702934A), in cells where there was only a low stimulus for

the cells to proliferate (2% serum). The TRPC3/6 channel activator (GSK1702934A) has not shown any augmented or inhibited effect in the presence of 10%FCS where the cells were stimulated to proliferate. It has been well documented that TRPC6 channel increase proliferation in different cancer cell lines (Jardin et al., 2018).

The major limitation with this kind of experiment in this study is related to the use of a nonspecific blocker (streptomycin). However, streptomycin provided a general guide to the potential roles of SACs in regulating different functions of valve cells. While 40-100 μ M of streptomycin inhibits SACs' activity, this concentration is routinely used in cell culture for its antibiotic properties and is therefore unlikely to affect other functions of the cell. In terms of specific blocker and activators, all compounds and their concentrations have been chosen based on selective publications.

7.6 Limitations and future work

In general, the specificities of some of the compounds that either inhibit or activate SACs are not specific to one channel, and further studies are required involving either compounds with greater specificities or that use molecular techniques to knock-out specific channel proteins that could lead to a specific determination of effects mediated by SAC. The transfection of vascular endothelial cells to generate SAC knockout mice was performed in different studies (Li et al., 2014). However, the knock-down technique may be difficult in the human primary valve cell line, and it is hard to get an efficient knock-down of protein expression. Also, the transfection lasts in the cells for 1-2 days and needs to be maintained during the experiments.

This study was also limited by the fact that FlexCell is a simplified system that lacks the 3-D and multicellular complexity of the tissue. FlexCell provides a multi-radial stretch whereas *in vivo*, the cells experience a circumferential and a radial stretch, each of which differs in magnitude to the other. In addition, different hemodynamic environments apply different stretch patterns and the mechanical force is also layer-dependent, with differences between the fibrosa and ventricularis layers due to differences in phenotypical cells and extracellular matrix (ECM) cues (Yip and Simmons, 2011). Therefore, different stretch patterns and pathological stretch should be considered in future works. Also, this experiment measures only collagen synthesis by VICs without the consideration of VECs and cellular interaction between VICs and VECs. It could be performed involving intact valve tissue or de-endothelized valve tissue to include the effects of VICs, VECs, and the interaction between valve cells and localized collagen expression in order to determine the individual effects of VICs and VECs. However, the approach used in this study provided insight into the potential role of SACs in regulating collagen production by VICs. Therefore, the future work clearly needs to focus on determining exactly the effect of VICs

and VECs on collagen synthesis. The experiments were carried out on fibroblast phenotypic condition of VICs which present the physiological conditions. The duration of this experiment did not allow for the assessment of functional and phenotypic changes of VICs used that related to collagen synthesis, such as changes in VIC differentiation.

Migration experiments have been carried out with an *in vitro* experimental wound made (scratch assay) in a confluent monolayer of VICs as a model of interstitial cell repair.

Notably, the scratch assay is an artificial situation that does not arise during the normal function of the cells in the valve. However, the scratch assay does not consider the effects of ECM on cells and hemodynamic forces that the valve is normally exposed to *in vivo*, though their role on regulating interstitial cell migration was reported (Durbin and Gotlieb, 2002). Also, it requires a relatively long time and consumes a large number of cells and materials. Despite these limitations, overall, *in vitro* scratch assay is a simple method to study cell migration, is compatible with microscopy, and does not require any expensive supplies. However, these experiments can be more useful and successful if they were designed to add *in vivo* components including mechanical forces and ECM either alone or in combination so as to investigate more complex regulation schemes of VIC migration.

In the proliferation studies, only the activation of TRPC3/6 was shown to promote VIC proliferation at one dose (0.25 Mm). Therefore, using lower doses is required to find where the threshold of this effect is. The subsequent loss of effect at the higher concentrations could be caused by channel desensitization due to over stimulation at the concentrations used. These findings are thus important from a therapeutic viewpoint because VICs appear to regulate valve repair and function. Furthermore, any valve therapies involving the modulation of VIC function would affect valve repair and maintenance. Investigations involving determining the correlations between SAC activity and collagen production as

well as the proliferation and migration of VICs will provide new insights into the cellular and molecular factors that regulate AV calcification.

7.7 Conclusions

- Some SACs promote collagen production in aortic VICs under stretch conditions and the inhibition of these channels leads to a reduction in collagen production.
- Some SACs modulate the migration ability of aortic VICs, where the activation increases the migration percentage and the inhibition of SACs reduces it.
- Some SACs play a regulatory role in the proliferation of aortic VICs.

Chapter 8

Discussion and Limitation and Future Work

8.1 Discussion

AV is a sophisticated structure that performs a complex function to prevent the backflow of blood into the left ventricle, optimise coronary blood flow, and maintain myocardial function. AV is located in a unique mechanical environment within the heart, wherein the opposing sides of the valve experience continuous, yet different, hemodynamic forces, including pressure, oscillatory shear stress, unidirectional shear stress, and cyclic strain. Adaption to the mechanical environment is a critical feature that is involved in the regulation of valve function; this adaption is based on the ability to sense mechanical forces (mechanotransduction). Although the mechanisms of valve mechanotransduction are ill-defined, this thesis has identified that stretch-activated channels (SACs) are expressed in VIC and VEC and have the capacity to be an important mechanotransduction element in AV cells. Stretch-activated channels are defined in the broadest sense by their ability to allow ions to pass through a cell membrane in response to mechanical stimuli, thus converting mechanical forces into intracellular signalling. Stretch-activated channels are functional mechanotransducers in different tissues, including the heart, and their role in heart disease has been documented (Reed et al., 2014).

The first question in this study addresses the current understanding of SACs in valve interstitial and endothelial cells. Prior studies have noted the importance of six SACs in the cardiovascular system, including TRPC6, TRPM4, TRPV4, KCNK2, KCNJ8, and Piezo1. Their importance is based on their regulatory roles in different functions: KCNK2 plays a role in differentiation and interactions between immune cells and muscle cells (Afzali et al., 2016); piezo1 aligns endothelial cells (Volkers et al., 2015), TRPV4 helps with the thermoregulation of peripheral vessels (Nilius et al., 2004b), TRPC6 plays a role in the transdifferentiation of cardiac fibroblasts (Nishida et al., 2015), and TRPM4 is used

in cardiac conduction (Abriel et al., 2012). Therefore, these channels were targeted in VECs and VICs, and their presence has been proven via different techniques.

TRPC6, TRPM4, TRPV4, KCNK2, KCNJ8, and Piezo1 channels were found to be expressed in valve interstitial and endothelial cells. These channels are considered one potential way to sense mechanical forces and translate them into inter-cellular signalling to regulate a range of different cell functions. With regard to VECs, this study finds that the expression patterns of TRPM4, TRPV4, TRPC6, KCNK2, KCNJ8, and Piezo1 is different between VECs from the aortic side and ventricular side of the valve. Previous studies have demonstrated that VECs from each side of the valve differ in their expression of pro- and anti-calcification / inflammatory gene, and differences in their regulation of ECM proteins in response to flow (Mongkoldhumrongkul et al., 2018, Simmons et al., 2005). This difference in function is most likely a reflection of the difference in the mechanical environment experienced by each side, caused by the patterns of flow seen by each surface of the valve. The variations in SAC expressed in aortic and ventricular VEC suggest that the mechanotransduction pathways of each side may also differ. The precise role of SAC in each side of the valve can only be confirmed by specific inhibition of SACs activity by either the use of specific channel blockers or by the knock-down the genes for the expression of these channels. Data from Chapter 6 was able to demonstrate an in-vitro role for SAC in valve endothelial cell alignment as an indicator of VEC response to shear stress. In this study, streptomycin was used as a general (non-selective) blocker of SACs under shear stress. The inhibitory effect of streptomycin confirms that SACs play a role in response to shear stress and that the inhibition of SACs reduces the alignment of VECs from both the aortic and ventricular sides of AV in a dose-dependent manner. The specific inhibitors of TRPC6/3, TRPV4, K⁺, Piezo1 channels in VECs from both sides suggested a role for these channels in the alignment of VECs in response to shear stress. However,

statistical analysis revealed that only the inhibition of the TRPC3/6 channels was significant in this regard. The TRPC6 channel regulates the actin cytoskeleton function, which is involved in stabilizing cell morphology and maintaining the internal structure of a cell (Zhao et al., 2015). The Piezo1 channel exhibited a promising result, as the Piezo1 channels clearly reduce the VEC alignment from both the aortic and ventricular sides of AV; however, this finding was not statistically significant. Nevertheless, recent studies have determined the importance of piezo1 channels in modulating the different functions of VECs, especially endothelial cell alignment (Volkers et al., 2015). Therefore, the non-significant result of the piezo1 channels could be due to a low “n” number (n=3). This is due in part to the difficulty in obtaining viable cultures of VEC from each side of the same valve. Additional studies are therefore required to confirm if there is a role for piezo channel in VEC alignment. The findings of this study are consistent with those of previous studies, which demonstrated differential responses to mechanical force by VECs from different sides of AV (Mongkoldhumrongkul et al., 2018, Simmons et al., 2005).

Furthermore, this study also aims to examine the role of SAC activity in the VIC function of the fibroblast phenotype, because it represents the predominated cell type found in healthy valves. This study shows that the expression levels of SAC in VIC different according to the phenotype of the cells. Potassium channels (KCNK2 and KCNJ8) were downregulated in fibroblast phenotypes, and TRP channels (TRPM4, TRPV4, and TRPC6) were upregulated in osteoblast phenotype. Given their expression pattern in VIC phenotypes, suggest that their expression and function may therefore change in disease processes -since myofibroblast and osteoblast are associated with pathological changes.

The main functions of VICs were investigated and the role of SACs in regulating these functions assessed. Firstly, it is established that VICs produce collagen in response to stretch (Ku et al., 2006). Changes in the collagen I and collagen III gene expression were

compared for three conditions: static, stretch, and stretch with the inhibition of SACs by streptomycin, which prevented the up-regulation of collagen I and collagen III gene expression by the stretch. This result suggests that the SACs play a regulatory role in the collagen production of VICs in AV. An attempt was made to determine the specific channel effects, and TRPC6/3, TRPV4, and Piezo1 were found to be effective, although no effect of potassium channels was detected. The next section of this study is concerned with the role of SACs in VIC migration. Similar to collagen production, the inhibition of all SACs significantly reduces the migration of VICs. The TRPV4 and TRPC6/3 channels modulated the migration of VICs, in that the activation of these channels increases the migration ability of VICs, while the inhibition of these channels decreases the migration ability of VICs. Finally, the activation of these channels by pharmacological activator in static culture was used to investigate the role of SACs in VIC proliferation. Four channels and channel families were targeted: Only the activation of the TRPC6/3 channels was found to play a regulatory role in the proliferation of VICs. Taken together, these results suggest that there is a regulatory relationship between SACs and the function of VICs within AV. As the mechanical forces show regulatory roles in valve cells, the mechanical forces transducers (SACs) show regulatory roles in valve cells. In recent years, growing evidence has been accumulated regarding the fundamental roles of SACs in SMCs, VSMC, and cardiomyocytes (Afzali et al., 2016, Smani et al., 2015). For example, downregulation of TRPC6 or TRPM4 significantly reduces pressure-induced depolarisation in arterial smooth muscle and decreases the myogenic vasoconstriction in an intact cerebral artery (Afzali et al., 2016, Smani et al., 2015). This study revealed the effects of SACs in different essential functions of valve cells, including collagen synthesis, migration, and proliferation of VICs and alignment of VECs. These results need more confirmation, investigation, and exploration of more channels in valve cells.

The differentiation of VICs into myofibroblasts and osteoblasts in AV is a key cellular mechanism in the calcification of AV (Wyss et al., 2012) and the expression of patterns in SACs. Thus, the expression of patterns in SACs was studied between non-calcified and calcified AV to determine the possible association of SACs to valve calcification. Various methods were used to compare SAC expression between non-calcified and calcified AV, including the WB of cells and tissue, the RT-PCR, and the paraffin section stain of non-calcified and calcified AV. Based on the WB of valve tissue and the paraffin section stain, SAC expression is more pronounced in the calcified AV than the non-calcified AV, and this difference is related to the upregulation of calcification markers in calcified AV. The upregulation of SACs in calcified valves might be caused by present VICs differentiated to osteoblast. It has been demonstrated in Chapter 4 that SACs were upregulated in VICs differentiated to osteoblast. Also, it could be a possible response to the increased stiffness of valve tissue in calcification, wherein calcification by valve interstitial cells is regulated by the stiffness of the extracellular matrix in vitro (Yip et al., 2009). These results advance the scientific community's understanding of AV calcification and new therapeutic strategies to target valve calcification by SACs.

Due to practical constraints, this study could not provide a comprehensive study of SACs channels activity using patch clamping techniques. Therefore, this study primarily depended on pharmacological and biological techniques. Streptomycin acted as an open channel blocker of all SACs and was therefore a useful way to provide a general overview of the potential role of SACs. Conversely, the specific pharmacological modulators emphasize the usefulness of these modulators to elaborate the channel effect, although this approach is still limited by the availability of these modulators and, in some channels, no specific modulators were reported. The best available option to study specific channels is to knock-down the expression of a gene for each channel. Despite the reasonableness of

this idea, it is difficult to perform in primary cultures of human cells and within the time constraints of this study. Therefore, the available pharmacological modulators were utilised to obtain an overview of SACs and their role in regulating valve cell functions.

In conclusion, further identification of SAC channels in AV cells will require new tools and experiments. Nevertheless, this study confirms the presence of SACs in VECs and VICs. Moreover, this study describes the recent findings on differences in the SACs present in VECs in the aortic and ventricular side at both the molecular and physiological levels. It further highlights the recent progress made in understanding the role of SACs in differentiating VICs and the possibility of controlling the differentiation of VICs.

8.2 Limitations

In this study, different techniques were used to identify and study SACs' presence and their potential roles in valve cells. Various techniques were used to investigate the presence of SACs, including electrophysiology and biology techniques. Also, the functional roles of SACs were investigated in different ways of activation of SACs by either mechanical force or pharmacological modulators. Therefore, the findings in this report were obtained from different approaches. These findings were subject to the limitations mentioned in relevant chapters. The main limitation was the lack of specific pharmacological modulators. The use of non-specific blocker (streptomycin) was helpful to provide a general idea or overview of the potential roles of SACs. On the other hand, the need for specific pharmacological modulators is critical to individually determine the exact role of every channel. However, the best available pharmacological modulators were used in this study, and their concentrations were considered efficient and did not affect cells' viability. Another important limitation in this study was performed in 2D cultures. It is known that cells respond differently when maintained in 3-D, which are a closer replication of the *in vivo* environments. .

In conclusion, although current biology and medicine have been developed over the centuries through the study of genetics, chemistry, and biology, recent work from different fields have discovered that mechanical forces play an important role in cell function control and the development of chemicals, biological elements and genes (Ingber et al., 2014). Subsequently, mechanotransduction has garnered the interest of scientists who want to understand cell behaviour in mechanical environments. One questions within the field of heart valve biology concern how AV cells sense and transduce the force at the molecular level and how these mechanotransducers regulate AV functions. This study has

defined the presence of some SACs and established possible roles for SACs in valve cells' functions.

8.3 Future Work

Further investigation and experimentation into the roles of SACs in cellular valve function are strongly recommended. More research should also investigate SACs that exhibit regulatory roles in valve cells, such as piezo1 and TRPC6. It would be appropriate to study individual SACs using molecular biology approaches, such as the siRNA technique, to overcome issues with the limited selectivity of pharmacological modulators. Another possible area of future research would be to investigate SACs in 3D cultures to mimic in vivo environments. It is also important to establish whether SACs regulate VECs in a site-specific manner, as the application of site-specific shear stress could provide more definitive evidence regarding the roles of different SACs on site-specific valve endothelial cells. Finally, future research regarding the role of SACs on AV calcification would undoubtedly be worthwhile to support extant research on AV calcification. More research is needed to better understand this role by studying the calcification process during the different level of SAC activation. These studies can help understand how SACs are involved in the mechanotransduction of the AV, as well as their roles in regulating valve functions.

References

- ABRIEL, H., SYAM, N., SOTTAS, V., AMAROUCHE, M. Y. & ROUGIER, J.-S. 2012. TRPM4 channels in the cardiovascular system: physiology, pathophysiology, and pharmacology. *Biochemical pharmacology*, 84, 873-881.
- AFZALI, A. M., RUCK, T., HERRMANN, A. M., IKING, J., SOMMER, C., KLEINSCHNITZ, C., PREUBE, C., STENZEL, W., BUDDE, T. & WIENDL, H. 2016. The potassium channels TASK2 and TREK1 regulate functional differentiation of murine skeletal muscle cells. *American Journal of Physiology-Cell Physiology*, 311, C583-C595.
- AGUIAR, C., THERRIEN, J., LEMIRE, P., SEGURA, M., SMITH, L. & THEORET, C. 2016. Differentiation of equine induced pluripotent stem cells into a keratinocyte lineage. *Equine veterinary journal*, 48, 338-345.
- AICHER, D., URBICH, C., ZEIHNER, A., DIMMELER, S. & SCHÄFFERS, H.-J. 2007. Endothelial nitric oxide synthase in bicuspid aortic valve disease. *The Annals of thoracic surgery*, 83, 1290-1294.
- AL-YAMANI, M. 2016. COX-2 and the vascular system: interactions with endothelial pathways and the eNOS system. Imperial College London.
- ARJUNON, S., DINH, A.-T., RATHAN, S. & AJIT YOGANATHAN, A. Y. 2012. Design of a novel ex vivo bioreactor to investigate the effect of pressure induced stretch on aortic valve biology. *QScience Proceedings*, 72.4.72
- ARJUNON, S., RATHAN, S., JO, H. & YOGANATHAN, A. P. 2013. Aortic valve: mechanical environment and mechanobiology. *Annals of biomedical engineering*, 41, 1331-1346.
- ARORA, P. D. & MCCULLOCH, C. A. 1994. Dependence of collagen remodelling on α -smooth muscle actin expression by fibroblasts. *Journal of cellular physiology*, 159, 161-175.
- AZIZ, Q., THOMAS, A. M., GOMES, J., ANG, R., SONES, W. R., LI, Y., NG, K.-E., GEE, L. & TINKER, A. 2014. The ATP-sensitive potassium channel subunit, Kir6.1, in vascular smooth muscle plays a major role in blood pressure control. *Hypertension*. 114.03116.
- BAE, C., SACHS, F. & GOTTLIEB, P. A. 2011. The mechanosensitive ion channel Piezo1 is inhibited by the peptide GsMTx4. *Biochemistry*, 50, 6295-6300.
- BALACHANDRAN, K., KONDURI, S., SUCOSKY, P., JO, H. & YOGANATHAN, A. P. 2006. An ex vivo study of the biological properties of porcine aortic valves in response to circumferential cyclic stretch. *Annals of biomedical engineering*, 34, 1655-1665.
- BALACHANDRAN, K., SUCOSKY, P., JO, H. & YOGANATHAN, A. P. 2009. Elevated cyclic stretch alters matrix remodeling in aortic valve cusps: implications for degenerative aortic valve disease. *American Journal of Physiology-Heart and Circulatory Physiology*, 296, H756-H764.
- BALACHANDRAN, K., SUCOSKY, P., JO, H. & YOGANATHAN, A. P. 2010. Elevated cyclic stretch induces aortic valve calcification in a bone morphogenic protein-dependent manner. *The American journal of pathology*, 177, 49-57.
- BAUM, J. & DUFFY, H. S. 2011. Fibroblasts and myofibroblasts: what are we talking about? *Journal of cardiovascular pharmacology*, 57, 376-379.
- BENEMEI, S., PATACCHINI, R., TREVISANI, M. & GEPPETTI, P. 2015. TRP channels. *Current opinion in pharmacology*, 22, 18-23.

- BLACKMAN, B. R., GARCÍA-CARDENA, G. & GIMBRONE, M. A. 2002. A new in vitro model to evaluate differential responses of endothelial cells to simulated arterial shear stress waveforms. *Journal of biomechanical engineering*, 124, 397-407.
- BLOOMFIELD, P. 2002. Choice of heart valve prosthesis. *Heart*, 87, 583-589.
- BRAYDEN, J. E., EARLEY, S., NELSON, M. T. & READING, S. 2008. Transient receptor potential (TRP) channels, vascular tone and autoregulation of cerebral blood flow. *Clinical and Experimental Pharmacology and Physiology*, 35, 1116-1120.
- BREHM, P., KULLBERG, R. & MOODY-CORBETT, F. 1984. Properties of non-junctional acetylcholine receptor channels on innervated muscle of *Xenopus laevis*. *The Journal of physiology*, 350, 631-648.
- BREWER, R., MENTZER JR, R., DECK, J., RITTER, R., TREFIL, J. & NOLAN, S. 1977. An in vivo study of the dimensional changes of the aortic valve leaflets during the cardiac cycle. *The Journal of thoracic and cardiovascular surgery*, 74, 645-650.
- BROHAWN, S. G. 2015. How ion channels sense mechanical force: insights from mechanosensitive K^{2P} channels TRAAK, TREK1, and TREK2. *Annals of the New York Academy of Sciences*, 1352, 20-32.
- BUBOLZ, A. H., MENDOZA, S. A., ZHENG, X., ZINKEVICH, N. S., LI, R., GUTTERMAN, D. D. & ZHANG, D. X. 2012. Activation of endothelial TRPV4 channels mediates flow-induced dilation in human coronary arterioles: role of Ca²⁺ entry and mitochondrial ROS signaling. *American Journal of Physiology-Heart and Circulatory Physiology*, 302, H634-H642.
- BUTCHER, J. T. & NEREM, R. M. 2007. Valvular endothelial cells and the mechanoregulation of valvular pathology. *Philosophical Transactions of the Royal Society of London B: Biological Sciences*, 362, 1445-1457.
- BUTCHER, J. T., PENROD, A. M., GARCÍA, A. J. & NEREM, R. M. 2004. Unique morphology and focal adhesion development of valvular endothelial cells in static and fluid flow environments. *Arteriosclerosis, thrombosis, and vascular biology*, 24, 1429-1434.
- CHANDRA, S., RAJAMANNAN, N. M. & SUCOSKY, P. 2012. Computational assessment of bicuspid aortic valve wall-shear stress: implications for calcific aortic valve disease. *Biomechanics and modeling in mechanobiology*, 11, 1085-1096.
- CHAWLA, M., CHANG, A., VYAVAHARE, N., LEVY, R., GRAHAM, L. & GANNON, F. 1999. Identification and characterization of calcifying valve cells from human and canine aortic valves. *The Journal of heart valve disease*, 8, 254-260.
- CHENG, H., YAO, Q., SONG, R., ZHAI, Y., WANG, W., FULLERTON, D. A. & MENG, X. 2017. Lysophosphatidylcholine activates the Akt pathway to upregulate extracellular matrix protein production in human aortic valve cells. *Journal of surgical research*, 213, 243-250.
- CHESTER, A. H. & BUTCHER, J. T. 2013. Side-Specific Endothelial-Dependent Regulation of Aortic Valve Calcification. *The American Journal of Pathology*, 182, 1922-1931.
- CHESTER, A. H., EL-HAMAMSY, I., BUTCHER, J. T., LATIF, N., BERTAZZO, S. & YACOUB, M. H. 2014. The living aortic valve: From molecules to function. *Global Cardiology Science and Practice*, 11, 52-77.

- CHESTER, A. H. & TAYLOR, P. M. 2007. Molecular and functional characteristics of heart-valve interstitial cells. *Philosophical Transactions of the Royal Society of London B: Biological Sciences*, 362, 1437-1443.
- CHIU, J.-J. & CHIEN, S. 2011. Effects of disturbed flow on vascular endothelium: pathophysiological basis and clinical perspectives. *Physiological reviews*, 91, 327-387.
- CHRISTENSEN, O. 1987. Mediation of cell volume regulation by Ca²⁺ influx through stretch-activated channels. *Nature*, 330, 66-68
- CLARK-GREUEL, J. N., CONNOLLY, J. M., SORICHILLO, E., NARULA, N. R., RAPOPORT, H. S., MOHLER III, E. R., GORMAN III, J. H., GORMAN, R. C. & LEVY, R. J. 2007. Transforming growth factor- β 1 mechanisms in aortic valve calcification: increased alkaline phosphatase and related events. *The Annals of thoracic surgery*, 83, 946-953.
- DARBY, W. G., POCOTNIK, S., RAMACHANDRAN, R., HOLLENBERG, M. D., WOODMAN, O. L. & MCINTYRE, P. 2018. Shear stress sensitizes TRPV4 in endothelium-dependent vasodilatation. *Pharmacological research*, 133, 152-159.
- DENG, Z., PAKNEJAD, N., MAKSAEV, G., SALA-RABANAL, M., NICHOLS, C. G., HITE, R. K. & YUAN, P. 2018. Cryo-EM and X-ray structures of TRPV4 reveal insight into ion permeation and gating mechanisms. *Nature structural & molecular biology*, 25, 252-260.
- DREGER, S., TAYLOR, P., ALLEN, S. & YACOUB, M. 2002. Profile and localization of matrix metalloproteinases (MMPs) and their tissue inhibitors (TIMPs) in human heart valves. *The Journal of heart valve disease*, 11, 875-80; discussion 880.
- DURBIN, A. D. & GOTLIEB, A. I. 2002. Advances towards understanding heart valve response to injury. *Cardiovascular Pathology*, 11, 69-77.
- EARLEY, S., STRAUB, S. V. & BRAYDEN, J. E. 2007. Protein kinase C regulates vascular myogenic tone through activation of TRPM4. *American Journal of Physiology-Heart and Circulatory Physiology*, 292, H2613-H2622.
- EARLEY, S., WALDRON, B. J. & BRAYDEN, J. E. 2004. Critical role for transient receptor potential channel TRPM4 in myogenic constriction of cerebral arteries. *Circulation research*, 95, 922-929.
- EISENBERG, L. M. & MARKWALD, R. R. 1995. Molecular regulation of atrioventricular valvuloseptal morphogenesis. *Circulation research*, 77, 1-6.
- ENYEDI, P. & CZIRJÁK, G. 2010. Molecular background of leak K⁺ currents: two-pore domain potassium channels. *Physiological reviews*, 90, 559-605.
- FERDOUS, Z., JO, H. & NEREM, R. M. 2013. Strain magnitude-dependent calcific marker expression in valvular and vascular cells. *Cells Tissues Organs*, 197, 372-383.
- FRISHMAN, W. H., HUBERFELD, S., OKIN, S., WANG, Y. H., KUMAR, A. & SHAREEF, B. 1995. Serotonin and serotonin antagonism in cardiovascular and non-cardiovascular disease. *The Journal of Clinical Pharmacology*, 35, 541-572.
- GOTLIEB, A. I., ROSENTHAL, A. & KAZEMIAN, P. 2002. Fibroblast growth factor 2 regulation of mitral valve interstitial cell repair in vitro. *The Journal of thoracic and cardiovascular surgery*, 124, 591-597.
- GOTTLIEB, P. A., SUCHYNA, T. M., OSTROW, L. W. & SACHS, F. 2004. Mechanosensitive ion channels as drug targets. *Current Drug Targets-CNS & Neurological Disorders*, 3, 287-295.
- GOULD, S. T., SRIGUNAPALAN, S., SIMMONS, C. A. & ANSETH, K. S. 2013. Hemodynamic and cellular response feedback in calcific aortic valve disease. *Circulation research*, 113, 186-197.

- GU, X. & MASTERS, K. S. 2010. Regulation of valvular interstitial cell calcification by adhesive peptide sequences. *Journal of Biomedical Materials Research Part A: An Official Journal of The Society for Biomaterials, The Japanese Society for Biomaterials, and The Australian Society for Biomaterials and the Korean Society for Biomaterials*, 93, 1620-1630.
- GUHARAY, F. & SACHS, F. 1984. Stretch-activated single ion channel currents in tissue-cultured embryonic chick skeletal muscle. *The Journal of physiology*, 352, 685-701.
- GUINAMARD, R., DEMION, M., MAGAUD, C., POTREAU, D. & BOIS, P. 2006. Functional expression of the TRPM4 cationic current in ventricular cardiomyocytes from spontaneously hypertensive rats. *Hypertension*, 48, 587-594.
- HARTENECK, C. 2005. Function and pharmacology of TRPM cation channels. *Naunyn-Schmiedeberg's archives of pharmacology*, 371, 307-314.
- HARTMANNGRUBER, V., HEYKEN, W.-T., KACIK, M., KAISTHA, A., GRGIC, I., HARTENECK, C., LIEDTKE, W., HOYER, J. & KÖHLER, R. 2007. Arterial response to shear stress critically depends on endothelial TRPV4 expression. *PLoS one*, 2, e827.
- HOEHN, D., SUN, L. & SUCOSKY, P. 2010. Role of pathologic shear stress alterations in aortic valve endothelial activation. *Cardiovascular Engineering and Technology*, 1, 165-178.
- HOLLIDAY, C. J., ANKENY, R. F., JO, H. & NEREM, R. M. 2011. Discovery of shear- and side-specific mRNAs and miRNAs in human aortic valvular endothelial cells. *American Journal of Physiology-Heart and Circulatory Physiology*, 301, H856-H867.
- HONORÉ, E. 2007. The neuronal background K_{2P} channels: focus on TREK1. *Nature reviews neuroscience*, 8, 251-261.
- HU, H. & SACHS, F. 1997. Stretch-activated ion channels in the heart. *Journal of molecular and cellular cardiology*, 29, 1511-1523.
- HUMPHREY, J. D., DUFRESNE, E. R. & SCHWARTZ, M. A. 2014. Mechanotransduction and extracellular matrix homeostasis. *Nature reviews Molecular cell biology*, 15, 802-812.
- INAI, T., MANCUSO, M. R., MCDONALD, D. M., KOBAYASHI, J., NAKAMURA, K. & SHIBATA, Y. 2000. Shear stress-induced upregulation of connexin 43 expression in endothelial cells on upstream surfaces of rat cardiac valves. *Histochemistry and cell biology*, 122, 477-483.
- INGBER, D. E., WANG, N. & STAMENOVIĆ, D. 2014. Tensegrity, cellular biophysics, and the mechanics of living systems. *Reports on Progress in Physics*, 77, 046603.
- ISOMOTO, S., KONDO, C. & KURACHI, Y. 1997. Inwardly rectifying potassium channels: their molecular heterogeneity and function. *The Japanese journal of physiology*, 47, 11-39.
- JAALOUK, D. E. & LAMMERDING, J. 2009. Mechanotransduction gone awry. *Nature reviews Molecular cell biology*, 10, 63-73.
- JANIN, A., KONTTINEN, Y., GRÖNBLAD, M., KARHUNEN, P., GOSSET, D. & MALMSTRÖM, M. 1990. Fibroblast markers in labial salivary gland biopsies in progressive systemic sclerosis. *Clinical and experimental rheumatology*, 8, 237-242.
- JARDIN, I., DIEZ-BELLO, R., LOPEZ, J., REDONDO, P., SALIDO, G., SMANI, T. & ROSADO, J. 2018. TRPC6 channels are required for proliferation, migration and invasion of breast cancer cell lines by modulation of Orail and Orail3 surface exposure. *Cancers*, 10, 331-339.

- JERMIHOV, P. N., JIA, L., SACKS, M. S., GORMAN, R. C., GORMAN, J. H. & CHANDRAN, K. B. 2011. Effect of geometry on the leaflet stresses in simulated models of congenital bicuspid aortic valves. *Cardiovascular engineering and technology*, 2, 48-56.
- KAKKAR, R., YE, B., GALLES, K., HADHAZY, M., STOLLER, D. A., MAKIELSKI, J. C. & MCNALLY, E. M. 2005. Spontaneous Coronary Vasospasm in Katp Mutant Mice Arises From a Smooth Muscle-extrinsic Process. *Circulation*, 112, II-I-II-J.
- KENNEDY, J. A., HUA, X., MISHRA, K., MURPHY, G. A., ROSENKRANZ, A. C. & HOROWITZ, J. D. 2009. Inhibition of calcifying nodule formation in cultured porcine aortic valve cells by nitric oxide donors. *European journal of pharmacology*, 602, 28-35.
- KONTTINEN, Y., NYKÄNEN, P., NORDSTRÖM, D., SAARI, H., SANDELIN, J., SANTAVIRTA, S. & KOURI, T. 1989. DNA synthesis in prolyl 4-hydroxylase positive fibroblasts in situ in synovial tissue. An autoradiography-immunoperoxidase double labeling study. *The Journal of rheumatology*, 16, 339-345.
- KU, C.-H., JOHNSON, P. H., BATTEN, P., SARATHCHANDRA, P., CHAMBERS, R. C., TAYLOR, P. M., YACOUB, M. H. & CHESTER, A. H. 2006. Collagen synthesis by mesenchymal stem cells and aortic valve interstitial cells in response to mechanical stretch. *Cardiovascular research*, 71, 548-556.
- KUNDROTAS, G. 2012. Surface markers distinguishing mesenchymal stem cells from fibroblasts. *Acta Medica Lituanica*, 19, 75-79.
- LATIF, N., QUILLON, A., SARATHCHANDRA, P., MCCORMACK, A., LOZANOSKI, A., YACOUB, M. H. & CHESTER, A. H. 2015. Modulation of human valve interstitial cell phenotype and function using a fibroblast growth factor 2 formulation. *PLoS One*, 10, e0127844.
- LATIF, N., SARATHCHANDRA, P., TAYLOR, P., ANTONIW, J. & YACOUB, M. 2005. Molecules mediating cell-ECM and cell-cell communication in human heart valves. *Cell biochemistry and biophysics*, 43, 275-287.
- LEWINSOHN, A. D., ANSSARI-BENHAM, A., LEE, D. A., TAYLOR, P. M., CHESTER, A. H., YACOUB, M. H. & SCREEN, H. R. 2011. Anisotropic strain transfer through the aortic valve and its relevance to the cellular mechanical environment. *Proceedings of the Institution of Mechanical Engineers, Part H: Journal of Engineering in Medicine*, 225, 821-830.
- LI, J., HOU, B., TUMOVA, S., MURAKI, K., BRUNS, A., LUDLOW, M. J., SEDO, A., HYMAN, A. J., MCKEOWN, L. & YOUNG, R. S. 2014. Piezo1 integration of vascular architecture with physiological force. *Nature*, 515, 279-282.
- LI, Z., LEE, H. & ZHU, C. 2016. Molecular mechanisms of mechanotransduction in integrin-mediated cell-matrix adhesion. *Experimental cell research*, 349, 85-94.
- LIU, A. C., JOAG, V. R. & GOTLIEB, A. I. 2007. The emerging role of valve interstitial cell phenotypes in regulating heart valve pathobiology. *The American journal of pathology*, 171, 1407-1418.
- LUMPKIN, E. A. & CATERINA, M. J. 2007. Mechanisms of sensory transduction in the skin. *Nature*, 445, 858-865.
- MALESTER, B., TONG, X., GHIU, I., KONTOGEORGIS, A., GUTSTEIN, D. E., XU, J., HENDRICKS-MUNOZ, K. D. & COETZEE, W. A. 2007. Transgenic expression of a dominant negative KATP channel subunit in the mouse endothelium: effects on coronary flow and endothelin-1 secretion. *The FASEB Journal*, 21, 2162-2172.

- MANDUTEANU, I., POPOV, D., RADU, A. & SIMIONESCU, M. 1988. Calf cardiac valvular endothelial cells in culture: production of glycosaminoglycans, prostacyclin and fibronectin. *Journal of molecular and cellular cardiology*, 20, 103-118.
- MARIOT, P., VANOVERBERGHE, K., LALEVÉE, N., ROSSIER, M. F. & PREVARSKAYA, N. 2002. Overexpression of an $\alpha 1H$ (CaV3.2) T-type calcium channel during neuroendocrine differentiation of human prostate cancer cells. *Journal of Biological Chemistry*, 277, 10824-10833.
- MARTINAC, B. 2004. Mechanosensitive ion channels: molecules of mechanotransduction. *Journal of cell science*, 117, 2449-2460.
- MAZELLA, J., PÉTRAULT, O., LUCAS, G., DEVAL, E., BÉRAUD-DUFOUR, S., GANDIN, C., EL-YACOUBI, M., WIDMANN, C., GUYON, A. & CHEVET, E. 2010. Spadin, a sortilin-derived peptide, targeting rodent TREK-1 channels: a new concept in the antidepressant drug design. *PLoS biology*, 8, e1000355.
- MENDOZA, S. A., FANG, J., GUTTERMAN, D. D., WILCOX, D. A., BUBOLZ, A. H., LI, R., SUZUKI, M. & ZHANG, D. X. 2009. TRPV4-mediated endothelial Ca^{2+} influx and vasodilation in response to shear stress. *American Journal of Physiology-Heart and Circulatory Physiology*, 298, H466-H476.
- MERRYMAN, W. D., LUKOFF, H. D., LONG, R. A., ENGELMAYR JR, G. C., HOPKINS, R. A. & SACKS, M. S. 2007. Synergistic effects of cyclic tension and transforming growth factor- $\beta 1$ on the aortic valve myofibroblast. *Cardiovascular pathology*, 16, 268-276.
- METZLER, S. A., PREGONERO, C. A., BUTCHER, J. T., BURGESS, S. C. & WARNOCK, J. N. 2008. Cyclic strain regulates pro-inflammatory protein expression in porcine aortic valve endothelial cells. *The Journal of heart valve disease*, 17, 571-578.
- MILLER, J. D., WEISS, R. M. & HEISTAD, D. D. 2011. Calcific aortic valve stenosis: methods, models, and mechanisms. *Circulation research*, 108, 1392-1412.
- MIRAGOLI, M., YACCOUB, M. H., EL-HAMAMSY, I., SANCHEZ-ALONSO, J. L., MOSHKOV, A., MONGKOLDHUMRONGKUL, N., PADALA, M., PARAMAGURUNATHAN, S., SARATHCHANDRA, P. & KORCHEV, Y. E. 2014. Side-specific mechanical properties of valve endothelial cells. *American Journal of Physiology-Heart and Circulatory Physiology*, 307, H15-H24.
- MISSIRLIS, Y. & CHONG, M. 1978. Aortic valve mechanics--Part I: material properties of natural porcine aortic valves. *Journal of bioengineering*, 2, 287-300.
- MOHLER, E. R. 2004. Mechanisms of aortic valve calcification. *American Journal of Cardiology*, 94, 1396-1402.
- MONGKOLDHUMRONGKUL, N., LATIF, N., YACCOUB, M. H. & CHESTER, A. H. 2018. Effect of side-specific valvular shear stress on the content of extracellular matrix in aortic valves. *Cardiovascular engineering and technology*, 9(2): 151-157.
- MUHAMED, I., CHOWDHURY, F. & MARUTHAMUTHU, V. 2017. Biophysical tools to study cellular mechanotransduction. *Bioengineering*, 4, 12-49.
- MUN, G. I., PARK, S., KREMERSKOTHEN, J. & BOO, Y. C. 2014. Expression of synaptopodin in endothelial cells exposed to laminar shear stress and its role in endothelial wound healing. *FEBS letters*, 588, 1024-1030.
- NGO, D. T., SVERDLOV, A. L., WILLOUGHBY, S. R., NIGHTINGALE, A. K., CHIRKOV, Y. Y., MCNEIL, J. J. & HOROWITZ, J. D. 2009. Determinants of occurrence of aortic sclerosis in an aging population. *JACC: Cardiovascular Imaging*, 2, 919-927.

- NILIUS, B., PRENEN, J., JANSSENS, A., VOETS, T. & DROOGMANS, G. 2004a. Decavanadate modulates gating of TRPM4 cation channels. *The Journal of physiology*, 560, 753-765.
- NILIUS, B., VRIENS, J., PRENEN, J., DROOGMANS, G. & VOETS, T. 2004b. TRPV4 calcium entry channel: a paradigm for gating diversity. *American Journal of Physiology-Cell Physiology*, 286, C195-C205.
- NISHIDA, M., KUWAHARA, K., KOZAI, D., SAKAGUCHI, R. & MORI, Y. 2015. TRP Channels: Their Function and Potentiality as Drug Targets. *Innovative Medicine*. Springer. 195-218.
- ODELL, G. M., OSTER, G., ALBERCH, P. & BURNSIDE, B. 1981. The mechanical basis of morphogenesis: I. Epithelial folding and invagination. *Developmental biology*, 85, 446-462.
- OSMAN, L., YACOUB, M. H., LATIF, N., AMRANI, M. & CHESTER, A. H. 2006. Role of human valve interstitial cells in valve calcification and their response to atorvastatin. *Circulation*, 114, I-547-I-552.
- OWENS, D. S. & OTTO, C. M. 2009. Is it time for a new paradigm in calcific aortic valve disease? : *JACC: Cardiovascular Imaging*. 59, 1, 78–83
- PACHA, J., FRINDT, G., SACKIN, H. & PALMER, L. G. 1991. Apical maxi K channels in intercalated cells of CCT. *American Journal of Physiology-Renal Physiology*, 261, F696-F705.
- PAGNOZZI, L. A. & BUTCHER, J. T. 2017. Mechanotransduction Mechanisms in Mitral valve Physiology and Disease Pathogenesis. *Frontiers in cardiovascular medicine*, 4, 83-89.
- PARANYA, G., VINEBERG, S., DVORIN, E., KAUSHAL, S., ROTH, S. J., RABKIN, E., SCHOEN, F. J. & BISCHOFF, J. 2001. Aortic valve endothelial cells undergo transforming growth factor- β -mediated and non-transforming growth factor- β -mediated transdifferentiation in vitro. *The American journal of pathology*, 159, 1335-1343.
- PARPAITE, T. & COSTE, B. 2017. Piezo channels. *Current Biology*, 27, R250-R252.
- PCHELINTSEVA, E. & DJAMGOZ, M. B. 2018. Mesenchymal stem cell differentiation: Control by calcium-activated potassium channels. *Journal of cellular physiology*, 233, 3755-3768.
- PEYRONNET, R., MARTINS, J. R., DUPRAT, F., DEMOLOMBE, S., ARHATTE, M., JODAR, M., TAUC, M., DURANTON, C., PAULAIS, M. & TEULON, J. 2013. Piezo1-dependent stretch-activated channels are inhibited by Polycystin-2 in renal tubular epithelial cells. *EMBO reports*, 14, 1143-1148.
- PEYRONNET, R., SHARIF-NAEINI, R., FOLGERING, J. H., ARHATTE, M., JODAR, M., EL BOUSTANY, C., GALLIAN, C., TAUC, M., DURANTON, C. & RUBERA, I. 2012. Mechanoprotection by polycystins against apoptosis is mediated through the opening of stretch-activated K2P channels. *Cell reports*, 1, 241-250.
- PLATT, M. O., XING, Y., JO, H. & YOGANATHAN, A. P. 2006. Cyclic pressure and shear stress regulate matrix metalloproteinases and cathepsin activity in porcine aortic valves. *Journal of Heart Valve Disease*, 15, 622-629.
- POGGIANTI, E., VENERI, L., CHUBUCHNY, V., JAMBRIK, Z., BARONCINI, L. A. & PICANO, E. 2003. Aortic valve sclerosis is associated with systemic endothelial dysfunction. *Journal of the American College of Cardiology*, 41, 136-141.
- POTTER, C. M., LUNDBERG, M. H., HARRINGTON, L. S., WARBOYS, C. M., WARNER, T. D., BERSON, R. E., MOSHKOV, A. V., GORELIK, J.,

- WEINBERG, P. D. & MITCHELL, J. A. 2011. Role of shear stress in endothelial cell morphology and expression of cyclooxygenase isoforms. *Arteriosclerosis, thrombosis, and vascular biology*, 31, 384-391.
- PREVARSKAYA, N., SKRYMA, R., BIDAUX, G., FLOURAKIS, M. & SHUBA, Y. 2007. Ion channels in death and differentiation of prostate cancer cells. *Cell death and differentiation*, 14, 1295-1304.
- PREVARSKAYA, N., SKRYMA, R. & SHUBA, Y. 2010. Ion channels and the hallmarks of cancer. *Trends in molecular medicine*, 16, 107-121.
- RABKIN, S. W. 2005. The association of hypertension and aortic valve sclerosis. *Blood pressure*, 14, 264-272.
- RAGAERT, K., DE SOMER, F., SOMERS, P., DE BAERE, I., CARDON, L. & DEGRIECK, J. 2012. Flexural mechanical properties of porcine aortic heart valve leaflets. *Journal of the mechanical behavior of biomedical materials*, 13, 78-84.
- RAJAMANNAN, N. M. 2011. Bicuspid aortic valve disease: the role of oxidative stress in Lrp5 bone formation. *Cardiovascular pathology*, 20, 168-176.
- RAJAMANNAN, N. M., EVANS, F. J., AIKAWA, E., GRANDE-ALLEN, K. J., DEMER, L. L., HEISTAD, D. D., SIMMONS, C. A., MASTERS, K. S., MATHIEU, P. & O'BRIEN, K. D. 2011. Calcific Aortic Valve Disease: Not Simply a Degenerative Process: A Review and Agenda for Research From the National Heart and Lung and Blood Institute Aortic Stenosis Working Group Executive Summary: Calcific Aortic Valve Disease—2011 Update. *Circulation*, 124, 1783-1791.
- RAJAMANNAN, N. M., SUBRAMANIAM, M., RICKARD, D., STOCK, S. R., DONOVAN, J., SPRINGETT, M., ORSZULAK, T., FULLERTON, D. A., TAJIK, A. & BONOW, R. O. 2003. Human aortic valve calcification is associated with an osteoblast phenotype. *Circulation*, 107, 2181-2184.
- REED, A., KOHL, P. & PEYRONNET, R. 2014. Molecular candidates for cardiac stretch-activated ion channels. *Global Cardiology Science and Practice*, 19, 9-25.
- RICHARDS, J., EL-HAMAMSY, I., CHEN, S., SARANG, Z., SARATHCHANDRA, P., YACOUB, M. H., CHESTER, A. H. & BUTCHER, J. T. 2013. Side-specific endothelial-dependent regulation of aortic valve calcification: interplay of hemodynamics and nitric oxide signaling. *The American journal of pathology*, 182, 1922-1931.
- SACHS, F. 2010. Stretch-activated ion channels: what are they? *Physiology*, 25, 50-56.
- SACKIN, H. 1995. Stretch-activated ion channels. *Kidney international*, 48, 1134-1147.
- SANSOM, M. S., SHRIVASTAVA, I. H., BRIGHT, J. N., TATE, J., CAPENER, C. E. & BIGGIN, P. C. 2002. Potassium channels: structures, models, simulations. *Biochimica et Biophysica Acta (BBA)-Biomembranes*, 1565, 294-307.
- SCHWARTZ, M. A. 2010. Integrins and extracellular matrix in mechanotransduction. *Cold Spring Harbor perspectives in biology*, 10, 1101-1115.
- SEGURA, A. M., LUNA, R. E., HORIBA, K., STETLER-STEVENSON, W. G., MCALLISTER, J. H., WILLERSON, J. T. & FERRANS, V. J. 1998. Immunohistochemistry of matrix metalloproteinases and their inhibitors in thoracic aortic aneurysms and aortic valves of patients with Marfan's syndrome. *Circulation*, 98, II331-7; discussion II337-8.
- SELL, S. & SCULLY, R. E. 1965. Aging changes in the aortic and mitral valves: histologic and histochemical studies, with observations on the pathogenesis of calcific aortic stenosis and calcification of the mitral annulus. *The American journal of pathology*, 46, 345-365.

- SHEETZ, M. P., FELSENFELD, D. P. & GALBRAITH, C. G. 1998. Cell migration: regulation of force on extracellular-matrix-integrin complexes. *Trends in cell biology*, 8, 51-54.
- SIMMONS, C. A., GRANT, G. R., MANDUCHI, E. & DAVIES, P. F. 2005. Spatial heterogeneity of endothelial phenotypes correlates with side-specific vulnerability to calcification in normal porcine aortic valves. *Circulation research*, 96, 792-799.
- SMANI, T., SHAPOVALOV, G., SKRYMA, R., PREVARSKAYA, N. & ROSADO, J. A. 2015. Functional and physiopathological implications of TRP channels. *Biochimica et Biophysica Acta (BBA)-Molecular Cell Research*, 1853, 1772-1782.
- SMITH, K. E., METZLER, S. A. & WARNOCK, J. N. 2010. Cyclic strain inhibits acute pro-inflammatory gene expression in aortic valve interstitial cells. *Biomechanics and modeling in mechanobiology*, 9, 117-125.
- STACY JR, G. P., JOBE, R., TAYLOR, L. K. & HANSEN, D. E. 1992. Stretch-induced depolarizations as a trigger of arrhythmias in isolated canine left ventricles. *American Journal of Physiology-Heart and Circulatory Physiology*, 263, H613-H621.
- STAMS, T. R., OOSTERHOFF, P., HEIJDEL, A., DUNNINK, A., BEEKMAN, J. D., VAN DER NAGEL, R., VAN RIJEN, H. V., VAN DER HEYDEN, M. A. & VOS, M. A. 2016. Beat-to-beat variability in preload unmasks latent risk of Torsade de Pointes in anesthetized chronic atrioventricular block dogs. *Circulation journal*, 80, 1336-1345.
- STEWARD JR, R., TAMBE, D., HARDIN, C. C., KRISHNAN, R. & FREDBERG, J. J. 2015a. alignment. *American Journal of Physiology-Cell Physiology*, 308, C657-C664.
- STEWARD JR, R., TAMBE, D., HARDIN, C. C., KRISHNAN, R. & FREDBERG, J. J. 2015b. Fluid shear, intercellular stress, and endothelial cell alignment. *American Journal of Physiology-Cell Physiology*, 308, C657-C664.
- SUCOSKY, P., BALACHANDRAN, K., ELHAMMALI, A., JO, H. & YOGANATHAN, A. P. 2009. Altered shear stress stimulates upregulation of endothelial VCAM-1 and ICAM-1 in a BMP-4–and TGF- β 1–dependent pathway. *Arteriosclerosis, thrombosis, and vascular biology*, 29, 254-260.
- SUCOSKY, P., PADALA, M., ELHAMMALI, A., BALACHANDRAN, K., JO, H. & YOGANATHAN, A. P. 2008. Design of an ex vivo culture system to investigate the effects of shear stress on cardiovascular tissue. *Journal of biomechanical engineering*, 130, 1115-1123.
- SUKUMARAN, S. V., SINGH, T. U., PARIDA, S., REDDY, C. E. N., THANGAMALAI, R., KANDASAMY, K., SINGH, V. & MISHRA, S. K. 2013. TRPV4 channel activation leads to endothelium-dependent relaxation mediated by nitric oxide and endothelium-derived hyperpolarizing factor in rat pulmonary artery. *Pharmacological research*, 78, 18-27.
- SUN, L., CHANDRA, S. & SUCOSKY, P. 2012. Ex vivo evidence for the contribution of hemodynamic shear stress abnormalities to the early pathogenesis of calcific bicuspid aortic valve disease. *PLoS one*, 7, e48843.
- SUN, W., ZHAO, R., YANG, Y., WANG, H., SHAO, Y. & KONG, X. 2013. Comparative study of human aortic and mitral valve interstitial cell gene expression and cellular function. *Genomics*, 101, 326-335.
- SZÜTS, V., ÖTVÖS, F., DÉZSI, L., VÁGVÖLGYI, C., SZALONTAI, B., DOBRZYNSKI, H., BOYETT, M., ZHANG, H., PAPP, G. & VARRÓ, A. 2012. What have we learned from two-pore potassium channels? Their molecular

- configuration and function in the human heart. *Acta Biologica Szegediensis*, 56, 93-107.
- TALLEY, E. M., SIROIS, J. E., LEI, Q. & BAYLISS, D. A. 2003. Two-pore-Domain (KCNK) potassium channels: dynamic roles in neuronal function. *The Neuroscientist*, 9, 46-56.
- TAN, J. C. & CORONEO, M. T. 2009. Are stretch-activated channels an ocular barometer? *Mechanosensitivity of the Nervous System*. Springer, 1, 133-144.
- TAYLOR, P., ALLEN, S. & YACOUB, M. 2000. Phenotypic and functional characterization of interstitial cells from human heart valves, pericardium and skin. *The Journal of heart valve disease*, 9, 150-158.
- TAYLOR, P. M., BATTEN, P., BRAND, N. J., THOMAS, P. S. & YACOUB, M. H. 2003. The cardiac valve interstitial cell. *The international journal of biochemistry & cell biology*, 35, 113-118.
- THAYER, P., BALACHANDRAN, K., RATHAN, S., YAP, C. H., ARJUNON, S., JO, H. & YOGANATHAN, A. P. 2011. The effects of combined cyclic stretch and pressure on the aortic valve interstitial cell phenotype. *Annals of biomedical engineering*, 39, 1654-1667.
- THUBRIKAR, M. J., AOUAD, J. & NOLAN, S. P. 1986. Comparison of the in vivo and in vitro mechanical properties of aortic valve leaflets. *The Journal of Thoracic and Cardiovascular Surgery*, 92, 29-36.
- TIAPKO, O. & GROSCHNER, K. 2018. TRPC3 as a target of novel therapeutic interventions. *Cells*, 7, 83-90.
- TZIMA, E., IRANI-TEHRANI, M., KIOSSES, W. B., DEJANA, E., SCHULTZ, D. A., ENGELHARDT, B., CAO, G., DELISSER, H. & SCHWARTZ, M. A. 2005. A mechanosensory complex that mediates the endothelial cell response to fluid shear stress. *Nature*, 437, 426.
- VINCENT, F. & AJ DUNCTON, M. 2011. TRPV4 agonists and antagonists. *Current topics in medicinal chemistry*, 11, 2216-2226.
- VOLKERS, L., MECHIOUKHI, Y. & COSTE, B. 2015. Piezo channels: from structure to function. *Pflügers Archiv-European Journal of Physiology*, 467, 95-99.
- WANG, H., SRIDHAR, B., LEINWAND, L. A. & ANSETH, K. S. 2013. Characterization of cell subpopulations expressing progenitor cell markers in porcine cardiac valves. *PLoS One*, 8, e69667.
- WANG, N. 2017. Review of cellular mechanotransduction. *Journal of physics D: Applied physics*, 50, 233-243.
- WARNOCK, J. N., BURGESS, S. C., SHACK, A. & YOGANATHAN, A. P. 2006. Differential immediate-early gene responses to elevated pressure in porcine aortic valve interstitial cells. *J Heart Valve Dis*, 15, 34-41.
- WARNOCK, J. N., NANDURI, B., GAMEZ, P., CAROL, A., TANG, J., KOBACK, D., MUIR, W. M. & BURGESS, S. C. 2011. Gene profiling of aortic valve interstitial cells under elevated pressure conditions: modulation of inflammatory gene networks. *International journal of inflammation*, 2011, 4016-4026.
- WEINHAUS, A. J. & ROBERTS, K. P. 2005. Anatomy of the human heart. *Handbook of cardiac anatomy, physiology, and devices*. Springer.
- WELLING, P. & O'NEIL, R. 1990. Cell swelling activates basolateral membrane Cl and K conductances in rabbit proximal tubule. *American Journal of Physiology-Renal Physiology*, 258, F951-F962.
- WESTON, M. W., LABORDE, D. V. & YOGANATHAN, A. P. 1999. Estimation of the shear stress on the surface of an aortic valve leaflet. *Annals of biomedical engineering*, 27, 572-579.

- WESTON, M. W. & YOGANATHAN, A. P. 2001. Biosynthetic activity in heart valve leaflets in response to in vitro flow environments. *Annals of biomedical engineering*, 29, 752-763.
- WIDMER, C., GEBAUER, J. M., BRUNSTEIN, E., ROSENBAUM, S., ZAUCKE, F., DRÖGEMÜLLER, C., LEEB, T. & BAUMANN, U. 2012. Molecular basis for the action of the collagen-specific chaperone Hsp47/SERPINH1 and its structure-specific client recognition. *Proceedings of the National Academy of Sciences*, 109, 13243-13247.
- WILLEMS, I., HAVENITH, M. G., SMITS, J. & DAEMEN, M. 1994. Structural alterations in heart valves during left ventricular pressure overload in the rat. *Laboratory investigation; a journal of technical methods and pathology*, 71, 127-133.
- WILSON, E., SUDHIR, K. & IVES, H. E. 1995. Mechanical strain of rat vascular smooth muscle cells is sensed by specific extracellular matrix/integrin interactions. *The Journal of clinical investigation*, 96, 2364-2372.
- WU, Q.-Q. & CHEN, Q. 2000. Mechanoregulation of chondrocyte proliferation, maturation, and hypertrophy: ion-channel dependent transduction of matrix deformation signals. *Experimental cell research*, 256, 383-391.
- WYLIE-SEARS, J., AIKAWA, E., LEVINE, R. A., YANG, J.-H. & BISCHOFF, J. 2011. Mitral valve endothelial cells with osteogenic differentiation potential. *Arteriosclerosis, thrombosis, and vascular biology*, 31, 598-607.
- WYSS, K., YIP, C. Y., MIRZAEI, Z., JIN, X., CHEN, J.-H. & SIMMONS, C. A. 2012. The elastic properties of valve interstitial cells undergoing pathological differentiation. *Journal of biomechanics*, 45, 882-887.
- XING, Y. 2005. Effects of mechanical forces on the biological properties of porcine aortic valve leaflets. Georgia Institute of Technology, Bioengineering Graduate Degree Program Theses and Dissertations.
- XING, Y., HE, Z., WARNOCK, J. N., HILBERT, S. L. & YOGANATHAN, A. P. 2004a. Effects of constant static pressure on the biological properties of porcine aortic valve leaflets. *Annals of Biomedical Engineering*, 32, 555-562.
- XING, Y., WARNOCK, J. N., HE, Z., HILBERT, S. L. & YOGANATHAN, A. P. 2004c. Cyclic pressure affects the biological properties of porcine aortic valve leaflets in a magnitude and frequency dependent manner. *Annals of biomedical engineering*, 32, 1461-1470.
- XU, X., LOZINSKAYA, I., COSTELL, M., LIN, Z., BALL, J. A., BERNARD, R., BEHM, D. J., MARINO, J. P. & SCHNACKENBERG, C. G. 2013. Characterization of small molecule TRPC3 and TRPC6 agonist and antagonists. *Biophysical Journal*, 104, 454a.
- YAP, C. H., SAIKRISHNAN, N., TAMILSELVAN, G. & YOGANATHAN, A. P. 2012a. Experimental measurement of dynamic fluid shear stress on the aortic surface of the aortic valve leaflet. *Biomechanics and modeling in mechanobiology*, 11, 171-182.
- YAP, C. H., SAIKRISHNAN, N. & YOGANATHAN, A. P. 2012e. Experimental measurement of dynamic fluid shear stress on the ventricular surface of the aortic valve leaflet. *Biomechanics and modeling in mechanobiology*, 11, 231-244.
- YIP, C. Y. Y., CHEN, J.-H., ZHAO, R. & SIMMONS, C. A. 2009. Calcification by valve interstitial cells is regulated by the stiffness of the extracellular matrix. *Arteriosclerosis, thrombosis, and vascular biology*, 29, 936-942.
- YIP, C. Y. Y. & SIMMONS, C. A. 2011. The aortic valve microenvironment and its role in calcific aortic valve disease. *Cardiovascular Pathology*, 20, 177-182.

- YOON, S.-H., SHARMA, R., CHAKRAVARTY, T., MIYASAKA, M., OCHIAI, T., NOMURA, T., GELLADA, N., NEMANPOUR, S., NAKAMURA, M. & CHEN, W. 2018. Transcatheter aortic valve replacement in bicuspid aortic valve stenosis: where do we stand? *The Journal of cardiovascular surgery*, 59, 381-391.
- YOUM, J. B., HAN, J., KIM, N., ZHANG, Y.-H., KIM, E., LEEM, C. H., KIM, S. J. & EARM, Y. E. 2005. Role of stretch-activated channels in the heart: action potential and Ca²⁺ transients. book.
- ZHAO, B., YANG, H., ZHANG, R., SUN, H., LIAO, C., XU, J., MENG, K. & JIAO, J. 2015. The role of TRPC6 in oxidative stress-induced podocyte ischemic injury. *Biochemical and biophysical research communications*, 461, 413-420.
- ZHENG, J. 2013. Molecular mechanism of TRP channels. *Comprehensive Physiology*, 3, 221-242.